Exploring the circulating biomarkers for prostate cancer progression and treatment monitoring

Submitted in partial fulfilment of the requirements of the Degree of Doctor of Philosophy

Tianyu Guo

Supervisors: Professor Wen Wang
Professor Yong-jie Lu
Queen Mary University of London
London, United Kingdom

Statement of originality

I, Tianyu Guo, confirm that the research included within this thesis is my own work or that where it has been carried out in collaboration with, or supported by others, that this is duly acknowledged below and my contribution indicated. Previously published material is also acknowledged below.

Dr. Yang Wang helped with a proportion of exosome isolation and RNA extraction. Dr. Lei Xu, Dr. Xueying Mao, Dr. Elzbieta Stankiewicz, Miss Caitlin R. Davies and Miss Edwina Burke helped with a proportion of clinical sample collection. Dr. Glenda Scandura helped collecting clinical information for recruited patients. Dr. Eva Wozniak, Dr. Anna Terry, and Dr. Charles Meins at Queen Mary University of London Genome Centre helped with performing library preparation, RNA-sequencing and alignment. Dr. Elzbieta Stankiewicz helped with immunohistochemistry staining of the tissue sections. Dr. Marc Yeste-Velasco helped with the mice xenograft work. Dr. Jacek Marzec provided some instructions for RNA-sequencing data analysis. Validation work in Department of Pathology and Cancer Centre, Medical College of Wisconsin was performed by Dr. Manish Kohli, Dr. Jing jia and Professor Liang Wang's team.

I attest that I have exercised reasonable care to ensure that the work is original, and does not to the best of my knowledge break any UK law, infringe any third party's copyright or other Intellectual Property Right, or contain any confidential material.

I accept that the College has the right to use plagiarism detection software to check the electronic version of the thesis.

I confirm that this thesis has not been previously submitted for the award of a degree by this or any other university.

Signature: Tianyu Guo

Date: 16/07/2019

Details of publications related to this study:

1. **Tianyu Guo**, Claire S. Wang, Wen Wang and Yongjie Lu. Culture of Circulating Tumor Cells - Holy Grail and Big Challenge. Int J Cancer Clin Res, 2016; 3:065.

2. Lei Xu, Xueying Mao, **Tianyu Guo**, Pui Ying Chan, Greg Shaw, John Hines, *et al.* The Novel Association of Circulating Tumor Cells and Circulating Megakaryocytes with Prostate Cancer Prognosis. Clin Cancer Res. 2017; 23(17): 5112–22.

3. **Tianyu Guo**, Yang Wang, Xueying Mao, Lei Xu, Jacek Marzec, Edwina Burke *et al*. Investigation of plasma exosomal miRNA as a biomarker and its potential function in prostate cancer castration resistant development [abstract]. Cancer Res 2019;79(13 Suppl):Abstract nr 2580.

Acknowledgement

I would like to thank my supervisors, Prof. Wen Wang and Prof. Yong-jie Lu for giving me this opportunity to pursue my PhD study. They have given me valuable support and guidance throughout the whole period of my study.

I would like to thank the members in our team and all my colleagues in Barts Cancer Institute and Institute of Bioengineering. They have been generous to offer help and suggestions for all my lab work and also my study life in UK.

I would like to thank China Scholarship Council for funding support of my PhD study. I would like to thank Great Britain-China Education Trust and Henry Lester Trust for their award support.

Special thanks go to my parents, Mr. Zhiqiang Guo and Ms. Li Wang, husband Mr. Zheyuan Liu, and other family members, for their unconditional support and encouragement.

Abstract

Prostate cancer (PCa) ranks as the second most frequent cancer and the fifth leading cause of cancer death in men worldwide. Androgen-deprivation therapy is the principal treatment for locally advanced and metastatic PCa. However, most patients will progress to castration-resistant PCa (CRPC), which contributes to the majority of PCa deaths. This project aims to investigate the utility of two main types of liquid biopsy, plasma exosomes and circulating tumour cells (CTCs), in monitoring PCa progression and treatment response.

We performed RNA-sequencing of plasma exosomal miRNAs in 24 treatment-naive PCa and 24 CRPC patients and identified different miRNA expression profiles. Several miRNAs were confirmed by reverse transcriptase quantitative polymerase chain reaction in 108 treatment-naive PCa, 42 CRPC and 36 treated non-CRPC patients. The most significantly differentially expressed miRNA, miR-423-3p, was also validated in 30 treatment-naive PCa and 30 CRPC patients at a separate centre. The differentially expressed exosomal miRNAs showed good prediction value for CRPC and showed better prediction value than prostate specific antigen when predicting CRPC from treated non-CRPC. The *in vitro* study of one miRNA, miR-423-3p, showed that it could enhanced LNCaP cell migration and invasion in hormone-depleted environment. The hormone-independent subline of LNCaP had higher miR-423-3p expression and increased migration and invasion ability.

CTC culture provides a good platform for establishing patient-specific tumour models and study of treatment response. I tested different CTC isolation methods and culture conditions for CTC propagation. Viable CTCs could be isolated from PCa patients' blood and potentially be propagated *in vitro*. However, the purity of tumour cells remain low in cultured population and long-term culture remains challenging.

This study demonstrated that plasma exosomal miRNAs play important roles in CRPC development and may serve as prediction biomarkers for CRPC occurrence. Long-term culture of PCa CTCs remains challenging and needs further investigation.

Table of Contents

Abbreviations

ADT	androgen deprivation therapy
AFMS	anterior fibromuscular stroma
AR	androgen receptor
AR-V7	androgen receptor splice variant 7
AS	active surveillance
AUC	area under the curve
BPH	benign prostatic hyperplasia
cfDNA	Cell-free DNA
CI	confidence interval
CK	cytokeratin
CPM	Counts per million
CRPC	Castration-resistant prostate cancer
CTCs	circulating tumour cells
ctDNA	circulating tumour DNA
CZ	central zone
DAPI	4,6-diamidino-2-phenylindole dihydrochloride
DEX	dendritic cell-derived exosomes
DHT	5α-dihydrotestosterone
dNTP	deoxy ribonucleotide triphosphate
DPX	Di-n-butyle phthalate in xylene

EpCAM	epithelial cell adhesion molecule
Evs	extracellular vesicles
FCS	Foetal Calf Serum
FDA	Food and Drug Administration
FFPE	formalin-fixed, paraffin-embedded
FISH	fluorescence *in situ* hybridisation
GS	Gleason score
GWAS	genome-wide association studies
HSPC	hormone-sensitive prostate cancer
IQR	interquartile range
ISUP	International Society of Urological Pathology
mCRPC	metastatic castration-resistant prostate cancer
miRNA	microRNA
mRNA	messenger RNA
MVBs	multivesicular bodies
NaCl	Sodium chloride
NSCLC	non-small-cell lung cancer
PBMCs	peripheral blood mononuclear cells
PBS	phosphate buffered saline
PCa	prostate cancer
pre-miRNA	precursor microRNA

pri-miRNA	primary microRNA
PSA	prostate-specific antigen
PSMA	Prostate-specific membrane antigen
PTEN	phosphatase and tensin homolog
PZ	peripheral zone
RT-qPCR	reverse transcriptase real-time quantitative polymerase chain reaction
ROC	Receiver operating characteristic
RPM	read counts per million mapped reads
RT	room temperature
SNPs	single-nucleotide polymorphisms
TBST	Tris Buffer Saline/0.1% Tween-20
TEPs	tumour-educated platelets
TMM	trimmed mean of M-value normalisation
TNM	Tumour-Node-Metastasis
TZ	transitional zone
Vim	Vimentin
V	volt
WB	Western-blotting
WW	watchful waiting
β-ME	β-mercaptoethanol

List of figures

List of tables

Chapter I Introduction and aims

1.1 Prostate cancer (PCa)

1.1.1 Prostate anatomy and physiology

The prostate is a tubuloalveolar exocrine gland of the male reproductive system. It is located between the bladder and the penis and is situated in front of the rectum, with the urethra running through its centre (Figure 1). There is a widely accepted anatomical model of the prostate established by McNeal in the early 1980s. This model describes the prostate as a gland consisting of three zones, namely, the central zone (CZ), the transitional zone (TZ), the peripheral zone (PZ), and a fibromuscular band of tissue named anterior fibromuscular stroma (AFMS) (Figure 2) [1]. The PZ is the largest area of the prostate, constituting about 70% of the glandular prostate. Most PCas start in the PZ. The TZ surrounds the part of the urethra which passes through the prostate (called the prostatic urethra), representing only 5% of the gland. The volume of the TZ increases with age and it is the primary site of benign prostatic hyperplasia (BPH). The CZ lies behind the TZ and surrounds the ejaculatory ducts, occupying approximately 25% of the glandular prostate. Very few PCas start in the CZ. The AFMS is a thickened area of tissue that surrounds the apex of the prostate. It is predominantly fibromuscular with little or no glandular structures [2, 3].

Adult prostate is composed of two compartments, the stroma and the epithelium. The epithelia include basal cells, secretory luminal cells, and rare intermediate and neuroendocrine cell populations. The epithelial ducts are adjacent to a stromal compartment that includes smooth muscle cells, fibroblasts, and vascular and neural components (Figure 3) [4]. The main function of the prostate is to secret prostatic fluid which constitutes approximately one-fifth to one-third of the volume of the entire ejaculate. The prostate epithelial compartment provides the main glandular function to secrete the prostatic fluid. Prostatic fluid contains a number of factors that control the ejaculation process and regulate proteins (from the other accessory gland secretions) that activate sperm maturation. These factors in prostatic fluid are necessary for semen liquefaction, the clotting cycle and sperm motility [3].

Androgen plays a pivotal role in prostate development and homeostatic maintenance. Testosterone is the principal circulating androgen in males. Approximately 90% of testosterone is from the testis and 10% from the adrenals. Within the prostate, testosterone is converted to 5α-dihydrotestosterone (DHT) by the 5α-reductase enzyme. The androgen receptor (AR) which presents in almost all prostate cells can bind both testosterone and DHT, though it has greater affinity for DHT. The androgen-AR complex then enters the nucleus and stimulates transcription of AR-regulated genes via binding to androgen responsive elements [5, 6].

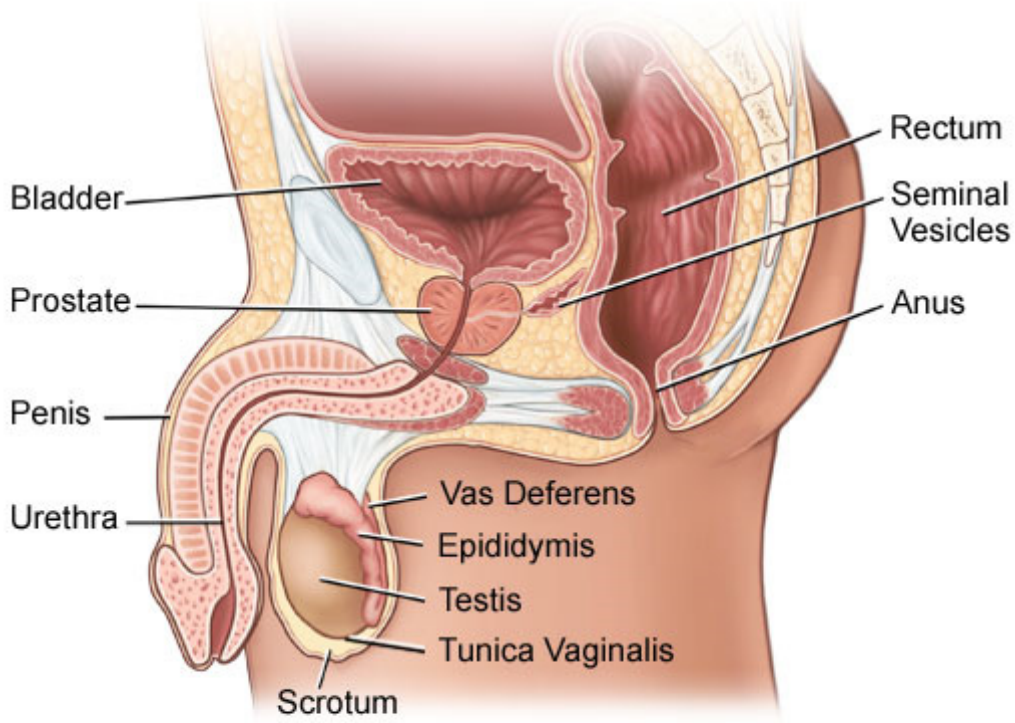

Figure 1. Location of human prostate gland. (Adapted from https://www.hopkinsmedicine.org/healthlibrary/conditions/prostate_health/anatomy_of_the_prostate_gland_85,P01257)

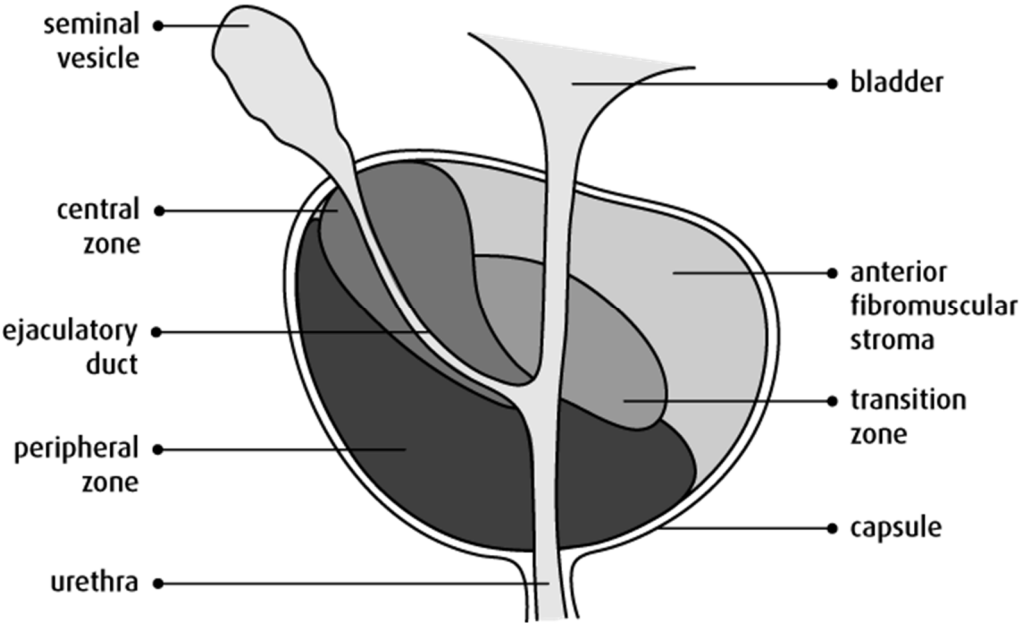

Figure 2. Zones of the prostate. (Adopted from http://www.cancer.ca/en/cancer-information/cancer-type/prostate/prostate-cancer/the-prostate/?region=on)

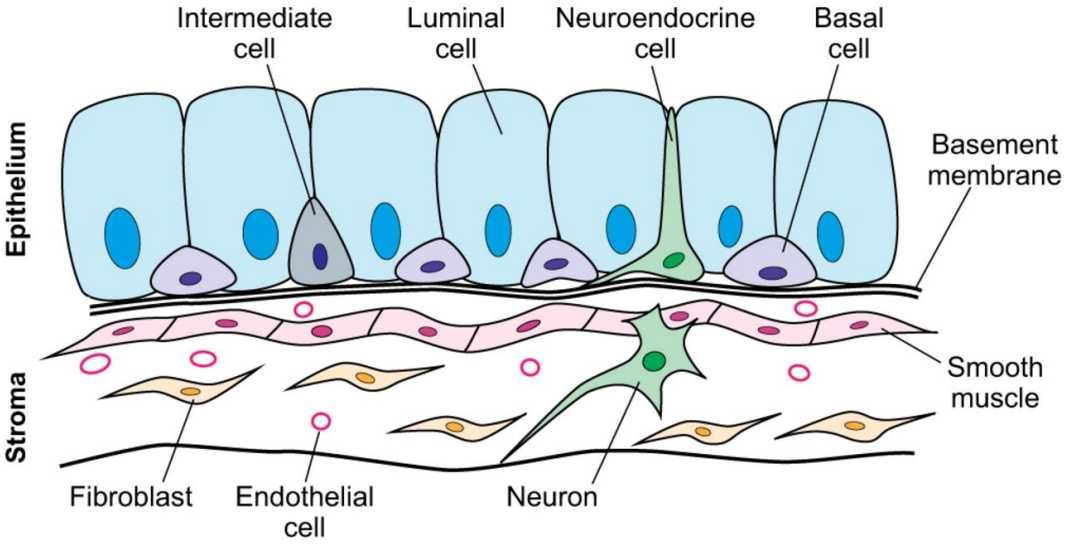

Figure 3. Differentiated cell types in the prostate. [4]

1.1.2 PCa incidence, mortality and survival

There was an estimate of 1,276,106 new cases and 358,989 deaths of PCa worldwide in 2018. PCa is the most frequently diagnosed cancer in male in 105

countries in a 185-country statistic. Globally, PCa is the second mostly diagnosed male cancer [7]. There are wide geographic variations of PCa incidence rate, as the highest incidence rate (in Australia/New Zealand) is around 17-fold higher than the lowest (in South Central Asia) [7]. In males in the United Kingdom (UK), PCa is the most common cancer, with around 47,200 new cases in 2015. PCa European age-standardised incidence rates have increased by 44% in the UK between 1993-1995 and 2013-2015. The incidence rates are projected to further rise by 12% in the UK between 2014 and 2035 [8]. This can be attributed to the practice of prostate-specific antigen (PSA) testing.

PCa is estimated as the fifth leading cause of cancer death in men worldwide, however the mortality rates also have geographical variations and they do not follow the variations of incidence [7]. In the UK, PCa is the second leading cause of cancer death in males [9]. The highest PCa mortality rates are among populations in the Caribbean and Southern Africa and the lowest PCa mortality rates are observed in South-central Asia [7].

Although PCa has high incidence rate, the survival is generally good. Age and the stage of the PCa at diagnosis have great effect on the survival. Five year survival gradually increases from 91% in men aged 15-49 and peaks at 94% in 60-69 year olds diagnosed with PCa. The survival falls thereafter, reaching its lowest point of 66% in 80-99 year olds patients diagnosed with PCa in England during 2009-2013 [10]. In cases where the cancer is localised or locally advanced at diagnosis, five year survival rate is almost 100%. However, for distant metastatic disease, five year survival rate is approximately 30% [10, 11].

1.1.3 Risk factors

Age, family history and race/ethnicity are the established risk factors for PCa. The risk of developing PCa increases with age, as PCa is rarely found in men younger than 40, but the risk increases significantly after the age of 50. A positive relationship between family history of PCa and PCa risk has been observed in many studies. Three systematic reviews and meta-analysis published in 2003 have shown consistent results that men with affected relative have greater risk of PCa [12-14]. The relative risk increases with decreasing age of the affected family

members at diagnosis, with increasing genetic relatedness of the affected relatives, and with increasing number of individuals affected [12-14]. Ethnicity is another main risk factor for PCa. In the United States (US), non-Hispanic black men have higher PCa incidence and mortality compared to men of other ethics [15]. In addition to age, family history, and race/ethnicity, there are also other risk factors reported, such as genetic factors, diet and obesity [16].

1.1.4 PSA test

PSA is a serine protease which is mainly responsible for gel dissolution in freshly ejaculated semen by proteolysis of the major gel-forming proteins, semenogelin I, semenogelin II and fibronectin. PSA is secreted by prostate epithelia. In normal males, PSA presents in the blood at very low concentration. Serum PSA level can elevate at the presence of PCa and other prostate diseases such as chronic inflammation and BPH, which is believed to result from the disruption of prostate architecture [17]. The PSA test is now routinely used for the diagnosis and monitoring of PCa, as well as PCa response to treatment.

In early 1990s, PSA screening was recommended for routine annual PCa screening in the US [18]. However, accumulating evidence raised concerns of PSA screening over the false-negative and false-positive issues and potential over-diagnosis and over-treatment. Two major screening trials, European Randomized Study of Screening for Prostate Cancer [19] and Prostate, Lung, Colorectal, and Ovarian Cancer Screening trial [20], published cancer survival data in 2009. The European Randomized Study of Screening for Prostate Cancer reported a modest PCa survival benefit with screening and a later follow up showed similar results [21], whereas the Prostate, Lung, Colorectal, and Ovarian Cancer Screening trial found no benefit of screening. Recent publication from the Cluster Randomized Trial of PSA Testing for Prostate Cancer in UK reported there was no significant difference in PCa mortality after a median follow-up of 10 years among practices randomised to a single PSA screening intervention compared to standard practice without screening, but the detection of low-risk PCa cases increased [22]. As data suggested more harm than benefit of PSA screening, current guidelines are against population-based screening of PSA and

propose individualised strategy and informed decision making for men to do the test [23].

Monitoring of PSA after definitive local therapy for PCa provides a mean of detecting recurrent PCa long before the tumour is detectable by any other means (for example, imaging or symptoms). This monitoring of PSA after treatment of localised PCa leads to the identification of men with a PSA-only (biochemical) recurrence, but the prognosis of men with PCa following a PSA relapse is diverse [24]. PSA is also used to monitor disease progression in patients undergoing androgen-deprivation therapy (ADT). However, PSA alone is not reliable enough for monitoring disease activity in advanced castration-resistant PCa (CRPC) as visceral metastases may develop in men without rising PSA [25]. Thus radiological tests are normally done to confirm the disease progression and facilitate clinical decisions.

1.1.5 Grading and staging of prostate adenocarcinoma

The grading system that is used for determining PCa aggressiveness is Gleason score (GS). In 1966, Dr. Donald Gleason created the grading system, which grades the different histologic patterns from 1 to 5, where a lower grade indicates well-differentiated glandular pattern. A GS contains two grades from the two most common grade patterns in a tumour, thus a GS scores range from 2 to 10 after added up the two grades. After that, the PCa grading system had undergone two major revisions in 2005 and 2014. In 2005, the International Society of Urological Pathology (ISUP) modified GS of biopsy-detected PCa comprising the GS of the most extensive pattern (primary pattern), plus the second most common pattern (secondary pattern). If only one pattern is present, it needs to be doubled to yield the GS. In cases with three or more grade patterns, the GS should comprise the most common grade plus the highest grade, irrespective of its extent. When a carcinoma is largely grade 4/5, identification of < 5% of grade 2 or 3 glands should not be incorporated in the GS. A GS < 4 should not be given based on prostate biopsies [26]. In 2014, ISUP consensus conference agreed upon a 5-tier ISUP grading system (Table 1), as grade 1 tumours being GS ≤6, grade 2 being GS 3+4, grade 3 being GS 4+3, grade 4 being GS 8, and grade 5 being GS 9 to 10 [27]. This new system eliminated the anomaly that the most highly differentiated

PCa have a GS 6 and further defined the clinically highly significant distinction between GS 7 (3 + 4) and 7 (4 + 3) PCa.

GS has been the single most powerful predictor of PCa prognosis, as higher GS correlates with poorer prognosis. Studies have grouped GS scores based on the assumption that patients diagnosed with these GSs have a similar prognosis, for example the most commonly used grouping is 2-6, 7, and 8-10 [28]. Although GS 7 has initially considered as a single score, later studies have found that 4+3 has significantly worse prognosis than 3+4 [29, 30]. GS 9 and 10 also showed significantly worse outcomes compared with GS 8 disease [31]. Thus, current ISUP grades has listed GS 3+4 and 4+3 as single grades and separated GS 8 and GS 9-10. Recent studies showed the new five-grade group system had great prognostic discrimination for biochemical recurrence [32, 33].

Table 1. International Society of Urological Pathology (ISUP) 2014 grades. Adapted from [27].

Gleason score	ISUP grade
2-6	1
7(3+4)	2
7(4+3)	3
8 (4+4 or 3+5 or 5+3)	4
9-10	5

Staging describes where the cancer is located, whether it has spread and where it has spread, and whether it has metastasis to other parts of the body. There are two types of staging for PCa, clinical staging and pathologic staging. The clinical staging is based on the results of digital rectum examination, lab tests, prostate biopsy, and imaging tests which are available prior to treatment or the surgical removal of the tumour. Pathologic staging is based on information gathered

during an examination of prostate tissue removed during radical prostatectomy and pelvic lymph nodes if pelvic lymph node dissection is performed. Staging is important to estimate prognosis and guide treatment decision making. Tumour-Node-Metastasis (TNM) classification system is the most widely used staging system for PCa. The American Joint Committee on Cancer published the first edition of the Cancer Staging Manual in 1977. Since then, they have published several editions. The recently updated edition was published in 2017 and has been implemented on January 1, 2018 [34] (Table 2).

Table 2. Definitions of American Joint Committee on cancer TNM criteria. (Adapted from [34]).

Clinical (cT)		
T category	TX	Primary tumour cannot be assessed
	T0	No evidence of primary tumour
	T1	Clinically inapparent tumour that is not palpable
	T1a	Tumour incidental histologic finding in 5% or less of tissue resected
	T1b	Tumour incidental histologic finding in more than 5% of tissue resected
	T1c	Tumour identified by needle biopsy found in one or both sides, but not palpable
	T2	Tumour is palpable and confined within prostate
	T2a	Tumour involves one-half of one side or less
	T2b	Tumour involves more than one-half of one side but not both sides
	T2c	Tumour involves both sides
	T3	Extraprostatic tumour that is not fixed or does not invade adjacent structures
	T3a	Extraprostatic extension (unilateral or bilateral)
	T3b	Tumour invades seminal vesicle(s)
	T4	Tumour is fixed or invades adjacent structures other than seminal vesicles, such as external sphincter, rectum, bladder, levator muscles, and/or pelvic wall
Pathologic (pT)		
T category	T2	Organ confined
	T3	Extraprostatic extension
	T3a	Extraprostatic extension (unilateral or bilateral) or microscopic invasion of bladder neck
	T3b	Tumour invades seminal vesicle(s)
	T4	Tumour is fixed or invades adjacent structures other than seminal vesicles, such as external sphincter, rectum, bladder, levator muscles, and/or pelvic wall
N category	NX	Regional lymph nodes were not assessed
	N0	No positive regional lymph nodes
	N1	Metastases in regional lymph node(s)
M category	M0	No distant metastasis
	M1	Distant metastasis
	M1a	Non-regional lymph node(s)
	M1b	Bone(s)
	M1c	Other site(s) with or without bone disease

1.1.6 Treatments for PCa

A risk classification system is used to assist offering appropriate treatment to patients diagnosed with PCa. Current clinical guidelines for PCa diagnosis and management published by the National Institute for Health and Clinical Excellence (https://www.nice.org.uk/guidance/ng131) and the European Association of Urology [23] categorise localised PCa to low, intermediate and high risk groups (Table 3) based on the risk of biochemical recurrence after surgery or external beam radiotherapy.

Table 3. Risk stratification for biochemical recurrence of localised and locally advanced PCa. Adapted from [23]

Low-risk	Intermediate-risk	High-risk	
PSA<10 ng/mL and GS<7(ISUP grade 1) and cT1-2a	PSA 10-20 ng/mL or GS 7(ISUP grade 2/3) or cT2	PSA >20 ng/mL or GS > 7(ISUP grade 4/5) or cT2c	any PSA any GS any ISUP cT3-4 or cN+
Localised			Locally advanced

1.1.6.1 Treatments for localised PCa

After diagnosis of localised PCa, there can be several options for patients, including active surveillance (AS), watchful waiting (WW) and several radical treatments. Radical prostatectomy is a surgery process which removes prostate cancer. It remains the most effective treatment and shows benefit over WW and AS [35-37]. However, as PCa often grows very slowly, some patients may not need active treatment and treatments will cause side effects and may affect the quality of life. AS, which conducts a routine protocol of close monitoring with digital rectal examination, periodic biopsy, and serial PSA testing and consultations, is often used as a mean to monitor the cancer more closely in low-risk patients who do not need active treatments [23]. A study with ten years of

follow up showed the similar cancer specific survival and overall survival (OS) between patients who were actively treated and on AS. However metastatic progression was higher in AS group (6% in the AS group as compared to 2.6% in the treated group) [35]. Although the metastatic progression risk needs to be considered, this study suggests that AS is as effective as active treatment at ten years, avoided unnecessary treatment for most patients. WW can be recommended to elderly patients with limited expectancy with no symptoms of PCa. WW normally has less tests than AS and relies on the changes of symptoms and of re-biopsy results to decide if treatment is needed [23].

1.1.6.2 Treatments for locally advanced PCa

Locally advanced PCa has extended clinically beyond the prostatic capsule, with invasion of the pericapsular tissue, bladder neck, or seminal vesicles, but without lymph node involvement or distant metastases. Treatment options for patients with locally advanced PCa include external beam radiotherapy with ADT (and sometimes with high dose-rate brachytherapy), radical prostatectomy (often followed by ADT and radiotherapy), ADT alone and WW [23]. There are different types of ADT which aim at reducing the effect of androgen. The main types of ADT include surgical castration which removes testicles, luteinizing hormone-releasing hormone agonists (e.g. Goserelin) and antagonists (e.g. degarelix) which lower the amount of androgen, anti-androgens (e.g. Flutamide, Enzalutamide, and Bicalutamide) which compete with androgen to reduce the binding of androgen to AR, and CYP17 inhibitor (e.g. Abiraterone) which blocks androgen formation[38].

1.1.6.3 Treatments for metastatic/ recurrent/ progressive diseases

As prostate epithelial cells and almost all PCa cells rely on androgen to grow, ADT is an efficient therapy for PCa. While in the case of local recurrence or local progression after radical treatment, consideration should be given to cancer re-staging and treating with further local radical therapy (radiotherapy or surgery), while ADT is the standard care for metastatic disease [39]. In recent years, three large clinical trials were conducted comparing ADT alone as the standard of care

to ADT combined with chemotherapy (docetaxel) in metastatic PCa patients within three months of ADT initiation [40-42]. In all three trials, ADT combined with docetaxel showed better OS. Based on these findings, docetaxel combined with ADT are now being considered as a new standard in men presenting with metastases at first presentation, providing they are fit enough to receive the drug [39].

ADT is initially effective in most patients, however, resistance inevitably arises. CRPC refers to a progressed disease, with evidence of either radiologic or biochemical progression, in the presence of castration level of circulating testosterone (< 50ng/dl) [43]. Of note, CRPC is not fully hormone refractory, as other forms of ADT as second line hormone therapies can be effective in CRPC [44].

CRPC is an incurable stage of PCa and the majority of patients have developed metastases with poor prognosis [45]. Treatment for CRPC was very limited with minimal survival benefits before the discovery of docetaxel. Two landmark phase III trials demonstrated better OS and improvement of pain in metastatic CRPC (mCRPC) patients treated with docetaxel [46, 47]. Docetaxel was then approval by the US Food and Drug Administration (FDA) in 2004 as a first-line chemotherapy agent and it has been a mainstay of therapy for patients with mCRPC. Currently, there are a few therapeutic options available for patients with mCRPC, for example ADT including abiraterone [48] and enzalutamide [49], immunotherapy sipuleucel-T which uses activated patient-derived antigen-presenting cells as an immune modulator or vaccine [50], and alpha emitter Ra 223 [51]. Many CPRC patients have benefited from these treatments with prolonged survival. However, not all patients respond well to the given therapy. For example, only approximately 50% of patients respond to first-line docetaxel [46, 47].

1.1.7 Molecular alterations in PCa

1.1.7.1 Germline variants in PCa patients

Multiple studies have demonstrated a genetic component to the aetiology of PCa. Evidence of the heritability of PCa from epidemiological as well as twin studies

point towards a significant genetic component contributing to PCa development [52]. Large-scale genome-wide association studies (GWAS), which screen for disease-related single-nucleotide polymorphisms (SNPs), have identified approximately 170 PCa susceptibility variants [53]. Most large-scale GWAS studies have been performed in European populations, but recent studies have also included some other populations and population-specific differences have been reported [54-56], which may help explain geographical and ethinic differences in PCa incidence rates. Linkage studies into the genetic predisposition in PCa had few significant findings, such as the identification of 8q24 as a significant PCa risk region [57, 58] and the identification of the missense G84E variant in *HOXB13* [59, 60]. SNPs have been found associated with aggressive disease [61] and lethal disease after radiotherapy [62]. Pathway-based analyses that examine GWAS loci have found genes assigned to risk loci are enriched in some pathways, for example the ERK-MAPK, WNT-β-catenin, p53 and ATM signalling pathways, G2-M DNA damage pathways and oestrogen-mediated S phase entry checkpoint regulation pathways [63, 64]. It has been shown that most of the GWAS-identified PCa variants are located in non-coding regions of the genome [65], which may modify transcriptional regulation. Identification of germline variants could facilitate the development of strategies for population-based risk stratification for PCa screening in men with an increased genetic risk of disease and, based on the genetic profile develop specific treatment strategies for PCa patients in early disease setting. However, the biological mechanisms underlying the susceptibility loci remain largely unknown [66].

1.1.7.2 Somatic alterations in PCa

Significant efforts have been made to characterise recurrent genomic alterations in PCa. Several large-scale genomic studies in both primary prostate tumours and mCRPC have identified recurrent DNA copy number changes, mutations, rearrangements, and gene fusions [67-71]. The most common alterations in PCa genomes are fusions of androgen-regulated promoters with ERG and other members of the ETS family of transcription factors. In particular, the fusion of 5′-UTR of TMPRSS2 (21q22) with 3′-end of ETS family member ERG (21q22) is the

most common molecular alteration [72, 73]. Significantly mutated genes include AR, SPOP, FOXA1, IDH1, TP53, MED12, and CDKN1B2 [68, 74]. In addition to somatic mutations, somatic copy number alterations are recurrently seen in PCa. In general, PCa exhibits more somatic copy number alterations than most of the other types of cancer [75]. Recurrent focal amplifications included known oncogenes such as CCND1, MYC, as well as FGFR1 and WHSC1L1 (8p11.23, 8%). Recurrent focal deletions were much more common, including homozygous deletions spanning the tumour suppressor PTEN, deletions of the region between the TMPRSS2 and ERG genes on 21q22.3 which result in TMPRSS2-ERG fusions, TP53, CDKN1B, MAP3K1, FANCD2, SPOPL, and the complex locus spanning FOXP1/RYBP/SHQ1 and MAP3K7 [68]. PTEN is one of the most frequently deleted tumour suppressor genes in PCa, leading to the activity of phosphoinositide 3-kinase-protein kinase B-mechanistic target of rapamycin (PI3K-Akt-mTOR) pathway. Monoallelic loss of PTEN is present in up to 60% of localised PCas [76]. In metastatic castration-resistant tumours, aberrations of AR, ETS genes, TP53 and PTEN are frequently (40-60% of cases) found, with TP53 and AR alterations enriched compared to primary tumour [68, 77, 78].

1.1.8 CRPC

CRPC, previously called hormone-refractory PCa or hormone-resistant PCa, is defined by disease progression despite normal testosterone level. The term change is based on the understanding that androgen axis still play important roles in CRPC [44]. The CRPC is usually suspected in patients with new symptoms on ADT. According to European Association of Urology (EAU) - European Society for Radiotherapy & Oncology (ESTRO) - International Society of Geriatric Oncology (SIOG) Guidelines on Prostate Cancer published in 2017(http://uroweb.org/guideline/prostate-cancer/), CRPC is diagnosed as patients with castrate serum testosterone < 50 ng/dL or 1.7 nmol/L with either, 1) Biochemical progression: Three consecutive rises in PSA one week apart resulting in two 50% increases over the nadir, and a PSA > 2 ng/mL or, 2) Radiological progression: The appearance of new lesion of either two or more new bone lesions on bone scan or a soft tissue lesion. CRPC is a late stage of disease with poor prognosis [45]. Most CRPCs are diagnosed with metastasis

and roughly one third of non-metastatic CRPCs with a rising PSA will develop bone metastases within two years [79]. Docetaxel is the standard first line chemotherapy for CRPC which significantly improved patients' survival compared to mitoxantrone [47, 80]. New systemic therapies, including the androgen biosynthesis inhibitor abiraterone acetate [48, 81], and the next-generation AR antagonist enzalutamide [49, 82] have demonstrated benefits in both before and post docetaxel settings and have been implemented in clinics. Other treatment options include Radium 223, and the immunotherapeutic sipuleucel-T [83] and the taxoid cabazitaxel [84].

Numerous mechanisms have been characterised in the development of CRPC. The majority of resistance mechanisms identified are AR or androgen axis-mediated [85]. In CRPC patients, low levels of androgen persist despite androgen blockade with ADT. Tumour cells could develop resistance either through amplification of the AR and overexpression of AR protein which causes AR hypersensitive to low level of androgen [86, 87], or development of AR mutations which could increase AR transactivation activity and decreased ligand specificity [88]. In recent years the role of AR splice variants in CRPC have been implicated. For example, AR-V7 has been found to be overexpressed in CRPC, localised in the nuclei and are constitutively active [89, 90]. Expression of AR-V7 has been associated with more advanced malignance and reduced survival in patients with mCRPC [90, 91]. Altered expression and function of AR co-regulators are also involved in CRPC development [92]. Synthesis of adrenal androgens and increased levels of intratumoural androgens is another mechanism that tumour cells sustain their growth with low circulating concentration of androgens [93]. Aberrant activation of other pathways such as PI3K-Akt-mTOR pathway, Src signalling pathway and growth factor pathways have also been identified in CRPC development [85]. Defects and mutations in DNA damage repair genes have been reported related to CRPC [77].

Identifying CRPC prognostic and treatment-response prediction markers have been intensively investigated. A number of factors such as PSA based testing results, performance status score, haemoglobin level, age, albumin, LDH or ALP levels, Gleason score, pain intensity and metastases characteristics, have been validated and included in nomograms, which help physicians to estimate patients'

survival [94, 95]. More recently, novel biomarkers from liquid biopsy have been extensively investigated. CTC enumeration has shown prognostic value [96-98]. Using CellSearch system, a cut-off of five CTCs per 7.5ml blood was set as favourable and unfavourable, correlating with good and poor CRPC prognosis respectively [96-98]. AR-V7 has not only showed functional role in CRPC, but also has emerged as a valuable marker in CRPC. In addition of detection in tissues, AR-V7 can be detected in CTCs, that expression of AR-V7 in CTCs is associated with poor response to abiraterone and enzalutamide [99], but has no predictive value for response to docetaxel or cabazitaxel [100-102]. Analyses of plasma exosomal miRNAs revealed that miR-1290 and miR-375 could be promising prognostic biomarkers for CRPC [103]. Other molecular prognostic and predictive biomarkers have also been identified, such RNA panel in whole blood [104, 105] and circulating cell-free DNA (cfDNA)[106].

Monitoring disease progression to CRPC has been relying on serum PSA levels along with serum testosterone measurements, and it is indeed effective in detecting mCRPC prior to clinical evidence of progression in most cases. However, disease progression may develop in men without rising PSA [25]. In addition, the serum level of PSA may be inconsistent to its tissue expression level during ADT, which challenged its use as a reliable surrogate for assessing tissue response to ADT [107]. Thus, there is a need for identifying new biomarkers for monitoring PCa progression. Studies of molecular mechanisms of CRPC development may reveal biomarkers for CRPC, while the detection methods of those molecular changes need further investigation for clinical use. CRPC prognostic and treatment-response predicting markers may also be evaluated as biomarkers for CRPC. For example, AR-V7 has been found functionally involved in CRPC development and its value as prognostic biomarker has been revealed [92, 99]. Further studies are needed to investigate its potential as a marker to monitor PCa progression to CRPC.

1.2 MicroRNA (miRNA)

1.2.1 MiRNA biogenesis

MiRNAs are short non-coding RNAs of ~22 nucleotides. The main process of mature miRNA biogenesis is characterised by several steps: transcription to primary miRNA (pri-miRNA), cropping to precursor miRNA (pre-miRNA), exporting to the cytoplasm and dicing to mature miRNA (Figure 4). The miRNA biogenesis begins with transcription by RNA polymerase II or RNA polymerase III [108], which results in a 5′ capped and 3′ polyadenylated large primary transcript known as pri-miRNA, containing a 33 bp hairpin stem, a terminal loop and a flanking single stranded sequence of hundreds of bases or even several kilobases [109]. The pri-miRNAs are then cleaved in the nucleus by a microprocessor complex, composed of RNA-binding protein DiGeorge syndrome critical region gene 8 (DGCR8) and type III RNase Drosha, into a small hairpin structure called precursor miRNA (pre-miRNA) [110, 111]. Then, pre-miRNAs are transported to the cytoplasm mediated by Exportin-5, a Ran-GTP-dependent double-strand RNA-binding protein, in a GTP dependent process [112, 113]. The pre-miRNA is processed in the cytoplasm by the RNAse III enzyme Dicer, producing a mature miRNA duplex of about 22 nucleotides [114]. During this process, Dicer is associated with other proteins like TAR RNA binding protein and protein kinase R-activating protein to increase its stability and its processing activity [115]. Following the Dicer cleavage, the miRNA double strands bind to the RNA-induced silencing complex (RISC) composed of TAR RNA binding protein, protein kinase R-activating protein and Argonaute 2 (Ago 2), where one strand of the miRNA duplex remains in Ago2 as a mature miRNA (the guide strand or miRNA), and the other strand (the passenger strand or miRNA*) is degraded [116]. The strand selection is often not a stringent process that miRNAs could be produced from both strands at comparable frequencies [117, 118].

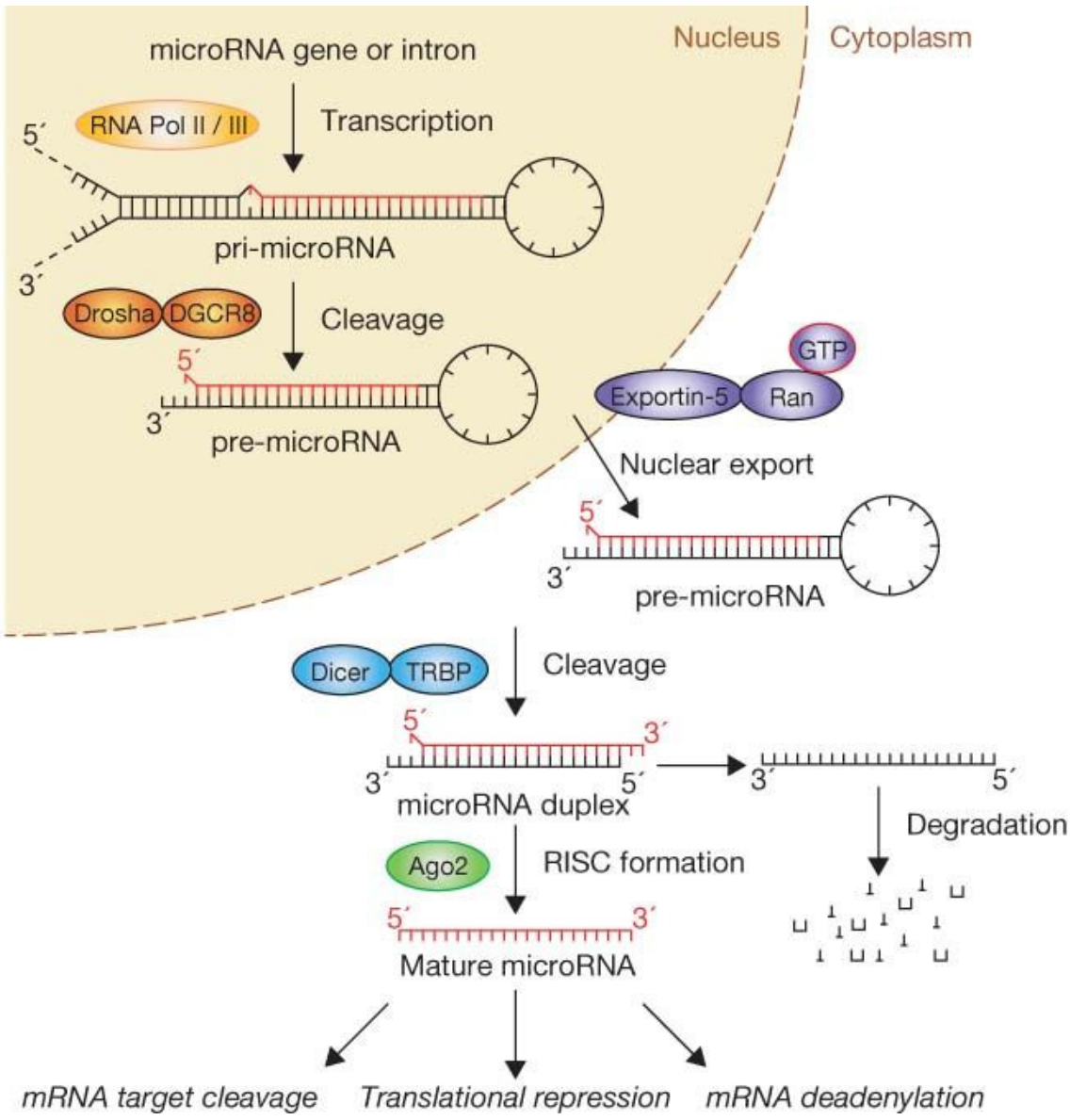

Figure 4. MiRNA biogenesis process in human. Adopted from [119].

MiRNAs typically direct the RISC to the target mRNAs through imperfect base pairing to their 3′ untranslated regions (3′UTR), leading to post-transcriptional repression through translation inhibition and mRNA destabilization [119, 120]. There is also evidence suggesting that some miRNAs could upregulate gene expression in specific cell types and conditions with distinct transcripts and proteins [121]. The miRNA-mRNA binding site is short (6-8 base pairs), and each miRNA has the potential to target multiple different mRNAs.

1.2.2 Deregulation of miRNAs in cancer

A number of miRNAs have been found up- or down-regulated in malignant tissues compared to the normal counterpart. They are considered as oncogenes or tumour-suppressors respectively. The earliest finding of a correlation between miRNA deregulation and cancer was reported by Croce and colleagues in 2002, revealing that the miR15a/16-1 cluster is frequently deleted in chronic lymphocytic leukemia [122]. After this, much work has been done identifying cancer-related miRNAs. Several studies showed that profiling of miRNA expression signatures could distinguish tumour from normal tissue and discriminate cancer tissue origin with high accuracy [123-125]. Recent years, large number of studies on miRNAs using microarrays, RT-qPCR and RNA-sequencing have provided more evidences that miRNA expression is dysregulated in cancer. The importance of miRNA alterations in cancer is further highlighted by functional studies in cancer cell lines and mouse models, revealing important roles of miRNAs in tumour initiation and progression. For example, it has been shown that miR-101 is down regulated in PCa and one or two of the genomic loci encoding miR-101 is lost in one-third of the localised PCa cells and in two-thirds of the metastatic cancer cells [126]. Overexpression of miR-101 could decrease PCa cell proliferation *in vitro* [127, 128]. MiR-101 expressing PCa cells also had decreased tumour growth in xenograft mouse models [128]. Studies also revealed the mechanisms underlying miRNA deregulation in cancer, which include chromosomal abnormalities, transcriptional control changes, epigenetic changes and defects in the miRNA biogenesis machinery [129].

1.2.3 MiRNAs as biomarkers

Due to the fact that miRNAs play vital roles in cancers and they are relatively stable, miRNAs have been an attractive source of biomarkers. It has been shown that miRNAs can be isolated and quantitated from fresh tissue samples, fresh-frozen specimens and formalin-fixed paraffin-embedded specimens [130-132]. MiRNA *in situ* hybridisation technology has been developed, which enables *in situ* detection of specific miRNAs in tissue samples [133-135]. MiRNAs in biofluids, for example blood and urine, have been particularly intensively studied

for biomarker value, as they are easy to access and be evaluated in a real-time manner.

For PCa research, massive studies have been done looking for miRNAs as biomarkers for PCa diagnosis, prognosis, disease progression and treatment response. The expression of aberrant miRNAs has been demonstrated in PCa using different materials and methods by multiple groups. However, each study identifies distinct miRNAs panels and some inconsistent outcomes regarding the miRNAs expression profile were raised, with only a few miRNAs presenting consistent effects [136]. MiR-21 is one of the oncomiRs that has been found overexpressed in multiple cancer types [137]. Several studies showed consistent results that miR-21 is up-regulated in PCa patients' tissue [133, 138, 139], serum/plasma [138, 140] and urine [141, 142]. Plasma/serum level of miR-21 has been found related to metastatic disease [143]. MiR-375 is another highlighted miRNA in PCa. It has been reported up-regulated in PCa patients' tissue [139, 144, 145], serum/plasma [138, 140, 146] and urine [144, 147], making it a good candidate of biomarker for PCa diagnosis. It has also been reported that miR-375 is correlated with high risk PCa (N1 or GS 8) and metastatic disease [145]. Exosomal miR-375 is also identified as a prognostic marker together with miR-1290 in CRPC [103]. Dysregulation of miR-141 is also frequently found up-regulated in PCa [138, 139, 146, 148, 149] and it is correlated with bone metastases[150]. A recent meta-analyses study on 104 studies published in between 2007 and 2017 showed miRNAs had great diagnostic and predictive potential to discriminate PCa from BPH/normal controls, to differentiate metastatic PC from local/primary PCa, and predict recurrence-free survival and OS of PCa [151]. However, inconsistent data for certain miRNAs from different sample resources were found. For example, the expression of miR-100 was increased in the patients' urine samples, which was contrary to its expression in cancer tissues [151]. The authors also pointed out that data for each single miRNA was limited which resulted in poor statistical significance [151]. The application value of miRNAs as biomarkers should be further investigated.

1.3 Exosomes

1.3.1 Biogenesis of exosomes

Exosomes are a type of small extracellular vesicle (EV) measuring around 30-150 nm that present in almost all body fluids. The process of exosome release was first visualized in rat reticulocytes in 1983 [152], and then in sheep reticulocytes in 1985 [153]. Rose M. Johnstone used the term “exosome” to name these membrane-bound vesicles in 1987 [154]. Early in 1983 when Hardings, *et al.* described the existence of these vesicles, they found that the vesicles were released from multivesicular endosomes (or “multivesicular bodies” (MVBs)) through exocytosis [152]. Further insight into this process has found that exosomes have unique biogenesis and release mechanisms different from that of microvesicles (MVs), which are generated from plasma membrane outbudding. The release of exosomes involves more complex cellular steps including formation of intraluminal vesicles in MVBs, transport of MVBs to the plasma membrane and fusion of MVBs with the plasma membrane [155]. Exosome biogenesis starts within the endosomal system. Early endosomes are formed from endocytosis processes and then undergo maturation, forming the late endosome or MVBs. During this process, early endosomes can communicate with the Golgi apparatus and the endoplasmic reticulum through bidirectional vesicle exchange. Inward budding of the membrane forms the intraluminal vesicles that will be released to the extracellular space as exosomes, or will fuse with lysosomes where an active degradation process will take place [156, 157]. MVBs then fuse with the plasma membrane and release exosomes (Figure 5) [157].

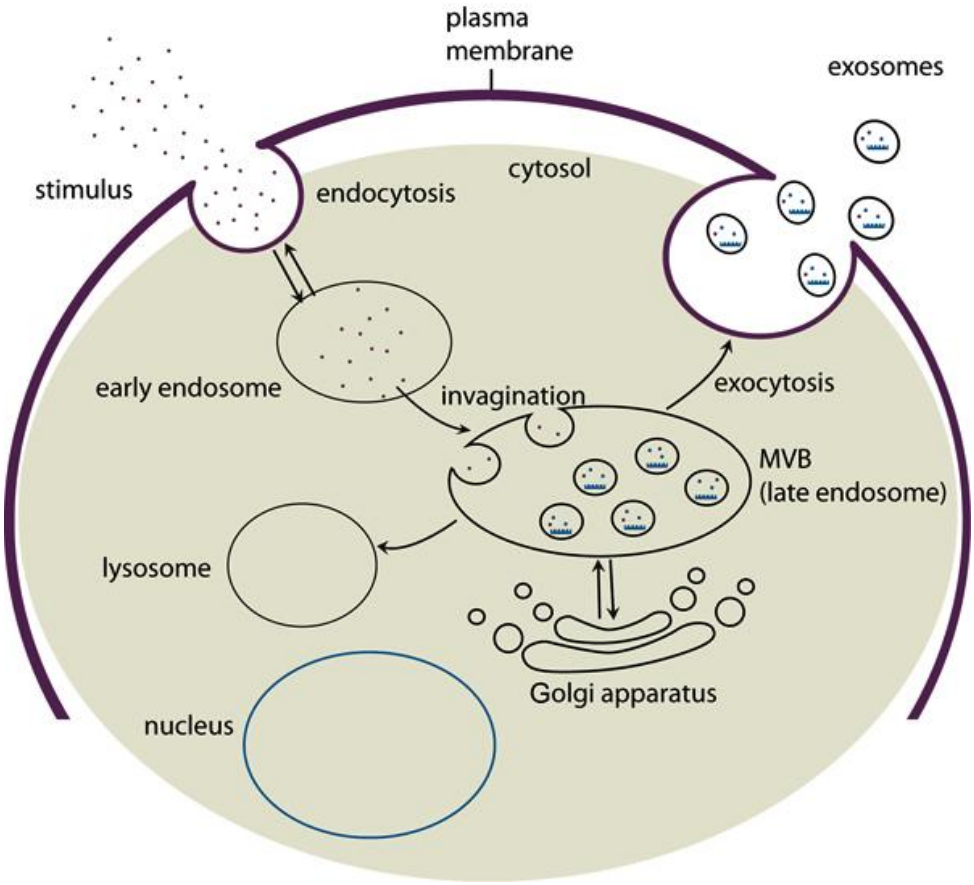

Figure 5. Exosome biogenesis and release process. (Adopted from Borges, F. T., 2013 [51])

1.3.2 Exosome cargos

Exosomes contain varies of proteins, lipids, RNAs and even DNAs. The contents of exosomes from different donor cells can have big difference. In fact, exosomes from single cell line present heterogeneous subpopulations carrying different cargos [158, 159].

Exosomes have been found enriched with tetraspanins (e.g. CD9 and CD63) [160] and proteins associated with endosomal sorting complexes required for transport machinery (e.g. TSG101 and ALIX) [161, 162]. These proteins are frequently used as markers for exosomes. Despite the fact that exosomes have some general protein families, vast diversity and variation still exists between exosomes from different donor cells and cells cultured under different conditions. The exosomal expression of known proteins in exosome have been massively evaluated by western-blotting (WB), ELISA and fluorescence-activated cell

sorting analysis [163]. In addition, a number of proteomics studies have been performed in exosomes isolated from different materials and have demonstrated the diversity of exosomal proteins and the specific protein expression under different conditions [164-166].

In terms of lipids, studies have analysed the composition of exosomal lipids and delivered general information that exosomes bear different lipid composition compared to the parental cells and exosomes from different cells in culture have different profiles [167, 168]. In general, exosomes are enriched in sphingolipids, CHOL, and PS compared with the donor cells. The lipid composition of exosomes shows similarities with lipid rafts, and exosomes have a higher lipid order and a higher stability against detergents than other EVs [169]. However, the lipid composition of exosomes in biofluids is poorly characterized and only limited data has been reported [170].

Several DNA species in exosomes/MVs have been identified including single strand DNA [171], mitochondrial DNA [172] and double strand DNA [173, 174]. These discoveries are exciting, however, the mechanism of DNA sorting into exosomes and the biological significance of exosomal DNA remain largely unknown.

RNA is one of the most-well studied contents in exosome. Large number of miRNAs and mRNAs have been detected in exosomes and other RNA types including ribosomal RNA (rRNA), long non-coding RNA, piwi-interacting RNA, transfer RNA, small nuclear RNA, and small nucleolar RNA have also been identified in exosomes [175-177]. Exosomes isolated from different biomaterial could have different RNA species representation. For example, it has been reported that exosomes from plasma contains more miRNA, while urine exosomes contained more rRNA[178]. Expression levels of RNAs in exosomes can also be different from those in the origin cells [179].

1.3.3 Exosome isolation and detection

The most commonly used isolation method for exosomes is ultra-centrifugation. Other methods include ultrafiltration and size-exclusion chromatography, antibody-based capture, polymer-based precipitation and microfluidics. Each

method has its advantages and limitations. Ultra-centrifugation is widely used to prepare fractionate exosomes for down-stream analysis. It is easy to use, requires very little technical expertise, and is able to process large volume samples (e.g. cell culture media) with little or no sample pre-treatment. There are two types of ultracentrifugation: differential ultracentrifugation and density gradient ultracentrifugation. Differential ultracentrifugation consists of a series of centrifugation cycles from low speed to high speed to separate exosomes from other components based on the size and density. Density gradient ultracentrifugation uses a density gradient medium to enrich exosomes in a certain range of medium from other solutes into a discrete zone exclusively depends on their density difference from those of other solutes [180, 181].

Ultrafiltration and size-exclusion chromatography isolate exosomes mainly base on size difference. Size-based isolation methods are capable of enriching exosomes with good purity and have good reproducibility, however, contamination of other nanoparticles (some non-vesicular) with the similar size as exosomes may occur. Size-exclusion chromatography needs dedicated equipment and its long run time limits its scalability for high throughput applications [180].

Antibody-based isolation and detection of exosomes relies on the specifically expressed proteins and receptors in the membrane of exosomes. CD9 and CD63 are commonly used as markers for exosome capture and using specific proteins enables selective capturing of exosomes of a specific origin or some subpopulations of exosomes. For example, isolation and analysis of glypican-1^{+} exosomes using flow cytometry in pancreatic cancer patients was found as a specific and sensitive method to distinguish healthy subjects and patients with a benign pancreatic disease from patients with early- and late-stage pancreatic cancer [182]. Prostate-specific membrane antigen (PSMA) was used as a tag for PCa exosome isolation [183, 184]. However, because of the heterogeneity of exosomes and cancer, only a subset of exosomes, expressing the antibody-recognised proteins, can be captured, potentially leading to low yield and false negative results. In addition, other biological material expressing the protein can also be captured.

Precipitation is another commonly used and efficient method for exosome isolation. Currently, several exosome precipitation kits are commercially available which utilise a decrease in the solubility of compounds in the solutions by a superhydrophilic polymer, polyethylene glycol [185, 186]. Mixing the sample with the precipitation reagent diminishing the hydration of the exosomes, which allows exosomes being pelleted via low-speed centrifugation. Exosome precipitation methods are attractive for clinical research as they are simple, time-saving and do not require special equipment, therefore enable processing of large number of samples. Other precipitation strategies were also proposed [187, 188], but haven't been broadly used.

Microfluidic devices have been developed in recent years to facilitate exosome isolation from various biological materials. Microfluidic devices employ a wide range of exosome isolation approaches, such as immunoaffinity, membrane-based filtration, trapping on nanowires, acoustic nanofiltration, and deterministic lateral displacement sorting. Integrated systems have been developed to perform downstream analysis of exosomes. Microfluidic technologies are fast developing and bear great potential for exosome isolation in clinical use [189, 190].

1.3.4 Exosome function

When exosomes were firstly characterised, they were reported as a means of cells to extrude unwanted membrane proteins [152]. With the improvement of isolation methods, more research has been conducted on exosomes and has revealed distinct biological functions of exosomes secreted by different cell types. As exosomes carry biologically active molecules including RNAs, lipids, and proteins and can transport between donor cells to recipient cells, they are believed to function as a novel mechanism for intercellular communication. Studies have demonstrated that exosomes play a significant role in various pathological conditions, such as different types of cancer [191], infectious diseases [192], metabolic diseases [193] and pregnancy [194].

Exosomes have been described as important mediators in cancer development, progression, metastasis and therapy response [195]. Many studies have reported the role of exosomes in influencing cancer cell proliferation and migration by

transferring specific cargos into the recipient cells [196-199]. The formation of pre-metastatic niches is one of the major events in cancer metastasis, which provides suitable environment for tumour cells to colonise in a distant site. Tumour-derived exosomes could prepare the pre-metastatic niche through a number of mechanisms such as inducing vascular leakiness and pro-inflammatory, reprograming metabolism, and remodelling extracellular matrix [200-203]. In turn, cells in the microenvironment could influence tumour cells via exosomes. For example, it is shown that tumour cells with normal expression of PTEN, an important tumour suppressor, could lose PTEN expression after dissemination to the brain, but not to other organs. This is regulated by astrocyte-derived exosomes which mediated an intercellular transfer of PTEN-targeting miRNAs [204].

Tumour-derived exosomes are found to be involved in immune response. It is reported that tumour exosomes could promote regulatory T cell expansion and induce the apoptosis of activated T cells, thus supress immune response facilitate immune-escape of tumour cells [205, 206]. It is found that exosomes secreted from tumour cells carry PD-L1 that could inhibit T cells function [207, 208]. Prostate-cancer-derived exosomes were found to be immunosuppressive by regulating dendritic cell function [209]. In addition, it is found that poorly metastatic melanoma cells can secret exosomes which stimulate an innate immune response, which then cause cancer cell clearance at the pre-metastatic niche [210].

1.3.5 Clinical applications of exosomes in cancer

1.3.5.1 Exosomes as biomarker

Exosomes are present in varies body fluids and stably carry different types of cellular cargos, making them a good candidate for non-invasive biomarkers. Many studies have demonstrated that exosomes hold potential as diagnostic, prognostic, and pharmacodynamic biomarkers in several cancer types, including breast cancer [211-213], PCa [214-216], lung cancer [217-219], colon cancer [220, 221], and pancreatic cancer [182, 222, 223].

Bryant *et al.* reported their study on circulating miRNAs in PCa. They identified miR-375 and miR-141 in plasma MVs and serum MVs and exosomes, which are correlated with metastatic disease, although MV miRNAs did not present better diagnostic value than PSA, nor increased diagnostic value of PSA when combined together [146]. Recently, McKiernan *et al.* developed a non-invasive detection test, ExoDx Prostate (IntelliScore) urine exosome assay, which has been approved by FDA for the detection of high-grade PCa. The assay which evaluates the expression level of three genes, PCA3, ERG (including TMPRSS2: ERG) and SPDEF (as normaliser) in urine exosomes and construct a score (ExoDx Prostate IntelliScore), which in combination with standard clinical parameters (PSA level, age, race, and family history), could discriminate high-grade PCa (Gleason score ≥7) from low-grade cancers and benign diseases [214, 224]. Huang *et al.* identified two miRNAs in plasma exosomes (miR-1290 and miR-375) as prognostic markers in castration-resistant PCa by RNA-sequencing and quantitative real-time polymerase chain reaction (RT-qPCR) [103]. Del Re *et al.* reported a method of using digital droplet PCR to detect AR-V7 in plasma exosomes. Their results showed that exosomal AR-V7 can be a predictive biomarker of resistance to second-line hormonal therapy in CRPC patients [225].

1.3.5.2 Exosomes as drug delivery tools

Recent years, there has been intense interest in exploiting exosomes as a tool for drug delivery. Exosomes have some ideal characteristics, such as stability in blood and can travel long distance, intrinsic ability to target tissues, good biocompatibility, and minimal or no inherent toxicity [226]. Therefore, exosomes emerge as ideal vehicles which can be isolated and modified for drug or gene delivery. To date, several studies have reported that administration of exosomes can potentially serve as therapeutic strategies. Kim *et al.* engineered macrophage exosomes loaded with paclitaxel to target pulmonary metastases and have good antineoplastic effect in a mouse model [227]. Kalimuthu *et al.* have demonstrated that paclitaxel-loaded mesenchymal stem cell exosomes could inhibit breast cancer growth *in vitro* and *in vivo* [228]. Ohno *et al.* reported that intravenously injected engineered exosomes could deliver miRNA to EGFR-expressing breast cancer tissue xenograft in RAG2$^{-/-}$ mice and supress tumour

growth [229]. Kamerkar *et al.* reported the study of using engineered exosomes from normal fibroblast-like mesenchymal cells carrying short interfering RNA or short hairpin RNA specific to oncogenic Kras mutation as therapy for pancreatic cancer [230, 231]. They showed that engineered exosomes could suppress cancer in multiple mouse models of pancreatic cancer and significantly increased OS [230, 231], revealing the clinical value of exosome-based therapies.

1.3.5.3 Exosomes as cancer vaccine and immunotherapy

The findings that exosomes are involved in modulating immune system illustrate the potential of exosomes as a cancer vaccine. Early in 1998, Zitvogel *et al.* reported that dendritic cell-derived exosomes (Dex) could present tumour-associated antigens and induce T-cell activation, resulting in the suppression of tumour growth *in vivo* [232]. Since then, Dex have received much attention as immunotherapeutic anticancer agents which can induce immune cell-dependent tumour rejection. Dex have been developed for use as cell-free cancer vaccines and put into clinical trials for melanoma [233] and lung cancer [234]. These two studies confirmed the safety of Dex administration in patients, however showed limited Dex-induced T cell responses. Later studies found that exosomes from matured dendritic cells can induce greater T cell stimulation [235-237], which led to second generation of Dex immunotherapies. However, a phase II trial in lung cancer patients after chemotherapy cessation using a second generation Dex as maintenance immunotherapy failed to detect T-cell response [238]. The patients showed good tolerance, which encourages further investigation of Dex immunotherapies to increase its efficiency.

1.4 Circulating tumour cells (CTCs)

Part of this section has been published[239].

1.4.1 Origin

Tumour cells can escape the primary tumour site (involving invasion and intravasation) and disseminated to distant sites (involving extravasation to distal tissues). The tumour cells which enter the bloodstream are referred to as

circulating tumour cells (CTCs). CTCs are a rare population of cell in the circulation blood at a ratio of one CTC to 10^6-10^7 nucleated blood cells. CTCs have long been considered as a substrate for cancer metastasis. Metastasis involves several main steps, starting with intravasation from the primary site which may be an active process supported by epithelial-to-mesenchymal transition (EMT). The CTCs then circulate in the blood stream as single cells or clusters. Then CTCs may extravasate to a new location, where CTCs may form a new metastasis site, and this extravasation is possibly supported by mesenchymal-to-epithelial transition (MET) [240, 241]. CTCs have been proposed as a main representative of “liquid biopsy” which may be used as biomarkers and provide a minimally invasive approach to the tumour tissue [242].

1.4.2 Isolation methods

CTCs were firstly described in 1869. However, the rarity of CTCs has largely hindered the research of them. Only in the past decades, owing to the development of technologies, researchers have achieved reasonable efficacy of enrichment of CTCs [243]. Current existing techniques of CTC isolation can be roughly divided into three types: antibody-based approaches, physical property-based approaches and function-based approaches [244].

Cell surface proteins are often used as targets in antibody-based CTC isolation methods. Due to the absence of strictly tumour-specific antigens, epithelial-specific proteins such as EpCAM and cytokeratins (CKs) have been employed for the positive selection of CTCs and antibodies against leukocyte-specific surface antigens, such as CD45, have been used to deplete leukocytes from the blood sample for negative selection [245]. Immune-magnetic separation [246, 247], flow cytometry [248], and immuno-affinity based microfluidic platforms have also been developed and employed to enrich CTCs. The representative platform of immune-magnetic separation CTC isolation is CellSearch, which is the first and the only CTC enumeration system cleared by FDA in clinic use for metastatic breast cancer, colorectal cancer and PCa [98, 249, 250]. A number of immune-affinity base CTC isolation platforms have been reported, for example, CTC-chip [251] and CTC-iChip [252, 253]. The overt drawback of positive selection is missing of heterogeneous CTCs, such as losing EMT cells when only epithelial

markers are used. Another strategy is negative selection, which depletes leukocytes, may circumvent the problem of losing some subtypes of CTCs. There are several commercially available products for negative selection. RosetteSep® antibody cocktail, which crosslinks unwanted cells in human whole blood to multiple red blood cells forming immunorosettes, has been used to enrich viable CTCs [247, 254]. However a negative selection will cause heavy leukocytes contamination, thus usually accompanied by further purification process or used for CTC culture where leukocytes can be eliminated during culture.

Physical property-based techniques take a large part in CTC isolation. “Ficoll,” a synthetic low-viscosity, high-molecular-weight hydrophilic sucrose, and epichlorohydrine polymer and sodium diatrizoate, has been extensively used for depleting red blood cells through density gradient centrifugation [255]. It is often used before further purification steps to deplete lymphocytes. Recently, a large number of size-based devices have been developed for CTC isolation, for example membrane capture of CTCs [256-260] and microfluidic devices [261-263]. They were designed based on the principle that tumour cells present different physical properties compared to blood cells, in size, deformability, density and electric properties [262, 264-267]. Physical property-based techniques are also facing the challenge of isolating heterogeneous tumour cells. For instance, although tumour cells are believed to be larger in size than blood cells, it cannot be guaranteed that all CTCs are bigger compared to blood cells and actually small CTCs have been identified [268, 269].

A unique strategy to enrich CTCs is taking the advantage of CTCs’ invasion ability. A method, which is based on tumour cells’ ability to attach and digest collagen adhesion matrix, has been described as collagen adhesion matrix (CAM) assay [270]. To enrich tumour cells, blood samples were simply transferred into a CAM-coated tube and incubated for several hours. Unattached cells were then washed off and adherent cells were collected [270, 271]. Similarly, Wang *et al.* developed an invasion assay to detect CTCs which could invade into Matrigel [272]. These methods enable enrichment of viable CTCs which are invasive. However, the captured CTCs cannot represent the whole population of CTCs in blood as apoptotic CTCs or fragmented CTCs are frequently found in the peripheral blood of patients with cancer [273].

1.4.3 Clinical applications of CTCs

The clinical value of CTCs has been revealed in many aspects. The prognostic value of CTC enumeration has been demonstrated in many cancer types [249, 274, 275]. Detection of CTCs has been associated with an increased risk of local and regional recurrence as well as the development of distant metastases [276]. In CRPC, enumeration of CTCs has been demonstrated as an independent predictor of OS in several cohorts [96, 97, 277-279]. It has been demonstrated that CTC counts hold independent prognostic value for OS similar to clinical and radiologic response in CRPC patients receiving docetaxel [278].

CTCs may also provide genetic information that can be used for cancer diagnosis and prognosis. Using high-quality whole-genome sequencing on single CTCs from a PCa patient, Jiang *et al.* identified shared genomic alterations between CTCs and tumour tissue [280]. Comprehensive sequencing and confident determination of genomic variants in CTCs could help understanding the heterogeneous between patients and monitoring the transiting status within single patient, thus facilitate targeted therapy [281].

Moreover, gene expression levels in CTCs has also been exploited as potential biomarkers for cancer diagnosis and prognosis [282-284]. AR-V7 in CTCs from CRPC patients was recently demonstrated to be associated with resistance to abiraterone and enzalutamide, but not taxanes [100]. Some markers for chemotherapy response have been demonstrated using cell lines or tumour tissue [285], but very few data has been published regarding detection of these markers in CTCs [286]. Some studies have also employed RNA-sequencing in CTCs to investigate the gene expression changes in primary, metastatic, and recurrent cancer non-invasively [287-289]. However, CTC sequencing still faces technical challenges for example different CTC isolation methods may affect CTC population, limited material could be obtained from CTCs for library preparation, and bioinformatics analysis could introduces bias [290].

1.4.4 CTC culture

Expanding CTCs bears great potential of providing material for functional study and establishing patient-specific tumour models for individualised therapeutic prediction. In the past decades, many research teams have attempted to establish CTC cultures. Although some achievements have been made, CTC culture remains challenging, especially for long-term culture.

1.4.4.1 Short-term culture

Some techniques have been developed for short-term *in vitro* culture of CTCs. An *in-situ* capture and culture methodology using MetaCell®, which is a size-based enrichment process is based on the filtration of peripheral blood through a porous polycarbonate membrane (pores with 8 μm diameter), has been used for CTC capture and short-term culture in non-small-cell lung cancer (NSCLC) [291], PCa [257, 292], pancreatic cancer [260] and gastric cancer patients [293]. In these studies, CTCs could be maintained on the membrane for over two weeks with some cells escaped the membrane. Some biological tests could be done in the cultured cells, characterising specific gene expression that are tumour-related [257, 291-293]. In 2015, Khoo *et al.* proposed a method which cultured breast CTCs in laser-ablated microwells under hypoxia condition after red blood cell lysis and indicated that the CTC cluster formation ability may predict treatment response [294]. Cells could form clusters in the microwells and could be maintained for over two weeks. In addition, several passages of the cultured clusters were achieved when cultured in Geltrex® or ultra-low adhesive dishes. It is also found that the cell cluster formation was not always correlated, indicating that the CTC enumeration methods may lead to an underestimation of a heterogeneous population of CTCs [294]. The authors reported that the method could enable establishment of clusters from >50% of clinical blood samples screened [295], which is promising for CTC culture. Recently, collecting mononuclear cells from apheresis and then isolating of CTCs has enabled enrichment of CTCs from large volume of blood that largely increased CTC yield [296, 297]. Maryou *et al.* reported that CTCs enriched from apheresis could form spheroids and could be cultured over 4-6 weeks [297]. However, this is a single case report that success rate is unknown. Short-term culture of CTCs bears the

advantages of short turn-over time for providing information and may potentially better representative of the original tumour with less passage and selection procedures compared to long-term culture. However, short-term culture also has limitations that limited material can be obtained from short-term culture with only a few analyses can be performed.

1.4.4.2 Long-term culture

Long-term culture of CTCs is more difficult with limited success cases reported. In 2013, Zhang et al. established CTC cell lines from three brain metastatic breast cancer patients [298]. Interestingly, in this study, only $EpCAM^-$ population survived over 14 days and be established to cell lines, but $EpCAM^+$ would die out during culture [298]. The $EpCAM^-/HER2^+/EGFR^+/HPSE^+/Notch1^+$ CTC lines were highly invasive and capable of generating brain and lung metastases when xenografted in nude mice, indicating the significance of $EpCAM^-$ CTCs in forming tumour metastasis [298]. In 2014, Yu *et al.* reported their success of developing CTC cell lines from six luminal subtype breast cancer patients, with 20% success rate [299]. Genome sequencing of the CTC lines revealed the same mutation status in the PIK3CA gene between CTC lines and primary tumours. Drug sensitivity screening on these cell lines showed that certain drug sensitivity features of the CTC cell lines were concordant with clinical response and revealed potential new therapeutic targets [299]. Although the success rate is low, this results is encouraging for CTC culture. One colon cancer CTC-derived cell line has been established [300]. For PCa, Gao *et al.* has reported success in long-term culture of CTCs from one mCRPC patient using organoid culture medium [246]. The *in vitro* expanded CTCs bear the potential to form xenograft when grafted to nude mice and some can form distant metastases, indicating the tumourigenic and metastatic ability of expanded CTCs. Both the CTC-derived organoid and xenograft histologically resembled the primary tumour [246]. In this study, 67% of point mutations found in the CTC-derived organoid line were identified in the lymph node metastasis of the same patient [246]. The additional mutations may be acquired during the cell culture. Directly injecting enriched CTCs into mice and generating CTC-derived xenografts is another strategy to establish CTC-derived tumour model. Dive's group reported their success in

generating CTC-derived xenografts of lung cancer [247, 254] and they later cultured the xenograft cells *in vitro* [301]. Rossi *et al.* also used a xenograft assay by injecting isolated $EpCAM^+$ CTCs from PCa patients into immunodeficient mice. Eight CTC xenografts were derived from 7 consecutive patients. However, after a median follow-up of 10.3 months (range 6.5-12 months) none of the CTC-injected mice developed clinical evidence of tumour, neither at the injection, nor at secondary sites, with only human CK^+ cells detected in the murine blood, bone marrow and spleen [302]. Bacelli *et al.* developed a CTC xenograft assay in a large set of luminal breast cancer patients by injecting CTCs to the femurs of NOD mice and showed that the luminal breast cancer CTCs bear the ability to form bone, lung and liver metastases in mice. However, only six recipient mice receiving at least 1,109 CellSearch-evaluated CTCs developed multiple bone, lung and liver metastases within 6-12 months after transplantation of CTCs from three patients, while injection of less than 1,000 CellSearch-evaluated CTCs from 106 samples did not lead to metastatic growth of human tumour cells within 15 months after transplantation [303]. Thus, studies on the CTC-derived xenograft models have revealed the potential of employing cultured CTCs as tractable platforms to study cancer biology, identify pharmacodynamic biomarkers and perform drug response tests for individualized medicine. However, the success rate remains low and high CTC number is important for developing xenografts.

1.5 Other liquid biopsy

Liquid biopsy is developed to detect informative tumour-associated components from various body fluids. Compared to conventional surgical biopsy, liquid biopsy holds several major advantages. Liquid biopsy provides an opportunity to obtain tumour-specific information with minimally invasive procedures and could be tested at successive time points providing real-time information on disease status. Tumours have been acknowledged with dynamic intra-tumour heterogeneity with presence of subpopulations of cells with distinct genotypes and phenotypes within a primary tumour and its metastases [304]. Liquid biopsy may better reflect the dynamic genetic profile of all tumour subclones present in a patient, unlike tissue biopsies which are obtained from only one tumour region at one fixed time [305, 306]. In addition to blood which has been the main source

of material for liquid biopsy, other body fluids have also been used, for example urine and salivary fluid [305, 307, 308]. Different circulating molecules have been exploited as materials for liquid biopsy. Beyond exosomes and CTCs which have been introduced in earlier chapters, there are other circulating molecules, such as cell-free nucleic acids and tumour-educated platelets (TEPs), which have been shown to contain tumour-derived genetic material.

CfDNA presents in the blood at very low concentration, mainly containing germline DNA from normal cells and a minority of a highly variable fraction of DNA from cancer cells, namely circulating tumour DNA (ctDNA). CfDNA has been massively investigated in recent decades owing to the technological advances in qPCR and next-generation sequencing. Analysis of ctDNA mainly focus on detection of gene mutations, structural chromosome rearrangements and somatic copy number variations, while some studies targeted on the ctDNA methylation patterns [309, 310]. The utility of ctDNA have been implicated at different stages of the management of patients with cancer, including diagnosis[311-313], prognosis [314-316], detection of residual disease[317-319] and treatment decision[315, 320, 321]. The US FDA has approved qPCR-based ctDNA test for mutated EGFR in patients with NSCLC target guild targeted therapy [322] and DNA methylation-based test of SEPT9 for the detection of colorectal cancer [323]. Large trials leading by one company, GRAIL, are currently ongoing aiming to develop blood tests of ctDNA for early cancer detection [313]. However, current released data showed the clinical use of ctDNA is still limited by low sensitivity and specificity, especially for asymptomatic tumour detection [324]. Combination of detection of cfDNA and other molecules may help to improve the sensitivity and specificity of the test for biomarker. A blood test, namely CancerSEEK, has been recently developed to detect eight common cancer types including ovary, liver, stomach, pancreas, esophagus, colorectum, lung, or breast through assessment of the levels of circulating proteins and mutations in cfDNA [325]. Evidence has showed that a large proportion of human blood plasma cfDNA is carried in extracellular vesicles [326, 327]. Thus enrichment of extracellular vesicles may help improve the sensitivity of cfDNA detection.

Circulating RNAs is another key member of liquid biopsy. Several studies have selectively evaluated some mRNAs and showed their potential as biomarkers [328]. Most studies were focused on analysing miRNA due to the stability issues of mRNA. A large proportion of cell-free RNA data came from analysis of EV RNAs [329], as EV could protect RNAs from degradation. However, it is indicated that EV-incorporated miRNAs and cell-free miRNAs in whole plasma may provide different information [140]. More studies are needed to explore the utility of circulating RNAs as biomarkers which may trigger new circulating biomarker discovery and functional implication for cancer biology.

TEPs have been exploited as an important source of circulating biomarker given the well-known interaction between blood platelets and tumour cells which could have an effect on the tumour-resident cancer cells as well as the cancer cells that have disseminated to the bloodstream [330-332]. TEPs are a fundamental component of the tumour microenvironment and they contribute to tumour initiation, progression, and therapy response [333]. Most recently, exciting findings were reported using thromboSeq, an RNA-sequencing-based methodology that enables identification of spliced RNA profiles from TEPs RNA combined with sophisticated machine learning-based classification algorithms, to discriminate patients with localised and metastasised cancer from healthy individuals [334]. This method also allowed to pinpoint the organ-of-origin of the primary tumour [334]. A follow-up study in large cohorts of NSCLC patients showed that TEPs spliced RNA panel could serve as robust biomarker for cancer detection [335]. Other studies also demonstrated the potential of evaluating TEPs RNA expression for cancer diagnosis and prognosis [336-338]. Although TEPs RNA has shown great value as biomarker, the study of TEPs RNA is still at an early stage that warrant validation in large scale cohorts with standardised blood storage conditions and processing protocol. In addition, further studies on other molecules in TEPs, for example, miRNAs and proteins, are needed.

1.6 Aims

The main aim of my PhD project is to explore the value of two main circulating subjects in peripheral blood, exosomes and CTCs, in monitoring PCa progression and predicting treatment response.

Exosomes will be isolated from the plasma of PCa patients and RNA will be extracted from the plasma exosomes. To identify plasma exosomal miRNAs associated with PCa castration-resistant acquisition, next-generation sequencing of exosomal RNA will be performed in treatment-naive PCa patients and CRPC patients. The differentially expressed miRNAs will be evaluated in more samples to validate the differential expression and explore the prediction value of exosomal miRNAs for CRPC. Some of the differentially expressed miRNAs will be selected based on literatures for further studies *in vitro* to understand the role of the miRNAs in CRPC development. The aim is to utilise exosomal miRNAs as a tool to monitor PCa progression to CRPC and potentially reveal new mechanism of CRPC development.

Our lab has previously developed CTC enumeration method and demonstrated the value of enumeration of CTCs as biomarker for PCa metastasis and prognosis [339]. Ongoing projects are aiming at exploring CTC enumeration as biomarker for PCa treatment response. Long-term culture of CTC isolated from the peripheral blood bears great potential to provide us patient-specific platforms to identify the most efficient treatment modality. For PCa, there are only few reports with limited cases on the successful *in vitro* culture of CTCs. Thus, I plan to assess different methods of isolating viable CTCs from prostate patients and optimise CTC *in vitro* culture methods. Investigations will be carried out using PCa cell lines first and optimised methods will be applied to clinical samples.

Chapter II Materials and methods

2.1 Cell lines

Five PCa cell lines, 22Rv1, PC3, DU145, LNCaP and VCaP were used in this project. Mouse embryonic fibroblasts, STO cells were also used as feeder cells for CTC culture. STO cells were sent for x-ray irradiation to inhibit proliferation before used as feeder cell.

Frozen cell stocks were stored in liquid nitrogen in Dulbecco's MEM (DMEM)(Gibco, Life Technologies, USA) or RPMI-1640 (Gibco, Life Technologies, USA) with 10% of DMSO and 20% of Foetal Calf Serum (FCS, Gibco, Life Technologies, USA). To recover cells from frozen stocks, cells were thawed at 37℃ water bath and the cell suspension was diluted in 5 ml of pre-warmed culture media (DMEM or RPMI-1640 supplemented with 10% FCS and 1% penicillin/streptomycin). The cells were then pelleted by centrifugation at 1200 rpm for 5 min and resuspended in culture medium. Cells were then maintained in a controlled standard condition (37°C and 5% CO_2) and passaged when reaching ~80% confluence. To passage cells, the old medium was taken out and cells were washed with phosphate buffered saline (PBS). Trypsin-EDTA solution (Sigma, UK) was added to detach the cells and then quenched by the addition of equal volume of culture media.

2.2 Patient samples

From St Bartholomew's Hospital, Barts Health NHS, London, UK, blood samples from 291 patients were collected with informed consents. Use of patient blood samples and clinical data in this study was approved by the London City & East Research Ethics Committee with a Research Ethics Committee reference of 09/H0704/4+5. From Department of Pathology and Cancer Centre, Medical College of Wisconsin (MCW), US, blood samples from 60 patients were collected by Dr. Manish Kohli, Dr. Jing jia and Professor Liang Wang with informed patients'

consents. Use of patients' blood samples and clinical data there was approved Institutional Review Board of Medical College of Wisconsin (PRO00017780).

2.3 Exosome isolation

2.3.1 Exosome isolation from cell culture media

Cells were seeded in T175 flasks with culture medium. When the cells reached 80% confluency, the cells were wash with PBS and 20 ml plain medium was added to each flask. The medium was collected after 24 h and centrifuged sequentially as following: the culture medium was firstly centrifuge at 2000 g for 15 min at room temperature (RT) and supernatant was collected into thin-wall, ultra-clear ultracentrifuge tubes (Beckman Coulter, US). The medium was then centrifuged at 10000 g for 40 min at 4 °C The supernatant was collected and transferred to new ultracentrifuge tubes and centrifuged at 100000 g for 2 h at 4 °C. Then the supernatant was taken out. PBS was added to repsuspend the pellet. Another centrifugation at 100000 g for 2 h at 4 °C was performed. The supernatant was taken out and the pellet was resuspended in PBS and filtered through 0.22 μm filter and stored at -20 °C.

2.3.2 Exosome isolation from plasma

Two kits were used for exosome isolation from plasma in Barts Cancer Institute, the total Exosome Isolation Kit (from plasma) (Invitrogen) and ExoEasy Maxi Kit (Qiagen). Total Exosome Isolation Kit (from plasma) (Invitrogen) was used to isolate exosomes from 200 μl plasma for method test and further clinical investigation. The plasma was thaw in RT and centrifuged at 2000 g for 10 min. The supernatant plasma to a new tube and centrifuged at 10,000 g for 20 min. The supernatant was taken out and mixed with 100 μl of PBS. RNase A was added to the plasma to a final concentration of 10 μg/ml. The sample was then incubated in 37°C water bath for 60 min. Then 2.25 μl (20 U/μl) RNase inhibitor (Applied Biosystems™) and 10 μl of Proteinase K from the Total Exosome Isolation Kit (from plasma) (Invitrogen™) were added to the sample. After mixed

well, the sample was incubated at 37 °C for 15 min. The sample was quickly cooled down on ice and 60 µl of the Exosome Precipitation Reagent (from plasma) from the Total Exosome Isolation Kit (from plasma) (Invitrogen) was added to the sample and mixed well. Then the sample was incubated at 4 °C for 2 h. Exosomes were then pelleted centrifugation at 10,000 g for 10 min and stored at -80 °C.

ExoEasy Maxi Kit (Qiagen) was used as a test method. 4 ml buffer XBP was added to 4 ml plasma and mixed inverting the tube for 5 times. The sample was then loaded onto the exoEasy spin column and centrifuged at 500 g for 1 min. The flow-through was discarded and the column was centrifuged at 5000 g for 1 min. After discarded the flow-through, 10 ml buffer XWP was added to the column and centrifuged at 5000 g for 5 min to remove residual buffer from the column. Then the spin column was transferred to a new collection tube. 400 µl Buffer XE was added to the membrane and incubated at RT for 1 min. The column was centrifuged at 500 g for 5 min. The eluate was collected and re-applied to the exoEasy spin column membrane and incubated at RT for 1 min. The column was then centrifuged at 5000 g for 5 min to and the eluate was collected as enriched EVs.

Validation work in Department of Pathology and Cancer Centre, Medical College of Wisconsin, US was performed by Dr. Jing Jia as following. 250 µl plasma from each patient was centrifuge at 500 g for 10 min at 4 °C. The supernatant was transferred to a new RNase-free tube and mixed with 2 µl of thrombin to a final concentration of 5 U/ml and incubated at RT for 5 min. The mixture was then centrifuged at 10000 g for 5 min at 4 °C. The supernatant was then mixed with 1/4 volume of ExoQuick exosome precipitation reagent (EXOQ5TM-1, SBI) and incubated at 4 °C for 1 h. The tube was rotated several times during the incubation to mix the sample. After the incubation, the sample was centrifuged at 1500 g for 15 min at 4 °C. Then the supernatant was aspirated. The sample was centrifuged again at 1500 g for 5 min at 4°C to remove residual ExoQuick solution. After removing the supernatant, the exosome pellet was resuspend in 100 µl PBS for following RNA extraction.

2.4 Nanoparticle tracking analysis

Nanoparticle tracking analysis was performed with some isolated exosome samples using NanoSight LM20 (NanoSight Ltd, UK). Exosomes isolated from plasma samples or cell culture media were diluted in PBS and loaded on NanoSight LM20. After loading the samples to the machine, 60 seconds videos were recorded to generate size distribution and concentration data.

2.5 RNA extraction

2.5.1.1 RNA extraction from plasma exosomes

30 µl Buffer RLT (Qiagen, UK) with 0.25% v/v Proteinase K (from the Total Exosome Isolation Kit (from plasma) (Invitrogen™)) was added to the exosome pellet to resuspend the exosomes. Exosomes were incubated at 50 °C for 30 min. Then RNA was then extracted with miRNeasy micro kit (Qiagen, UK) according to the manufacturer's protocol. 700 µl of QIAzol Lysis Reagent (Qiagen, UK) was added, vortexed and incubated at RT for 10 min. 140 µl of chloroform was added and the sample was shaken vigorously then incubated at RT for 5 min. The sample was then centrifuged for 15 min at 12,000 g at 4 °C. The upper aqueous phase (about 400 µl) was carefully transferred to a new 1.5 ml Eppendorf tube. Then 1.5 volumes of 100% ethanol was added to the upper aqueous phase and mixed thoroughly. The mixture was then transferred into a RNeasy MinElute spin column in a 2 ml collection tube and centrifuged at 8600 g for 15 s. The flow-through was discarded. 700 µl Buffer RWT from the kit was added to the spin column. The column was centrifuged for 15 s at 8600 g and the flow-through was discarded. 500 µl Buffer RPE was added to spin column. The column was centrifuged for 15 s at 8600 g at RT and the flow-through was discarded. Then 500 µl of 80% ethanol was added to the spin column. The column was centrifuged for 2 min at 8600 g and the flow-through was discarded. The spin column was placed in a new 2 ml collection tube (supplied in the kit) and centrifuged at 10000 g for 5 min with the column lid open. The spin column was then placed in a new 1.5 ml collection tube (supplied in the kit). 12 µl RNase-free water was added at the centre of the spin column membrane. The column was then centrifuged for 3

min at 13200 g at RT and RNA was eluted in the collection tube. RNA was stored at -80 °C.

For plasma samples from Department of Pathology and Cancer Centre, Medical College of Wisconsin (MCW), US, the RNA extraction was performed by Dr. Jing Jia. Plasma exosome sample resuspended in 100 µl PBS was mixed with 500 µl QIAzol Lysis Reagent and vortexed and incubated at RT for 5 min. 100 µl chloroform was added to the sample and vortexed vigorously for 15 s and then incubated at RT for 2 min. After incubation, the sample was centrifuged for 15 min at 12000 g at 4 °C. The upper aqueous phase was transferred to a new collection tube and mixed with 1.5 volumes of 100% ethanol. The sample was then loaded in a RNeasy MinElute spin column with a 2 ml collection tube and centrifuged at 12000 g for 30 s. 350 µl Buffer RWT (prepared with isopropanol) was added into the RNeasy MinElute spin column and centrifuge for 30 s at RT at 12000 g to wash. The flow-through was discarded. 80 µl Buffer RDD supplied with DNase from the RNase-Free DNase Set (QIAGEN) was added to the column and the column was incubated at RT for 15 min. 500 µl Buffer RWT (prepared with isopropanol) into the RNeasy MinElute spin column and centrifuge for 30 s at 12000 g. The flow-through was reapplied to the column and centrifuged for 30 s at 12000 g. After discarding the flow-through, the column was loaded with 500 µl Buffer RPE and centrifuged for 30 s at 12000 g. After discarded the flow-through, the column was loaded with 500 µl of 80% ethanol and centrifuged for 2 min at 12000 g. Then column was placed into a new 2 ml collection tube and centrifuged at full speed for 5 minutes with the lid open. Then the column was place in a new 1.5 ml collection tube. 14 µl RNase-free water was added to the column. The column was centrifuged for 1 min at full speed to elute the RNA.

2.5.1.2 RNA extraction from cell line exosomes

100 µl Buffer RLT (Qiagen, UK) with 0.25% v/v Proteinase K (from the Total Exosome Isolation Kit (from plasma) (Invitrogen™)) and 0.1% v/v β-mercaptoethanol (β-ME) was added to the 200 µl of exosomes. The mixture was incubated at 50 °C for 30 min. Then RNA was extracted with miRNeasy micro kit (Qiagen, UK) according to the manufacturer's protocol as described in 2.5.1.1.

2.5.1.3 RNA extraction from cell lines

Total RNA from cell lines was extracted with miRNeasy micro kit (Qiagen, UK) according to the manufacturer's protocol as described in 2.5.1.1.

MiRNAs from PC3 cells were extracted using AllPrep® DNA/RNA/Protein Mini kit (Qiagen) and miReasy micro kit (Qiagen). 350 µl of RLT buffer (with 1% v/v β-ME) was added to 10^6 cells and mixed well by pipetting up and down. The lysate was transferred to an ALLPrep DNA spin column placed in a 2 ml collection tube and centrifuged at 9000 g for 30 s. The liquid passed through was mixed with 250 µl of 100% ethanol, mixed well and added to a RNeasy mini spin column placed in a 2 ml collection tube. The column was then centrifuged at 9000 g for 15 s. The liquid passed through was mixed with 600 µl Buffer APP and incubated at RT for 10 min. Then the liquid was centrifuged at 13200 g for 10 min to precipitate protein. The supernatant was taken out and mixed with 600 µl of ethanol. The sample was then added to a RNeasy MinElute spin column placed in a 2 ml collection tube and centrifuge at 9000 g for 15 s. The flow-through was discarded and the column was washed by 700 µl Buffer RWT and centrifuged at 9000 g for 15 s. 500 µl Buffer RPE was added to the column and centrifuged at 9000 g for 15 sec. After discarding the flow-through, another 500 µl Buffer RPE was added to the column and centrifuged at 9000 g for 2 min. Then the column was placed in a new 2 ml collection tube and centrifuged at 13200 g for 2 min. The column was placed in a 1.5 ml collection tube. 14 µl RNase-free water was added to the column and centrifuged at 13200 g for 1 min.

2.6 RNA detection assays

2.6.1 Reverse transcription real-time quantitative polymerase chain reaction (RT-qPCR)

2.6.1.1 cDNA synthesis

The traditional reverse transcription was performed using miScript II RT Kit (Qiagen). RNA was thawed on ice. 10× miScript Nucleics Mix, RNase-free water, and 5× miScript HiFlex Buffer were thawed at RT. The reverse-transcription reaction mix was prepared on ice according to Table 4. The reactions were

incubated for 60 min at 37 °C following an incubation at 95 °C for 5 min. The reactions were then placed on ice to cool down. The cDNA was then diluted 10 times with RNase-free water and stored at -20 °C for later use.

Table 4. Reverse-transcription reaction components for cDNA preparation for RT-qPCR.

Components	Volume
5x miScript HiFlex Buffer	2 µl
10x miScript Nucleics Mix	1 µl
miScript Reverse Transcriptase Mix	1 µl
Template RNA	6 µl
Total volume	10 µl

2.6.1.2 RT-qPCR

RT-qPCR was performed with miScript SYBR® Green PCR Kit (Qiagen) and miScript Primer Assays (Qiagen). MiScript Primer Assays (Qiagen) were reconstituted in 550 µl RNase-free water. The RT-qPCR mix was prepared on ice according to Table 5.

Table 5. RT-qPCR reaction components.

Components	Volume/reaction(384-well plate)
2x QuantiTect SYBR Green PCR Master Mix	5 µl
10x miScript Universal Primer	1 µl
10x miScript Primer Assay	1 µl
RNase-free water	2 µl

Template cDNA	1 µl
Total volume	10 ul

Reactions were loaded in optical 384-well reaction plates and run the programme (Table 6) on The Applied Biosystems™ QuantStudio™ 7 Flex Real-Time PCR System. Water was loaded as negative control. PC3 miRNA sample was loaded in every plate as normaliser between plates. All reactions were run as triplicates.

Table 6. Cycling conditions for RT-qPCR.

Step	Time	Temperature
PCR initial activation step	15 min	95 °C
3-step cycling		
Denaturation	15 s	94 °C
Annealing	30 s	55 °C
Extension	30 s	70 °C
Cycle number	40 cycles	

2.6.2 Fluidigm multiple RT-qPCR

Samples for Fluidigm multiple RT-qPCR were prepared using the miScript Microfluidics PreAMP Kit (Qiagen), miScript Microfluidics PCR Kit (Qiagen), and miScript Primer Assays (Qiagen).

2.6.2.1 cDNA synthesis

Reverse transcription was performed using miScript II RT Kit (Qiagen). RNA was thawed on ice. 10× miScript Nucleics Mix, RNase-free water, and 5× miScript

HiSpec Buffer were thawed at RT. The reverse-transcription reaction mix was prepared on ice according to Table 7. The reactions were incubated for 60 min at 37 °C following another incubation at 95 °C for 5 min. The reactions were then placed on ice to cool down. The cDNA was then diluted 5 times with RNase-free water and store at -20 °C for later use.

Table 7. Reverse-transcription reaction components for cDNA preparation for Fluidigm.

Components	Volume
5× miScript HiSpec Buffer	2 µl
10× miScript Nucleics Mix	1 µl
miScript Reverse Transcriptase Mix	1 µl
Template RNA	6 µl
Total volume	10 µl

2.6.2.2 Pre-amplification

The pre-amplification was performed using miScript Microfluidics PreAMP Kit (Qiagen) and miScript Primer Assays (Qiagen). MiScript Primer Assays (Qiagen) were reconstituted with 27.5 µl RNase free water to make a concentration of 100 µM. List of primer assays is shown in Table 8. To make miScript PreAMP Primer Mix, 2.2 µl of each primer assay was taken and mixed together with 1030 µl of RNase free water. The pre-amplification reactions were prepared according to Table 9.

Table 8. List of primer assays used in Fluidigm multiple RT-qPCR.

MS00031829 - Hs_miR-375_2 miScript Primer
MS00008932 - Hs_miR-193a-5p_1 miScript Primer

MS00003640 - Hs_miR-184_1 miScript Primer
MS00010752 - Hs_miR-9_1 miScript Primer
MS00031703 - Hs_miR-320b_2 miScript Primer
MS00003738 - Hs_miR-200a_1 miScript Primer
MS00008372 - Hs_miR-101_3 miScript Primer
MS00003556 - Hs_miR-148a_1 miScript Primer
MS00003577 - Hs_miR-150_1 miScript Primer
MS00032158 - Hs_miR-99a_2 miScript Primer
MS00004179 - Hs_miR-423_1 miScript Primer
MS00014707 - Hs_miR-320a_1 miScript Primer
MS00004242 - Hs_miR-451_1 miScript Primer
MS00003416 - Hs_miR-122a_1 miScript Primer
MS00031234 - Hs_miR-100_2 miScript Primer
MS00031710 - Hs_miR-320d_2 miScript Primer
MS00009366 - Hs_miR-30c_2 miScript Primer
MS00006552 - Hs_miR-24_1 miScript Primer
MS00041867 - Hs_miR-320c_3 miScript Primer
MS00048510 - Hs_miR-7706_1 miScript Primer
MS00043491 - Hs_miR-1246_2 miScript Primer
MS00048538 - Hs_miR-4433b-3p_1 miScript
MS00009142 - Hs_miR-22*_1 miScript Primer
MS00003535 - Hs_miR-146a_1 miScript Primer
MS00003206 - Hs_miR-20b_1 miScript Primer
MS00010549 - Hs_miR-744_1 miScript Primer
MS00006629 - Hs_miR-125b_1 miScript Primer
MS00008554 - Hs_miR-125a-3p_1 miScript

MS00008281 - Hs_let-7b*_1 miScript Primer
MS00009408 - Hs_miR-30e*_1 miScript Primer
MS00007350 - Hs_miR-30a-5p_1 miScript Primer
MS00003129 - Hs_let-7c_1 miScript Primer

Table 9. Pre-amplification reaction components for Fluidigm sample preparation.

Component	Volume per sample
5× miScript PreAMP Buffer	5 µl
HotStarTaq DNA Polymerase	2 µl
miScript PreAMP Primer Mix	5 µl
RNase-free water	7 µl
miScript Microfluidics Universal Primer	1 µl
Diluted cDNA	5 µl
Total volume	25 µl

Pre-amplification was then performed in thermal cycler according to Table 10.

Table 10. Cycling conditions for pre-amplification for Fluidigm sample preparation.

Step	Time	Temperature
PCR initial activation step	15 min	95 °C
2-step cycling:		
Denaturation	30 s	94 °C

Annealing/extension	3 min	60 °C
Cycle number	12 cycles	

After the run was finished, 2 µl Side Reaction Reducer was added to each pre-amplified reaction. The samples were mixed well, and centrifuged briefly to collect any liquid on the tube wall.

2.6.2.3 Multiple RT-qPCR

To perform multiple RT-qPCR, primers were further diluted from 100 µM to 40 µM by adding 7.5 µl RNase free water to 5 µl primer (100 µM). Pre-amplified cDNA samples were used without dilution. Multiple RT-qPCR was performed by Barts and the London Genome centre using BioMark HD system (Fluidigm, USA). Reactions were assayed in 96.96 Dynamic Array Integrated fluidic circuit. PCR was performed with 40 cycles.

2.6.3 RNA-sequencing

2.6.3.1 Exosome RNA-sequencing

Exosome RNA from 24 treatment-naive PCa and 24 CRPC samples were sent for RNA-sequencing to the Barts and the London Genome Centre core facility. Indexed libraries were prepared from exosomal RNA as instructed by the NEBNext Multiplex Small RNA Library Prep Set for Illumina (New England Biolabs) according to the manufacturer's instructions without size selection. RNA-sequencing was performed on Illumina NextSeq 500 platform and run twice.

2.6.3.2 RNA-sequencing data analysis

Unaligned reads were trimmed and aligned against mirBase mature miRNA (Release 20) within Partek® Genomics Suite®. Low expression miRNAs (expressed in less than 25% of samples) were removed. The miRNA read counts were then analysed using three methods to identify differentially expressed

miRNAs. 1) Linear Models for Microarray and RNA-sequencing Data (Limma) [340] was performed using functions implemented in edgeR and limma() in R studio. 2) Counts per million (CPM): Read counts were transformed to CPM using cpm() function implemented in R package edgeR (version 2.4.0) and then Welch's t-test were performed in SPSS 24. 3) The trimmed mean of M-value normalisation (TMM)[341] was performed using functions implemented in the edgeR in R studio and ExactTest() function in edgeR was used to find differentially expressed miRNAs.

2.7 Transient miR-423-3p over-expression

Cells were seeded in CellBind 6-well plates (Corning) with phenol red-free RPMI-1640 (Gibco, US) supplemented with 10% charcoal-depleted FCS (Gibco) and 1% penicillin/streptomycin at a density of 2×10^5 cells per well. After 24 h when the cells were 70%-80% confluency, the medium was changed to phenol red-free RPMI-1640 (Gibco, US) supplemented with 1% penicillin/streptomycin (plain medium). For each well of the 6-well plate, 25 nmol of mirVana miR-423-3p mimics (Invitrogen)/ mirVana miRNA mimics Negative Control #1 (Invitrogen) and 7.5 µl Lipofectamine® RNAiMAX Reagent (Invitrogen) were used. MirVana miR-423-3p mimics (Invitrogen)/ mirVana miRNA mimics Negative Control #1 (Invitrogen) and Lipofectamine® RNAiMAX Reagent (Invitrogen) were separately diluted in 150 µl plain medium, incubated for 5 min and then mixed together and incubated for 20 min at RT. The mixture was then added to the cells. After 6 h of transfection, the transfection medium was aspirated and replaced with phenol red-free RPMI-1640 (Gibco, US) supplemented with 10% charcoal-depleted FCS (Gibco) and 1% penicillin/streptomycin.

2.8 Cell viability assay

Cell viability assay was performed at 72 h of seeding using the CellTiter 96 Aqueous Non-radioactive cell proliferation assay (Promega, UK). The assay is composed of a tetrazolium compound (3-(4,5-dimethylthiazol-2-yl)-5-(3-carboxymethoxyphenyl)-2-(4-sulfophenyl)-2H-tetrazolium, inner salt; MTS) and an electron coupling reagent (phenazine methosulfate; PMS). MTS is bioreduced

by cells into a formazan product that is soluble in tissue culture medium. The quantity of formazan product as measured by the amount of 490 nm absorbance is directly proportional to the number of living cells in culture. After 24 h of transfection, the transfected cells were trypsinised and centrifuged at 1000 rpm for 5 min. Cells were then resuspended and seeded in a 24-well plate at a density of 2×10^5 cells per well in same volume of medium. At 72 h of seeding, 200 µl of MTS and PMS mixture (1:20) was added to each well and incubated at 37 °C for 3 h. Absorbance was then measured at 495 nm using SPECTROstar Nano Absorbance plate reader (BMG LABTECH).

2.9 Cell migration assay

Cell migration was assayed by transwell migration assay. After 24 h of transfection, the transfected cells were trypsinised and centrifuged at 1000 rpm for 5 min. Cells were then resuspended as single cell solution in phenol red-free RPMI-1640 medium supplemented with 1% charcoal-depleted FCS and 1% penicillin/streptomycin and counted. 24-well plates were filled with 500 µl phenol red-free RPMI-1640 medium supplemented with 10% charcoal-depleted FCS and 1% penicillin/streptomycin per well and transwell inserts with 8 µm pores (Corning, US) were placed on top. A total of 8×10^4 cells per well were seeded into the inserts. Cells were incubated for 24 h to migrate. Depending on the cell type, different number of cells will be migrated after 24h. Cells were fixed in cold methanol for 20 min and cells in the inner side of the insert membrane were removed. The membranes were then stained with 0.057% sulforhodamine B for 30 min and rinsed in 1% acetic acid. Membranes were cut from the inserts and rinsed in xylene and mounted on the glass slides in DPX mounting medium. Slides were scanned using Hamamatsu NanoZoomer S210 system. Cell number was counted from equal size of each membrane.

2.10 Cell invasion assay

Cell invasion for non-transfected LNCaP and C4-2 was determined by transwell invasion assay using Corning® BioCoat™ Growth Factor Reduced Matrigel Invasion Chambers with 8.0 µm PET Membrane as previously described [23].

Cells were seeded at 8×10^4 cells per well into the invasion chambers in phenol red-free RPMI 1640 medium supplemented with 1% charcoal-depleted FCS. Phenol red-free RPMI 1640 medium with 10% charcoal-depleted FCS was added in the 24-well plates to attract invasion. Depending on the cell type, different number of cells will be migrated after 24h. Cells were incubated for 24 h before they were fixed, stained and counted using the same method as for migration assay.

Invasion ability of transfected LNCaP cells was assayed by single cell invasion assay through collagen type-I/Matrigel matrix. Cells were seeded onto the matrix of 1.6 mg/ml collagen type-I (BD Biosciences) and 50% growth factor-reduced Matrigel™ (BD Biosciences) as single cell suspension in phenol red-free RPMI 1640 medium with 10% charcoal-depleted FCS. 24 h later, cells with pseudopodia-like extensions were counted as invaded cells.

2.11 WB

2.11.1 Protein extraction

Cells were lysed in lysis buffer (Table 11) on ice for 20 min with vortex every 5 min. Cell debris were pelleted by centrifugation at 2000 g for 2 min. The supernatant was collected and stored at -80 °C until use. For protein extraction from exosomes, 50 µl of 10% Triton-100, 71.5 µl of Protease inhibitor cocktail 7×, and 2.5 µl of Phosphatase inhibitor were directly added to 376 µl of isolated exosomes (which were resuspended in PBS) and incubated on ice for 30 min with vortex every 5 min. To concentration the protein, the exosome protein lysate was mixed with 4 volumes of cold acetone (-20 °C) and incubated at -20 °C for 2 h. The mixture was then centrifuged at 12000 g at 4 °C for 10 min. The supernatant was discarded. The protein pellet was air-dried and then dissolved in PBS.

Table 11. Cell lysis buffer for protein extraction.

Reagent	**Volume (µl)**
50 mM Tris/HCl pH8.0	752

10% Triton-100	100
Protease inhibitor cocktail 7×	143
Phosphatase inhibitor	5
Total volume	1000

2.11.2 Bradford assay

Cell lysates were defrosted on ice and the concentration of protein was measured by Bradford assay. 10 µl of each protein solution or standard solutions (bovine serum albumin (BSA) solutions at 100/200/400/500/1000/2000 µg/ml) was added to 190 µl of diluted 1×Protein Assay Dye Reagent Concentrate (BioRad, UK) in triplicates in 96-well plate. Absorbance at 565 nm was measured on SPECTROstar® Omega absorbance microplate reader (BMG LABTECH, Germany). The standard curve was made using the readings of the standard solutions and the concentrations of cell lysates were calculated from the standard curve.

2.11.3 Sodium Dodecyl Sulphate-Polyacrylamide gel electrophoresis and Polyvinylidene difluoride (PVDF) membrane transfer

Protein samples (30 µg) were mixed with loading buffer and reducing buffer. Samples were denatured at 95°C for 5 min and then loaded on the gel prepared according to Table 12. The denatured protein samples were loaded on the gel and run in 1× Tris Glysine with SDS at 80 V for 20 min and then 110 V for 80 min. PVDF membrane (Immobilon-P Membrane, 0.45 µm, Millipore, UK) was pre-treated for 1 min in 100% methanol. After electrophoresis, proteins were transferred on PVDF membrane for 120 min at 200 mA in using standard transfer buffer (10% 10× Tris-Glycine buffer (0.25 M Tris base and 1.92 M glycine, National Diagnostics, UK), 20% methanol, 70% water).

Table 12. Sodium Dodecyl Sulphate-polyacrylamide gel preparation.

12% resolving gel		Stacking gel	
Reagents	**volume**	**Reagents**	**volume**
ProtoFlowgel (Flowgen Bioscience, UK)	8 ml	ProtoFlowgel (Flowgen Bioscience, UK)	1.3 ml
4×ProtoFLOWGel Resolving Buffer (Flowgen Bioscience, UK)	5 ml	ProtoFLOWGel Stacking Buffer (Flowgen Bioscience, UK)	2 ml
water	6.8 ml	water	6.1 ml
TEMED (Sigma, UK)	20 µl	TEMED (Sigma, UK)	10 µl
10% Amonium persulphate (Sigma, UK)	200 µl	10% Amonium persulphate (Sigma, UK)	50 µl

2.11.4 Antibody incubation and protein detection

The PVDF membrane with proteins was blocked in 5% BSA in Tris Buffer Saline/0.1% Tween-20 (TBST) at RT for 1h. After blocking, the membrane was incubated with primary antibody diluted in 3% BSA at 4 °C overnight. Next day, the membrane was washed in TBST for 5 min three times. Then the membrane was incubated in secondary peroxidase conjugated antibody diluted in 3% BSA at RT for 1 h, followed by washes in TBST for 5 min three times. All antibodies used are listed in Table 13.

Table 13. Antibodies and dilutions used for Western-blotting.

Primary antibody	Dilution/concentration	Secondary antibody	Dilution
anti-MEIS1 (Rabbit, ab229962, Abcam, UK)	1:2000	Goat Anti-Rabbit IgG (H+L), Peroxidase Conjugated	1:2000

		(32430, Fisher Scientific, UK)	
anti-β-actin (13E5, Rabbit, Rabbit mAb (HRP Conjugate) #5125, Cell Signalling Technology, US)	1:2500	Goat Anti-Rabbit IgG (H+L), Peroxidase Conjugated (32430, Fisher Scientific, UK)	1:2000
anti-ALIX (Rabbit, ab76608, Abcam, UK)	1 µg/ml	Goat Anti-Rabbit IgG (H+L), Peroxidase Conjugated (32430, Fisher Scientific, UK)	1:2000

Protein detection was done with Immobilon Western Chemiluminescent HRP Substrate (Millipore, UK). 1 ml of Chemiluminescent HRP Substrate was added on the membrane. Protein bands were detected using X-ray film (Fuji Photo Flim, Fisher Scientific, UK).

2.12 CTC isolation

Several CTC isolation methods were used in this project for enumeration and/or culture.

2.12.1 Ficoll centrifugation

50 ml LeucoSep tube was filled with 15.3 ml of Ficoll-Paque PLUS (Greiner Bio-One, Germany), and spun at 1000 g for 30 sec at RT. Whole blood was added to the LeucoSep tube with same volume of PBS. The mix was centrifuged at 1000 g for 15 min with breaks off. After the spin, a layer of peripheral blood mononuclear cells (PBMC) was shown above the frit in the LeucoSep tube. All

liquid above the frit was moved to a 50 ml conical tube and PBMC was pelleted at 200 g for 8 min.

2.12.2 Parsortix™

The Parsortix™ system (ANGLE, UK) is a micro-fluidic CTC isolation platform which captures CTCs in cassettes (Figure 6) based on their less deformable nature and larger size as compared to other blood components.

2.12.2.1 For CTC enumeration

7 ml blood was used in the Ficoll centrifugation step. After the Ficoll centrifugation step, the cell pellet was resuspended in 4 ml isolation buffer (PBS with 2 mM EDTA and 1% BSA) and added back to the original EDTA blood tube containing 0.5 ml whole blood.

Sample was then loaded onto Parsortix and cells were separated in the 10 µm-gap cassette using installed program PX2_S26. The enriched cells in the cassette were eluted to a low retention 1.5 ml tube and centrifuged at 1000 g for 3 min. Cell pellet was resuspended in 10 µl of 0.075 M KCl and transferred onto poly-L-lysine coated slides with Supersilk™ surface and wide orfice pipet tips (VWR, UK). Another 10 µl of 0.075 M KCl was used to rinse the tube and liquid was transferred onto the same slide. Slides were air-dried. Cells were fixed with cold acetone on ice for 20 min and air-dried and kept at 4 °C up to one week for later staining.

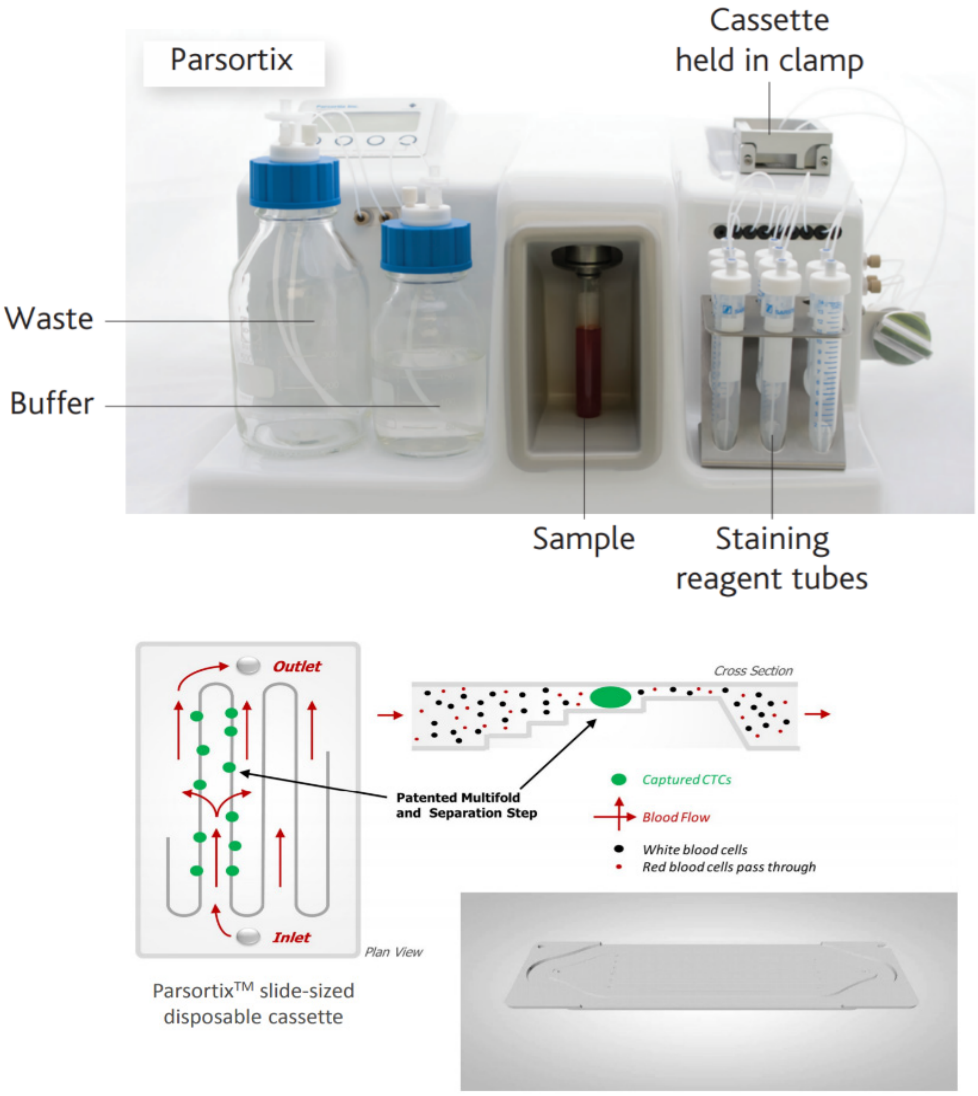

Figure 6. Parsortix system overview and cassette design.

2.12.2.2 For CTC culture

Various volumes of blood were used in the Ficoll centrifugation step. If more than 10 ml of blood was used, blood was separated into two equal portions and processed in two LeucoSep tube during the Ficoll centrifugation step. After the Ficoll centrifugation step, the cell pellet was resuspended in a total of 4 ml isolation buffer (PBS with 2 mM EDTA and 1% BSA) and added back to the original EDTA blood tube containing 0.5 ml of whole blood.

Sample was then loaded onto Parsortix and cells were separated in the 10 µm-gap cassette using installed program PX2_S26. The enriched cells in the cassette were eluted to a low retention 1.5 ml tube and centrifuged at 1000 g for 3 min. Cell pellet was then resuspended in cell culture media.

2.12.3 EasySep™

EasySep™ is an immuno-magnetic system for CTC isolation (Figure 7). After the Ficoll centrifugation step, the cell pellet was repsupended in 200 µl of EasySep™ buffer (PBS containing 2% FCS and 1 mM EDTA) and transferred to a Falcon 5 ml polystyrene round-bottom tube with Supersilk™ surface and wide orfice pipet tips. Conical tube was rinsed with 200 µl of EasySep buffer twice and liquid was transferred to the Falcon 5 ml polystyrene round-bottom tube. Then 30 µl of EasySep CD45 cocktail antibody (included in EasySep™ Human CD45 Depletion kit) (STEMCELL, Canada) was added into the sample, mixed well and incubate at RT for 15 min. 60 µl EasySep magnetic nanoparticles (included in EasySep™ Human CD45 Depletion kit) was added to the sample, mixed well, and incubated at RT for 10 min. EasySep™ buffer was added to top up the sample to a total volume of 2.5 ml. Cells were mixed and the tube (without cap) was placed into EasySep™ Violet Magnet rack (STEMCELL) and set aside for 10 min. Then the sample was poured into a new Falcon 5 ml polystyrene round-bottom tube. Remained cells in the old tube were washed with 100 µl of EasySep™ buffer and transferred to the new tube. The new tube with cells was placed into the magnet and set aside for 10 min. Cells were then poured out and pelleted by centrifugation at 1000 g for 3 min.

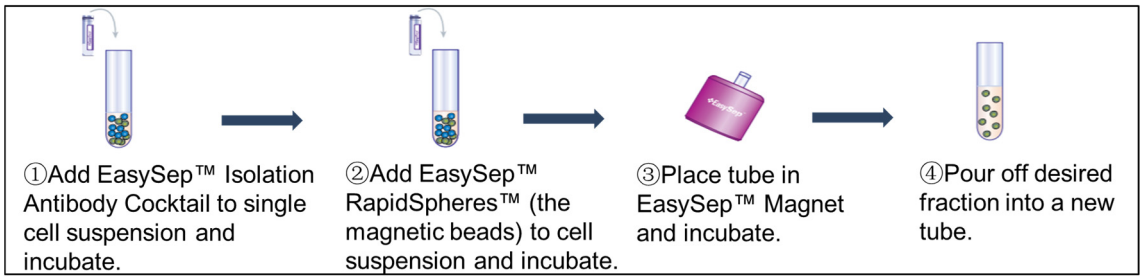

Figure 7. Illustration of EasySep work flow for CTC enrichment.

2.12.4 RossetteSep™

RosetteSep™ is an immunodensity procedure for the isolation of cells from whole blood (Figure 8). By crosslinking unwanted cells to red blood cells (RBCs) present in the sample, target cells are purified during standard density gradient centrifugation. RosetteSep™ CTC enrichment cocktail containing anti-D56 (STEMCELL) contains tetrameric antibody complexes recognizing CD3, CD14, CD16, CD19, CD38, CD45, CD56, CD61, CD66b and crosslinks cells positive for these antigens with red blood cells and deplete them via centrifugation with density gradient medium. 50 µl of RosetteSep™ CTC enrichment cocktail containing anti-D56 (STEMCELL) was added per 1 ml whole blood and mixed well. Sample was then incubated for 20 min at RT. Then the sample was diluted with an equal volume of PBS (with 2% FCS). The diluted sample was slowly added on top of 15 ml Lymphoprep™ (STEMCELL). The sample was then centrifuged at 1200 g for 20 min with the brake off. The enriched cells were taken from the density gradient medium/plasma interface and washed with cell culture medium twice and pelleted by centrifugation at 1200 rpm for 5 min.

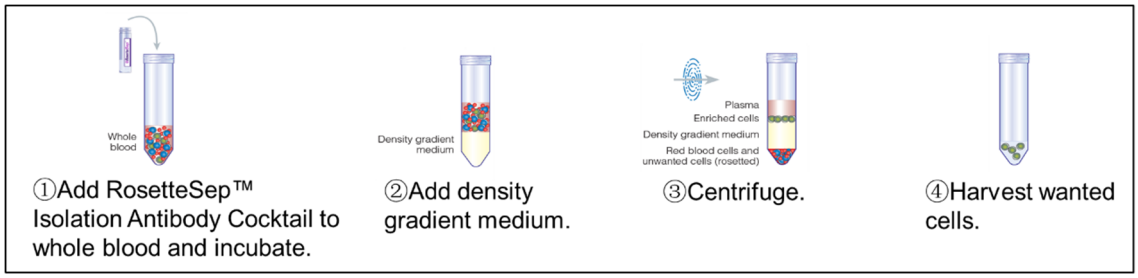

Figure 8. Illustration of RossetteSep work flow for CTC enrichment.

2.13 CTC culture

2.13.1 Culture media

Several culture media were used for *in vitro* culture of CTCs:

1) RPMI-1640 supplemented with 1% FCS and 1% penicillin/streptomycin (for CTC culture using clinical samples, 1% penicillin/streptomycin was replaced with 1×antibiotic&antimycotic (Sigma)).

2) Clonetics™ Prostate Epithelial Cell Growth Medium (PrEGM) (Lonza, Walkersville, Inc., USA) [342].

3) F-medium[343]: 3:1 (v/v) F-12 Nutrient Mixture (Ham)–Dulbecco's modified Eagle's medium (Invitrogen) containing 5% FCS, 0.4 μg/mL hydrocortisone (Sigma-Aldrich), 1ml per liter insulin solution human (Sigma-Aldrich), 8.4 ng/ml cholera toxin (Sigma-Aldrich), 10 ng/ml epidermal growth factor (Peprotech), 24 μg/ml adenine (Sigma-Aldrich),10 μmol/L Y-27632 (Selleckchem), and 1×antibiotic antimycotic(Sigma-Aldrich).

4) Organoid culture medium [246]. Advanced DMEM/Ham's F-12 (ADMEM/F-12) (Gibco) was used as basal media with supplements listed in Table 14.

Table 14. Supplements in organoid culture medium.

Reagents	Final concentration	Company
Recombinant human EGF	5 ng/ml	Peprotech
Recombinant Human Noggin	100 ng/ml	Peprotech
Recombinant Human R-spondin-1	500 ng/ml	Peprotech
A83-01	500 nM	Tocris
Prostaglandin E2	1 μM	Tocris
human FGF10	10 ng/ml	Peprotech
human FGF-basic	5 ng/ml	Peprotech
Nicotinamide	10 mM	Sigma
SB202190	10 μM	Sigma
n-Acetyl-cysteine	1.25 mM	Sigma
Dihydrotestosterone	1 nM	Sigma

Y-27623 2HCl	10 µM	Selleckchem.com
B-27	1×	Life technology
HEPES	10 mM	Sigma
Glutamax	1×	Life technology
Antibiotic&antimycotic	1×	Sigma

5) CTC culture Plating medium and Base medium (Xcell Biosciences, San Francisco, US).

2.13.2 Culture condition

2D culture was performed in normal cell culture plates. Spheroid culture was performed in ultra-low attachment plate (Corning). For 2.5D culture, 100 µl of Matrigel® Growth Factor Reduced (GFR) Basement Membrane Matrix (Corning) was added to each well in 96-well plate and incubated in 37 °C for 1 h to solidify. Cells were then added on top. When using CTC culture Plating media and Base media (Xcell Biosciences, San Francisco, US), cell were cultured in XCM 6-well plates (Xcell Biosciences, San Francisco, US) in Avatar system or under hypoxia condition (1% O_2, 5% CO_2, 37 °C).

2.14 Immunofluorescence staining

Fixed CTC slides were rehydrated with PBS for 3 min. Unspecific background was blocked by incubating slides with 10% normal donkey serum (Sigma, UK) for 10 min. After PBS wash 2× 2 min, slides were stained with rabbit polyclonal PE conjugated anti-human CD45 antibody (Miltenyi Biotec) for 15 min. Antibody excess was washed with PBS for 3 min. Cells were then permeabilized with 0.1% Triton X-100 for 10 min followed by staining with FITC conjugated anti-CK (Miltenyi Biotec) and Alexa Fluor® 647 conjugated anti-Vimentin (Abcam) for 30 min. Slide were washed in PBS 3× 3 min, dried and mounted in SlowFade® gold

antifade mountant with DAPI. All antibodies were diluted in dilution buffer (2% BSA, 2 mM EDTA in PBS) as detailed in Table 15. Slides were scanned using Ariol image analysis system (Leica Microsystems (Gateshead) Ltd, UK), equipped with an Olympus BX61 microscope. For CTC enumeration, the number of cells in the following categories were counted: $CK^+Vim^-CD45^-$ (epithelial type), $CK^+Vim^+CD45^-$ (EMT type) and $CK^-Vim^+CD45^-$ (mesenchymal type).

Table 15. Antibodies and dilution used in immunofluorescence staining.

Antibody	Clone	Dilution
FITC conjugated anti-CK, Miltenyi Biotec, 130-080-101	CK-6H5	1:30
PE conjugated anti-CD45, Miltenyi Biotec, 130-080-201	5B1	1:10
Alexa Fluor 647 conjugated anti-vimentin, Abcam, ab194719	EPR3776	1:75

2.15 Fluorescent *in situ* hybridisation (FISH)

The cultured CTC slides used previously for IF were incubated in stripping buffer (containing 2% SDS, 0.0625 M Tris-HCL pH 6.8 and 0.8% β-ME) at 50 °C for 20 min to wash off the immunofluorescence signal, following three 5 min PBS washes. The slides were then fixed in methanol: acetic acid (3:1) for 10 min and stripped of cytoplasm by incubation in 70% acetic acid for 10 min. After 3× 5 min PBS washes, slides were dehydrated through 3 min incubation in series of 70%, 90% and 100% ethanol, and air-dried. *AR* (RP11-479J1) and *PTEN* (CTD-846G17) BAC probes were used for subsequent FISH. FISH probes were prepared by Dr Xueying Mao. The *AR* (red) probe was labelled with Tetramethunl-rhodamine-5-dUTP (Roche, US) and *PTEN* probe (green) was labelled with Fluorecein-12-dUTP (Roche, US). Probes labelling was performed with BioPrime DNA Labelling System (Invitrogen, Life Technologies, UK)

according to the manufacturer's protocol. For each probe, 300 ng of amplified BAC DNA was diluted in water to a final volume of 24 µl and mixed with 20 µl of random primers (octamers). The mixture was denatured at 95°C for 5 min and cooled on ice for 10 min. Next, the *AR* DNA solution was mixed with 1.75 µl of Tetramethunl-rhodamine -5-dUTP and the *PTEN* DNA solution was mixed with 1.75 µl of Fluorescein-12-dUTP. 5 µl of the special 10×dNTP (1mM dATP, dGTP, dCTP, 0.65 mM dTTP) and 1 µl of Klenow enzyme (BioPrime DNA Labeling kit) were added to both solutions. The labelling was performed at 37 °C for 3 h and stopped by adding 5 µl of stop buffer. Labelled probes were cleaned with Microspin G50 columns (GE Healthcare, UK). Purified DNA was mixed with 30 µl of COT-1 DNA (Roche, UK) and 1 µl of salmon sperm DNA (Sigma, UK). Next, DNA was precipitated with 4 M NaCl (1/10 of DNA volume) and 2.5 volumes of ethanol at -80 °C for 30 min. The samples were then centrifuged at 13000 rpm for 20 min at 4 °C. The DNA pellet was washed with 200 µl of fresh 80% ethanol and centrifuged at 13000 rpm for 10 min at 4 °C. The pellet was air-dried and resuspended in 20 µl of nuclease-free water. 10 µl of hybridisation buffer (60% formamide, 12%w/v dextran sulphate, 2.4×SSC, 0.14 mM EDTA pH 8.0, 400 µg/ml salmon sperm in water) was mixed with 1 µl of AR probe and 1 µl of PTEN probe and applied to each CTC slide. The slides were covered with coverslips, sealed with liquid rubber and denatured at 95 °C for 10 min. Finally, the slides were put in a humid box and incubated at 37 °C overnight to allow probes hybridisation. Next day the coverslips were removed and the excess of probes was washed off through series of washes performed at 42 °C: quick rinse in 2×SSC to remove hybridisation solution, 4 min in 50% formamide/2×SSC twice and 5 min in 2×SSC twice. Finally, slides were washed twice in PBS for 5 min, dehydrated in 70% ethanol for 2× 20 s, air-dried and mounted in mounting medium with DAPI. Slide were then scanned using Ariol image analysis system.

2.16 Mouse engrafting and xenograft cells *in vitro* culture

The mouse engrafting and sacrifice were performed by Dr. Marc Yeste-Velasco. The NU Foxn1nu nude mouse was housed in the Biological Services Unit of the Barts Cancer Institute, Queen Mary University of London according to our institutional guidelines, and the United Kingdom Home Office regulations.

Procedures were performed under the personal license number: P1EE3ECB4. 8.8×10^6 of cultured prostate cancer CTC cells were suspended in PBS, mixed with same volume of Matrigel and injected into the flank of nude mouse. Tumour was allowed to grow for 11 weeks before the mouse was sacrificed. The tumour tissue was then separated into three parts:

1) Part of the tissue was put in gentleMACS™ C tube (Miltenyi Biotec) containing 6 ml of 0.33% collagenase (STEMCELL Technologies) diluted in plain RPMI-1640. Collagenase tissue digestion was performed at 37 °C for 90 min, with shred on gentleMACS dissociator system (Miltenyi Biotec) every 30 min. To stop enzymatic reaction, 10 ml of RPMI-1640 (supplemented with 10% FCS and 1% antibiotic & antimycotic) was added to the cells suspension and mixed well. After 5 min centrifugation at 1300 rpm, the supernatant containing suspended cells was filtered through 70 µl filter. The pass through cells were centrifuged at 1300 rpm for 5 min. The cell pellet was resuspended in PBS and filtered through 40 µl filter. The pass through cells were centrifuged at 1300 rpm for 5 min. The cell pellet was resuspended in RPMI-1640 (supplemented with 10% FCS and 1% antibiotic & antimycotic) to create single cell suspension and cultured at 37 °C and 5% CO_2.

2) Part of the xenograft tissue was cut to small clumps and cultured in RPMI-1640 (supplemented with 10% FCS and 1% antibiotic & antimycotic) in 6-well plates at 37 °C and 5% CO_2.

3) Part of xenograft tissue was fixed in 10% formalin at 4 °C overnight. The fixed tissue was then moved to 70% ethanol and sent to Barts Cancer Institute pathology service, where the tissue was embedded in paraffin and sectioned by Mr George Elia.

2.17 Metaphase spreads preparation

After reaching 70% confluence, cultured xenograft-derived cells were treated for 4 h with 0.04 ug/ml of colcemid to arrest cultured cells in metaphase. After 4 h treatment of colcemid, cells were trypsinised and pelleted by centrifugation at 1000 rpm for 3 min. The cell pellet was resuspended in pre-warmed (37 °C) 0.075 M KCl and incubated at 37 °C for 15 min. 1 ml of fixation solution (methanol: acetic acid (v:v)=3:1) was added to 8 ml of cell suspension and mixed. Cells were

pelleted by centrifugation at 1000 rpm for 6 min. The supernatant was aspirated and cells were resuspended in 10 ml of fixation solution. After 15 min incubation at RT, cells were pelleted by centrifugation at 1000 rpm for 6 min. The supernatant was then aspirated and cells were resuspended in 200 µl of fixation solution. Glass slides used for metaphase spreads preparation were previously cleaned with 100% ethanol, treated in 100% acetic acid overnight, washed in distilled water and kept in distilled water at 4 °C. The fixed cells were then dropped on the glass slides and air-dried. SlowFade® gold antifade mountant with DAPI was added on the dried slides and the slides were covered with cover slips. The metaphase spreads were checked under Axioplan fluorescent microscope (Zeiss).

2.18 Immunohistochemistry (IHC) staining

IHC on formalin-fixed, paraffin-embedded (FFPE) xenograft sections were performed by Dr. Elzbieta Stankiewicz. The tissue slides were dewaxed in xylene for 5 min twice. Then the slides were incubated in 100% ethanol for 5 min, following 10 min incubation in 3% H_2O_2 in methanol solution. The slides were then washed under running water for 2 min. Next, the slides were sunk in pre-boiled antigen retrieval solution (Vectastain, H3300) and boiled in a pressure cooker for 10 min. After antigen retrieval, slides were rinsed in water, spread onto the staining tray and equilibrated in TBST for 5 min. Next, the TBST was removed and the slides were incubated with the primary antibodies (diluted in 1% BSA in PBS with azide) for 60 min at RT. Antibodies and dilutions used for IHC are listed in Table 16. After incubation, the slides were rinsed with TBST for 3 min twice. Then the slides were incubated for 30 min at RT with secondary biotinylated universal antibody (Vector Lab, Vectastain Universal Elite ABC Kit, PK6200). After incubation, the slides were rinsed with TBST buffer for 3 min twice. Then complex avidin + biotinylated horseradish peroxidise (Vector Lab, Vectastain Universal Elite ABC Kit, PK6200) was applied to the slides and incubated for 20 min. After incubation, the slides were rinsed with TBST for 3 min twice. The slides were then incubated with DAB solution (BioGenex, HK153-5KE) for 10 min. Finally, the slides were counterstained in Hematoxylin solution Gill's No. 2 (Sigma) for 3 min, washed in water and dehydrated through series of ethanol solutions:

70%, 90% and 100% ethanol for 3 min each. The slides were then cleared in xylene for 3 min twice and mounted with xylene based mounting medium (DPX).

Table 16. Primary antibodies used for IHC and their dilutions.

Primary antibodies	Dilution
Anti-AR antibody, monoclonal, mouse, clone 441 (Abcam, ab9474)	1:800
Anti-Human PSA, Polyclonal, Rabbit (Dako, A0562)	1:8000

2.19 Statistical analysis

For RT-qPCR results, ΔCt value for each mature miRNA profiled was calculated using the formula ΔCt = sample (Ct^{miRNA} - average $Ct^{Normalisers}$) - PC3 (Ct^{miRNA} - average $Ct^{Normaliser}$). $2^{-\Delta Ct}$ was used to compare the expression levels of each miRNA in different groups of patients. Expression levels were compared by Mann-Whitney U tests. Receiver operating characteristic (ROC) curve analysis was used to test the performance of predictors in distinguishing CRPC patients. Area under the curve (AUC) was used to evaluate the prediction value of parameters

For Fluidigm, results were reported as Ct values and quality threshold was set at 0.65. ΔCt value for each mature miRNA profiled was calculated using the formula ΔCt = Ct^{miRNA} - average $Ct^{Normaliser}$. $2^{-\Delta Ct}$ was used to compare the expression levels of each miRNA in different groups of patients. Expression levels were compared by Mann-Whitney U tests. Bivariate logistic regression was performed to combine several predictors. ROC curve analysis was used to test the performance of predictors in distinguishing CRPC patients. AUC was used to evaluate the prediction value of parameters. Spearman correlation tests were used to evaluate the correlation of miRNA expression levels and PSA levels and the correlation of Ct values generated from different methods. Two-tailed Student-t-test was used to compare cell proliferation, migration and invasion. Statistical analyses were performed in SPSS 24 and GraphPad Prism 5.1.

Chapter III Identification of plasma exosomal miRNA profile in PCa and CRPC-associated miRNAs by RNA-sequencing

3.1 Introduction

Exosomes are cell-derived small membrane vesicles (<150 nm) existing in various body fluids that are believed to be involved in various biological functions including angiogenesis, cell proliferation, tumour cell invasion and metastasis, immune response through intercellular transfer of their protein or RNA content [344]. Studies have demonstrated their important roles in intercellular communication, as well as the potential of using exosomes as vehicles to deliver therapeutic agents [195, 345].

It has been reported that EVs contains a variety of RNA species, the majority being small non-coding RNAs [178, 346]. MiRNAs are stably preserved in plasma exosomes [347] and can be functionally active, making them an ideal source of non-invasive biomarker and good material to study cancer biology. A number of studies have been reported investigating exosomal miRNAs as diagnostic biomarker for PCa [348]. However, there is currently limited data generated from clinical samples, especially comprehensive analysis of plasma exosomal miRNAs in CRPC [103, 175, 346]. Plasma exosomal miRNAs associated with CRPC development have not been investigated.

RNA-sequencing has quickly emerged as the preferred platform for studying miRNA expression in recent years. The key advantage of RNA-sequencing over microarray or qPCR-based miRNA expression profiling techniques is that it enables examining the differential expression of all small RNAs in samples without target RNA pre-selection. It has been previous reported that RNA-sequencing can be used to profile the RNA contents in exosomes, and RNAs in exosomes bear great value as biomarker [103, 175, 346].

This chapter aims to identify the miRNA expression profile of plasma exosomes from treatment-naive PCa and CRPC patients and identify the differentially expressed miRNAs using RNA-sequencing.

3.2 Results

3.2.1 Enrichment of exosomes

Exosomes from PCa patients' plasma were firstly isolated by precipitation using the commercial kit, the total Exosome Isolation Kit (from plasma) (Invitrogen). To check the purity and concentration of enriched exosomes, we sent exosome from three samples for nanoparticle tracking analysis. The nanoparticle tracking analysis results showed that plasma exosomes isolated with this precipitation commercial kit had good purity, with mean sizes and mode sizes from three samples were all smaller than 150 nm, though they had slightly different size distribution (Figure 9). Most of the particles fell in <150 nm range. Exosomes from different patients had varies concentrations, but all three samples had more than 10^8 particles obtained from 200 µl plasma (Figure 9).

In comparison, we used ExoEasy kit, which is a membrane-based affinity binding step to isolate exosomes and other EVs from plasma, to enrich exosomes and EVs from BCI150. The exosomes and EVs isolated using exoEasy kit showed larger particle size than our exosome precipitation kit and the particles sizes mainly fell into two ranges, <100 nm and 200-300 nm (Figure 10). Comparing to ExoEsy, the total Exosome Isolation Kit (from plasma) (Invitrogen) showed better specificity of isolating exosomes (which are of smaller sizes than other EVs). Therefore, the total Exosome Isolation Kit (from plasma) (Invitrogen) was used for exosome isolation from clinical plasma samples for studying exosomal miRNAs.

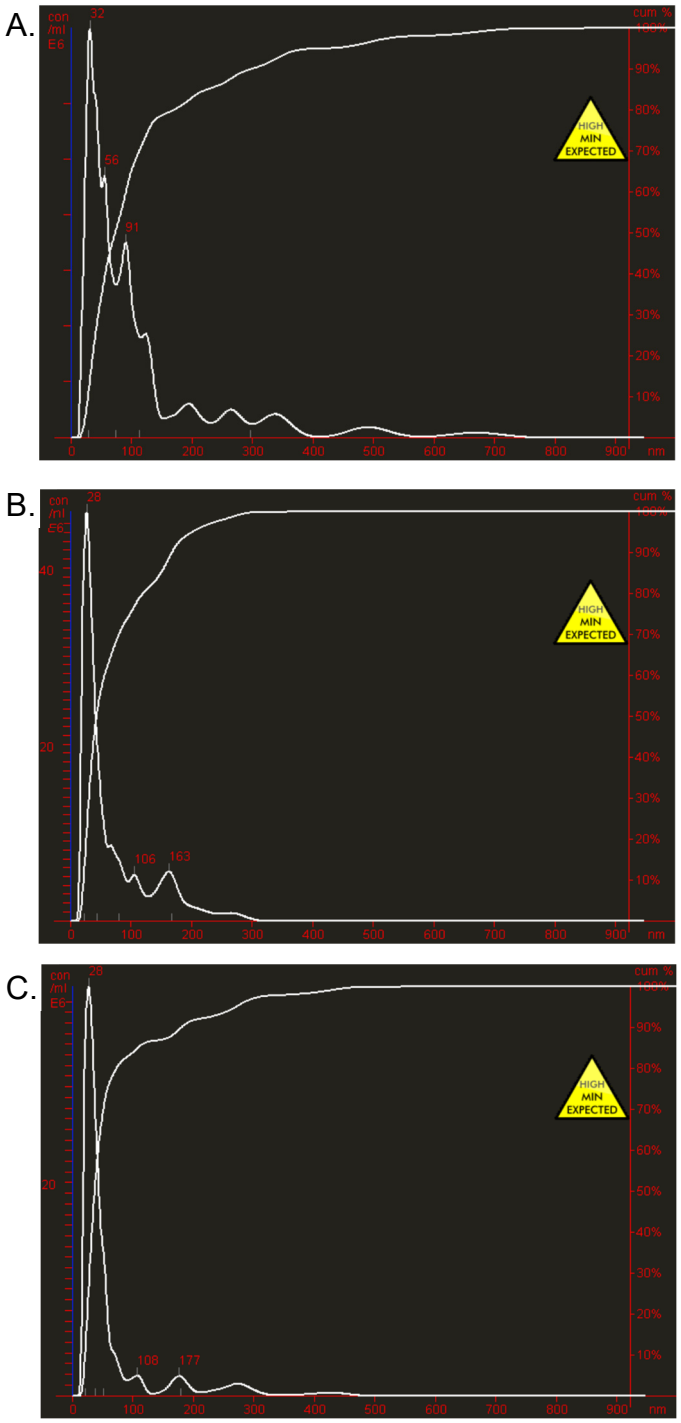

Figure 9. Nanoparticle tracking analysis of exosomes isolated from plasma of PCa patients using the Total Exosome Isolation Kit (from plasma) (Invitrogen). A. Exosomes from BCI150, mean size=122 nm, mode size=32 nm, concentration=5.47×10^8 particles/ml; B. Exosomes from BCI025, mean size=73 nm, mode size=28 nm, concentration=19.51×10^8 particles/ml; C. Exosomes from BCI158, mean size=69 nm, mode size=28 nm, concentration=13.96×10^8 particles/ml. X-axis: size (nm), Y-axis: Concentration (10^6 particles/ml)

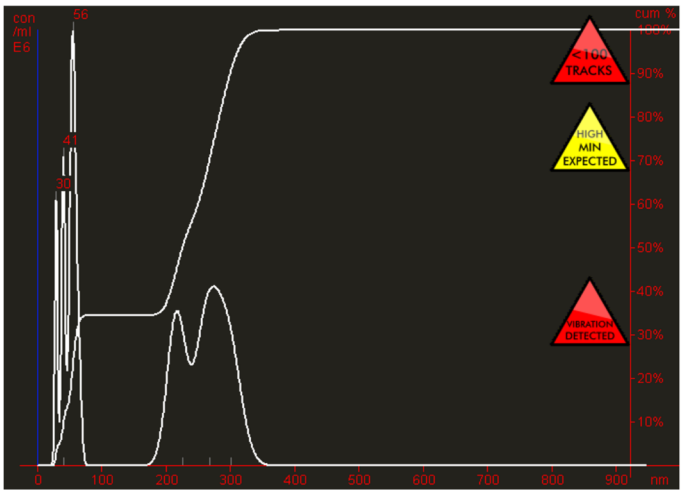

Figure 10. Nanoparticle tracking analysis of exosomes and EVs isolated from plasma of BCI150 with ExoEasy kit (Qiagen). Mean size=188nm, mode size=56nm, concentration= 0.99×10^{8} particles/ml. X-axis: size (nm), Y-axis: Concentration (10^{6} particles/ml).

3.2.2 Analysis of exosomal miRNA by RNA-sequencing

To profile the plasma exosomal miRNA expression pattern in treatment-naive PCa and CRPC, exosomes were isolated from 200 µl plasma of 24 treatment-naive PCa patients and 24 CRPC patients using the Total Exosome Isolation Kit (from plasma) (Invitrogen) and exosomal RNA was extracted from each sample (these samples were processed together with Dr. Yang Wang). All treatment-naive PCa had no metastasis. Most CRPC patients had metastasis that 20 out of the 24 CRPC patients had metastasis including regional lymph nodes metastasis and metastasis information for 2 patients was unavailable. Patients' data was summarised in Table 17. Detailed information for each patients was listed in **Appendix I** .

Exosomal RNA samples were sent for bioanalyzer, but the concentration was very low that did not show clear bands in bioanalyzer (Figure 11). To determine the existence of miRNA, RT-qPCR of miR-17, which was used as miRNA endogenous control in previous studies, was performed (performed by Dr. Yang Wang), In RT-qPCR, Ct of miR-16 were all less than 27, showing the potential of evaluating miRNA expression in these samples.

Table 17. Summary of clinical characteristics of patients in the RNA-sequencing.

	Treatment-naive PCa	**CRPC**
Number of cases	24	24
Age at sample collection, year, median(IQR)	65.15 (56.125-70.725)	75.55 (68.75-81.875)
Gleason score at diagnose		
6	8	1
7	16	2
8	0	5
>=9	0	9
unknown	0	7
Median PSA at sample collection, ng/ml (IQR)	9.9(6.9-12.75)	51(17.75-241.8)

IQR: interquartile range; Prostate cancer: PCa; CRPC: castration-resistant prostate cancer; PSA: prostate-specific antigen.

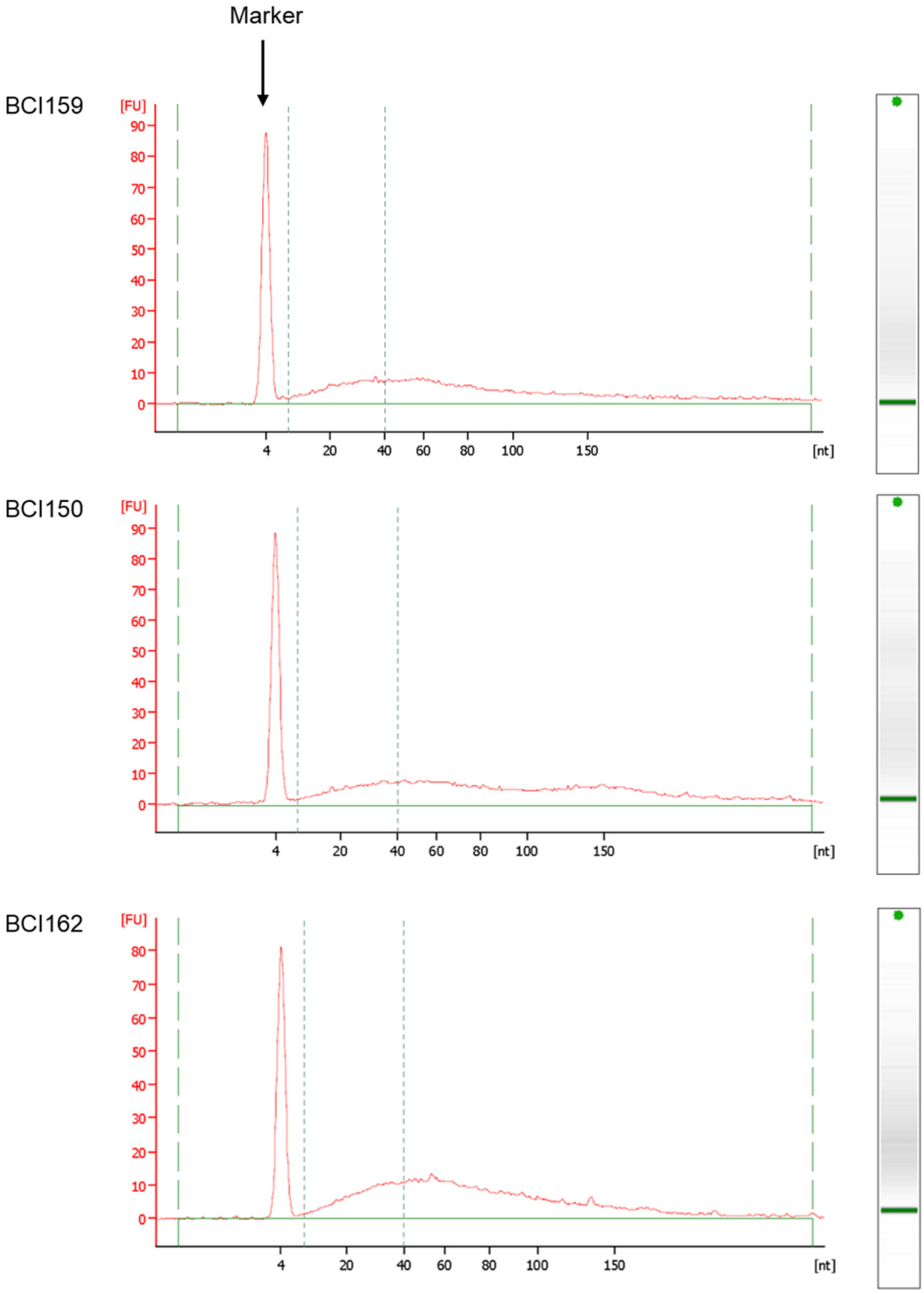

Figure 11. Representative Bioanalyzer results of exosomal RNA.

Due to the low amount of RNA that we could obtained from exosomes from small volume of plasma, first attempt of library preparation with size selection failed. Thus, we later did not perform size selection and RNA-sequencing was run twice for each sample and reads from two runs were combined. From the two runs, an average of 5-million reads per sample was generated. As no size selection was performed during sample preparation, large number of the reads were from other RNA species and primer dimers. After alignment and annotation, 0.2% of raw reads were aligned to mature miRNAs. A total of 612 plasma exosome miRNAs were detected, with 483 detected in treatment-naive PCa and 499 in CRPC. Reads of all miRNAs for all samples are provided in **Appendix II**.

There were 37 miRNAs which consistently expressed in all samples (Table 18). 45 miRNAs expressed in all CRPC samples (Table 18) and 45 miRNAs expressed in all treatment-naive PCa samples (Table 18). On average, miR-451a was the most abundant miRNA in both treatment-naive PCa and CRPC. The top ten most abundant miRNAs detected in two groups were same and list in Table 19. Although the rankings for each miRNAs in two groups are different, in general, the top ten most abundant miRNAs are the same within two groups.

Table 18. Plasma exosomal miRNAs expressed in all RNA-sequencing samples/ all treatment-naive PCa samples/ all CRPC samples.

All samples	**treatment-naive PCa**	**CRPC**
let-7a-5p	let-7a-5p	let-7a-5p
let-7b-5p	let-7b-5p	let-7b-5p
let-7c-5p	let-7c-5p	let-7c-5p
let-7f-5p	let-7d-5p	let-7d-3p
let-7g-5p	let-7f-5p	let-7e-5p
let-7i-5p	let-7g-5p	let-7f-5p
miR-10a-5p	let-7i-5p	let-7g-5p
miR-10b-5p	miR-101-3p	let-7i-5p
miR-122-5p	miR-10a-5p	miR-10a-5p
miR-126-3p	miR-10b-5p	miR-10b-5p
miR-128-3p	miR-122-5p	miR-122-5p
miR-148a-3p	miR-126-3p	miR-125a-5p
miR-150-5p	miR-128-3p	miR-126-3p
miR-151a-3p	miR-148a-3p	miR-128-3p
miR-181a-5p	miR-150-5p	miR-143-3p
miR-183-5p	miR-151a-3p	miR-146a-5p
miR-191-5p	miR-16-5p	miR-148a-3p
miR-192-5p	miR-181a-5p	miR-150-5p
miR-21-5p	miR-183-5p	miR-151a-3p
miR-22-3p	miR-185-5p	miR-155-5p
miR-24-3p	miR-191-5p	miR-181a-5p
miR-25-3p	miR-192-5p	miR-183-5p
miR-26a-5p	miR-21-5p	miR-191-5p
miR-27a-3p	miR-22-3p	miR-192-5p
miR-30a-3p	miR-24-3p	miR-21-5p
miR-30d-5p	miR-25-3p	miR-22-3p
miR-30e-3p	miR-26a-5p	miR-24-3p
miR-320a	miR-27a-3p	miR-25-3p
miR-320b	miR-30a-3p	miR-26a-5p

miR-423-3p	miR-30c-5p	miR-27a-3p
miR-423-5p	miR-30d-5p	miR-30a-3p
miR-451a	miR-30e-3p	miR-30a-5p
miR-486-5p	miR-3168	miR-30d-5p
miR-532-5p	miR-320a	miR-30e-3p
miR-92a-3p	miR-320b	miR-320a
miR-99a-5p	miR-363-3p	miR-320b
miR-99b-5p	miR-423-3p	miR-423-3p
	miR-423-5p	miR-423-5p
	miR-451a	miR-451a
	miR-486-5p	miR-486-3p
	miR-532-5p	miR-486-5p
	miR-629-5p	miR-532-5p
	miR-92a-3p	miR-92a-3p
	miR-99a-5p	miR-99a-5p
	miR-99b-5p	miR-99b-5p

Table 19. The top ten most abundant miRNAs in plasma exosomes from RNA-sequencing.

miRNA	**Read counts**	
	treatment-naive PCa	CRPC
let-7a-5p	10785	11740
let-7b-5p	21445	23510
let-7i-5p	9428	13628
miR-122-5p	6840	32435
miR-126-3p	25910	18888
miR-148a-3p	5696	13845
miR-423-5p	17712	18064
miR-451a	65849	59687
miR-486-5p	32939	30138
miR-92a-3p	13134	14054

3.2.3 MiRNAs differential expression analysis

Three analysis methods (Limma, TMM and CPM) were applied to identify differentially expressed exosomal miRNAs in treatment-naive PCa and CRPC patients. These three analyses resulted in three different lists of differentially expressed miRNAs with 13, 13, and 11 miRNAs with $p<0.01$ for Limma, TMM and CPM respectively (Table 20). There are five miRNAs (miR-423-3p, miR-99a-5p, miR-320a, miR-200a-3p and miR-193a-5p) showed significant differential expression ($p< 0.01$) between treatment-naive PCa and CRPC patients in three analyses (Table 20). These five miRNAs were all higher expressed in CRPC exosomes.

Table 20. Significantly differentially expressed plasma exosomal miRNAs with $p<0.01$ between treatment-naive PCa and CRPC identified by RNA-sequencing.

Limma		**TMM**		**CPM**	
MiRNA	*p*-value*	MiRNA	*p*-value*	MiRNA	*p*-value*
miR-375	0.000373	miR-375	5.71×10^{-11}	**miR-423-3p**	0.00042
miR-193a-5p	0.000393	**miR-193a-5p**	1.32×10^{-5}	miR-21-5p	0.00106
miR-101-3p	0.000907	miR-9-5p	1.56×10^{-5}	**miR-320a**	0.0011
miR-451a	0.001702	miR-184	9.39×10^{-5}	**miR-193a-5p**	0.00207
miR-320b	0.001728	**miR-200a-3p**	0.0004	miR-451a	0.00261
miR-320a	0.003068	miR-320b	0.00049	miR-24-3p	0.00325

miR-423-3p	0.004791	miR-148a-3p	0.00104	**miR-99a-5p**	0.00474
miR-148a-3p	0.005329	**miR-99a-5p**	0.0017	miR-146a-5p	0.00778
miR-150-5p	0.005872	miR-150-5p	0.00263	**miR-200a-3p**	0.00833
miR-342-5p	0.006394	miR-320d	0.0029	miR-22-5p	0.00921
miR-200a-3p	0.00655	**miR-320a**	0.00326	miR-320d	0.00982
miR-99a-5p	0.008049	**miR-423-3p**	0.00327		
miR-30c-5p	0.008837	miR-122-5p	0.00707		

*_p_-values without multiple test adjustment. MiRNAs showed significant difference in all three analyses are in bold. Limma: Linear Models for Microarray and RNA-sequencing Data; CPM: counts per million transformation; TMM: the trimmed mean of M-value normalisation.

3.2.4 Prediction value of exosomal miRNA for CRPC

To evaluate the predictive value of plasma exosomal miRNAs for CRPC, I performed ROC curves analysis using the CPM values of the five exosomal miRNAs which showed significant difference between treatment-naive PCa and CRPC in all three analyses. The AUC values of miRNAs were similar as the AUC of PSA, which all showed moderate prediction efficiency of CRPC (Figure 12, Table 21).

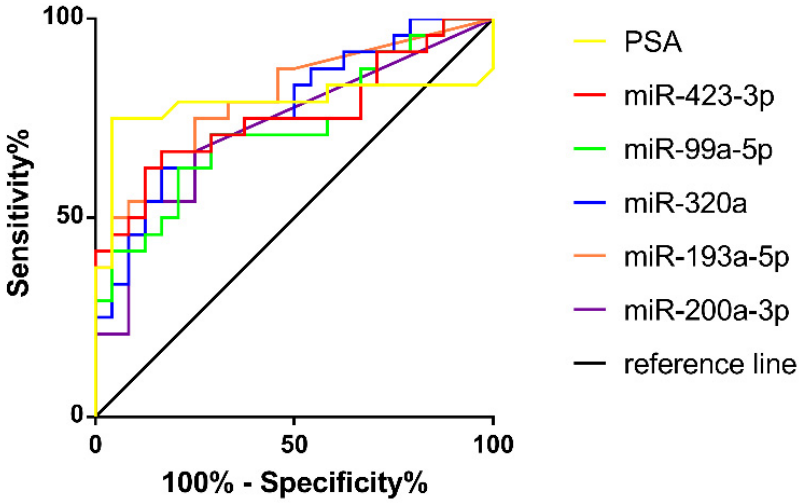

Figure 12. ROC curves analyses of PSA and miRNAs which showed significant difference between treatment-naive PCa and CRPC in all three RNA-sequencing analyses. This ROC curves analyses of miRNAs were performed using the count-per-million values from RNA-sequencing data. Large under the curve area indicates good prediction value with high sensitivity and high specificity.

Table 21. AUCs and p-values from ROC curves analysis results of PSA level and miRNAs which showed significant difference between treatment-naive PCa and CRPC in all three RNA-sequencing analyses for CRPC prediction.

	AUC	**95% CI**	***p*-value**
miR-423-3p	0.7587	0.6185 to 0.8988	0.0021
miR-99a-5p	0.7257	0.5811 to 0.8703	0.0074
miR-320a	0.7674	0.6347 to 0.9001	0.0015
miR-193a-5p	0.8038	0.6791 to 0.9286	0.0003
miR-200a-3p	0.7292	0.5842 to 0.8742	0.0065
PSA	0.7865	0.6342 to 0.9388	0.0007

3.2.5 In silicon analysis of published publically available plasma exosomal RNA-sequencing

To date, exosomal RNA-sequencing data in PCa has mainly come from studies from Liang Wang's group [103, 175, 346]. Huang *et al.* reported their study of plasma exosomal RNA in 2016 using RNA-sequencing, which included samples from 50 healthy individuals, 100 colorectal cancer, 15 hormone-sensitive PCa (HSPC), 21 CRPC and 6 pancreatic cancer patients [346]. They scaled their sequencing data as read counts per million mapped reads (RPM, which is equal to CPM). I took the data of their list of the RNA transcripts with average log2 transformed RPM >5, which were in total 187 human mature miRNAs with average log2 RPM>5 (as in their supplementary table 1), and did further analysis of the PCa and healthy control data.

204 human mature miRNAs with average log2 CPM>5 were detected in our study, where 113 are shared with the 187 miRNAs detected in Huang's study. 32 of their 187 miRNAs were not detected in our mapped reads. The top ten most abundant miRNAs detected in Huang's study are listed in Table 22. Although the rankings (by abundance) for each miRNAs in each sample groups are different, in general, the top ten most abundant miRNAs were the same within three groups. Let-7i-5p was within the top ten most abundant miRNAs in both our study and Huang's. The top ten most abundant exosomal miRNAs detected in our study all present in top 65 in Huang's data. The top ten most abundant exosomal miRNAs detected in Huang's study were all detected in our study, with seven miRNAs ranked in top 37 most abundant. The other three miRNAs had lower expression as miR-181b-5p ranked at 111, miR-129-5p ranked at 166, and miR-9-3p ranked at 542 with expression in only one sample.

Table 22. Top ten most abundant miRNAs in plasma exosomes in data from Huang *et al.* [346].

N	**HSPC**	**CRPC**
miR-99a-5p	miR-99a-5p	miR-99a-5p

miR-128-3p	miR-129-5p	miR-129-5p
miR-129-5p	miR-22-3p	miR-22-3p
miR-22-3p	hsa-let-7i-5p	miR-128-3p
miR-181a-5p	miR-128-3p	miR-9-3p
miR-9-3p	miR-181a-5p	miR-181a-5p
miR-100-5p	miR-320a	miR-100-5p
miR-181b-5p	miR-9-3p	miR-181b-5p
hsa-let-7i-5p	miR-181b-5p	miR-320a
miR-320a	miR-100-5p	hsa-let-7i-5p

N: healthy individual; HSPC: hormone-sensitive prostate cancer; CRPC: castration-resistant prostate cancer.

I analysed differentially expressed miRNAs in plasma exosomes between healthy individuals and HSPC patients in Huang's study using the RPM data and Welch's t-test [346]. The top ten most significantly differentially expressed miRNAs are listed in Table 23**.** None of the identified top ten differentially expressed miRNAs shown significant difference in our RNA-sequencing data comparing treatment-naive PCa and CRPC.

Table 23. Top ten differentially expressed miRNAs in plasma exosomes between healthy individuals and hormone-sensitive PCa patients in data from Huang *et al.* [346].

miRNA	***p*-value**
miR-490-5p	2.77×10^{-6}
miR-1343-3p	9.19×10^{-5}
miR-204-3p	0.000161
let-7i-3p	0.000228
miR-181b-5p	0.000325
miR-130a-3p	0.000515
miR-125a-5p	0.000803
miR-874-3p	0.001184
miR-423-5p	0.001921
miR-7-5p	0.002411

I then identified differentially expressed miRNAs in plasma exosomes between HSPC and CRPC patients in Huang's study using the RPM data and Welch's t-test [346]. The top ten most significantly differentially expressed miRNAs are listed in Table 24**.** Six of the top ten most significantly differentially expressed miRNAs had low expression in our sequencing (expressed in less than 25% samples) and had been filtered out before our differentially expression analyses. The remaining four miRNAs were not significantly differentially expressed in our CPM analysis (unadjusted *p*-value for miR-125b-5p, miR-425-5p, miR-99b-3p and miR-652-3p was 0.085, 0.150, 0.414, and 0.533, respectively). I identified 11 miRNAs differentially expressed between treatment-naive PCa and CRPC by CPM method in our data, among which miR-193a-5p and miR-320d had low expression in Huang's data and were filtered out before analysis. The remaining nine miRNAs did not show difference at $p<0.01$ in the Huang's data (unadjusted *p*-value for miR-423-3p, miR-21-5p, miR-320a, miR-451a, miR-24-3p, miR-99a-5p, miR-146a-5p, miR-200a-3p, and miR-22-5p was 0.1572, 0.5134, 0.2342, 0.8675, 0.1139, 0.0318, 0.0102, 0.0442, and 0.8801, respectively).

Table 24. Top ten most significantly differentially expressed miRNAs in plasma exosomes between hormone-sensitive PCa and CRPC patients in data from Huang *et al.* [346]

miRNA	p-value
miR-490-5p	0.001165
miR-105-5p	0.00134
miR-132-5p	0.001527
miR-652-3p	0.002409
miR-99b-3p	0.002864
miR-125b-5p	0.002935
miR-885-3p	0.003477
miR-425-5p	0.00397
miR-4448	0.004029
miR-181c-3p	0.005081

3.3 Discussion

3.3.1 Exosomal miRNA profiling

Exosome is a major member of cell-derived vesicles that has been massively investigated in recent years. It has been demonstrated that exosomes play important roles for intercellular communication and could serve as potential biomarkers for particular disease status. MiRNAs, as important small non-coding RNAs, play important roles in post-transcriptional regulation of biological processes [349]. The expression profiles of miRNAs vary widely in normal and tumour tissues [123-125]. Study of miRNAs carried in exosomes have shown that miRNAs are stably protected by exosomes in circulation and can be functionally active and transferred between cells [347, 350, 351]. Thus, investigation of miRNA contents in exosomes may shed light on discovery of new non-invasive biomarkers, as well as providing novel insight into the biological roles mediated by exosomes. Up to date, several resources have deposited the RNA contents in

exosomes, such as ExoCarta [352] , EVpedia [353], exoRBase [354] and EVmiRNA [355], which collect RNA expression data from publications. However, the most extensive exosomal RNA profile data in PCa has mainly come from RNA-sequencing studies from Wang's group [103, 175, 346]. In the current study, we used RNA-sequencing to generate miRNA expression profile in plasma exosomes from treatment-naive PCa and CRPC patients. We generated individual libraries from 24 treatment-naive PCa and 24 CRPC patients without pooling cases together, thus significantly contributed to the current data for exosomal miRNAs in PCa.

Our data present similar features in terms of the most abundant miRNAs from published exosomal RNA-sequencing data from other groups [350, 356, 357], which showed the reliability of our RNA-sequencing results. In our cohort, we found examples of highly expressed exosomal miRNAs that were previously reported as abundant circulating miRNAs in serum/plasma. Among the top ten highly expressed exosomal miRNAs, 5 miRNAs (miR-122-5p, miR-148-3p, miR-423-5p, miR-486-5p, miR-451a) were also identified as top ten highly expressed miRNAs in a previous RNA-sequencing study evaluating RNAs in healthy donors' serum [358]. MiR-451a is the most abundant miRNA we detected, and it is also reported as the most abundant miRNA in plasma from participants of an on-going cardiovascular disease study [359]. As we used RNase to treat our plasma samples to degrade RNAs outside exosomes, these shared abundant miRNAs in our exosomes and previous reported miRNAs in plasma/serum may suggest that most detectable miRNAs in plasma/serum are embedded in exosomes.

To be noted, our RNA-sequencing profiles present slightly different features in terms of most abundant miRNAs as previous published data from Wang's group [103, 175, 346]. We observed that the top ten most abundant miRNAs were all the same within different sample groups in each study, but different across two studies. As the exosome isolation methods, RNA-sequencing library preparation and reads alignment methods used in two studies were totally different. This may indicate that the workflow used could significantly influence the miRNA detection in RNA-sequencing and may have certain bias on detecting some miRNAs. The effects of vesicle isolation methods, RNA extraction, sequencing library preparation or gel size selection on RNA profiling using RNA-sequencing have

been previously demonstrated by Huang *et al.* [346]. After RNA-sequencing, the software packages and methods for miRNA-sequencing data processing and alignment to generate miRNA reads could also affect the final results [360]. The different workflows used between studies makes it difficult to compare miRNA expression across studies. Thus, it is critical to establish a standardised pipeline for studies of exosomal RNAs.

3.3.2 Differentially expressed miRNAs between treatment-naive PCa and CRPC identified by RNA-sequencing

After generating RNA read counts in RNA-sequencing, RNA read counts are normally sent for normalisation to remove variations in the data which were caused by non-biological effects. Several normalisation methods for RNA-sequencing data have been proposed, but no standard method has currently be established. We employed three methods, Limma, CPM and TMM, to analyse our sequencing data to identify differentially expressed gene. Limma is a commonly used package for the analysis of gene expression data arising from microarray or RNA-sequencing technologies by using of linear models to assess differential expression in the context of multifactor designed experiments [340]. CPM is a simple normalisation method to be applied. However some studies have shown that it may not be sufficient to account for technical differences across samples [360, 361]. The TMM method estimates scale factors between samples and assumes that most genes are not differentially expressed. Tam *et al.* assessed several normalisation methods and demonstrated the advantage of using of TMM for the miRNA-sequencing normalisation over other methods [360]. In our study, we used three methods and the differentially expressed miRNAs lists generated from these three methods were different but sharing some miRNAs. The difference mainly came from normalisation strategy rather than statistical tests. It has been previously demonstrated that different normalisation methods for miRNA sequencing data could cause bias [360]. Our results showed that different normalisation methods would affect the analyses of differentially expression genes with different significance levels (*p*-values). As there are many methods available, it is worth to consider using different methods when analysing RNA-sequencing data for a particular study.

In our study, there are five miRNAs (miR-423-3p, miR-99a-5p, miR-320a, miR-200a-3p and miR-193a-5p) showed significant differential expression ($p < 0.01$) between treatment-naive PCa and CRPC patients in three analyses. The prediction values of all these miRNAs were similar to PSA for CRPC as determined by AUC, though miR-193a-5p showed slightly higher AUC than PSA. These data suggested potential biomarker value of exosomal miRNAs for CRPC. However, as the sample number is small, further validation in larger cohorts is required.

Chapter IV Identification of plasma exosomal miRNAs as biomarkers for CRPC

4.1 Introduction

Currently, CRPC is usually diagnosed based on biochemical and radiographic progression [39]. Radiographic progression is hard to detect in a timely fashion and needs frequent bone scans and CT scans. Biochemical progression relies on PSA level despite castrate levels of serum testosterone. However, there are various reasons for raised PSA level and the serum PSA level is not always correlated with the clinical status of CRPC [362]. Studies of CRPC biomarkers have been mainly focused on identifying prognostic markers and markers for prognosis and therapy response in CRPC [95]. Some studies have investigated CRPC-related miRNAs in cell lines [363, 364], but their clinical utility as biomarker remain invalidated. Thus, it is important to further identify biomarkers for the prediction of CRPC occurrence.

As described in Chapter III, RNA-sequencing has enabled us to characterise exosomal miRNA profiles of treatment-naive PCa and CRPC patients and identify differentially expressed exosomal miRNAs between these two groups of patients. RNA-sequencing has been commonly used in various biological applications in recent years. However, as demonstrated in previous chapter, several aspects including technique issues and data analysis methods could affect the results of differentially expressed miRNA. In addition, RNA-sequencing is much more expensive than other RNA quantification method, which, in most studies, caused limited sample number. Currently, it is still difficult to apply RNA-sequencing in daily clinic tests.

RT-qPCR is a commonly used method for quantifying gene expression in clinic. It bears several advantages including being fast, accurate, sensitive, high-throughput in terms of the number of clinical samples that can be analysed, cost-effective and requiring a small amount of sample [365]. It is the current gold standard for the evaluation and validation of miRNA biomarkers. In this chapter, we examined candidate miRNAs identified by exosome RNA-sequencing in Chapter III in a larger cohort of patients using RT-qPCR and investigated the value of exosomal miRNAs as biomarker for CRPC.

4.2 Results

4.2.1 Fluidigm validation of differentially expressed exosomal miRNAs

To facilitate the validation of a large number of miRNAs from the RNA-sequencing data in a large number of samples, we firstly selected 32 miRNAs including 3 endogenous control candidates (miR-30e-3p, miR-30a-5p and let-7c-5p) and quantified their expression levels with Fluidigm in a cohort of 52 treatment-naive PCa and 42 CRPC patients. Most treatment-naive PCa had no metastasis (92.3%), with only four patients had N1 disease (7.7%). Most of the CRPC patients had metastasis (90.5%), with only two patients without metastasis (4.8%) and four patients had no information for metastasis status. Patients' information is summarised in Table 25. The detailed patients' information is provided in **Appendix I**.

Table 25. Summary of clinical characteristics of patients in the Fluidigm validation cohort.

	Treatment-naive PCa	**CRPC***
Number of cases	52	42
Age at sample collection, yr, median (IQR)	65.45 (58.63-69.75)	74.5 (69.02-81.25)
Gleason score at diagnose		
6	27	1
7	17	2
8	2	3
>=9	5	14
unknown	1	10 (including one NEC)

Median PSA at sample collection, ng/ml (IQR)	7.5 (5.32-11.93)(missing two patients' data)	65 (20.5-335)(missing one patient's data)

IQR: interquartile range; PCa: prostate cancer; CRPC: castration-resistant prostate cancer; PSA: prostate-specific antigen; NEC: neuroendocrine carcinoma. * including 21 patients used for RNA-sequencing.

Three miRNAs were initially selected as endogenous controls based on their stable expression across all samples in RNA-sequencing and previous reports [103, 175, 346]. However, in Fluidigm, miR-30e-3p was undetectable in five samples (Ct > 40 in two or all three technical replicate wells). Thus, miR-30a-5p and let-7c-5p were used as endogenous control. After Bonferroni correction of the *p*-values, there were 13 miRNAs showed significant difference between treatment-naive PCa and CRPC with $p< 0.05$ (Table 26).

.

Table 26. List of plasma exosomal miRNAs and their *p*-values/ corrected p-values evaluetd using Fluidigm.

MiRNA	*p*-value	Corrected *p*-value
miR-99a-5p	8.81×10^{-10}	2.55×10^{-08}
miR-100-5p	2.73×10^{-09}	7.91×10^{-08}
miR-125b-5p	1.23×10^{-08}	3.55×10^{-07}
let7b-3p	3.02×10^{-06}	0.00009
miR-320b	4.36×10^{-06}	0.00013
miR-320a	0.00001	0.00019
miR-744-5p	0.00001	0.00039
miR-200a-3p	0.00001	0.00042
miR-24-3p	0.00010	0.00277
miR-193a-5p	0.00013	0.00367
miR-148a-3p	0.00032	0.00933
miR-146a-5p	0.00059	0.01703
miR-4433b-3p	0.00087	0.02509

miR-30c-5p	0.00358	0.10390
miR-150-5p	0.01038	0.30102
miR-9-5p	0.01133	0.32845
miR-22-5p	0.01317	0.38181
miR-184	0.02637	0.76481
miR-451a	0.02637	0.76481
miR-122-5p	0.03138	0.91000
miR-320d	0.05247	
miR-423-3p	0.07148	
miR-1246	0.08990	
miR-125a-3p	0.14011	
miR-101-3p	0.26359	
miR-7706	0.27014	
miR-320c	0.44695	
miR-20b-5p	0.67574	
miR-375	0.91521	

I performed ROC analysis of PSA and the plasma exosomal miRNAs, which showed Bonferroni corrected $p<0.05$ from Fluidigm data, for the correlation with CRPC. The result showed that many plasma exosomal miRNAs had high AUCs and the AUC of miR-99a-5p was better than PSA (Figure 13, Table 27).

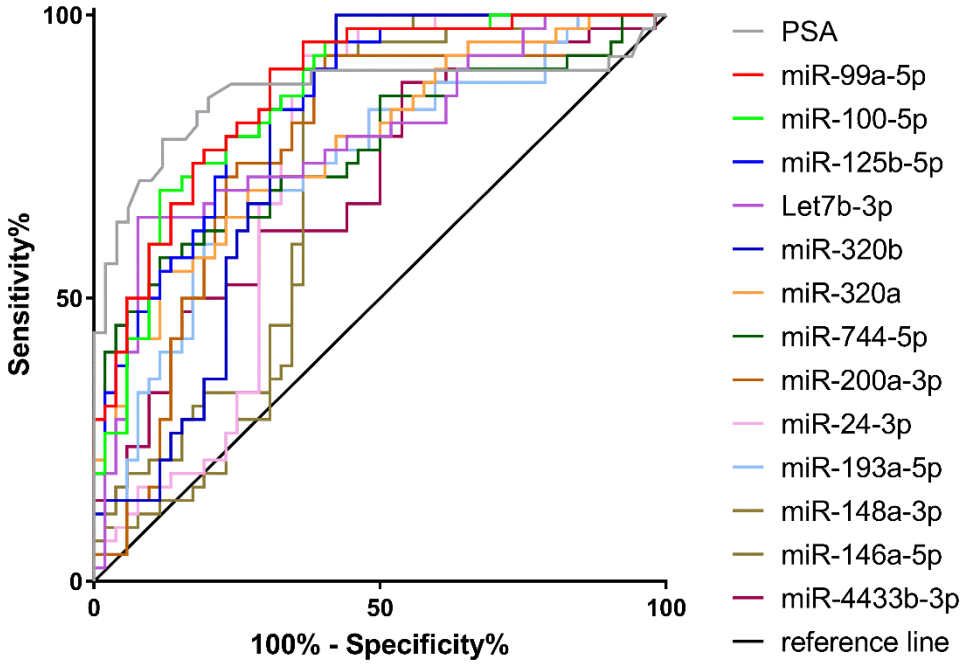

Figure 13. ROC analysis of Fluidigm data of plasma exosomal miRNAs and PSA for prediction of CRPC from treatment-naive PCa. Large under the curve area indicates good prediction value with high sensitivity and high specificity.

Table 27. ROC curves to predict CRPC from treatment by Fluidigm data of plasma exosomal miRNAs and PSA level.

	Area	**95% confidence interval**	***p*-value**
PSA	0.861	0.7714 to 0.9505	<0.0001
miR-99a-5p	0.869	0.7989 to 0.9392	<0.0001
miR-100-5p	0.8581	0.7841 to 0.9320	<0.0001
miR-125b-5p	0.8429	0.7659 to 0.9200	<0.0001
let7b-3p	0.7811	0.6852 to 0.8771	<0.0001
miR-320b	0.7766	0.6803 to 0.8728	<0.0001
miR-320a	0.7715	0.6769 to 0.8661	<0.0001

miR-744-5p	0.7619	0.6614 to 0.8624	<0.0001
miR-200a-3p	0.761	0.6594 to 0.8626	<0.0001
miR-24-3p	0.7349	0.6295 to 0.8402	<0.0001
miR-193a-5p	0.7308	0.6277 to 0.8338	0.0001
miR-148a-3p	0.7166	0.6103 to 0.8229	0.0003
miR-146a-5p	0.707	0.5968-0.8171	0.0006
miR-4433b-3p	0.7005	0.5944-0.8067	0.0009

The Fluidigm results showed plasma miRNAs had great prediction value for CRPC. However, within the 13 miRNAs which showed significant (adjusted p< 0.05) difference between treatment-naive PCa and CRPC in Fluidigm, there are four miRNAs which had opposite expression pattern as they were identified in RNA-sequencing (Table 28). MiR-100-5p was found expressed higher in CRPC in the Fluidigm validation but expressed lower in CRPC in the RNA-sequencing data. MiR-320b, miR-320a and miR-744-5p were found expressed lower in CRPC in the Fluidigm validation but expressed higher in CRPC in the RNA-sequencing. These conflict results led to our further validation of plasma exosomal miRNA expression using traditional RT-qPCR.

Table 28. Summary of significantly differentially (adjusted p-value <0.01) expressed plasma exosomal miRNAs between treatment-naive PCa and CRPC identified by Fluidigm and their expression patterns in RNA-sequencing*.

MiRNA	Fluidigm result	adjusted p-value	RNA-sequencing result
miR-99a-5p	high in CRPC	2.5537×10^{-08}	high in CRPC
miR-100-5p	**high in CRPC**	**7.9124×10^{-08}**	**low in CRPC**

miR-125b-5p	high in CRPC	3.5530×10^{-07}	high in CRPC
let-7b-3p	high in CRPC	8.7559×10^{-05}	high in CRPC
miR-320b	**low in CRPC**	**1.2643×10^{-04}**	**high in CRPC**
miR-320a	**low in CRPC**	**0.0002**	**high in CRPC**
miR-744-5p	**low in CRPC**	**0.0004**	**high in CRPC**
miR-200a-3p	high in CRPC	0.0004	high in CRPC
miR-24-3p	high in CRPC	0.0028	high in CRPC
miR-193a-5p	high in CRPC	0.0037	high in CRPC
miR-148a-3p	high in CRPC	0.0093	high in CRPC
miR-146a-5p	high in CRPC	0.01703	high in CRPC
miR-4433b-3p	high in CRPC	0.02509	high in CRPC

*MiRNAs showed opposite expression pattern between Fluidigm and RNA-sequencing are in bold.

4.2.2 RT-qPCR confirmation of differentially expressed plasma exosomal miRNAs in treatment-naive PCa and CRPC patients

As the Fluidigm system results are inconsistent to RNA-sequencing data, I used the conventional RT-qPCR to investigate the plasma exosomal miRNA expression between treatment naive PCa and CRPC patients in a larger cohort of cases. MiRNAs were re-selected based on the RNA-sequencing data and many of them have been included in the Fluidigm analysis. Plasma samples from 108 treatment-naive PCa and 42 CRPC patients (including 24 patients whose plasma exosomal miRNAs had been analysed both by in RNA-sequencing and the Fluidiam) were used. Most treatment-naive PCa patients had no metastasis (95.4%), with only five patients bearing metastasis including regional lymph nodes metastasis. Most of the CRPC patients had metastasis including regional

lymph nodes metastasis (81%), with only two patients without metastasis (4.8%) and six patients had no metastasis information. Patients' data were summarised in Table 29 and detailed information is listed in **Appendix I.**

Table 29. Summary of clinical characteristics of patients in the RT-qPCR validation cohort.

	Treatment-naive PCa	**CRPC***
Number of cases	108	42
Age at sample collection, yr, median (IQR)	65.90 (57.875-72.1)	72.65 (68.375-80.875)
Gleason score at diagnose		
6	36	1
7	58	7
8	6	8
>=9	8	16
unknown	0	10
Median PSA at sample collection, ng/ml (IQR)	8.9 (5.75-13)	57 (21.5-192.25)

IQR: interquartile range; PCa: prostate cancer; CRPC: castration-resistant prostate cancer; PSA: prostate-specific antigen. * including 24 patients used for sequencing

There are five miRNAs which showed significant difference in three sequencing data analyses. Among them, one miRNA, miR-200a-3p expressed at very low level which cannot be detected by our RT-qPCR method in many samples. In the 126 evaluated sample, 76 samples had Ct larger than 35 or undetected of miR-200a-3p. This is consistent to Fluidigm data, in which 35 out of 94 samples had no detection of miR-200a-3p. Out of the remaining four miRNAs, three miRNAs, miR-423-3p, miR-320a and miR-99a-5p were significantly differentially expressed between treatment-naive PCa patients and CRPC (p= 7.3×10^{-8}, 0.002 and 0.0186, respectively) (Figure 14A). Consistent to the RNA-sequencing data, these three miRNAs expressed at higher levels in CRPC compared to treatment-naive PCa. MiR-193a-5p did not show significant difference between treatment-naive PCa and CRPC in the RT-qPCR cohort (Figure 14A).

We also tested six miRNAs which showed significant difference in two of the three analysis methods of RNA-sequencing data. Among these six miRNAs, miR-375 could not be detected efficiently by our RT-qPCR method, with 118 out of 126 samples evaluated presented Ct over 30 while Ct of negative control (water) presented at 32.9 which was close to the Ct of samples. This problem was also observed in Fluidigm, where 41 out of the 94 samples had more than 2 or 3 wells of three technical replicates had failed quality score. Of the remaining five miRNAs, three miRNAs, miR-320d, miR-320b and miR-150-5p were significantly differentially expressed (p= 0.0028, 0.0013 and 0.0058, respectively) (Figure 14B) and miR-148a-3p and miR-451a showed no difference between treatment-naive PCa and CRPC (p= 0.95 and 0.98 respectively) (Figure 14B).

Four miRNAs which showed significant difference in one of the three analysis methods were also checked. MiR-101-3p, miR-21-5p and miR-24-3p showed no difference in the RT-qPCR validation (p= 0.086, 0.17 and 0.075, respectively)

(Figure 15). MiR-9 had too low expression to be detected, as 92 out of 126 evaluated samples had undetected level or Ct>35.

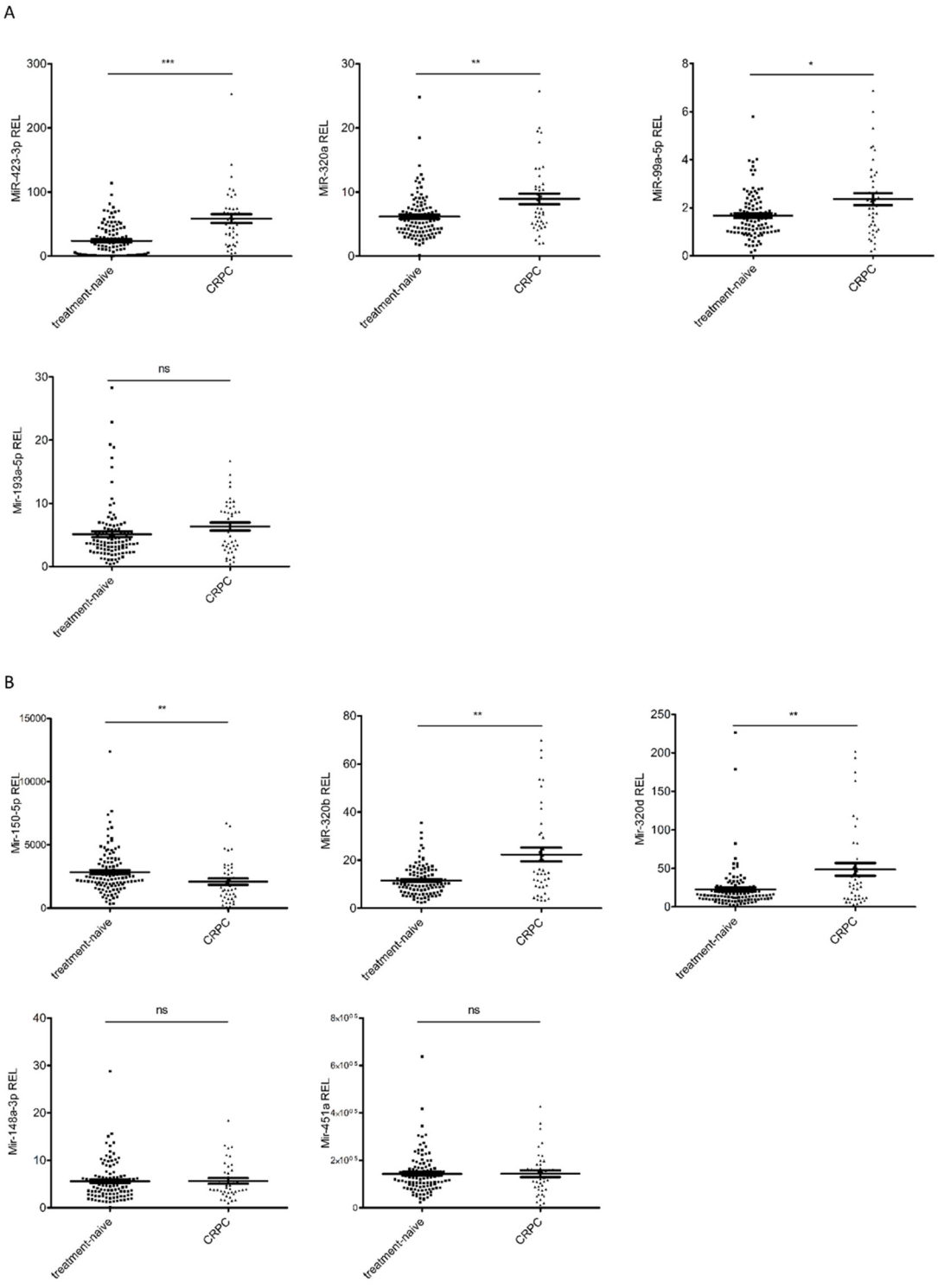

Figure 14. RT-qPCR evaluation of plasma exosomal miRNAs in treatment-naive PCa and CRPC. A. MiRNAs identified by three RNA-sequencing analyses; B. MiRNAs identified by two RNA-sequencing analyses.

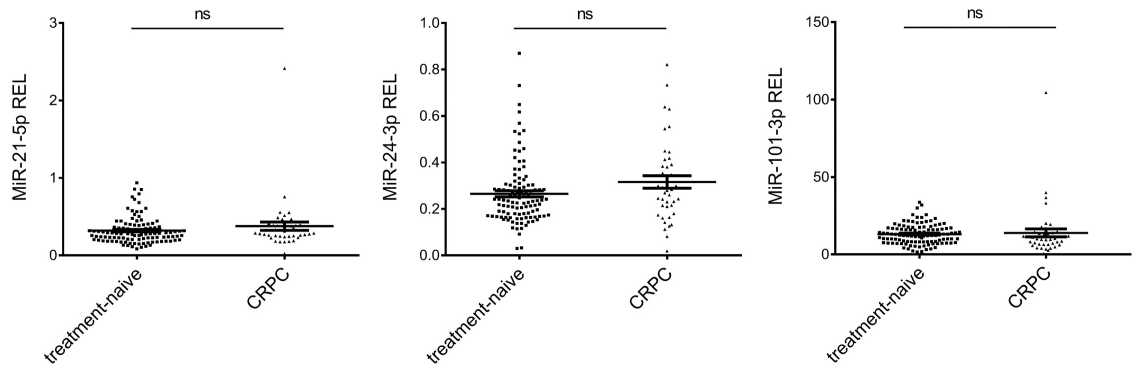

Figure 15. RT-qPCR evaluation of plasma exosomal miRNAs in treatment-naive PCa and CRPC which were identified by one RNA-sequencing analysis.

4.2.3 Independent validation of miR-423-3p in MCW centre

The most significantly differentially expressed plasma exosomal miRNA, miR-423-3p, was then evaluated in MCW by Professor Liang Wang's team. 30 treatment-naive PCa and 30 CRPC samples were used. The patients' information is summarised in Table 30. Although different exosomal isolation method was used, in the MCW cohort, miR-423-3p also showed significant difference in the plasma exosomes between treatment-naive PCa and CRPC with p= 0.0163 (Figure 16A). AUC of miR-423-3p was 0.679 (95% CI= 0.542-0.817, p= 0.017). Using the same combination model generated in the Barts cohort of treatment-naive PCa and CRPC described in 4.2.5(combine model= 0.026*PSA+0.033*miR-423-3p), miR-423-3p in combination with PSA improves the prediction value of PSA alone from AUC = 0.716 (95% CI=0.5822-0.8499, p= 0.0044) to AUC = 0.729 (95% CI= 0.5963-0.8612, p= 0.0026) for CRPC (Figure 16B).

Table 30. Summary of clinical characteristics of patients in the MCW centre validation cohort.

	Treatment-naive PCa	CRPC
Number of cases	30	30
Age at sample collection, yr, median(IQR)	67.30 (63.38-80.55)	71.70 (65.85-76.58)
Gleason score at diagnose		
<=6	2	4
7	14	9
8	3	4
>=9	8	10
unknown	3	3
Median PSA at sample collection, ng/ml (IQR)	7 (1.75-28.55)(missing one patient's data)	47.7 (9.35-119)

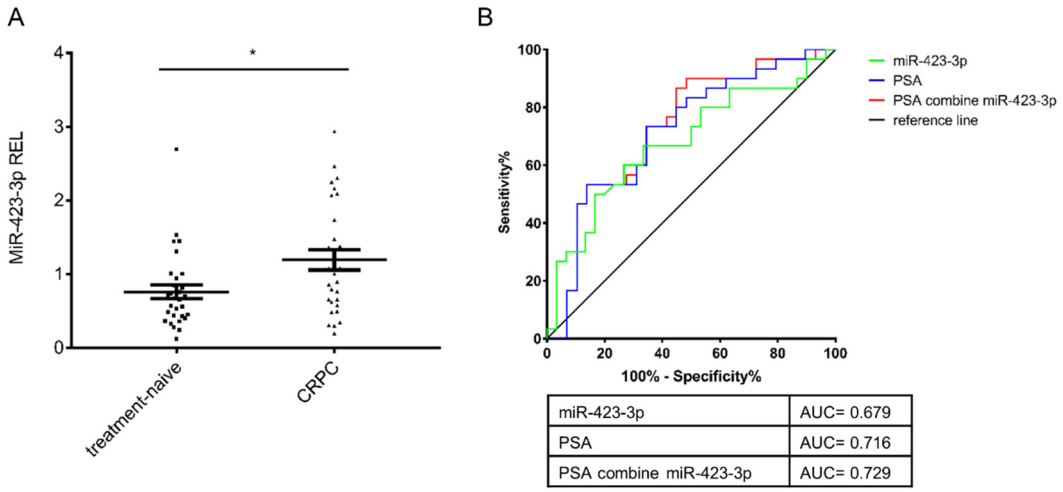

Figure 16. RT-qPCR evaluation of miR-423-3p for its CRPC prediction value in a MCW cohort. A. Scatter plots of plasma exosomal miR-423-3p expression levels; significance is defined by raw *p*-value (*p< 0.05); B. ROC analysis of the

efficiencies of miR-423-3p (AUC= 0.679, *p*= 0.017), serum PSA (AUC = 0.716, *p*= 0.0044) and the combination model of PSA and miR-423-3p (AUC = 0.729, *p* = 0.0026) in discriminating CRPC from treatment-naive PCa. Large under the curve area indicates good prediction value with high sensitivity and high specificity.

4.2.4 RT-qPCR identified differentially expressed plasma exosomal miRNAs between treated non-CRPC and CRPC patients

For above, we have validated differentially expressed exosomal miRNAs between untreated PCa and CRPC. Considering the management of PCa patients in clinics where patients receive hormone therapy before diagnosis of CRPC, I further checked the miRNAs levels in 36 PCa patients who were receiving hormone therapy but had not developed CRPC (non-CRPC). Most patients had metastasis including regional lymph nodes metastasis (75%), with eight patients (22.2%) had no metastasis and one patient had no metastasis information. The six exosomal miRNAs validated by RT-qPCR comparing untreated and CRPC patients showed interesting expression patterns within treatment-naive PCa, non-CRPC and CRPC (Figure 17). Five of the six miRNAs, miR-423-3p (*p*< 0.0001), miR-320a (*p*< 0.0001), miR-320b (*p*< 0.0001), miR-320d (*p*< 0.0001) and miR-99a-5p (*p*< 0.0001) showed significant difference between non-CRPC and CRPC. In addition, treatment-naive miR-320a (*p*= 0.0047), miR-320b (*p*< 0.0001), miR-99a-5p (*p*< 0.0001), miR-320d (*p*< 0.0001), and miR-150-5p (*p*= 0.0013) showed significant difference between treatment-naive PCa and non-CRPC, while the expression level of miR-423-3p had no significant difference in this comparison (*p*= 0.3353).

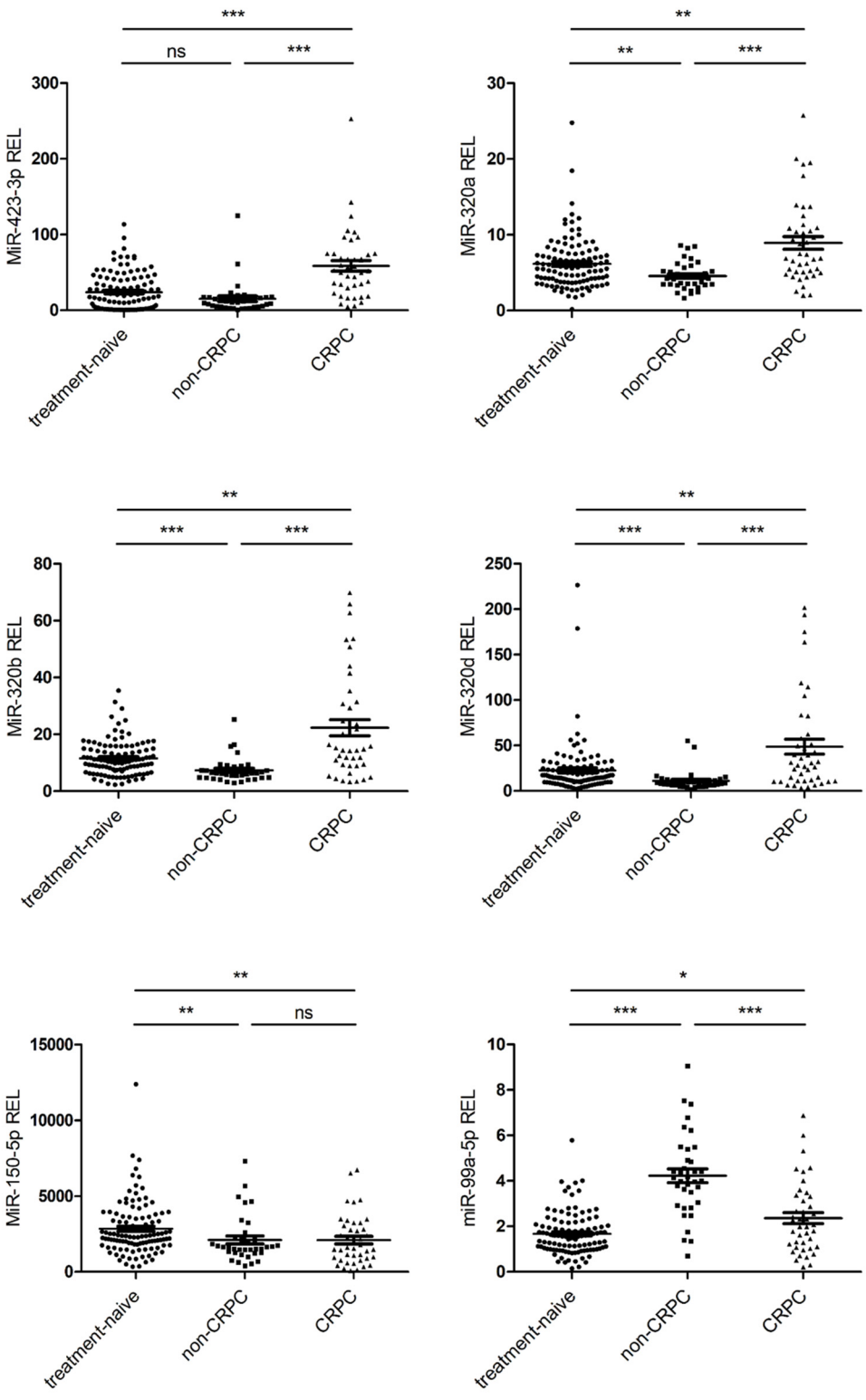

Figure 17. RT-qPCR evaluation of plasma exosomal miRNAs in treatment-naive PCa, non-CRPC and CRPC.

I then checked the expression level of five miRNAs which showed no difference between treatment-naive PCa and CRPC. Surprisingly, three of them (miR-101-3p, miR-193a-5p and miR-148a-3p) were significantly differentially expressed between treated non-CRPC and CRPC with $p<0.001$ (Figure 18).

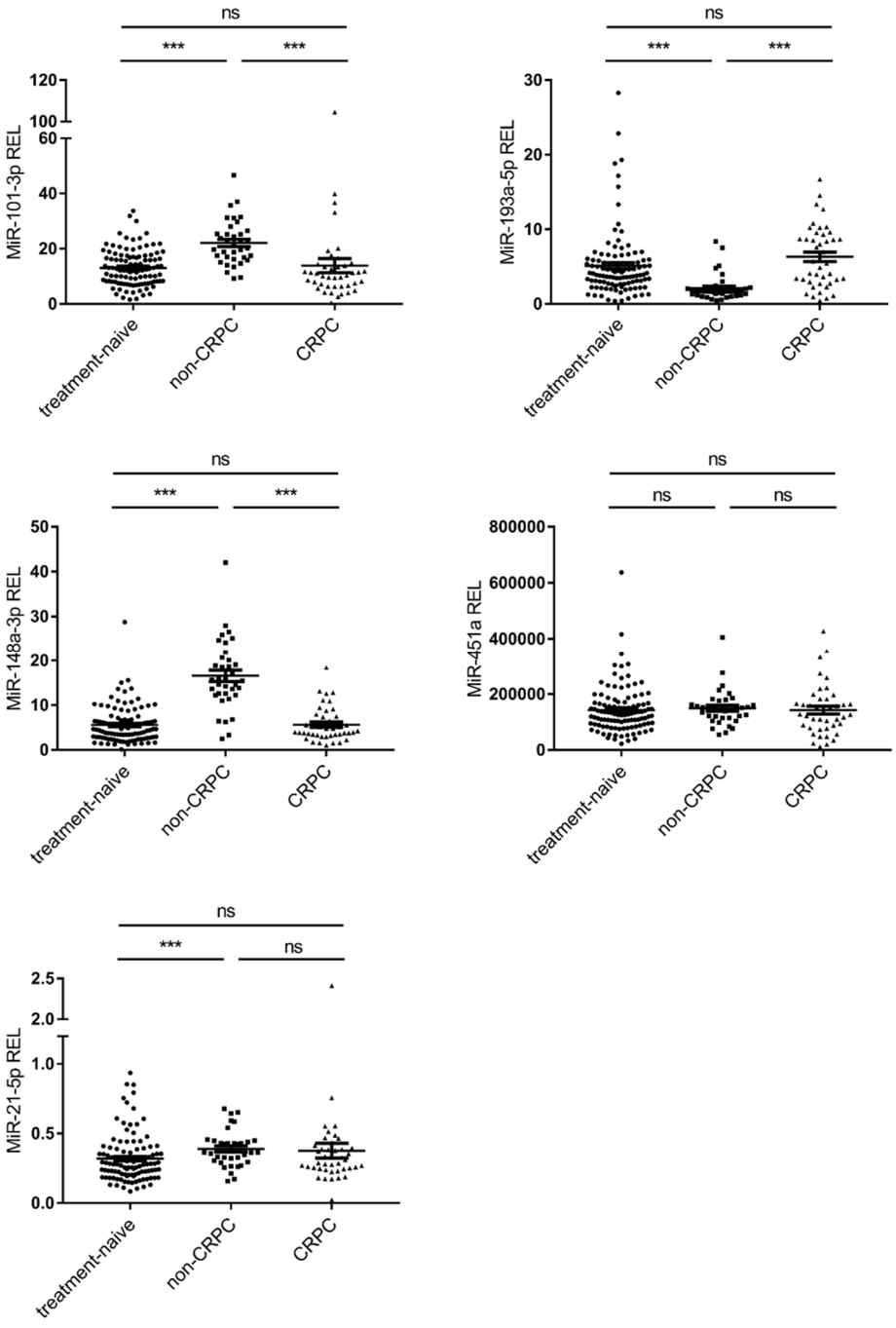

Figure 18. RT-qPCR evaluation of plasma exosomal miRNAs which showed no difference in treatment-naive PCa and CRPC.

4.2.5 Evaluation of plasma exosomal miRNAs as potential biomarkers for CRPC

To evaluate the predictive value of plasma exosomal miRNAs for CRPC, we performed ROC curves analysis based on the RT-qPCR results. When comparing the treatment-naive PCa and CRPC, miR-423-3p showed best prediction value with AUC= 0.7835 (95% CI: 0.707- 0.860, $p< 0.0001$)(Figure 19A, Table 31) among the miRNAs. Any combination of miRNAs did not show better performance than miR-423-3p alone. Although its efficiency was lower than PSA (AUC= 0.837, 95% CI: 0.740- 0.934, $p< 0.0001$), when combined with PSA in a logistic binominal regression model (combine model= 0.026*PSA+0.033*miR-423-3p REL), the performance improved to AUC= 0.9076 (95% CI: 0.861- 0.955, $p< 0.0001$)(Figure 19B, Table 31).

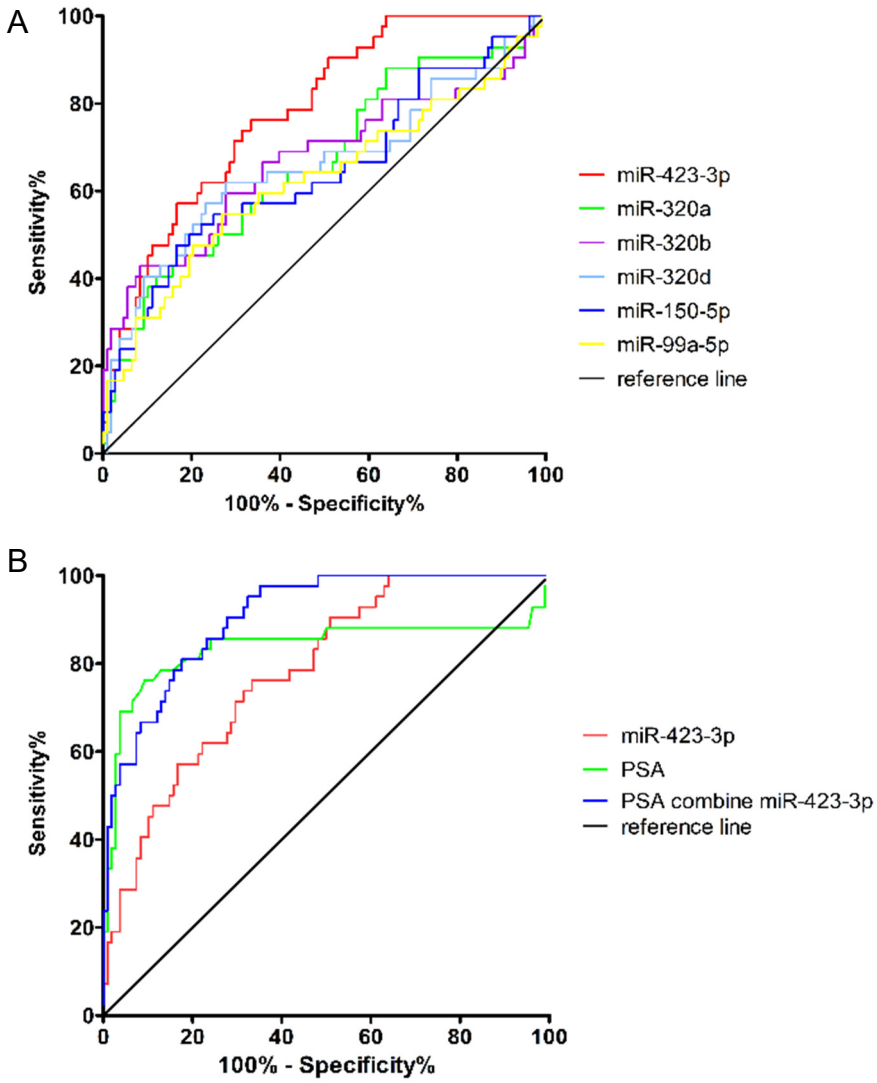

Figure 19. ROC analyses of exosomal miRNAs for prediction of CRPC from treatment-naive PCa using RT-qPCR data. A. MiRNAs showed significant different expression between CRPC and treatment-naive PCa; B. MiR-423-3p, PSA and miR-423-3p combine PSA. Large under the curve area indicates good prediction value with high sensitivity and high specificity.

Table 31. ROC curves to predict CRPC from treatment-naive PCa by exosomal miRNAs and PSA level.

	AUC	95% CI	*p*-value
miR-423-3p	0.7835	0.707- 0.8601	<0.0001
miR-320a	0.6627	0.5615- 0.7639	0.002
miR-320b	0.6695	0.5602- 0.7788	0.0013
miR-99a-5p	0.6241	0.5144- 0.7339	0.0184
miR-320d	0.6574	0.5486- 0.7662	0.0028
miR-150-5p	0.6453	0.5392- 0.7514	0.0058
PSA	0.8368	0.7401- 0.9334	<0.0001
PSA combine miR-423-3p	0.9076	0.8607 to 0.9545	<0.0001

When comparing the treated non-CRPC and CRPC, exosomal miRNAs except for miR-150-5p showed good AUCs and PSA showed worst prediction value of CRPC from non-CRPC with AUC= 0.6521 (95% CI: 0.5282-0.776, p=0.211). Five miRNAs showed significant difference between CRPC and treatment-naive also had good prediction value for CRPC when comparing CRPC and non-CRPC (Table 32, Figure 20A). Three miRNAs which showed no difference between CRPC and treatment-naive PCa but showed significant difference between CRPC and non-CRPC had high AUCs for CRPC (Table 32, Figure 20B), while the best performance comes from miR-148a-3p with AUC= 0.9087 (95% CI: 0.8383 to 0.9792, p< 0.0001).

Table 32. ROC curves to predict CRPC from non-CRPC by plasma exosomal miRNAs and PSA level.

	AUC	95% CI	P value
miR-423-3p	0.879	0.7981 to 0.9599	<0.0001
miR-320a	0.7923	0.6921 to 0.8925	<0.0001
miR-320b	0.8009	0.6972 to 0.9047	<0.0001
miR-99a-5p	0.795	0.6937 to 0.8963	<0.0001
miR-320d	0.8175	0.7205 to 0.9144	<0.0001
miR-150-5p	0.5192	0.3887 to 0.6496	0.7713
miR-101-3p	0.8406	0.7457 to 0.9355	<0.0001
miR-148a-3p	0.9087	0.8383 to 0.9792	<0.0001
miR-193a-5p	0.8313	0.7361 to 0.9266	<0.0001
PSA	0.6521	0.5282 to 0.776	0.0211

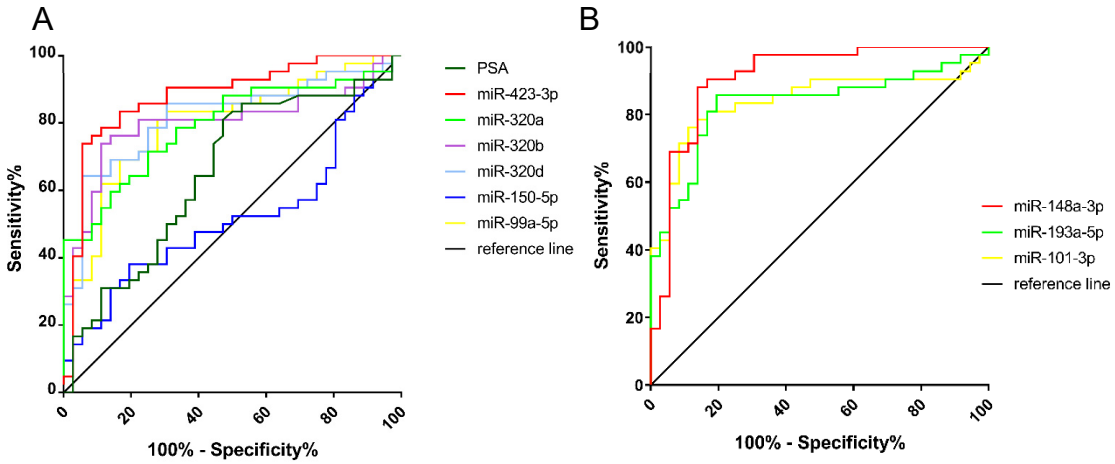

Figure 20. ROC analysis of exosomal miRNAs for prediction of CRPC from non-CRPC using RT-qPCR data. A. MiRNAs showed significant different expression between CRPC and treatment-naive PCa also showed significant different expression between CRPC and treated non-CRPC; B. MiRNAs showed significant different expression only between CRPC and non-CRPC. Large under the curve area indicates good prediction value with high sensitivity and high specificity.

4.2.6 Association of exosomal miRNA expression with serum PSA level

As PSA level is an important parameter in CRPC detection, we analysed the correlation of six plasma exosomal miRNA expression levels and serum PSA level in all Barts samples. The Spearman's rank order correlation test showed only miR-150-5p had weak reverse correlation with PSA level, while the other five miRNAs were not correlated to PSA levels (Figure 21). The Spearman r for miR-423-3p, miR-320a, miR-320b, miR-320d, miR-150-5p and miR-99a-5p were 0.1770, 0.1136, 0.1129, 0.1188, -0.2358 and 0.1404, respectively and only miR-423-3p and miR-150-5p reached $p < 0.05$.

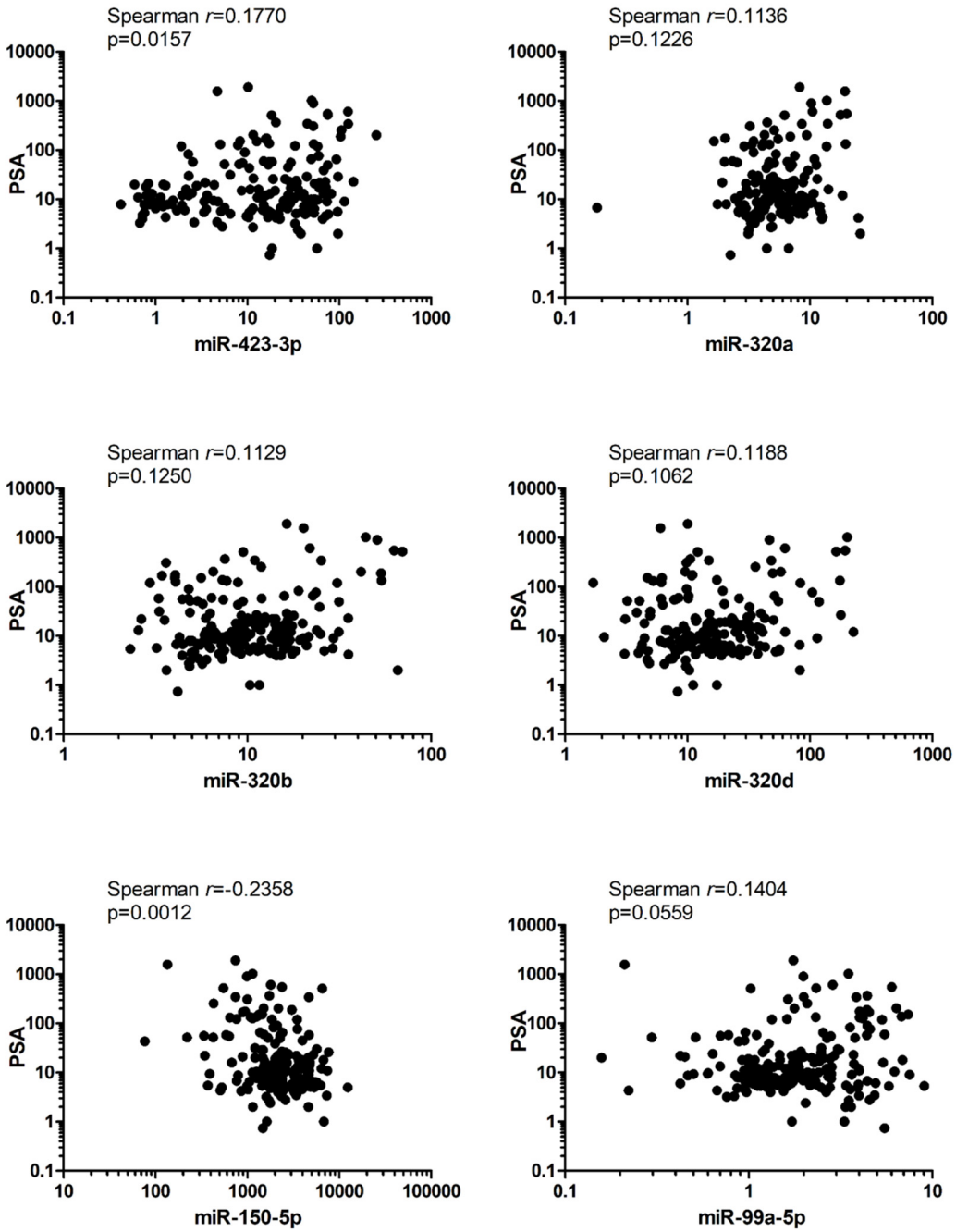

Figure 21. Correlations of expression levels of plasma exosomal miRNAs with PSA.

4.2.7 Technical investigation of the reason for inconsistence results between techniques used for plasma exosomal miRNA detection

Fluidigm and traditional RT-qPCR are both RT-qPCR based methods for RNA quantification. However, it is found in this study that Fluidigm showed very different results from RNA-sequencing that some plasma exosomal miRNAs showed opposite expression patterns, while traditional RT-qPCR showed consistent results to RNA-sequencing. I then wanted to find the potential reason. The main difference between these Fluidigm and traditional RT-qPCR is the cDNA preparation process. When preparing cDNA for Fluidigm, pre-amplification was performed. I performed traditional RT-qPCR of let-7b in 23 cDNA samples used for Fluidigm PCR analysis with and without pre-amplification to compare the Cts to data derived from Fluidigm system. cDNA samples with amplification showed clearly lower Ct in the RT-qPCR (Figure 22). Cts of amplified cDNA correlates better with Cts obtained from Fluidigm run with Spearman r=0.8557 with the best fit linear regression R^2=0.8254, compared to non-amplified DNA with Spearman r=0.7826 with the best fit linear regression R^2=0.7475 (Figure 22).

When performing reverse transcription, different types of buffer in the miScript II RT Kit (Qiagen) were used: HiFlex buffer was used for RT-qPCR and HiSpec buffer was used for Fluidigm. To examine if different buffer used in the reverse transcription step affected final miRNA quantification, I performed reverse transcription using HiSpec buffer for 26 samples and ran RT-qPCR of miR-320b and compared to the results from HiFlex buffer. Spearman correlation analysis showed that the Cts generated from the same samples using HiSpec buffer and HiFlex buffer for reverse transcription had Spearman r=0.7338 and the best fit linear regression R^2=0.7503 (Figure 23).

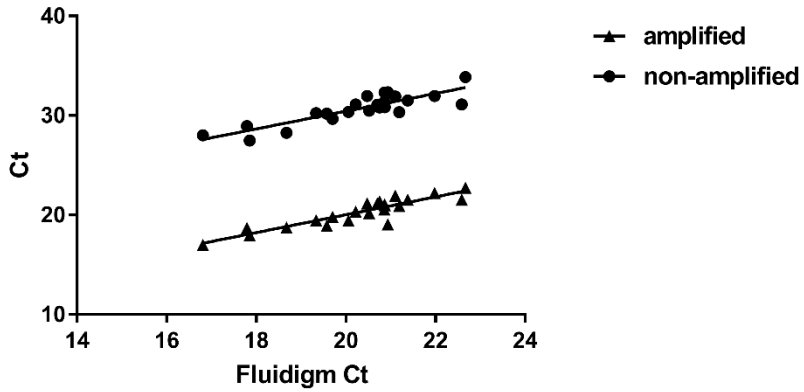

Figure 22. Correlation of Cts of let7b-3p from Fluidigm and RT-qPCR using pre-amplified and non-amplified cDNA.

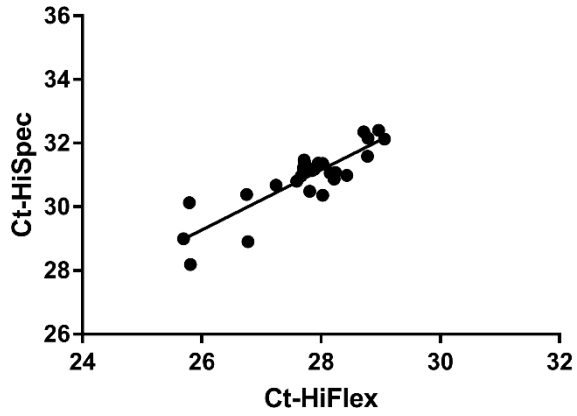

Figure 23. Correlation of Cts of miR-320b using cDNA sythesized with HiFlex buffer and HiSpec buffer.

4.3 Discussion

4.3.1 The potential prediction value of plasma exosomal miRNAs for CRPC

The study was initiated by comparing two distinct groups of PCa patients: treatment-naive PCa and CRPC and this strategy was adopted by most studies for CRPC-specific genes [366]. Within these two groups of patients, I identified several exosomal miRNAs that have prediction value for CRPC. Although none

of them overtook PSA level individually, exosomal miRNA improved prediction value of PSA when combined.

As CRPC developed when patients' are undergoing hormone therapy, I later checked the miRNAs levels in PCa patients who were receiving hormone therapy but had not developed CRPC (referring to treated non-CRPC). Five of the six exosomal miRNAs which were differentially expressed between treatment-naive PCa and CRPC also showed significant difference between treated non-CRPC and CRPC. In addition, three out of five miRNAs which were not differentially expressed between treatment-naive PCa and CRPC also showed significant difference between treated non-CRPC and CRPC. Importantly, all differentially expressed exosomal miRNAs had better prediction value for CRPC from treated non-CRPC than PSA. In our cohort, PSA had good AUC when comparing treatment-naive PCa and CRPC maybe because most (87%) of the treatment-naive PCa patients were low/intermediate risk who had low PSA level at 8.9 (5.75-13) ng/ml. In the treated non-CRPC group, the PSA levels fell in a wide range 15.5 (6.26-112.65) ng/ml. The expression level of miRNAs in treated non-CRPC was not consistent to it in treatment-naive PCa, as 9 out 11 miRNAs I validated had significant difference between treatment-naive PCa and treated non-CRPC. Some miRNAs showed consistent aberrant expression in CRPC compared to non-CRPC and treatment-naive PCa, while some miRNAs showed fluctuated expression level along treatment-naive PCa, non-CRPC and CRPC. It is possible that these miRNAs are involved in different biological processes in the development of CRPC. These results showed the importance of evaluating plasma exosomal miRNA levels in treated non-CRPC patients for developing clinically useful CRPC predictive biomarkers.

The miRNAs I identified in the current study have been previously reported in tissues, plasma/serum and some functional studies. However, the findings were not consistent. In my RT-qPCR validation, I found four exosomal miRNAs (miR-423-3p, miR-320a, miR-320b and miR-320d) that were consistently higher expressed in CRPC compared to treatment-naive PCa and treated non-CRPC. In line with our finding, miR-423-3p has been previously found highly expressed in the plasma of patients with mCRPC compared to localised disease [366]. Mir-423-3p was also found up-regulated in the serum of lung cancer patients (n=40)

compared to the benign pulmonary disease (n=40) and healthy control (n=40) [367]. However, in an earlier study analysing one patient's non-metastatic and metastatic xenograft lines, mir-423-3p was not identified as significant differentially expressed miRNA [368].

Except for miR-423-3p, the other three miRNAs I found consistently higher expressed in CRPC compared to treatment-naive PCa and treated non-CRPC are all from miR-320 family. Several studies have reported the tumour suppressor role of miR-320 family members in PCa [369-371] as well as many other cancer types [372-375]. MiR-320a level has been found high in non-cancer prostate tissue compared to PCa tissue and CRPC metastasis [371]. In a study of serum level of miR-320a/b/c, the healthy control group showed the lowest median levels of miR-320a/b/c followed by the PCa group, while the BPH group showed the highest median expression levels of these miRNAs [376]. Changes of the levels of these miRNAs before and after radical prostatectomy and increased levels of these miRNAs after radical prostatectomy were correlated to better PSA-recurrence-free survival [376]. Based on these findings, miR-320a/b/d are expected to be less abundant in plasma exosomes of CRPC patients, which is opposite to our findings.

In our study, miR-193a-5p was significantly higher expressed in plasma exosomes of CRPC compared to treated non-CRPC, while there was no difference between treatment-naive PCa and CRPC. Different studies have shown different expression levels of miR-193-5p in PCa tissues. It has been found upregulated in PCa tissues and PCa cell lines, with significant suppression of PC3 cell apoptosis induced by oxidative stress [377, 378]. However, in a study examining 20 primary PCa tissues and their paired adjacent benign tissues, miR-193a-5p was found lower expressed in the tumour tissues [379].

I also observed that miR-99a-5p, miR-101-3p and miR-148a-3p were expressed at significantly lower levels in plasma exosomes of CRPC compared to treated non-CRPC. MiR-99a-5p was previously demonstrated as a tumour suppressor [380]. However, miR-99a has been found higher expressed in the plasma of mCRPC compared to localised PCa [366]. MiR-101-3p was found downregulated in metastatic PCa tissue compared to primary PCa tissue [381]. Tumour suppressor role of miR-148a-3p has been reported in many cancer types [382-

384]. However, in PCa, miR-148a has been reported as an androgen-responsive miRNA which could promote LNCaP cell growth by repressing its target CAND1 expression [385]. I also found miR-150-5p was expressed lower in plasma exosomes of CRPC when compared to treatment-naive PCa, but there was no difference between treated non-CRPC and CRPC. Both miR-150-3p and mir-150-5p have been found as tumour suppressor in PCa [386, 387] and other cancer types [388]. However, one study reported elevated serum level of miR-148a-3p and miR-150-3p in PCa patients (n=19) compared to healthy controls (n = 19) by RNA-sequencing and RT-qPCR [389].

The inconsistency of the expression levels of miRNAs found in the same sample source, for example in blood or tissue, could be largely caused by the small number of samples used and different techniques used to detect miRNAs. However, evidence shown there are biological reasons supporting the different expression of miRNAs in circulation and tissues. MiRNAs are found to be generally downregulated in cancer [390], but in a review of serum/plasma miRNA in PCa, most miRNAs were found up-regulated in malignant diseases [391]. Studies evaluating miRNAs in tumour tissue and serum/plasma of the same patient also found big difference of miRNA expression patterns [138, 392]. One potential explanation could be that miRNAs in circulation were originated from various cell types. For plasma exosomes, the exosomal miRNA profile in plasma represents the collective miRNA contributions from various cell types. It has been reported that although miR-320a is highly expressed in the non-small cell lung cancer patients and it plays a tumour suppressor role [393, 394]. miR-320a is expressed by different cell types of the microenvironment but absent in epithelial cells both from normal and tumour lung tissues [395]. It is found that miR-320a is higher expressed in activated polymorphonuclear leukocytes and M2 macrophages and could induced M2-polarization of macrophages [395]. Thus, the miRNAs we detected in plasma exosomes may reflect the tumour microenvironment and immune response status, resulting in different expression levels in tumour cells. Currently, it is difficult to identify the origin of exosomes. One potential approach is to selectively pull down EVs derived from specific tissues by immuno-capture specific membrane proteins. However, this approach may have sensitivity issue due to the heterogeneity of exosomes.

4.3.2 Different techniques influence evaluation of miRNA expression

In this study, I applied two qPCR-based methods for exosomal miRNA quantification: the traditional RT-qPCR and Fluidigm multiple RT-qPCR. The main advantage of Fluidigm is that it enables detecting multiple gene targets in a large number of samples at one time with little amount of starting RNA material, making it an ideal platform for screening genes in large sample sets. However, the Fluidigm results are inconsistent to the RNA-sequencing data. Therefore, the conventional RT-qPCR method, which is not a good choice for validation of a large panel of miRNAs using very limited number of clinical samples, were used for the plasma exosomal miRNA validation. Each of the three miRNA analysis methods used different reverse transcription methods, with or without cDNA amplification step. Hence, certain degree of discorrelation is expected. My data showed that the traditional RT-qPCR is generally consistent to RNA sequencing data and the invalidated miRNAs are more likely due to false discovery rather than technically inconsistence. However, data from the Fluidigm were very different from the traditional RT-qPCR. As RT-qPCR and Fluidigm multiple RT-qPCR should perform similar RT-qPCR reactions, consistent results were expected from these two methods. The main difference between these two methods is the cDNA preparation process. As Fluidigm used small amount of material and the reaction was done in extreme small volume, when preparing samples for Fluidigm, additional step of pre-amplification of the cDNA is required. When I performed traditional RT-qPCR using the cDNA prepared for Fluidigm before and after the pre-amplification, Cts of amplified cDNA correlates better with Cts obtained from Fluidigm compared to non-amplified DNA. This indicates that traditional RT-qPCR and Fluidigm can generate consistent results when using the same starting cDNA samples. However, pre-amplification would slightly affect the quantification. When performing reverse transcription, different types of buffer in the miScript II RT Kit (Qiagen) were used: HiFlex for RT-qPCR and HiSpec for Fluidigm. To examine if different buffer used in the reverse transcription step would affect final miRNA quantification, I performed reverse transcription using both HiSpec and HiFlex buffers for the same samples and ran RT-qPCR. It showed that the correlation between Cts generated from cDNA

samples reverse transcribed with HiSpec and HiFlex buffers was poor (Spearman R^2=0.7503). This indicates the cDNA synthesis methods may affect miRNA quantification. In summary, the cDNA preparation process could affect the results from Fluidigm and RT-qPCR, especially for detection of differentially expressed miRNAs when the expression difference among samples is small.

4.3.3 Validation of RNA-sequencing data by RT-qPCR

There are different techniques to quantify RNA expression. RNA-sequencing has been intensively used in recent decades for RNA expression profiling, however, RT-qPCR validation is often requested to provide evidence from a different method as well as to evaluate more samples. In our RT-qPCR validation step, we selected a number of differentially expressed miRNAs from our RNA-sequencing data and checked their expression in a larger cohort. Despite the miRNAs which we were not able to validate due to low-expression issue, the results showed the benefit of using different methods for RNA-sequencing data analysis. 75% (3/4) miRNAs which showed significant difference in three RNA-sequencing analysis methods and 60% (3/5) miRNAs which showed significant difference in two RNA-sequencing analysis methods were validated in RT-qPCR, while none of the three miRNAs which showed significant difference in only one method was validated in RT-qPCR. The overall precision of our RNA-sequencing in comparison to RT-qPCR is 0.5, which is slightly lower than a previous report [396]. Although high consistency of the fold changes estimated from RNA-sequencing and from the RT-qPCR were reported [396, 397], it was also common observed that some genes could not be validated and even had opposite expression direction [220, 396, 398]. Thus, it is important to recognise the false positive and false negative signals from using different techniques and cross validate the target genes using different methods.

Chapter V Function of miR-423-3p for castration-resistance acquisition

5.1 Introduction

Understanding the mechanisms of resistance that cause hormone-naive prostate cancer to progress to castration-resistance is the key to developing future therapy. Lots of studies have been done investigating the mechanism under CRPC development. Multiple mechanisms have been demonstrated, which can mainly be divided into AR-androgen axis-dependent mechanisms and AR-androgen axis independent mechanisms [85]. The majority of mechanisms identified leading to castration-resistant are mediated by AR or the androgen axis. In CRPC patients, low levels of androgen persist despite androgen blockade with ADT. Tumour cells can develop resistance either through overexpression of AR protein to cause AR hypersensitive to low level of androgen [86], or AR mutations/variants to increase AR transactivation activity and decreased ligand specificity [88]. Amplification of the AR gene, overexpression of the AR protein, AR mutation are commonly observed among patients with CRPC. In recent years, the role of AR splice variants in CRPC have been implicated. For example, the presence of AR-V7 has been found associated with more advanced malignance and reduced survival in patients with mCRPC [90]. Altered expression and function of AR co-regulators are also involved in CRPC development [92]. AR-independent mechanisms mainly involves aberrant activation of other pathways such as PI3K-Akt-mTOR pathway, Src signalling pathway, growth factor pathways [85].

Alterations of miRNAs expression have been reported in CRPC. However, the mechanism of how miRNAs regulate CRPC development remain largely unknown. Pathway analyses suggested that miR-218, miR-145, miR-197, miR-149, miR-122, and let-7b may contribute to the development of CRPC through the influence of Ras, Rho proteins, and the SCF complex [364], but lack of experimental validation. Several miRNAs have been identified as AR regulators or AR-regulated miRNAs, thus potentially involved in the development of CRPC [399].

MiR-423 gene is located in chromosome 17q11.2 and can produce two mature sequences: miR-423-3p and miR-423-5p. As described in previous chapters,

miR-423-3p expressed at significantly higher level in the plasma exosomes of CRPC compared to treatment-naive-PCa and treated hormone-sensitive PCa patients. MiR-423-3p has been found overexpressed in PCa tissue compared to non-malignant tissue [400]. It has also been found upregulated in the plasma of metastatic CRPC (mCRPC) compared to localised PCa and associated with higher Gleason score, metastasis and poorer outcome [366]. Functional studies have demonstrated the tumour promoting role of miR-423-3p by targeting different genes in different cancer types. For example, miR-423-3p was found to promote cell proliferation, migration, and invasion in gastric cell lines by targeting Bcl-2-interacting mediator of cell death [401]. It has been reported that miR-423-3p could promote tumour progression via modulation of AdipoR2 in laryngeal carcinoma [402]. In glioma, miR-423-3p was found enhancing cell growth through inhibition of PANX2 [403]. However, its functional role in PCa has not been elucidated. Thus, we sought to study the potential function of miR-423-3p in CRPC development in this chapter.

5.2 Results

5.2.1 Overexpression of miR-423-3p did not affect LNCaP cell proliferation in hormone-depleted medium

To study the potential function of miR-423-3p in CRPC development, I transiently transfected miR-423-3p mimics in hormone-dependent PCa cell line, LNCaP, and cultured the cells in hormone-depleted medium. RT-qPCR showed that transfection of miR-423-3p mimics significantly increased the miRNA level in LNCaP cells compared to negative control and the high level of miR-423-3p could maintain for at least 72 h (Figure 24).

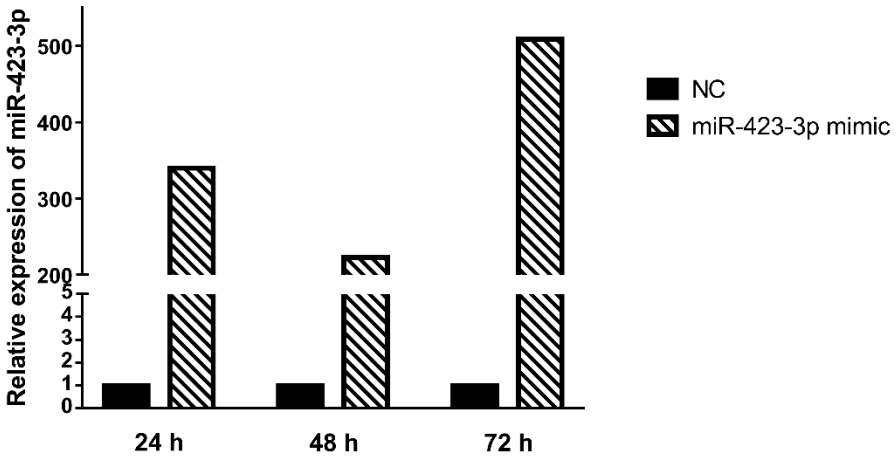

Figure 24. Transient overexpression of miR-423-3p in LNCaP cells. MiR-423-3p level was measured at different time points after transfection. NC, negative control. Expression of miR-423-3p was normalised to U6.

To evaluate the effect of miR-423-3p on cell proliferation, MTS assays were performed on the LNCaP cells transfected with miR-423-3p or negative control miRNA. The MTS assay results showed that overexpression of miR-423-3p did not affect LNCaP cell viability (Figure 25) in hormone-depleted medium.

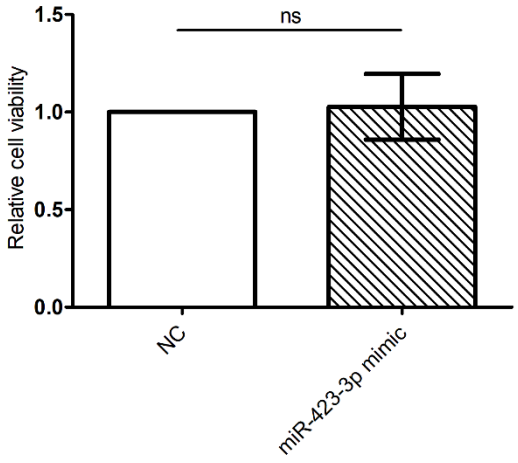

Figure 25. The effect of miR-423-3p overexpression of LNCaP cell proliferation. Cell viability measured by MTS assay at 96 h post transfection showed that the proliferation of LNCaP cells transfected with miR-423-3p mimics and negative control (NC) were not different. Relative cell viability was normalised to NC. Data

were obtained from three experiments and triplicate wells were used in each experiment.

5.2.2 Overexpression of miR-423-3p leads to increased cell migration and invasion

I then evaluated the effect of overexpression miR-423-3p on cell migration using transwell assay. Overexpression of miR-423-3p led to significantly (p= 0.023) increased cell migration (Figure 26) (1.5 fold) of LNCaP cells in hormone-depleted medium. On the migration membrane, more round cells sitting on the membrane were observed in the control group, while migrated cells in the miR-423-3p overexpression group had more stretched morphology (Figure 26C).

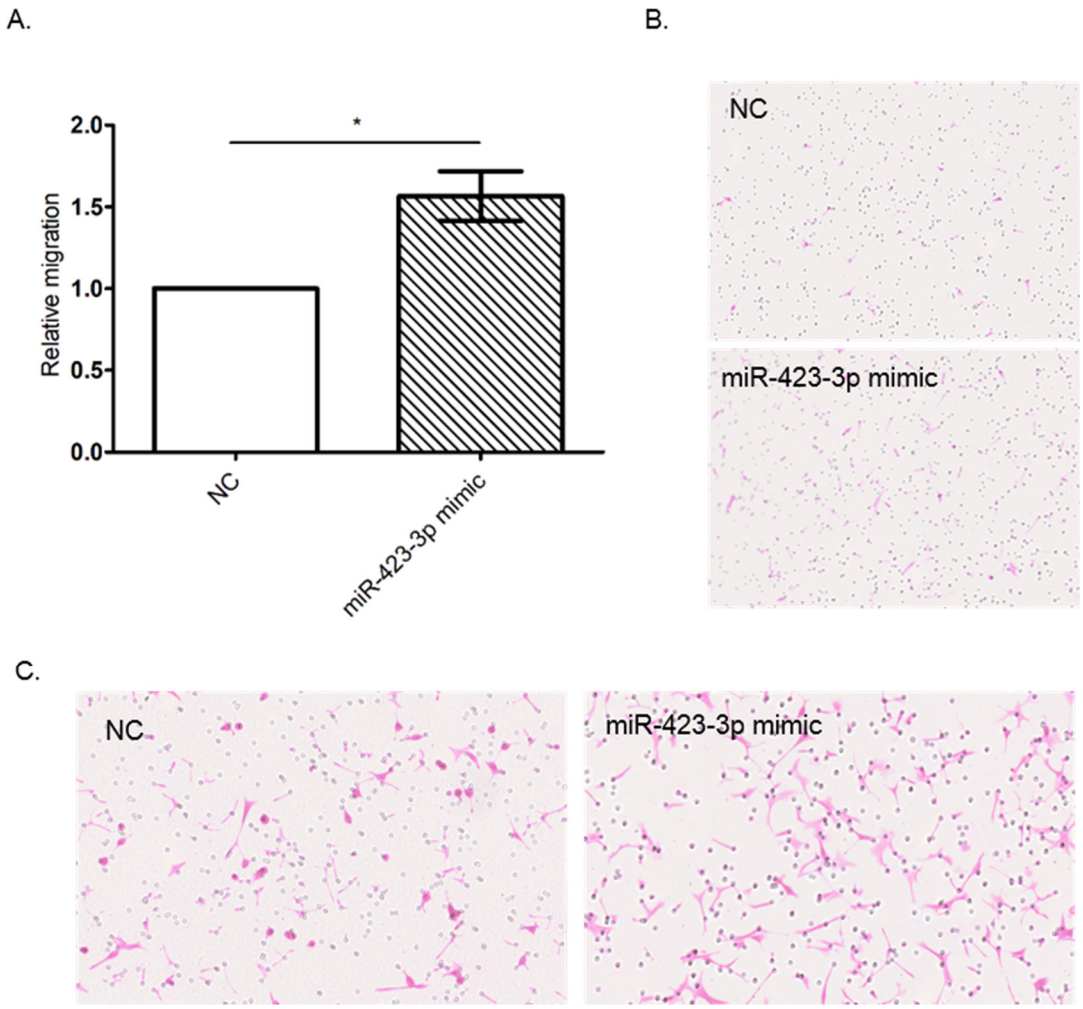

Figure 26. Overexpression of miR-423-3p leads to increased LNCaP cell migration in hormone-depleted medium. A. Transwell migration assay showed 1.5 fold increased cell migration in LNCaP transfected with miR-423-3p mimics compared to negative control (NC); B. Representative images of transwell membranes to show increased cell number in LNCaP transfected with miR-423-3p mimics compared to NC; C. Morphology difference was observed between LNCaP cells overexpressing miR-423-3p and LNCaP cells transfected with negative control, that LNCaP cells overexpressing miR-423-3p had more stretched morphology. Cells were incubated for 24 h to migrate. Photos were taken using Hamamatsu NanoZoomer S210 system under 200× magnification. Data were obtained from three experiments and triplicate wells were used in each experiment. Relative migration was normalised to NC. *p<0.05.

I then attempted to evaluate the effect of miR-423-3p on cell invasion. Invasion

chambers with Matrigel-coated membranes were firstly used, but LNCaP cells were easy to float after transfection and the invasion ability of LNCaP after transfection was extremely poor that it is difficult to be examined by invasion chambers. Thus, I performed single cell invasion assay through collagen/Matrigel matrix and determined 1.6 fold increased (p= 0.0134) invasion ability of LNCaP cells overexpressed miR-423-3p (Figure 27).

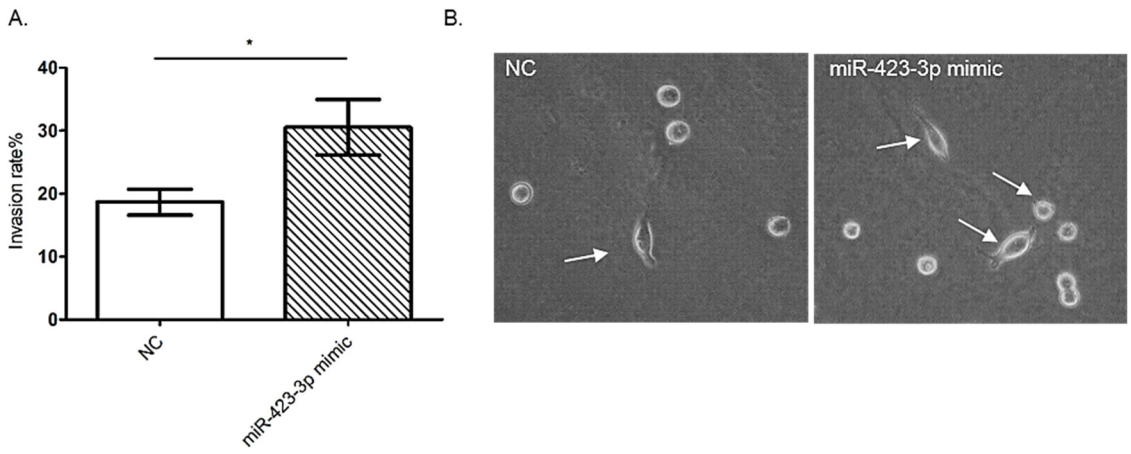

Figure 27. Overexpression of miR-423-3p leads to increased LNCaP cell invasion in hormone-depleted medium. A. Single cell invasion assay showed increased cell invasion (1.6 fold) in LNCaP transfected with miR-423-3p mimics compared to negative control (NC); data were obtained from three experiments and triplicate wells were used in each experiment; *p<0.05. B. Representative images of single cell invasion assay showing increased invading cells (arrow) after LNCaP cell overexpressing miR-423-3p. Cells were incubated for 24 h to invade. Photos were taken under 400× magnification.

5.2.3 MiR-423-3p expressed at higher level in the C4-2 cells and C4-2 cells have better migration and invasion ability

C4-2 is an androgen-independent isolated from LNCaP cell subcutaneous xenograft tumour of castrated mouse [404]. I checked the expression level of miR-423-3p in LNCaP and C4-2 cells and found that C4-2 cells have 1.6 fold higher expression of miR-423-3p (p= 0.019) than LNCaP cells (Figure 28).

I then compared the migration and invasion ability of LNCaP and C4-2 cells in hormone-depleted environment and C4-2 cells showed significant better migration (p= 1.3×10^{-04}) which was 3.8 folds better than LNCaP cells. C4-2 cell also showed 3.7 folds better invasion (p= 0.0005) ability compared to LNCaP cells (Figure 29).

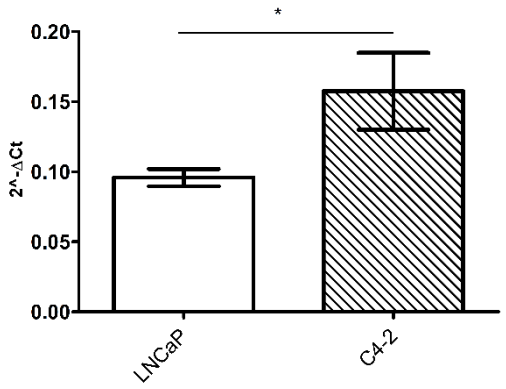

Figure 28. Expression level of miR-423-3p in LNCaP and C4-2 cells evaluated by RT-qPCR showed C4-2 cells have 1.6 fold higher expression of miR-423-3p than LNCaP cells. Expression of miR-423-3p was normalised to U6. *p <0.05

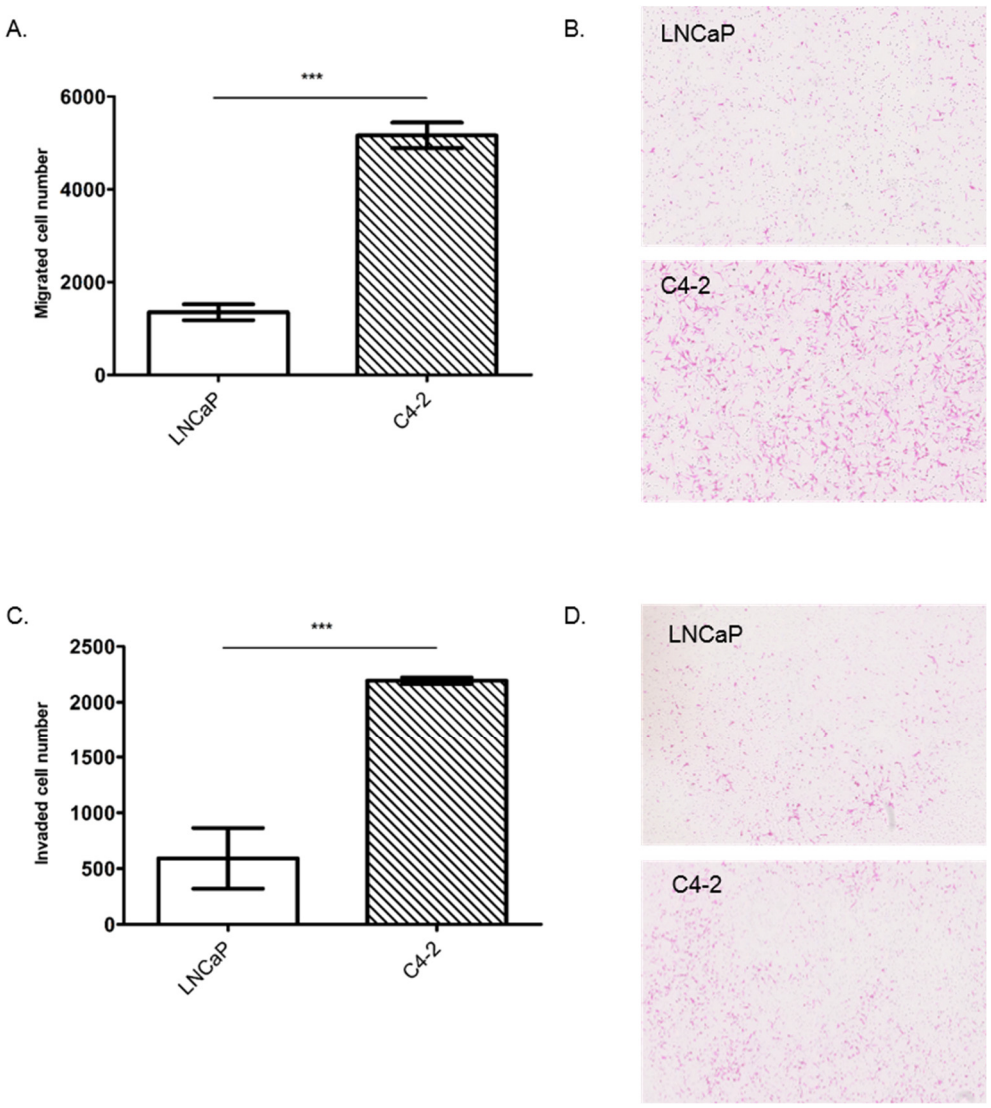

Figure 29. C4-2 cells have better migration and invasion ability compared to LNCaP cells in hormone-depleted medium. A. Transwell migration assay showed better migration ability of C4-2 (3.8 folds) compared to LNCaP; B. Representative images of transwell membranes to show better migration ability of C4-2 compared to LNCaP cells; C. Matrigel invasion chamber assay showed better invasion ability of C4-2 (3.7 folds) compared to LNCaP cells; D. Representative images of Matrigel invasion chamber membranes, showing C4-2 has more cells invaded than LNCaP. Data were obtained from three experiments and triplicate wells were used in each experiment. Cells were incubated for 24 h to migrate/invade. Photos were taken using Hamamatsu NanoZoomer S210 system under 200× magnification. ***p<0.001.

5.2.4 Investigation of potential MiR-423-3p targets

In silicon analysis of miR-423-3p target genes were performed using TargetScan 7.1 (http://www.targetscan.org/vert_71/) and miRDB (http://mirdb.org/). By TargetScan 7.1 analysis, there are several hundreds of target predicted genes. However, there are only 18 target genes of miR-423-3p with conserved sites (which tends to be more effective)(Table 33). There are 30 targets predicted in miRDB, with four shared genes with Targetscan 7.1, PABPC1, RAP2C, BCORL1, and LGALSL. However, the literature on the role of PABPC1 in PCa against our observation and the other three genes have not been reported for their involvement in PCa.

MEIS1 is ranked third of the predicted miR-423-3p targets by TargetScan 7.1 with one predicted target site. It has been identified as an AR negative regulator [413] and found with decreased expression in metastatic tissue. However, there is no experimentally confirmation if MEIS1 is a miR-423-3p target. As I found miR-423-3p could induce PCa cell migration and invasion, it is interesting to investigate if overexpression of miR-423-3p contribute to CRPC development through down-regulation of MEIS1. I checked if miR-423-3p overexpression affects MEIS1 protein expression level by WB. Biological replicates of WB analysis were carried out in LNCaP cells cultured in hormone-depleted medium with and without miR-423-3p overexpression. WB showed that overexpression of miR-423-3p decreased MEIS1 protein expression when normalised to β-actin, though the degree of this effect varied in the biological replicates. WB images were shown in Figure 30.

Table 33. Predicted targets of miR-423-3p with conserved sites in TargetScan 7.1*.

Orthologue of target gene	Gene name	Conserved sites total	Conserved 8mer sites	Conserved 7mer-m8 sites	Conserved 7mer-A1 sites	Cumulative weighted context++ score
FAM222B	family with sequence similarity 222, member B	1	1	0	0	-1.23
RAP2C	RAP2C, member of RAS oncogene family	1	1	0	0	-0.85
MEIS1	Meis homeobox 1	1	1	0	0	-0.78
PABPC1	poly(A) binding protein, cytoplasmic 1	1	1	0	0	-0.72
BCORL1	BCL6 corepressor-like 1	1	1	0	0	-0.61
GBX2	gastrulation brain homeobox 2	1	0	1	0	-0.54
KCTD2	potassium channel tetramerization domain containing 2	1	0	1	0	-0.52
LGALSL	lectin, galactoside-binding-like	1	0	1	0	-0.51
CINP	cyclin-dependent kinase 2 interacting protein	1	0	1	0	-0.42

AC007375.1	Uncharacterized protein; cDNA FLJ43210 fis, clone FEBRA2020582	1	0	1	0	-0.29
VLDLR	very low density lipoprotein receptor	1	0	1	0	-0.29
WTIP	Wilms tumour 1 interacting protein	1	0	1	0	-0.28
MYO9A	myosin IXA	1	0	1	0	-0.26
ARFGAP1	ADP-ribosylation factor GTPase activating protein 1	1	0	0	1	-0.26
ZXDC	ZXD family zinc finger C	1	0	1	0	-0.25
RNF19B	ring finger protein 19B	1	0	1	0	-0.15
ZBTB7A	zinc finger and BTB domain containing 7A	1	0	1	0	-0.14
WDR91	WD repeat domain 91	1	0	1	0	-0.13

***The table is sorted by cumulative weighted context++ score (http://www.targetscan.org/cgi-bin/targetscan/vert_71/targetscan.cgi?species=Human&gid=&mir_sc=&mir_c=&mir_nc=&mir_vnc=&mirg=mir-423-3p).**

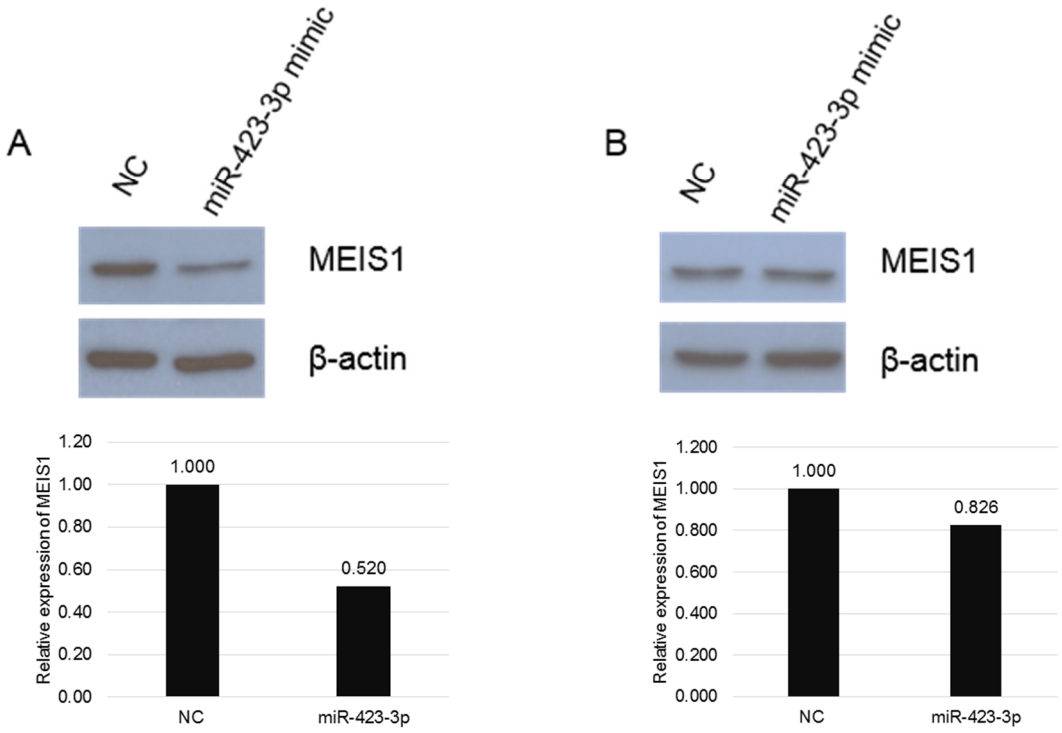

Figure 30. Images of two WB showing that overexpression of miR-423-3p slightly down-regulated MEIS1 protein expression in LNCaP cells in hormone-depleted medium. Band density was measured using ImageJ. The relative expression of MEIS1 in each sample is firstly normalised to β-actin and expression in cells transfected with miR-423-3p mimic was further normalised to negative control (NC).

5.2.5 Technical development for functional evaluation of exosome miRNAs *in vitro*

I found different expression levels of miR-423-3p in plasma exosomes of CRPC and non-CRPC patients, indicating that PCa may release miR-423-3p through exosomes into the cancer microenvironment to facilitate their castration resistant growth. Therefore, it is logical to explore the potential role of exosomal miR-423-3p in CRPC development. For the preparation of this study, I attempted to establish and evaluate the efficiency of the exosome isolation method from cell culture media in our laboratory together with Dr. Yang Wang. Exosomes from cell culture media of PC3 and DU145 cells have been isolated by ultracentrifugation.

I further confirmed the purity of exosomes by Nanosight nanoparticle tracking analysis, which showed exosomes isolated from cell culture media has high purity (Figure 31). Exosomes isolated from PC3 cell culture media presented mean exosome isolated from DU145 cell culture media presented mean size=52 nm, mode size=32 nm, size=71 nm, mode size=35 nm, concentration=13.81×10^{8} particles per ml and concentration=9.3×10^{8} particles per ml.

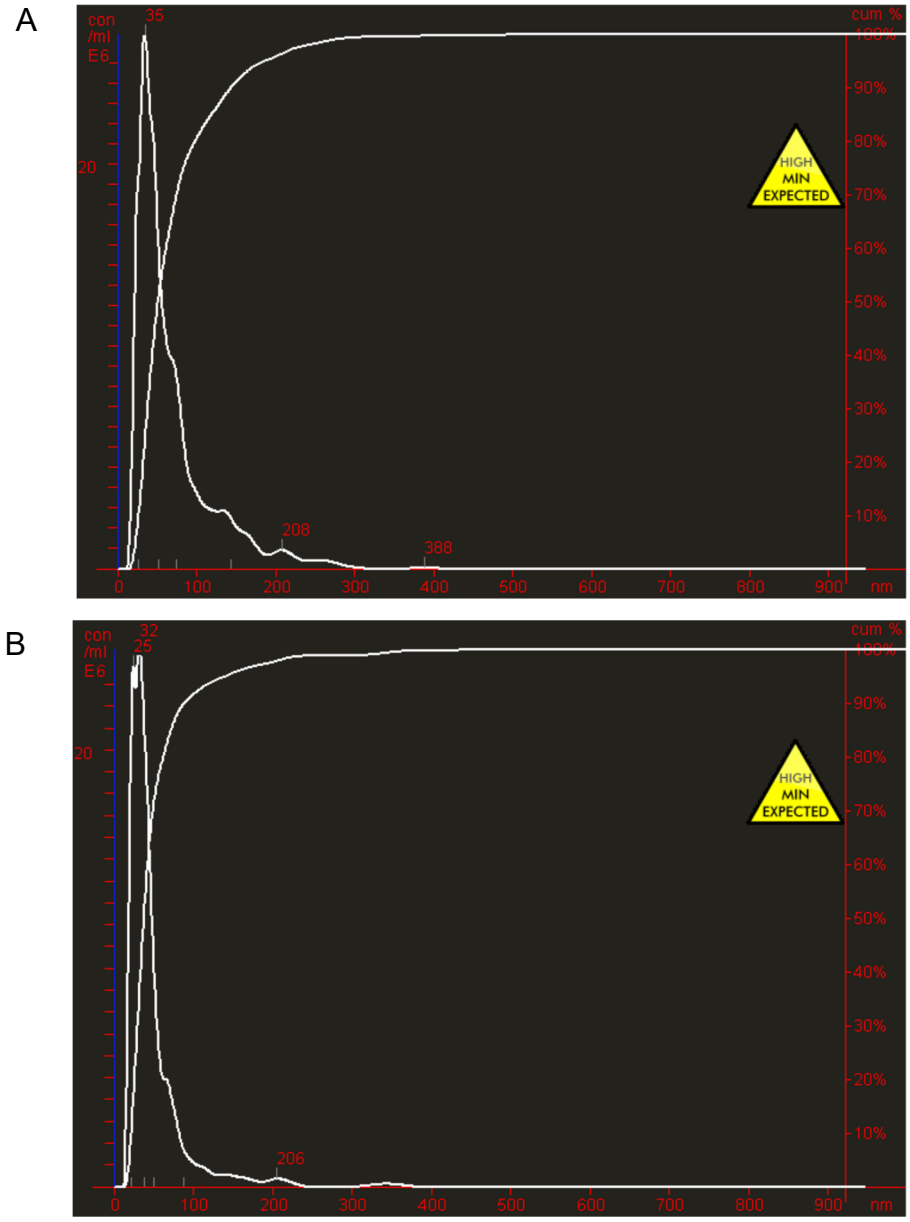

Figure 31. Nanosight nanoparticle tracking analysis of exosomes isolated from cell culture media by ultracentrifugation. A. Exosome isolated from PC3 cell culture media, with mean size=71 nm, mode size=35 nm, concentration=13.81×10^8 particles per ml; B. Exosome isolated from DU145 cell culture media, with mean size=52 nm, mode size=32 nm, concentration=9.3×10^8 particles per ml. X-axis: size (nm), Y-axis: Concentration (10^6 particles/ml).

Protein was extracted from exosomes from DU145 and PC3 cells. WB detected ALIX expression in the isolated DU145 and PC3 exosomes (Figure 32) (Protein extraction and WB were done by Dr Yang Wang). ALIX is a member of exosome proteome, which plays important role in exosome biogenesis. It is frequently used as a marker for exosomes. The detection of ALIX by WB indicated success isolation of exosomes.

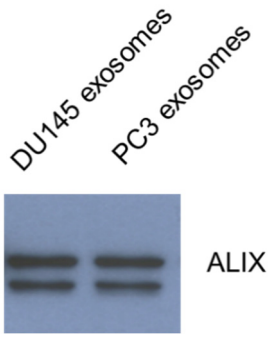

Figure 32. WB detection of ALIX in exosomes from DU145 and PC3 cells. Both bands are ALIX.

RNA was extracted from exosomes from PC3 cells and DU145 cells. Bioanalyzer showed existence of small RNAs in the exosomes from the cell culture media (Figure 33). From the Bioanalyser, tRNA was enriched in the exosomes (~60nt). I then performed RT-qPCR and detected two endogenous controls miR-30a-5p and let-7c-5p expression in the cell line exosomes with Ct<30.

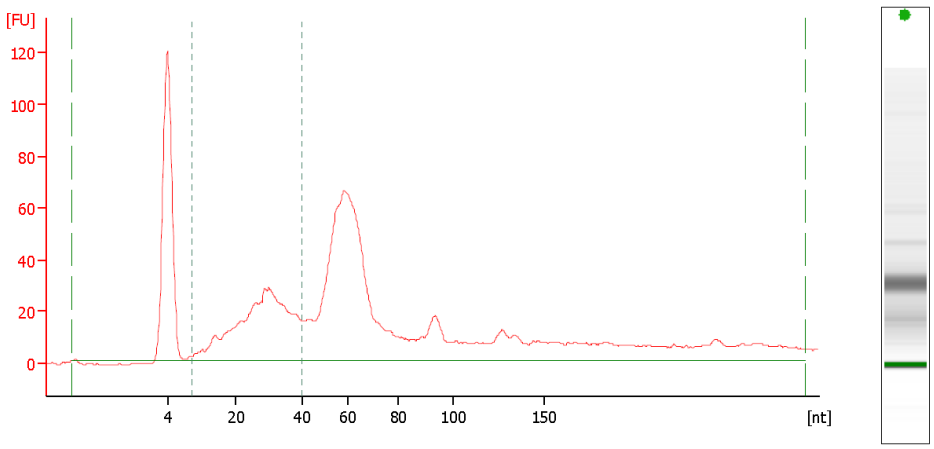

Figure 33. Bioanalyzer evaluation of RNA extracted from PC3 cell exosomes. MiRNAs are < 40 nt and the peak at 60 nt represents tRNAs.

The method of isolating high purity exosomes from cell cultures has been established to facilitate further study of the miRNAs packaged in exosomes and the study of miRNAs delivery via exosome in the future, but I ran out of time to fully investigate the role of exosomal miR-423-3p in CRPC.

5.3 Discussion

Higher level of miR-423-3p in CRPC exosomes suggested that miR-423-3p could potentially promote tumour progression. To evaluate the function of miR-423-3p prostate cancer cells in relation to CRPC development, I overexpressed miR-423-3p in hormone-dependent PCa cell line, LNCaP, and evaluated the cell proliferation, migration and invasion under the hormone-depleted environment. The increased migration and invasion ability of LNCaP cells overexpressing miR-423-3p indicated that miR-423-3p could induce hormone-independent migration and invasion of LNCaP cells. The higher expression of miR-423-3p in C4-2 cells and higher migration and invasion ability of C4-2 cells compared to LNCaP cells also supported CRPC development is associated with increased cancer cell migration/invasion ability and miR-423-3p could promote CRPC via promoting hormone-independent migration and invasion.

MiR-423-3p has been reported to act as an oncogene via promoting cell proliferation, cell migration and invasion [402, 405, 406]. However, I did not observe changes in cell proliferation when I overexpressed miR-423-3p in LNCaP cells in hormone-depleted medium. My data indicated that miR-423-3p is mainly associated with cell migration and invasion in castration environment. Some studies have revealed that miR-423-3p is involved in cancer metastasis. In lung adenocarcinoma, miR-423-3p was found highly expressed in patients with brain metastasis [406] and overexpression of miR-423-3p promoted lung cancer cell migration [407]. CRPC is highly related to metastasis, as only small proportion of CRPC patients have non-metastatic disease when diagnosed with CRPC and about half of the non-metastatic CRPC patients would develop metastasis within 3 years of diagnosis [408]. Thus, it is potential that miR-423-3p promoted CRPC development by inducing cell migration and invasion. Further study is warranted to understand the role of miR-423-3p in CRPC and the association of cancer cell invasion with CRPC development.

MiRNAs downregulate gene expression through incorporation into the RISC, which then binds to partially complementary sites mainly in the 3′UTR (also can be in 5’ UTR) of their mRNA targets. According to TargetScan 7.1, there are in total 18 predicted target genes of miR-423-3p with conserved sites and MEIS1 is the top third target. Although it is not predicted by other prediction tool, this lower expression of this gene has shown positive association with PCa progression, while there is limited information of other predicted targets based on literatures. MEIS1 is a homeodomain transcription factor. In PCa, MEIS1 level exhibits a stepwise decrease in from benign epithelia, to primary tumour, and then to metastatic tissues and low expression of MEIS1 is associated with poor prognosis [409, 410]. MEIS1 has been identified as an AR negative regulator, which could inhibit the AR transcriptional activity and reduced the expression of AR target gene as well as disrupt the cytoplasm to nucleus translocation of AR in response to androgen [411]. Thus, I decided to explore if miR-423-3p could function as a regulator of MEIS1 in PCa cells. My WB results showed that over-expression of miR-423-3p decreased the protein level of MEIS1, but the effect was not big. This result cannot rule out the potential that MEIS1 is a miR-423-3p target. Further studies will be done to investigate if MEIS1 is a direct target of miR-423-3p.

Other genes may also be involved in the development of CRPC via regulation by miR-423-3p. In hepatocellular carcinoma [412], lung adenocarcinoma[406], and colorectal cancer [405], it has been demonstrated that miR-423-3p induces cell proliferation and invasion by directly targeting p21 (WAF1/CIP1), a cyclin dependent kinase inhibitor, although p21 (WAF1/CIP1) is not predicted as target of miR-423-3p either by Targetscan or miRDB. Previous reports of p21 (WAF1/CIP1) function in PCa progression are controversial. Early studies found p21 (WAF1/CIP1) is highly expressed in androgen-independent tumours and correlates with poor prognosis [413, 414], while other studies showed increased p21(WAF1/CIP1) production directly suppresses proliferation of PCa cells regardless of androgen sensitivity [415] and downregulation of both p21(WAF1/CIP1) and p27/Kip1 could produces a more aggressive prostate cancer phenotype[416]. Further studies should be done to determine the interaction of miR-423-3p and p21(WAF1/CIP1) and their role in PCa progression.

As I found different expression levels of miR-423-3p in plasma exosomes of CRPC and non-CRPC patients, it would be interesting to explore the potential role of exosomal miR-423-3p. The exosomes in plasma may come from various cell types. Currently we do not have evidence of the source of the exosomes. However, we observed higher levels of miR-423-3p in C4-2 cells compared to LNCaP cells, indicating that plasma exosomes miR-423-3p expression potentially resembles that in the tumour tissue. It has been demonstrated that exosomes from malignant cells could deliver miRNAs to recipient cells and induce their change from non-malignant to malignant [197, 417]. Due to short of time, the role of exosome-derived miRNAs in CRPC development have not been elucidated in the present study. However, I have tested method of ultracentrifugation to enrich exosomes from cell culture medium, which may facilitate further studies exploring the mechanism of miR-423-3p packaging in exosomes, and investigation of whether exosomes can deliver exogenous miR-423-3p to LNCaP cells and mediate its hormone-sensitivity. Exosomal miRNAs have also been demonstrated to playing important roles in regulating cancer microenvironment and promoting metastasis [203, 418, 419]. The effect of exosomal miRNAs on other cells, for example cancer-associated fibroblast and immune cells may also be explored.

Chapter VI *In vitro* propagation of PCa CTCs

6.1 Introduction

Patient-derived *in vitro* models will enable the investigation of the biology and genetics of PCa progression, in particular the mechanism under therapy response and drug resistance. Consequently, it will facilitate the identification of new biomarkers and the improvement of PCa clinical management. Expanding CTCs has offered the opportunity to establish patient-specific tumour models for individualised therapeutic prediction where tissue samples are not available. In the past decades, many research teams have attempted to establish CTC cultures, however limited achievements have been made.

There is only one case report on long-term culture of CTCs from PCa which cultured CTCs from peripheral blood of a mCRPC patient in organoid condition *in vitro* [246]. The CTC-derived cell line could facilitate detection of gene mutations and aberrant gene expression. It was also amenable to drug testing [246]. Attempts for short-term culture of CTCs have also been reported. Using an *in-situ* size-based capture and culture method, MetaCell®, CTCs from PCa patients could be cultured for over two weeks [257, 292]. The limited number of CTCs in blood has been the main issue that hampered CTC culture. Recently, CTC isolation method using mononuclear cells from apheresis has been developed that showed promises of high yield of CTCs [296, 297], which enable the formation of organoids and culture for over 4-6 weeks [297].

Our laboratory has explored a size-based CTC isolation system, Parsortix and demonstrated its high efficiency in capture CTCs [261] and the value of enumeration of CTCs as biomarker for PCa metastasis and prognosis [339]. Ongoing projects are aiming at exploring CTC enumeration as biomarker for PCa treatment response, especially for CRPC development and docetaxel response. My project was focused on CTC culture. This chapter aims to develop the method for PCa CTC culture in order to explore the value of CTC propagation for the study of PCa genetics and therapeutic response.

6.2 Results

6.2.1 CTC enumeration using Parsortix

For each clinical sample used for CTC culture, parallel assessment of CTC number using 7.5 ml blood was done using Ficoll-Parsortix and immunofluorescence staining as described in the method Chapter II. From the immunofluorescence staining, we detected different populations of CTCs: $CK^+Vim^-CD45^-$(epithelial type), $CK^+Vim^+CD45^-$(EMT type) and $CK^-Vim^+CD45^-$ (mesenchymal type). Representative images of each population of cells are shown in Figure 34. The CTC enumeration for each sample is presented in later section together with CTC culture results.

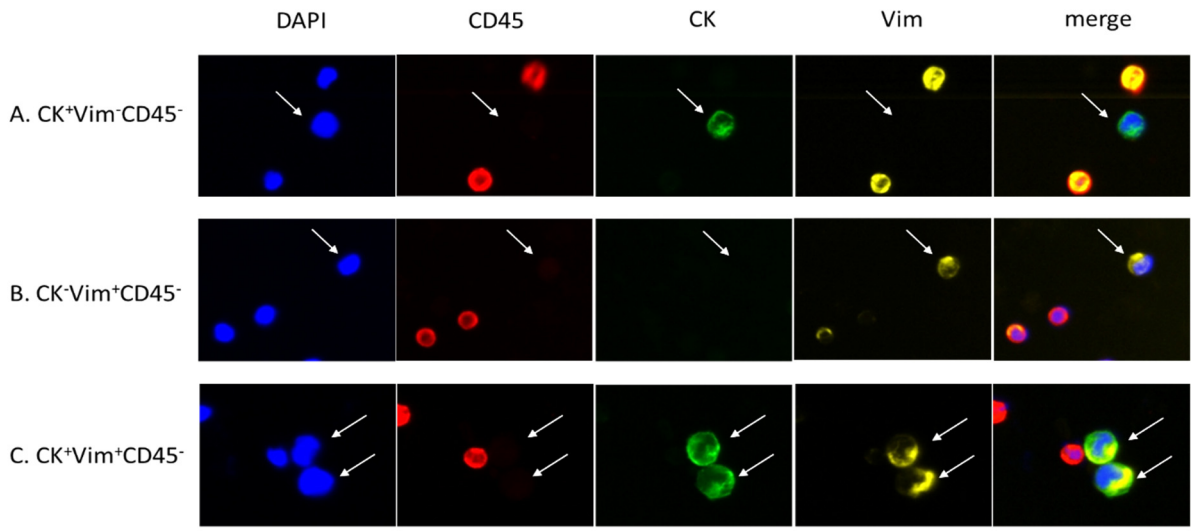

Figure 34. Representative immunofluorescence images for different types of cells in PCa patients. A. A representative $CK^+Vim^-CD45^-$ cell (arrow); B. A representative $CK^-Vim^+CD45^-$ cell (arrow); C. Two representative cells with $CK^+Vim^+CD45^-$ (arrow). Photos were taken using Ariol under 200× magnification. Part of this image has been published [339].

6.2.2 Initial test of CTC culture from clinical samples

To culture CTCs, I initially tried several samples with different isolation methods and culture media. Previously our group has shown Parsortix is an efficient CTC isolation platform with >50 harvest rate when testing with PCa cell lines [261].

Thus, it was used as one of the CTC isolation methods for initial test for CTC culture from clinical samples. EasySep is a negative selection method for CTC enrichment, which has been tested by Dr. Lei Xu in our group to further purify CTCs enriched from Parsortix. To shorten processing time and avoid cell loss, I used Ficoll-EasySep for CTC culture instead of Ficoll-Parsortix-EasySep. PrEGM media is designed for primary prostate cell culture and feeder cells are commonly used for primary prostate cell culture [343, 420]. Organoid culture medium and Matrigel has previously been used for PCa cells primary culture and PCa CTC culture [246]. I therefore tested three culture conditions 1) PrEGM medium with 5% Matrigel; 2) PrEGM with STO cells as feeder cells seeded at the bottom of the culture plate; 3) Organoid culture medium in Matrigel-coated plates (Figure 35). Three cases were isolated with Ficoll-Parsortix. However, all three cases got bacteria contamination shortly in culture. Eight samples were isolated by Ficoll-EasySep and no bacteria contamination was observed in these samples.

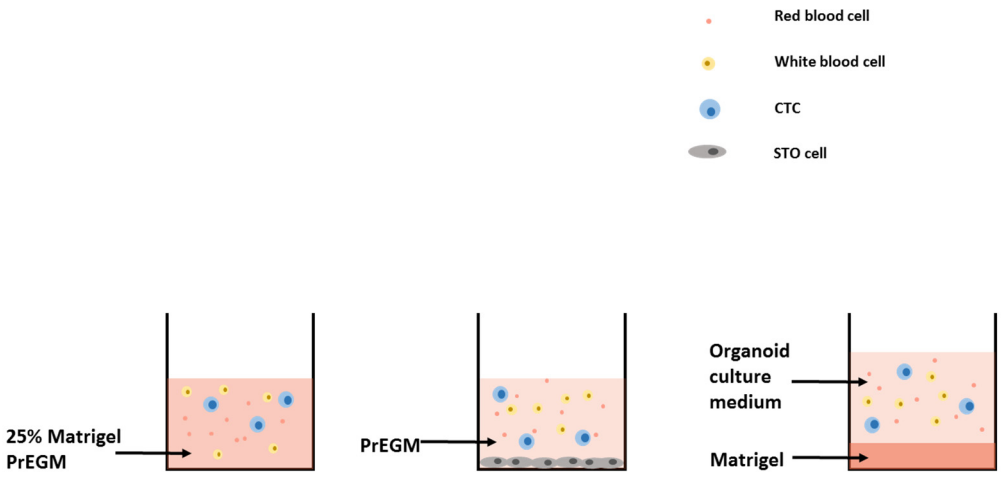

Figure 35. Illustration of three cell culture conditions for initial test of CTC culture from clinical samples.

When PrEGM medium is mixed with 25 % Matrigel, the medium is semisolid and cells remain in their position. White blood cell and red blood cell contamination severely affected the growth and observation of CTCs in culture in PrEGM medium mixed with 25 % Matrigel. Thus I gave up this culture condition as I tested it in only one sample. In the three samples which I PrEGM with feeder cells, it was difficult to distinguish CTC cells from feeder cells. All cells died out after

two weeks including the feeder cells, indicating the failure of CTC expansion. In the four samples which I used organoid culture medium with Matrigel, attached cells were observed at the first 3-5 days. However, there was no live cells observed after two weeks.

Table 34. Summary of CTC culture using blood samples from prostate cancer patients.

ID.	blood volume (ml)	isolation methods	culture condition	Total CTC counts/7.5 ml	Outcome
BCI188	7.5	Ficoll-Parsotix	PrEGM and feeder cells	0	contaminated
BCI189	7.5	Ficoll-Parsotix	Organoid culture medium+Matrigel-coated plates	0	contaminated
BCI255	7.5	Ficoll-Parsotix	Organoid culture medium+Matrigel-coated plates	1	contaminated
BCI254	16.5	Ficoll-EasySep	PrEGM with 25% Matrigel	0	too many red blood cell contamination
BCI141	8.5	Ficoll-EasySep	PrEGM and feeder cells	0	no live cell after 2 weeks
BCI142	7.5	Ficoll-EasySep	PrEGM and feeder cells	0	no live cell after 2 weeks
BCI152	12	Ficoll-EasySep	PrEGM and feeder cells	14	no live cell after 2 weeks
BCI145	7.5/2	Ficoll-EasySep	Organoid culture medium+Matrigel-coated plates	8	no live cell after 2 weeks
BCI146	7.5/2	Ficoll-EasySep	Organoid culture medium+Matrigel-coated plates	0	no live cell after 2 weeks
BCI266	7.5/2	Ficoll-EasySep	Organoid culture medium+Matrigel-coated plates	No enumeration done as no enough blood	no live cell after 2 weeks
BCI147	11.5	Ficoll-EasySep	Organoid culture medium+Matrigel-coated plates	3	no live cell after 2 weeks

6.2.3 Test of CTC isolation methods and culture conditions

Following the failure of the initial test of CTC culture, PCa cell lines were used to test different CTC isolation methods and culture media and conditions.

6.2.3.1 Test of CTC isolation methods

Although Ficoll-Parsortix and Fioll-EasySep did not work in initial test of CTC culture from clinical samples, there may be various reasons for the failure. Thus, there two methods were further tested using PCa cells lines. In addition, another negative-selection method which has been previously reported for CTC culture, RossetteSep [246], was also tested.

2400 VCaP cells, which are difficult to culture at low cell density, were spiked in 7.5 ml healthy donors' blood for each method. VCaP cells were then isolated by Ficoll-Parsortix, Ficoll-EasySep or RossetteSep. Harvested cells were resuspended in RPMI-1640 and equally aliquoted and used for culture in four different conditions: 2D culture in normal 96-well plate, 2.5D culture on Matrigel-coated 96-well plate, organoid culture mixed with Matrigel and suspension culture in low-attachment 96-well plate. Cells ran through Parsortix were quickly contaminated with bacteria within one week under all culture conditions. Viable cells could be isolated by EasySep and RossetteSep, but only limited cells survived at the beginning of culture and the cells gradually died off. This is mainly because VCaP cells are too difficult to be expanded when start with small number of cells (Figure 36). It is difficult to draw a conclusion of which isolation method and culture condition is the best for CTC culture based on the test results using VCaP cells.

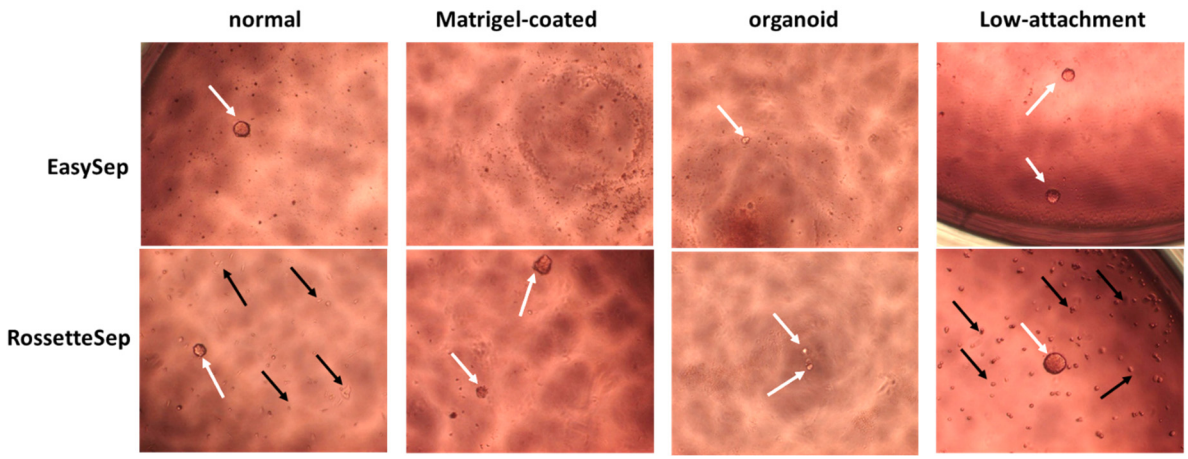

Figure 36. Image of VCaP cells harvested from different CTC isolation methods and cultured in four different conditions. No image shown for VCaP cells harvested from Parsortix as the cells were contaminated. White arrows indicate spheres; Black arrows indicate single cells. Photos were taken uder 40× magnification.

I then used PC3 cells for spiking test using different isolation methods and culture conditions. 240 PC3 cells were spiked in 7.5 ml healthy donors' blood and then isolated by Parsortix, EasySep or RossetteSep. Harvested cells were resuspended in RPMI-1640 (supplemented with 10% FCS and 1×antibiotic&antimycotic) and equally aliquoted and used for culture in four different conditions. Parsortix still had contamination problem but viable cells were isolated and could proliferate well (Figure 37). PC3 cells enriched by EasySep grown better than the other two isolation methods. Normal culture plates and Matrigel-coated plates were both good for cell proliferation (Figure 37).

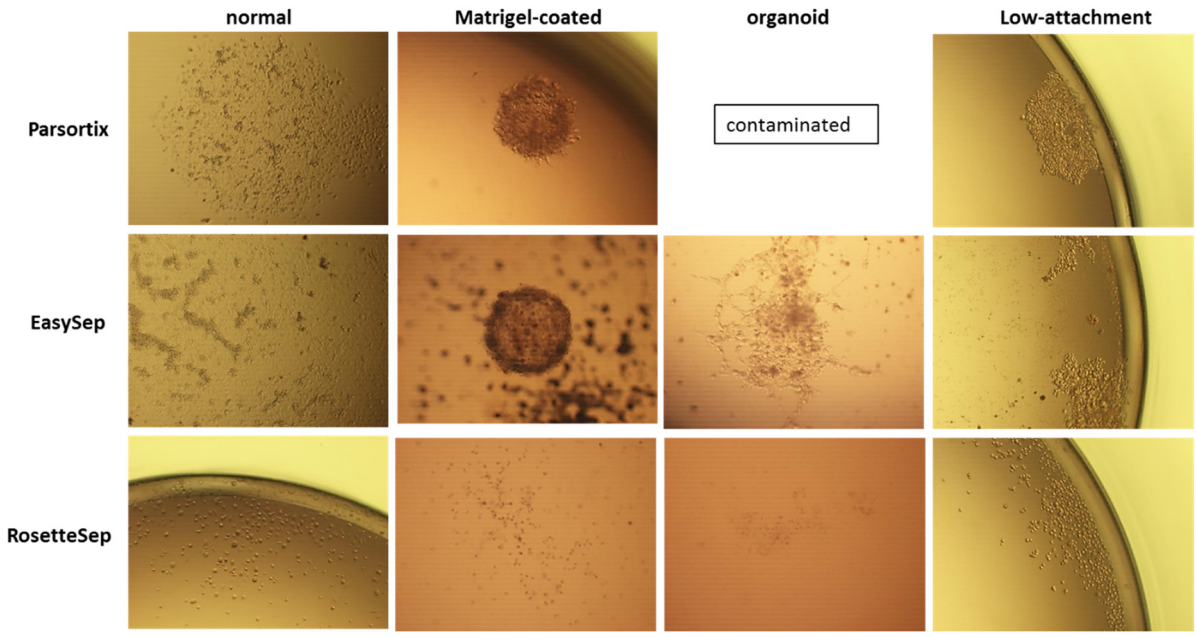

Figure 37. Image of PC3 cells harvested from three different CTC isolation methods and cultured in four different conditions. Photos were taken uder 40× magnification.

6.2.3.2 Test of culture media and conditions

VCaP cells were used to model CTC culture as VCaP cells are difficult to grow when starting with low number of cells. 200 VCaP cells were counted and directly seeded in each well of 96-well plates of three conditions and with four different culture media. After culturing for two weeks, cells were checked under microscope. It showed that RPMI-1640 (supplemented with 10% FCS and 1×antibiotic&antimycotic) was the most suitable medium for VCaP cells that cells formed large colonies in normal plate and low-attachment plate (Figure 38). VCaP cells grown well in organoid culture medium in Matrigel-coated plates, but only as single cells in normal plate and low-attachment plate (Figure 38). PrEGM and F-medium were not as good as RPMI-1640 (supplemented with 10% FCS and 1×antibiotic&antimycotic) under any condition (Figure 38).

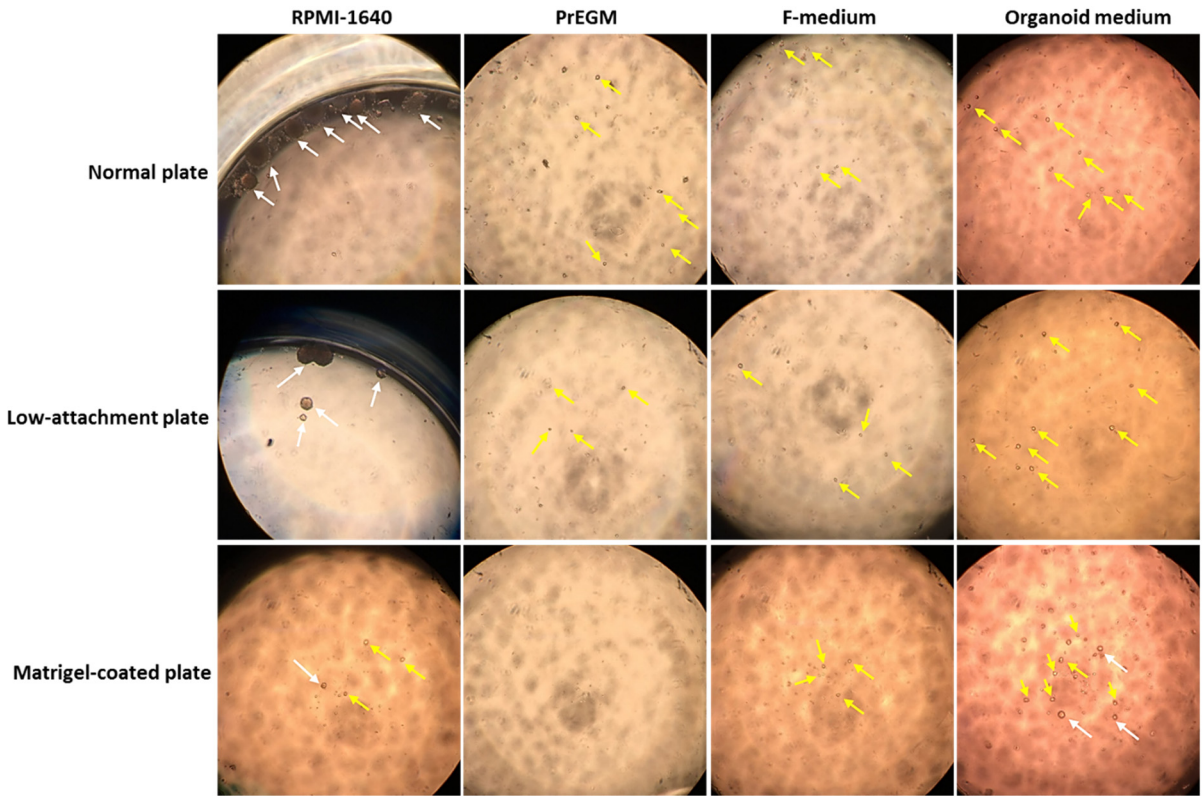

Figure 38. VCaP cells cultured in different media and conditions. Three replicates were done for each condition. White arrows indicate colonies; yellow arrows indicate single cells. White arrows indicate spheres; yellow arrows indicate single cells. Photos were taken uder 40× magnification.

To test if the culture conditions have the same effect to other PCa cell lines, similar tests were also performed using DU145 and 22Rv1 cells. As DU145 and 22Rv1 cells are easier to expand compared to VCaP cells, in addition to testing using 200 cells per well, another group using 30 DU145/22Rv1 cells per well was tested.

In normal plates, DU145 grown best in RPMI-1640 that the wells were confluent (Figure 39A). DU145 cells did not grown well in low-attachment plate and there was no difference between three media (Figure 39B). In Matrigel-coated plate, DU145 cells grew well in RPMI-1640 and organoid culture medium and formed more colonies (Figure 39C) than in F-medium. Least colonies formed in PrEGM (Figure 39C).

For 22Rv1, in normal plates, cells grown well in RPMI-1640 and F-medium as the wells were confluent (Figure 40A). Cells formed small spheroids in organoid

culture medium, but the total live cell number was low (Figure 40A). In low-attachment plate, 22Rv1 formed large spheres in RPMI-1640 and F-medium. Small spheroids were observed in organoid culture medium while very few live cells found in PrEGM (Figure 40B). In Matrigel-coated plates, 22Rv1 cells grew well in RPMI-1640 and organoid culture medium and formed more colonies than in F-medium (Figure 40C). Very few single live cells were observed in PrEGM (Figure 40C).

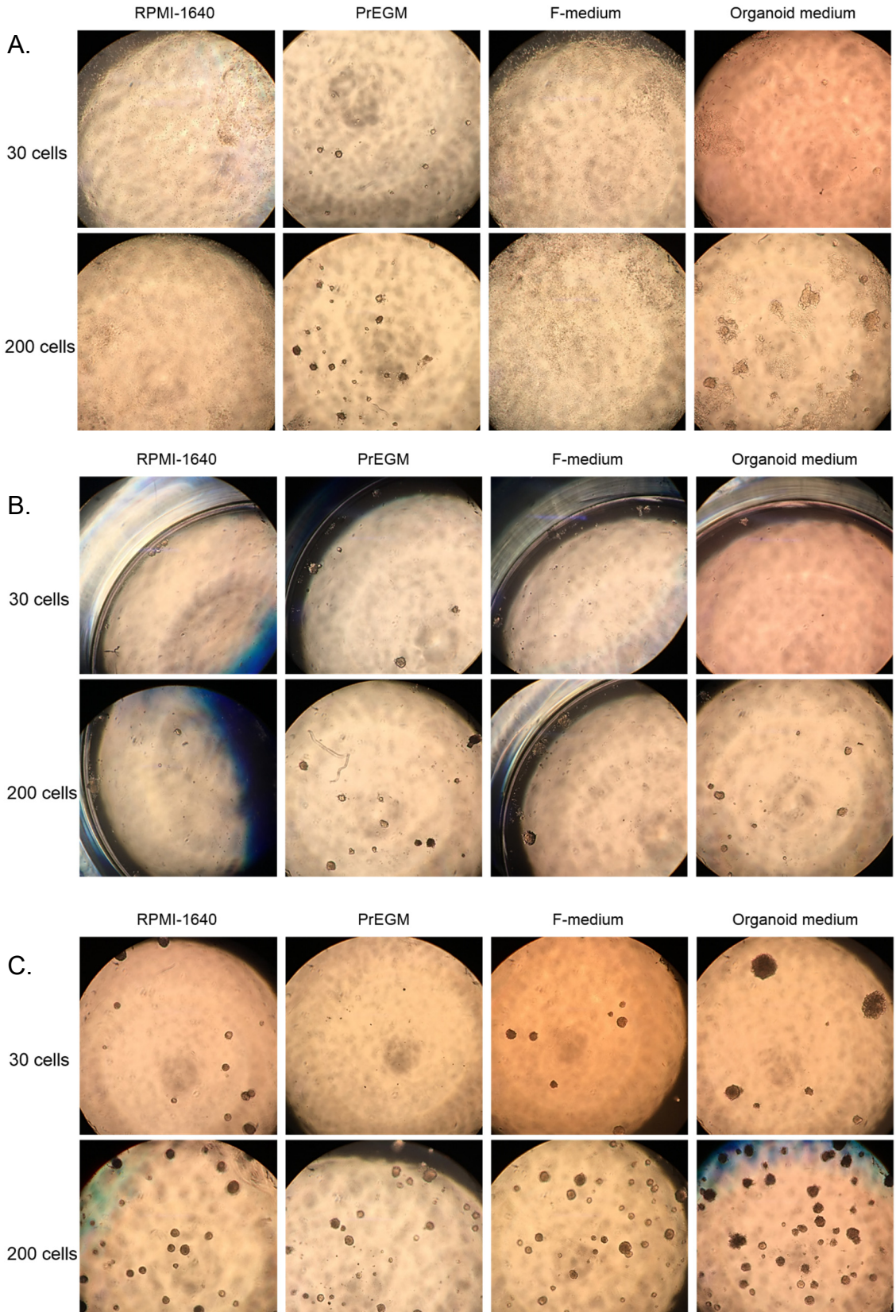

Figure 39. Test of different culture media and conditions using DU145 cells. A. Cells grown in normal plates; B. Cells grown in low-attachment plates; C. Cells grown in Matrigel-coated plates. Three replicates were done for each condition. Photos were taken uder 40× magnification.

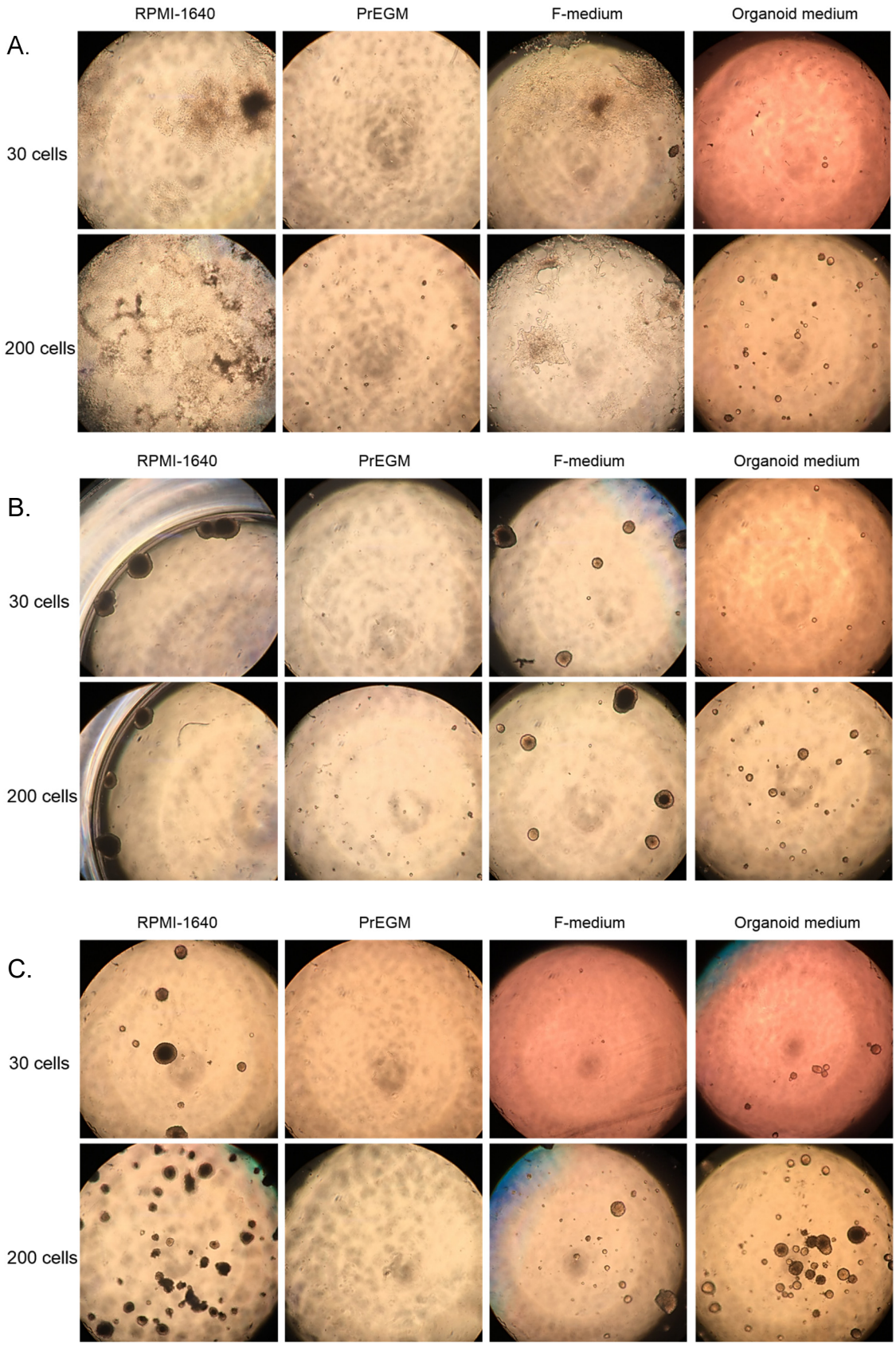

Figure 40. Test of different culture media and conditions using 22Rv1 cells. A. Cells grown in normal plates; B. Cells grown in low-attachment plates; C. Cells grown in Matrigel-coated plates. Three replicates were done for each condition. Photos were taken uder 40× magnification.

I also tried an rotary cell culture system (SYNTHECON, US) (Figure 41) which could help 3D cell culture. 20000 VCaP cells were seeded in the 10 ml vessel. The cells formed large spheres. However, the cell count after one-week culture was even lower than the seeded count. Considering the system requires large number of cells to start and did not help VCaP cell expansion, I later did not apply this system for CTC culture.

Figure 41. The rotary cell culture system.

6.2.4 CTC culture using Avatar system and Xcell liquid biopsy kit

Avatar system is a cell culture incubator which could provide hypoxia and pressure condition similar to that in the blood circulation. At this stage, a CTC isolation and culture workflow developed by Xcell bioscience (US) using Xcell liquid biopsy kit and Avatar cell incubator system was introduced to me. Thus I tested Xcell liquid biopsy kit and Avatar system with modifications on the manufacturer's protocol to culture CTCs from clinical samples.

As RPMI-1640 had best performance for cell culture in my previous tests, I firstly tested five samples isolated by Ficoll-Parsortix, EasySep or Ficoll only and cultured the cells in RPMI-1640 in Avatar incubator (Table 35). The sample isolated by Ficoll-Parsortix was not contaminated by bacteria, but no cells live after 3 weeks of culture. The sample isolated by Ficoll-Easysep had attached cells in culture but the cell morphology showed the cells were unhealthy and cells gradually died off (Figure 42). Three samples were isolated by Ficoll and cultured in RPMI-1640 in Avatar system. One sample had no attached cells at day 4 of culture and the attached cells from other two samples died off within 3 weeks of culture. In summary, using RPMI-1640 and Avatar system could not facilitate CTC culture when I tested with clinical samples.

Figure 42. Cells from BCI255 isolated by Ficoll-Easysep and cultured in RPMI-1640 in Avatar system at day 4. Photos were taken uder 100× magnification.

Table 35. Summary of samples used for CTC culture with RPMI-1640 in Avatar system and the CTC counts.

ID	Blood vol for culture (ml)	CTC culture medium	Blood collection tube	CTC culture plate	Isolation method	Incubator	Epithelial CTC	Mesenchymal CTC	EMT CTC
BCI169	9	RPMI-1640	EDTA	low-attachment	Ficoll-Parsortix	Avatar	0	5	0
BCI255	8.5	RPMI-1640	EDTA	normal	Ficoll-Easysep	Avatar	2	0	0
BCI256	15	RPMI-1640	EDTA	normal	Ficoll	Avatar	0	2	0
BCI257	15	RPMI-1640	ACD	normal	Ficoll	Avatar	0	0	0
BCI258	13	RPMI-1640	ACD	normal	Ficoll	Avatar	0	1	0

Xcell liquid biopsy kit was designed for CTC culture which includes seeding medium, culture medium, and 6-well plates which are coated-specially for CTC culture. Thus, I decided to try Xcell media and plates for CTC culture. According to the Xcell bioscience suggestion, CTCs were enriched by Ficoll only to reduce processing time and avoid further cell loss during the process. As Avatar system broke down and we had limited time for the demo machine, hypoxia incubator was used later instead of Avatar. I employed Avatar system/hypoxia incubator and Xcell liquid biopsy kit to culture CTCs from 27 PCa patients' blood. For each sample, we also did parallel CTC enumeration using 7.5 ml blood. Table 33 shows the CTC isolation method, culture method used for CTC culture of each sample and the CTC counts.

Table 36. Summary of samples used for CTC culture using Avatar system and Xcell liquid biopsy kit and the CTC counts.

ID	Blood vol for culture (ml)	CTC culture medium	Blood collection tube	CTC culture plate	Isolation method	Incubator	Epithelial CTC	Mesenchymal CTC	EMT CTC
BCI173	15	XCR	ACD	XCR	Ficoll	Avatar	0	2	0
BCI243	15	XCR	ACD	XCR	Ficoll	Avatar	0	3	0
BCI262	18	XCR	ACD	XCR	Ficoll	Avatar	2	1	0
BCI263	18	XCR	ACD	XCR	Ficoll	Avatar	0	2	1
BCI244	18	XCR	ACD	XCR	Ficoll	Avatar	0	6	0
BCI265	18	XCR	ACD	XCR	Ficoll	Avatar	2	0	1
BCI266	18	XCR	ACD	XCR	Ficoll	Avatar	0	0	0
BCI267	18	XCR	ACD	Half in XCR	Ficoll	Avatar	0	1	0

				Half in Matrigel-coated 24-well plate					
BCI174	18	XCR	ACD	Half in XCR Half in Matrigel-coated 24-well plate	Ficoll	Avatar	0	1	0
BCI125	16.5	XCR	ACD	XCR	Ficoll	Avatar	0	9	0
BCI270	8	XCR	ACD	XCR	Ficoll	Avatar	0	9	2
BCI271	18	XCR	ACD	XCR	Ficoll	Avatar	0	0	0
BCI159	18	XCR	ACD	XCR	Ficoll	hypoxia	1	3	0
BCI273	18	XCR	ACD	XCR	Ficoll	hypoxia	0	2	0
BCI274	18	XCR	ACD	XCR	Ficoll	hypoxia	0	2	0
BCI275	17	XCR	ACD	XCR	Ficoll	hypoxia	1	3	0
BCI276	17	XCR	ACD	XCR	Ficoll	hypoxia	not countatble		

BCI277	18	XCR	ACD	XCR	Ficoll	hypoxia	0	0	0
BCI278	18	XCR	ACD	XCR	Ficoll	Avatar moved to hypoxia	0	0	0
BCI279	16.5	XCR	ACD	XCR	Ficoll	Avatar moved to hypoxia	0	0	0
BCI245	17	XCR	ACD	XCR	Ficoll	Avatar-hypoxia	3	0	0
BCI281	18	XCR	ACD	XCR	Ficoll	hypoxia	0	0	0
BCI282	18	XCR	ACD	XCR	Ficoll	hypoxia	3	0	0
BCI283	18	XCR	ACD	XCR	Ficoll	hypoxia	5	0	1
BCI290	18	XCR	ACD	XCR	Ficoll	hypoxia	0	0	0

BCI291	18	XCR	ACD	XCR	Ficoll	hypoxia	2	3	1
BCI287	17	XCR	ACD	XCR+Matrigel-coated plate	Ficoll	hypoxia	0	1	0
BCI246	17	XCR	ACD	Matrigel-coated 24-well plate	Ficoll	hypoxia	0	4	0
BCI285	17	XCR	ACD	Matrigel-coated 24-well plate	Ficoll+EasySep	hypoxia	0	0	0
BCI175	17	XCR	ACD	Matrigel-coated 24-well plate	Ficoll	hypoxia	0	0	0
BCI288	18	XCR	ACD	low-attachment 96-well plate	Ficoll	hypoxia	0	0	0
BCI289	18	XCR	ACD	low-attachment 96-well plate	Ficoll	hypoxia	0	2	1

Cultured CTCs in XCR 6-well plate were attached to the plates as single cells or colonies, exhibiting different morphologies (Figure 43). Some attached cells exhibited cell membrane ruffling and some exhibit elongated morphology (Figure 43). In 26 samples which we used Xcell liquid biopsy kit and Avatar/hypoxia incubator, we managed to culture 15 samples for over one month, and I froze cells from another two samples within one-month culture. The longest culture I kept reached five month.

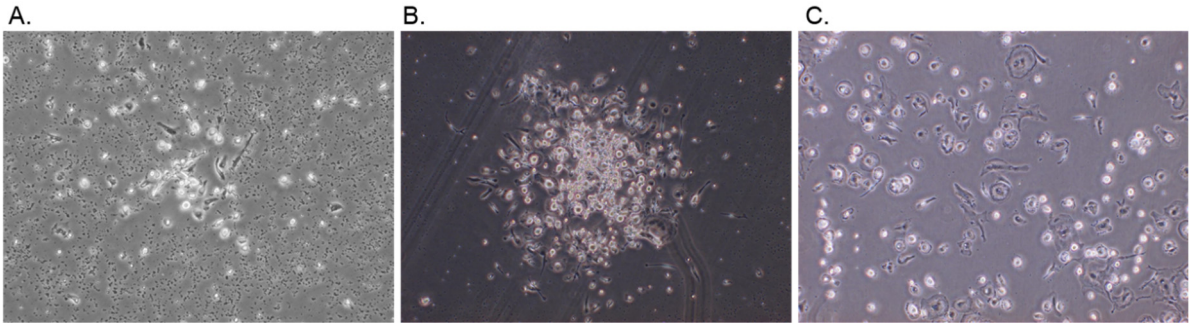

Figure 43. Representative images of cultured CTCs in XCR 6-well plate with different morphologies. A. Culture cells from BCI263 at day 14; B. Cultured cells from BCI125 at day 18; C. Cultured cells from BCI267 at day 25. Photos were taken uder 100× magnification.

Enriched CTCs from BCI267 and BCI174 were split into two portions and cultured in XCR 6-well plate and Matrigel-coated plate separately (Table 33). Cells in XCR 6-well plate were attached to the plate as mono layers. In Matrigel-coated plate, some cells spread as single cells and some formed spheres (Figure 44).

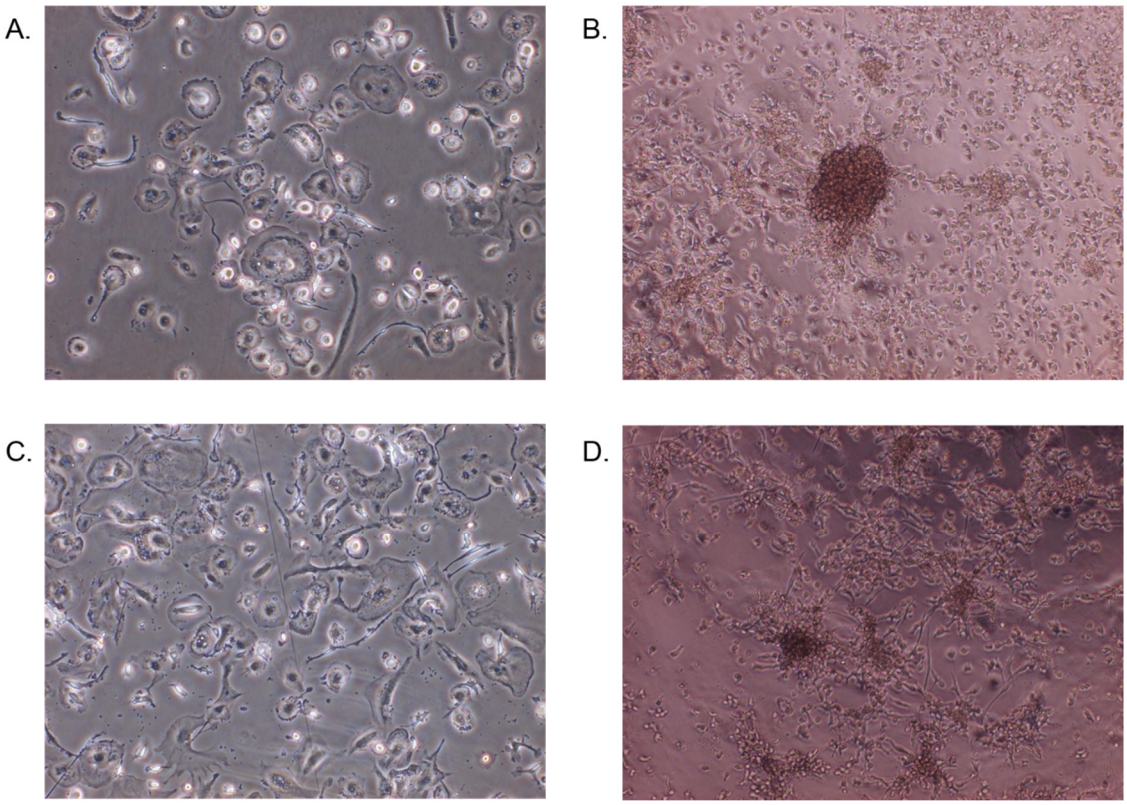

Figure 44. Representative image of culture CTCs in XCR 6-well plates and Matrigel-coated plates. A. BCI267 cells cultured in XCR 6-well plate at day 25; B. BCI267 cells cultured in Matrigel-coated plate at day 28; C. BCI174 cells cultured in XCR 6-well plate; D. BCI174 cells cultured in Matrigel-coated plate at day 28. Photos were taken uder 100× magnification.

Three samples were used to culture in Matrigel-coated plates using Xcell media, but cells gradually died off. Two samples were used to culture in low-attachment plate using Xcell media, but no spheres formed and cells could be easily removed via medium change.

6.2.5 Immunofluorescence-staining and FISH analysis of cultured CTCs

In certain cases, the enriched CTCs were able to be propagated using XCR CTC culture medium in hypoxia incubator for over 3 weeks. However, the cells exhibited different morphologies which were not typical epithelial cell morphology. We then sought to identify the cell type of living cells in the culture by immunofluorescence-staining and FISH. Cells of BCI267 cultured in XCR 6-well plate were harvested, dropped and fixed on glass slides. Then the cells were fixed and stained with CK, Vim, CD45 and DAPI. Most of the cells showed strong Vim stain and different levels of CD45 expression. No or very weak CK expression was observed. Some cells shown multiple nucleus (Figure 45).

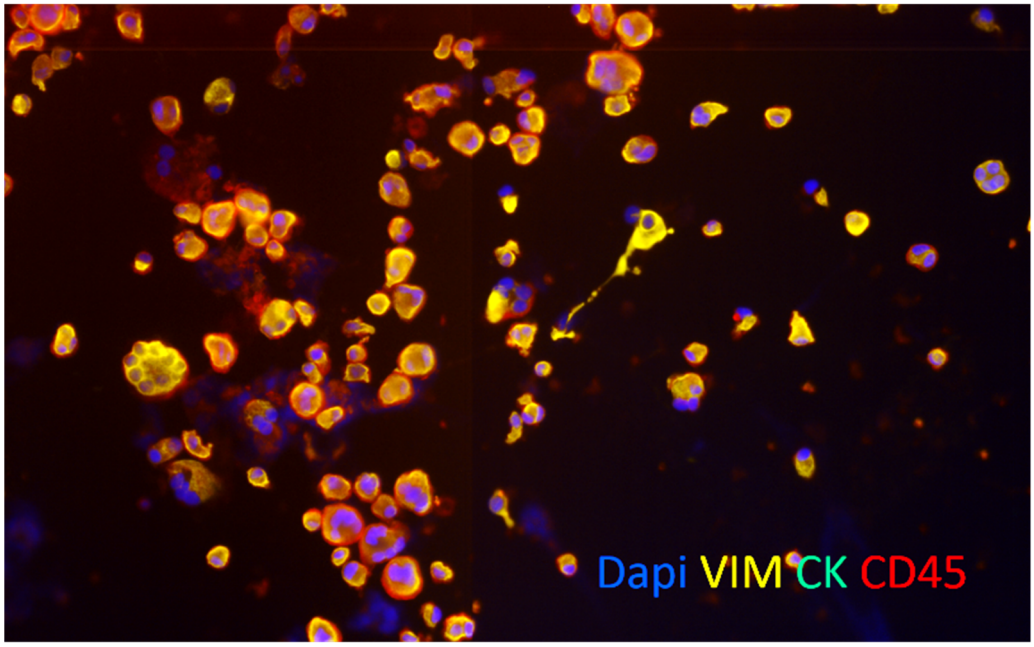

Figure 45. Immunoflorescence-staning of cultued CTCs from BCI267 that dropped on slide. Photos were taken using Ariol under 200× magnification. Blue: DAPI; Yellow: Vimentin; Green: CK, Red: CD45.

To clearly observe the cell morphology at culture condition, I harvested cells of BCI278 cultured in XCR 6-well and cultured them on the glass coverslip. 24 h after the cells were attached, cells were fixed and stained with CK, Vim, CD45 and DAPI. Similar as cells from BCI267, most of the cells shown strong Vim stain

and different levels of CD45 expression. No or very weak CK expression was observed. Some cells shown multiple nucleus (Figure 46). Most cells showed elongated morphology, while small portion of cells were round (Figure 46).

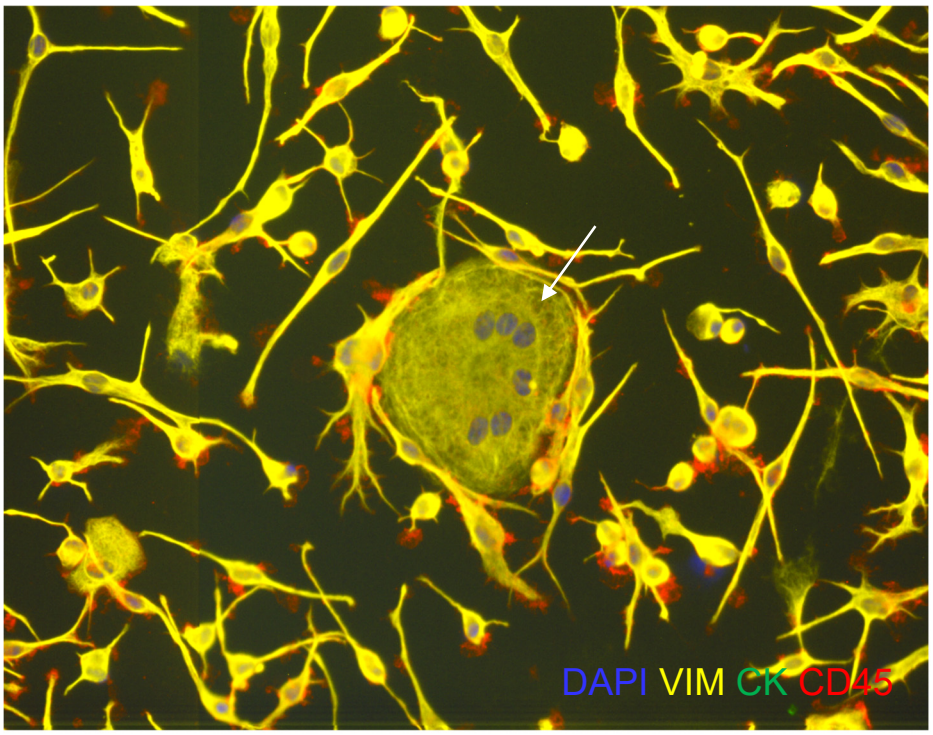

Figure 46. Immunoflorescence-staining of cultured CTCs from BCI278 that grown on slide. A big multi-nucleus cell is indicated by arrow. Photos were taken using Ariol under 200× magnification. Blue: DAPI; Yellow: Vimentin; Green: CK, Red: CD45.

PTEN is one of the most frequently deleted tumour suppressor gene in PCa. Monoallelic loss of *PTEN* is present in up to 60% of localised prostate cancers and complete loss of *PTEN* in PCa has been found linked to metastasis and androgen-independent progression [76]. *AR* amplification were reported in 20-30% of CRPC and has been suggested to develop during hormone deprivation therapy. Thus, I decided to perform FISH to detect *AR* and *PTEN* in the cultured CTCs to identify potential tumour cells. The immunofluorescence signal was washed off and FISH of *AR* and *PTEN* was applied on the slide of BCI267. The cell nuclei morphology changed potentially during FISH, but the cells could be located between FISH image and immunofluorescence image based on the relative cell position.

Most of the cells present normal *AR* (one copy per cell) and *PTEN* (two copies per cell) copy number. However, I also observed cells with *AR* gain or *PTEN* loss genotype (Figure 47). In 211 cells examnined, nine cells were found to bear copy number changes.

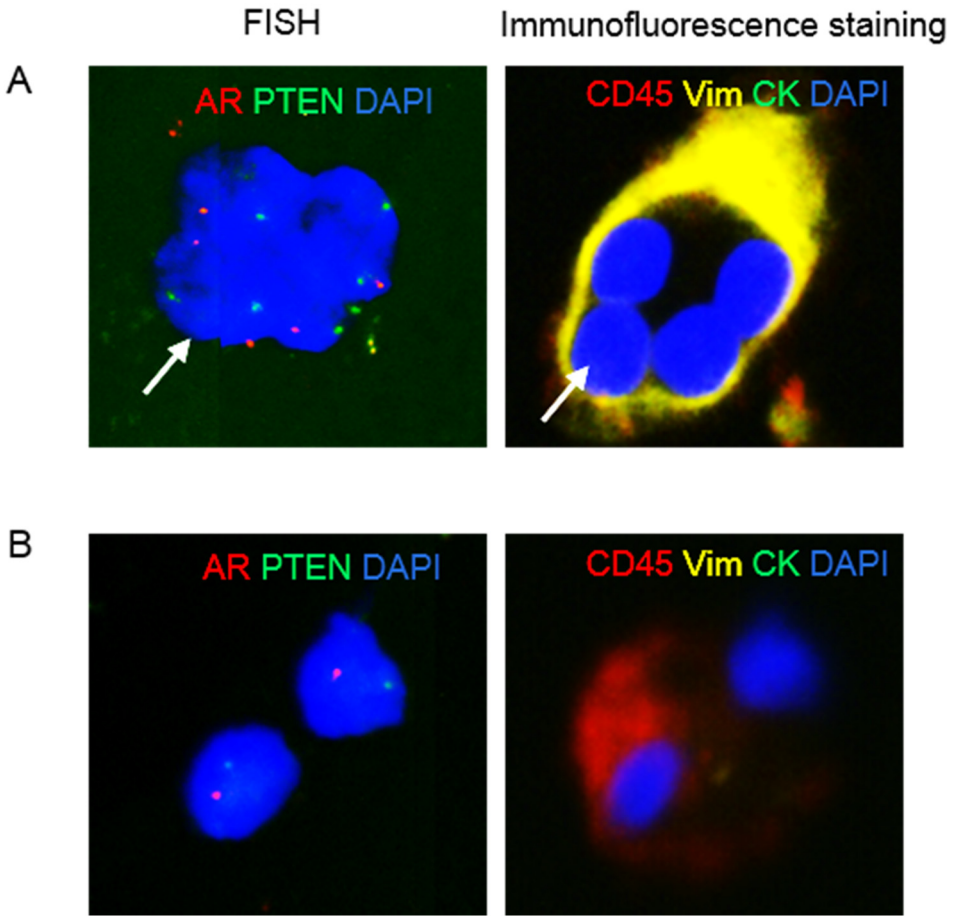

Figure 47. FISH images (left) and corresponded immunofluorescence-staining (right) of cultured CTC cells from BCI267. A. White arrow indicates a cell with *AR* gain; B. Two cells with *PTEN* loss. Immunofluorescence-staining images were taken using Ariol under 200× magnification and FISH images were taken using Ariol under 400× magnification.

6.2.6 Xenografts of cultured CTCs

Cultured CTCs were also obtained from Dr. Lei Xu. These CTCs were initial cultured with mitomycin treated mouse fibroblast cell NIH/3T3 in F medium. However, NIH/3T3 cells maintained proliferation ability. Initial immunofluorescence staining performed by Dr Lei Xu showed that only small

portion of the cultured cells expressed CK, indicating the cultured CTCs are mixed with NIH/3T3 cells with the later as dominant.

I recovered the cultured CTCs from Dr. Lei Xu's frozen stock and performed immunofluorescence staining of the cultured CTCs and NIH/3T3 cells. Immunofluorescence staining showed both cultured CTCs and NIH/3T3 cells expressed Vim. However, only in cultured CTCs, CK expression was observed and cells presented different intensity of CK staining (Figure 48).

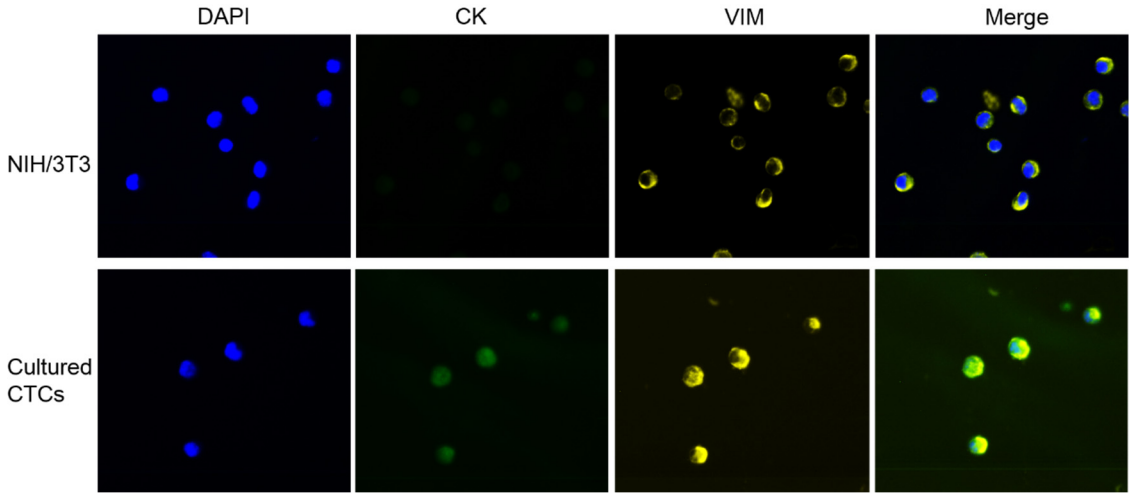

Figure 48. Immunofluorescence staining of NIH/3T3 cells and mixed population of cultured CTCs. Immunofluorescence-staining images were taken using Ariol under 200× magnification.

To enrich the tumour cells from the mixed population, the cultured CTCs were engrafted into the nude mouse flank (the mouse engrafting and sacrifice was

Figure 49. Nude mouse engrafted with cultured CTCs in the flank formed tumour (red circle) after 11 weeks.

performed by Dr. Marc Yeste-Velasco). Injected cells formed tumour after 11 weeks (Figure 49).

The xenograft tumour was taken out and part of the tumour tissue was cut to small clumps or digested and shredded into single cells. The clumps and singles cells were cultured *in vitro*. The left tissue was formalin-fixed paraffin-embedded. After 3 days of culture, cells climbed out the clumps (Figure 50A). From the shredded tumour tissue, attached cells were observed in the culture (Figure 50B). The cells could be passaged and proliferated quickly. However, from the cell morphology, it is difficult to determine the cells were tumour cells or fibroblast cells.

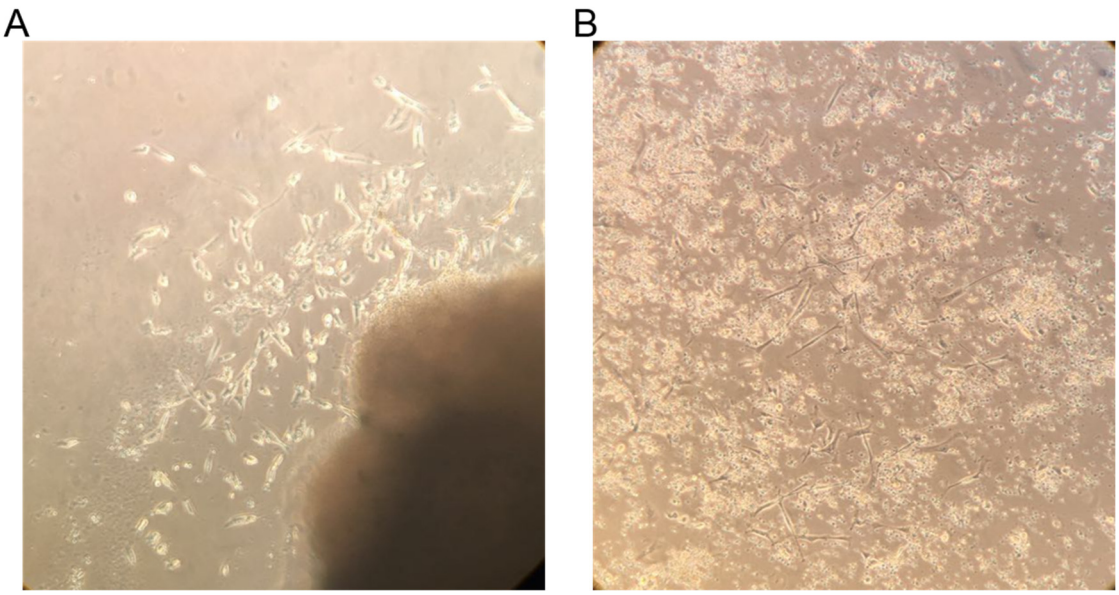

Figure 50. *In vitro* culture of cells from CTC xenograft. A. Cells climbed out of tissue clump; B. Some cells attached in the shredded tissue culture. Photos were taken under 40× magnification.

To examine the cell type, we prepared the metaphase chromosome spread slides of the cultured cells. The metaphase spreads showed that most of the chromosomes were telocentric but metacentric chromosomes were also present (Figure 51), indicating potential hybrid human and mouse cells. Two karyotypes with 61 and 125 chromosomes were observed (Figure 51). The karyotypes

present different chromosome numbers to NIH/3T3 cells which were reported having 52 to 82 chromosomes[421].

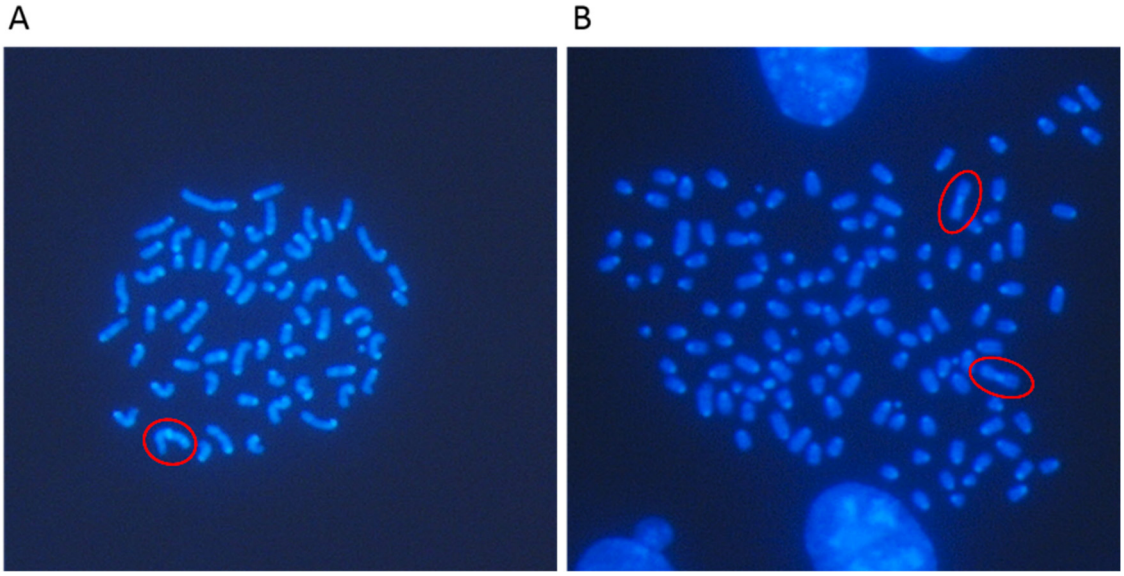

Figure 51. Metaphase spread analysis of cultured cells from CTC xenograft. The cells presented two karyotypes with 61 chromosomes (A) and 125 chromosomes (B). Red circles label metacentric chromosomes. Images were taken under 600× magnification.

We then performed IHC on the FFPE sections of the CTC derived tumour tissue (Dr. Elzbieta Stankiewicz helped to perform the IHC). The CTC-derive xenograft present cytoplasmic AR stain (Figure 52). IHC for PSA showed the xenograft had moderate PSA expression (Figure 53).

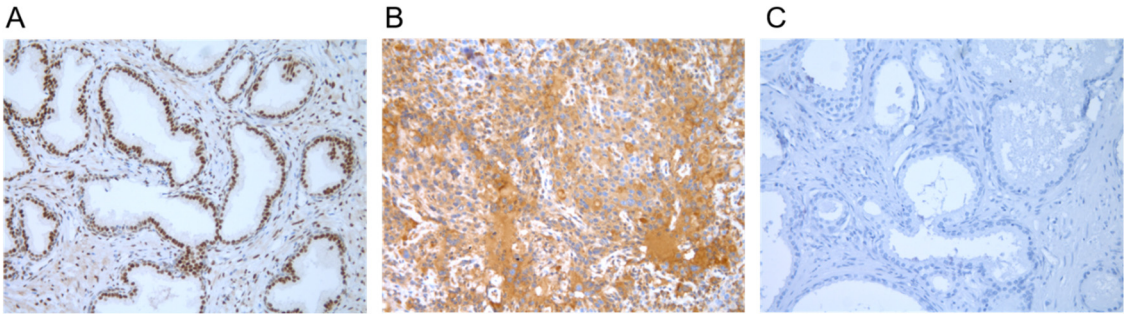

Figure 52. Detection of AR expression in FFPE sections by IHC. A. Human BPH section as positive control where AR present nuclear stain; B. CTC-derived xenograft tissue section where AR present cytoplasmic stain; C. Human BPH section without primary antibody. Images were taken under 200× magnification.

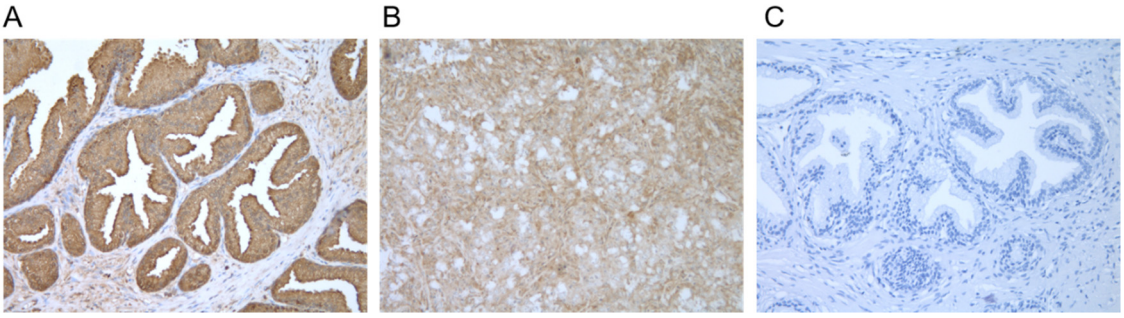

Figure 53. Detection of PSA expression in FFPE sections by IHC. A. Human BPH section as positive control; B. CTC-derived xenograft tissue section; C. Human BPH section without primary antibody. Images were taken under 200× magnification.

6.3 Discussion

6.3.1 CTC isolation methods for CTC culture

Isolation and analysis of CTCs from blood have provided significant implications in diagnosis and therapeutic treatment of cancers. There are various techniques have been developed to isolate CTCs. However, isolation of CTCs remains a technological challenge due to their rarity and low recovery rate. The requirements for CTC isolation methods are different for different purposes. CTC isolation for CTC culture may require preservation of the cell viability and high harvest rate, while the demand on purity is not strict. To find a CTC isolation method suitable for prostate CTC *in vitro* culture, in this study, I tested several CTC isolation methods which enrich CTCs based on different principles. Ficoll-Paque PLUS is a density gradient medium that has been recognised standard in laboratories worldwide for the isolation of mononuclear cells. Ficoll centrifugation provides a quick process to enrich mononuclear cells from whole blood. Using red blood cell lysis buffer to deplete red blood cells is another commonly used method to enrich nucleated cells. Parsortix is a size-based microfluidic system

that could enrich CTCs and keep cell viability [261]. Our lab has developed the method using Ficoll-Parsortix for CTC enumeration [261]. EasySep and RossetteSep used in this study are immuno-based methods to deplete white blood cells. EasySep depletes unwanted cells by first incubating samples with the magnetic nanoparticles and tetrameric antibody complexes targeting CD45. Then the magnetically labelled cells are separated from unlabelled cells by placing the sample-containing tube into the EasySep magnet, which creates a magnetic field that holds labelled cells on the tube wall that unlabelled cells can be poured out. RossetteSep crosslinks red blood cells and white blood cells that can deplete red blood cells and white blood cells at the same time by density centrifugation of Ficoll. Several studies of CTC culture have used RossetteSep to enrich CTCs [246, 247, 300]. I tested Ficoll-Parsortix, Ficoll-EasySep and RossetteSep using VCaP and PC3 cells. When using PC3 cells, viable cells could be harvested from Ficoll-Parsortix and cultured *in vitro*. However, using Parsortix had high bacteria contamination risk as Parsortix is an open system that samples would be exposed to the outside environment at several steps during the process. Both my CTC culture attempts using spiking and clinical blood samples all showed that cells isolated from Parsortix were easy to be contaminated by bacteria. Both Ficoll-EasySep and RossetteSep enabled viable cells isolation. However, when testing with PC3 cells using RossetteSep, the cells in culture showed different morphology compared to them in routine culture. The morphology of PC3 cells isolated using RossetteSep indicates the reagents used in RossetteSep may affect cell property or induce blood cell growth. Thus, Ficoll-EasySep is the best CTC enrichment method among our tests to deplete white blood cells for *in vitro* culture. However, EasySep has its drawbacks including long processing time and potential influence of remaining magnetic beads on cell proliferation. As blood cells can be depleted during cell culture and additional step would inevitably reduce harvest rate, Ficoll centrifugation alone may be sufficient to preliminary enrich CTCs from whole blood.

6.3.2 Culture media and conditions for CTC culture

In the published articles of CTC *in vitro* culture, various culture media and culture conditions were used without sufficient comparison to other culture methods. For

PCa CTC culture, limited reports have been published. For short-term culture, RPMI-1640 supplemented with FCS were used [257, 292]. Organoid culture medium was used to establish long term culture of PCa cells from CTCs and specimens [246]. In a recent study, organoid culture medium was used to culture PCa CTCs from one mCRPC patient. The spheroids were maintained for 4 to 6 weeks [297]. PrEGM is a serum-free medium designed for prostate epithelial cell primary culture. I also included a modified medium, F-medium which has been previously reported [343] and used by Dr. Lei Xu for CTC culture. In addition to different media, we also included several culture conditions for test. 2D adherent condition is most commonly used for *in vitro* culture. However, it is claimed that non-adherent conditions are important for long-term expansion of CTCs, as CTCs would senesce after a few cell divisions in adherent monolayer culture [422]. A growing body of evidence has suggested that 3D culture represents more accurately the actual microenvironment where cells reside in tissues [423]. Thus, I also used Matrigel to provide extracellular matrix condition for CTC culture. Ultra-low attachment culture dish and rotary cell culture system, which force cells to stay in unattached conditions to minic the blood circulation situation for cancer cells, were also tested. When I tested different culture media and conditions with cell lines, we observed different cell proliferation pattern in different media and conditions. Different cells lines also suited differently.

In general, all cell lines tested maintained in good condition in RPMI-1640, but did not survive well in PrEGM. Organoid media worked specifically in Matrigel-coated condition that supported cells to form organoids. Cells in F-medium had slightly poorer organoid-forming ability as in organoid medium, but had better proliferation in 2D condition. RPMI-1640 was initially used as a control condition in our test, but turned out to be the most efficient culture medium for cell proliferation in the low cell density PCa cell line culture test. The limitation of this culture test is that the cells used are from established cell lines which are get used to cell culture condition and were maintained in RPMI-1640, which may bias the culture ability towards this culture medium. In a previously study which successfully established long-cultures of breast CTCs, several media were also tried but only RPMI-1640 with serum-free supplements achieved success CTC culture from 6 patients out of 36 patients [299]. In my CTC culture test using the Avatar system, RPMI-1640 supplemented with FCS was not successful for long-

term propagation of CTCs, which was potentially due to the use of FCS. Our tests indicated that these existing media and conditions I tested may not be sufficient to achieve the best CTC culture condition. The composition of cell culture media is complicated and each study used different media and condition. Further development of specific cell culture media is needed and more comprehensive comparison of different conditions is warranted.

6.3.3 *In vitro* culture of prostate CTCs

I used several conditions to isolate and culture CTCs from PCa patients. When I used EasySep or Parsortix to further enrich CTCs after Ficoll centrifugation and cultured the cells in different conditions, I observed attached live cells in culture in 7 out of 11 samples. However, no cell survived over two weeks. Thus, I changed strategy that I enriched CTCs by Ficoll centrifugation only and cultured CTCs using Avatar system and Xcell liquid biopsy kit.

Avatar is a high pressure and hypoxia system for cell culture. Hypoxia is a common feature of solid tumours [424] and it had been demonstrated that solid tumours present an increased interstitial fluid pressure[425]. The Avatar system provided an environment that mimics the environment in solid tumour, in order to help tumour cell *in vitro* propagation. As we have limited volume of blood for each clinical samples, it is difficult to compare Avatar and hypoxia incubator using the same clinical sample. However, using Avatar did not helped us to expand CTCs with different CTC isolation and culture media. In addition, I did not observe clear different of cell morphology and success culturing rate when using Avatar and hypoxia incubator to culture CTCs. Although previous studies showed that increased pressure has shown benefit for tumour cell proliferation *in vitro* [426, 427], the effect of pressure for CTC or primary cell culture needs further investment.

I tried low-attachment plate, Matrigel-coated plate and XCR plate to culture CTCs with XCR media. In low-attachment plate, cells could form clusters. However it is difficult to deplete blood cells. The clusters were easy to be broke when I change the medium, indicating the clusters were of loose structure and were not organoids or spheroids formed via cell proliferation. In addition, media change

caused cell loss that in short term no live cells left. In Matrigel-coated plate, cells could form colonies but did not form spheroids. Only when using XCR plate and media, I was able to culture enriched CTCs for over 2 weeks *in vitro*. Although we were not able to establish CTC cell line, the cultured CTCs could be used for further genetic analysis, such as immunofluorescence-staining, FISH and potentially transcriptional analysis.

The propagation of CTCs in our study was not related to CTC counts isolated by Parsortix. The longest culture of CTCs were achieved in BCI267 and BCI174. However, there was only one CTC/7.5 ml blood detected in these two samples respectively in the parallel CTC enumeration. The CTC enumeration method may selectively detect some subpopulations of the CTCs and the CTC enumeration results may not represent the viable CTC counts in blood circulation. Previous report also found it is possible to establish CTCs-derived colonies in samples with undetectable levels of CTC detected in parallel analysis by CellSearch [294]. Another study showed none of the CK^+ CTCs they detected express proliferation marker Ki-67, indicating most CTC were apoptotic [428]. Thus, CTC culture may add great values to current analysis of CTC enumeration in terms of detecting viable CTCs and understanding CTC heterogeneity.

It is difficult to identify the cell types in my CTC cultures from clinical samples according to their morphology. Most cells were macrophage-like. Later immunofluorescence-staining also indicated that most cells expressed Vim and CD45, which are expressed in macrophage cells. However, macrophage cells normally die off within one month *in vitro* culture, while we have cells culture over one month and much longer. In a previous study which cultured CTCs from breast cancer patients, the cultured CTCs also present similar morphology as we observed in our study that the attached cells exhibited cell membrane ruffling [429]. The authors explained that the presence of cell membrane ruffling demonstrated the selective expansion of epithelial cells and improved cell motility and they identified the cultured cells as EpCAM positive [429]. Although we observed very weak or no CK expression in our cultured cells, it may because of the CTCs underwent EMT that present mesenchymal features. Our FISH analysis showed the existence of potential tumour cells in culture that exhibit abnormal *AR* and *PTEN* copy number change. This also demonstrate that using cultured CTCs,

we may be able to detect the genetic characteristics which are similar to those detected in the primary tumour tissues. However, it is very likely that many cultured cells are not CTCs, but they have long-term survival in this specific cell culture medium.

Among the cultured CTCs using Xcell kit, I observed some multinucleated cells. The multinucleated cells we observed may be the multinucleated giant cells that have been previously demonstrated originate from fusion of monocytes or macrophages [430]. Another potential is that tumour cells may fuse with macrophage cells. Powell *et al.* demonstrated *in vivo* that macrophages could fuse with intestinal tumour epithelial cells during the tumourigenesis [431]. The fusion cell could exhibit both epithelial and macrophage markers [431]. Similar tumour cell-macrophage fusion was also proposed in cultured melanoma CTCs [432]. Charles E. Gast *et al.* reported evidence of fusion hybrids harbouring hematopoietic and epithelial properties existence in cell culture, tumour-bearing mice and in the peripheral blood of human cancer patients [433]. The tumour cell-macrophage fusion may contribute to the CTC heterogeneity and may be one of the mechanisms of how tumour cells gain the physical macrophage-attributed properties, which may facilitate tumour metastasis in extravasation, migration and immune evasion. Using cultured CTCs, we may potentially demonstrate the tumour cell-macrophage fusion in PCa and explore the correlation of tumour cell-macrophage fusion in tumour metastasis and treatment response in the future.

Feeder cells are commonly used for primary cell culture to support target cells. Mitomycin C and irradiation treatments are commonly used to prepare nonproliferating feeder cells. However, in our study, mitomycin C treatment was not sufficient to supress NIH/3T3 cell proliferation, which resulted in mixed population of NIH/3T3 cells and cultured CTCs. As the effect of mitomycin C treatment may be affect by cell concentration and condition, and it is practically difficult to test for the efficiency of mitomycin C treatment, special attention should be paid when using this method. Some studies also showed mitomycin C treated feeder cells are less preferable to support the target cell proliferation [434]. Thus, irradiation may be used for feeder cell preparation when applicable.

We generated xenografts using the mixed cells of NIH/3T3 cells and CTCs, aiming to enrich cancer cells during this process, as NIH/3T3 cell was not

supposed to form tumour in nude mice. However, our analysis on the *ex vivo* cultured cells from the xenograft and on the xenograft itself could not confirm the cell origin. The metaphase spreads showed majority mouse chromosomes which were telocentric, indicating the xenograft was largely mouse cell originated. However, metacentric chromosomes also present and the chromosome numbers were not representative for NIH/3T3 cells. IHC of AR and human PSA on the xenograft section shown untypical staining patterns, which could not help us to discriminate the cell type. One explanation for these observations may be that cultured CTCs could fuse with mouse fibroblast cells, generating a type of hybrid cells which bear contents from both human and murine genomes. Mouse embryonic fibroblast and melanoma cell fusion has been observed in co-culturue system [435]. It has also been reported that androgen-dependent LNCaP cells could fuse with stromal cells in *in vitro* culture, forming a hybrid cell with type androgen-independent phenotype [436]. The mechanism under the cell-cell fusion remain further investigation. However, this phenomenon may bring about problems of using feeder cells for cell culture and establishing mouse xenografts, where the cells may not resemble their original properties.

Chapter VII Final discussion and future research

7.1 Final discussion

PCa is estimated as the most frequently diagnosed male cancer and the second-leading cause of male oncological mortality in 2019 in the US [437]. While the prognosis for localised or locally spread disease is very good, the prognosis for locally advanced and metastatic PCa disease is poor. ADT is the standard of care for initial management of locally advanced and metastatic PCa. However, the progression of PCa remains a major issue of PCa management as patients inevitably progress, leading to a lethal stage of disease, CRPC [44]. PSA level is not only one of the main factors to guide risk stratification and treatment decisions for men with newly diagnosed PCa, it is also the only widely used blood-based biomarker for routine monitoring of disease progression in patients receiving treatment. In metastatic settings, PSA level at the seventh month of ADT initiation [438] and time to PSA nadir after ADT initiation [439] have shown prognostic value for patients' OS. It is also an important parameter for CRPC diagnosis. However, the PSA test has its limitations in assessing disease progression [440]. PSA level may not always reflect the disease burden. PCa patients with wide-spread metastatic disease who have poorly differentiated tumour or neuroendocrine differentiation on histology may present low levels of PSA [441-443]. Progression of PCa may also occur despite undetectable or low PSA levels [443, 444]. Imaging methods have been widely implemented in confirmation of PCa progression. However, imaging procedures are difficult to be conducted frequently due to high cost and expertise required for image analysis, thus delayed detection of progression may occur resulting in early metastasis being missed. Therefore, studies of new biomarkers for PCa progression and monitoring are needed to identify non-invasive markers with high sensitivity and specificity to routinely monitor PCa progression and guide clinical decisions. These studies will also help to identify novel biological mechanisms of PCa progression, facilitating discovery of new treatment strategies. Therefore, in the present study, I explored the value of two main circulating elements in peripheral blood, exosomes and CTCs, in monitoring PCa progression and predicting treatment response. There are other research groups working on plasma exosomes and CTCs in PCa progression and treatment response. However,

none of them investigated their role and biomarker potential in CRPC development. Due to time limitation, my plasma exosomal miRNA studies were mainly focused on CRPC development and prediction biomarkers as there are no previous studies in this area; and my CTC study was focused on CTC cultures to facilitate the establishment of patient specific molecular characteristics and patient drug sensitivity test, which is critical for patient treatment decision/selection making.

Exosomes, a type of small vesicle that carries varieties of biologically active molecules, have been investigated in different cancer types. Biomarker mining from exosomes has emerged as an attractive research area. MiRNAs in exosomes has been a main focus of research as they bear several advantages: 1) miRNAs are enriched in exosomes thus facilitate biomarker detection using only a small volume of sample [350]; 2) miRNAs are stably protected in exosomes upon RNase treatment [350] and are minimally affected by storage conditions [347], providing an ideal source of biomarkers; 3) miRNAs in exosomes are functionally active, thus can be transferred from donor cells to the receiver cells and play important functional roles [351].

In PCa, exosomal miRNAs have demonstrated their biomarker potential under several pathological conditions. However, only limited data has been reported for comprehensive analysis of the exosomal miRNA profile and no study has focused on miRNAs correlated to CRPC development. In this study, we generated a plasma exosomal miRNA profile in treatment-naive PCa and CRPC patients in order to identify novel biomarkers for CRPC via extensive, unbiased screening. Although the case number is still limited especially for CRPC, we identified several exosomal miRNAs correlated with CRPC which were validated by RT-qPCR for discriminating CRPC from treatment-naive PCa. Among those differentially expressed miRNA, miR-423-3p showed great CRPC prediction value (high AUC value), in particular when combined with PSA level. This data remained true with different exosome isolation methods, as the differential expression level of miR-423-3p in plasma exosomes was validated between treatment-naive PCa and CRPC in another centre.

While differential expression of plasma miRNAs have been correlated to CRPC, the expression level of plasma exosomal miRNAs may be affected by the

treatment given to the patients. As patients receive hormone therapy before diagnosis of CRPC, I included a group of patients with early hormonal therapy without progression to minimise the effect of treatments on discovery of plasma exosomal miRNA biomarker. MiR-423-3p also showed significant differential expression between treated non-CRPC and CRPC and over-performed PSA in predicting CRPC, but showed no difference between treatment-naive PCa and treated non-CRPC. These results indicate that change of plasma exosomal miR-423-3p level is not a response of ADT treatment, but is associated with the occurrence of CRPC. These data together strongly support the hypothesis that plasma exosomal miR-423-3p could be used as a predictive biomarker for CRPC. In addition, the *in vitro* study showed that miR-423-3p is expressed at a higher level in castration-resistant cells (C4-2) compared to hormone-sensitive cells (LNCaP) and its upregulation in LNCaP cells induce cancer cell migration/invasion under castration culture condition, further support that miR-423-3p is associated with CRPC development and plasma exosomal miR-423-3p may be released from cancer cells instead of the environmental cells in response to PCa progression.

One problem in the study of CRPC monitoring biomarkers is that it is difficult to determine if the differentially expressed miRNAs are metastatic-related or CRPC related when comparing treatment-naive PCa vs CRPC. Indeed, CRPC is highly correlated with metastasis as a large proportion of patients treated with ADT are diagnosed with metastatic disease and metastasis is the common sign of CRPC development for patients starting with ADT for locally advanced PCa. CRPC is a therapeutic resistance issue, presenting with a distinct mechanism of disease progression to cancer metastasis. The link between them has rarely been investigated. My *in vitro* data of miR-423-3p expression changes in LNCaP and C4-2 cells indicate that cancer metastasis and CRPC may be linked in cancer progression process that miR-423-3p overexpression may induce both cancer metastasis and castration-resistance by promoting cancer invasion under castration condition. In addition to miR-423-3p in cancer cells, cancer cell secreted exosomal miR-423-3p might also play a role in the promotion of mCRPC. It has been demonstrated that exosomes from metastatic cells can induce non-metastatic cells to undergo EMT [445, 446]. Tumour cells can also secret exosome carrying miRNAs and transport them to distant sites, regulating the

microenvironment and promoting metastasis [203, 418, 419]. My data suggests that PCa cells may secret exosomes acting as delivery vesicles that shuttle miR-423-3p to other cells, even at distant sites, and induce metastasis under castration environment. However, currently our functional data is limited and the underlying mechanism should be further investigated.

In this study, I included three groups of patients, treatment-naive PCa, treated non-CRPC and CRPC, and evaluated the plasma exosomal miRNA expression. To our knowledge, this is the first study that report data from these three groups of patients, as most studies only recruited treatment-naive localised PCa and CRPC. Interestingly, we observed novel expression patterns of plasma exosomal miRNAs between these three groups of patients. MiR-423-3p was the only miRNA that showed significant difference when comparing treatment-naive PCa vs CRPC and treated non-CRPC vs CRPC, but no difference between treatment-naive PCa and treated non-CRPC. This may suggest exosomal miR-423-3p is a true CRPC development related miRNA. MiR-150-5p showed significant difference when comparing treatment-naive PCa vs CRPC and treatment-naive PCa vs treated non-CRPC, but no difference between treated non-CRPC vs CRPC, suggesting miR-150-5p may be a metastasis-related marker, supported by other studies [15, 447]. We also identified seven miRNAs (miR-320a, miR-320b, miR-320d, miR-99a-5p, miR-101-3p, miR-193a-5p, miR-148a-3p) that showed fluctuated expression levels among treatment-naive PCa, treated non-CRPC and CRPC. One explanation of the fluctuated expression may be that these plasma exosomal miRNA levels change are reflective of the tumour burden. In the treated non-CRPC group, when the disease was under control, fluctuations across these miRNAs were observed in comparison to the treatment-naive PCa group. When the disease progressed, these miRNAs underwent expression changes respective to the untreated stage. Our study demonstrated that plasma exosomal miRNAs could serve as biomarkers for CRPC with some also having potential value as biomarkers for metastatic disease. Further studies will be needed to evaluate these miRNAs in larger cohorts, and potentially in serial blood collection in the same patients, to investigate their utility for disease progression.

CTCs has been intensively investigated in recent years owing to the development of CTC detection methods. CTC enumeration has shown promising value as a

biomarker for PCa prognosis. Recent molecular analysis of CTCs, for example the detection of AR-V7 in CTCs [448, 449], further elucidated the value of CTCs as a biomarker and for study of tumour biology. However, limited number of CTCs remains a problem and has hindered comprehensive studies. Propagation of CTCs has aroused research interests as a novel approach to non-invasively obtain tumour cells and study their molecular features and to establish patient-specific models to test drug sensitivity. As plasma exosomal miRNAs provide systematic information of disease status and we have investigated the potential of using plasma exosomal miRNA as biomarkers to detect PCa progression, CTC culture may enable us to obtain tumour specific molecular information and establish patient-specific models for precision medicine.

PCa cell primary culture is difficult, and there are very limited reports on successful culture of PCa CTCs [246, 297]. In this study, I tested different CTC isolation methods, culture media and culture conditions for PCa CTC *in vitro* propagation. We demonstrated that for CTC culture, one-step enrichment of mononuclear cells via Ficoll centrifugation without further purification of CTCs may be adequate for CTC culture. Although I tried several culture media and conditions, we found they were not efficient enough to propagate PCa CTCs when using clinical samples. Eventually, I used Xcell liquid biopsy kit, composing of special cell culture media and collagen-based pre-coated cell culture plate, and hypoxia incubator to culture PCa CTCs. This protocol enabled us to culture CTCs for over one month in 15 out of 27 samples with the longest culture reaching five months. Although I was not able to establish a CTC cell line, my data showed good success rate for short-term CTC culture. In addition, I managed to perform immunofluorescence-staining and FISH on the cultured CTCs and I froze some cells down for future analysis. AR-gain and PTEN-loss in the cultured CTCs were identified by FISH analysis, indicating the presence of viable tumour cells in our culture. Unfortunately, we did not have access to the patient's parallel tissue sample. Thus, we were not able to confirm these genetic changes in the patient's tissue.

In parallel to CTC culture, we performed CTC enumeration using the Parsortix system [339]. I did not observe correlation of CTC number and CTC culture outcome. In a previous study of short-term culture of CTCs as clusters, it was

also found that CTC cluster formation was not always correlated with the detected CTC counts [294]. Park *et al.* showed that CTCs from CRPC patients were similar in size to leukocytes (around 8 m) with significant shape variability and many cells having an elongated shaped [450]. As very few CTCs were detected, it is possible that our size-based CTC enumeration method may have missed some small CTCs. It has also been demonstrated that CTCs bear high heterogeneity with different proliferative capacity [451, 452]. Thus, it is difficult to link CTC culture outcomes with CTC enumeration directly. However, it is commonly accepted that more CTCs raises higher chance to establish culture and thus isolating CTCs from an apheresis product may provide an access to more starting material for CTC culture [296, 297].

It is confirmed by FISH that there were tumour cells existent in our cultured cells. However, most cultured cells presented normal *AR* and *PTEN* copy numbers. The cells also displayed different morphologies and heterogeneous CK, Vim and CD45 expression. Thus, we could assume that our cultured cells were a mixed population of different cell types. Further identification of the cell types may be conducted using the frozen cells we have. Notably, we observed extremely weak or no CK expression in our cultured CTCs. In line with our observation, Zhang *et al.* reported their success in establishing $EpCAM^-$ CTC lines from breast cancer patients with undetectable CTC level using CellSearch, while the $EpCAM^+$ CTCs were not able to be expanded [298].

Our data showed the possibility to culture PCa CTCs and to perform molecular analysis using cultured CTCs. However, the study is still at an early stage and the CTCs did not grow vigorously to allow drug sensitivity testing. More thorough investigations are needed. Our CTC culture conditions should be further improved to facilitate long-term CTC propagation in order to perform drug sensitivity tests.

7.2 Future plans

7.2.1 Further evaluation of plasma exosomal miRNAs as biomarkers

In this study, we have evaluated the expression levels of several plasma exosomal miRNAs in three groups of patients: treatment-naive PCa, treated non-

CRPC and CRPC. We identified plasma exosomal miRNAs that could potentially be used as biomarkers for CRPC. However, the sample number is still small, especially for non-CRPC and CRPC groups. Further validation of our miRNAs is needed in a larger cohort of treated non-CRPC and CRPC patients. In addition, the prognostic value of the identified exosomal miRNAs in treated non-CRPC may be evaluated when follow-up data is obtained.

To further evaluate the potential of using plasma exosomal miRNAs to monitor disease progression, exosomal miRNAs may be evaluated in serial collection of blood in patients starting hormone therapy. Our lab have started sample collection in patients with recurrent disease or newly diagnosed advanced disease, who are assigned for hormonal therapies or hormone combined with docetaxel chemotherapy. Plasma exosomes will be isolated from the serial collection of samples and the expression levels of exosomal miRNAs in serial blood collections in these patients will be evaluated by RT-qPCR. The exosomal miRNA levels will be compared with other clinical parameters and follow-up data for disease progression such as PSA level and imaging information, to investigate if plasma exosomal miRNAs can detect early disease progression.

Plasma exosomal miRNAs significantly differentially expressed between treated non-CRPC and CRPC but not between untreated and CRPC cases were observed in this study. RNA-sequencing of plasma exosomal RNA will be performed in the treated non-CRPC and CRPC, to comprehensively evaluate the differentially expressed plasma exosomal miRNAs between treated non-CRPC and CRPC. This may help us identity important biomarkers for CRPC.

In this study, we identified several miRNAs associated with CRPC using RNA-sequencing. RT-qPCR enabled us to further validate some of them in larger cohorts. However, there are some miRNAs that may have significant CRPC biomarker potential which were not able to be evaluated due to technique issues. For example, miR-375, miR-200 and miR-9 have previously been demonstrated for their correlation with PCa development and progression and bear biomarker value [151, 453]. Further evaluation of these miRNAs using more sensitive approach, for example digital qPCR, may reveal their value in monitoring PCa progression.

While evaluating miRNAs expression using different methods, I found inconsistent results generated from traditional RT-qPCR and Fluidigm. Although I found different cDNA preparation procedures may be responsible, this technical issue may be further elucidated in future research. Nevertheless, for a biomarker, as long as it is clinically useful if detected using a specific measurement method, it will be valuable biomarker. The plasma exosomal miRNAs correlated to CRPC as detected by Fluidigm, although were not consistent to RNA sequencing and RT-qPCR results, achieved better AUCs than those detected by RT-qPCR. They should be further validated in a large cohort of patient blood samples for their CRPC predictive biomarker potential using the Fluidigm system.

7.2.2 Investigation of exosomal miRNAs function

In this study, I explored potential functional role of miR-423-3p. I showed that overexpression of miR-423-3p induced cell migration and invasion in a hormone-depleted condition without affecting cell proliferation. Future studies will be done to determine if down-regulation of miR-423-3p would reduce cell proliferation, migration and invasion ability, which may reveal a novel PCa treatment strategy. MiR-423-3p inhibitors will be transfected to down-regulate the miRNA in LNCaP and C4-2 cells. Cell proliferation, migration and invasion ability will be examined using the methods described in Chapter VI.

The mechanism of miR-423-3p induced cell migration and invasion remain to be studied. I observed the effect of miR-423-3p on MEIS1 protein expression and the changes of MEIS1 mRNA level will be evaluated and whether MEIS1 is a direct target of miR-423-3p should be confirmed later by luciferase-reporter assay. Further studies will be done to determine the interaction of miR-423-3p and p21(WAF1/CIP1) and their role in PCa progression. WB will be performed to check if over-expression or inhibition of miR-423-3p will affect protein level of P21 in PCa cells. MRNA level will be checked by RT-qPCR.

As overexpression of miR-423-3p induced cell migration and invasion, it is possible that it induced EMT in the cells. Thus, EMT-related markers such as Vim and N-cadherin will also be investigated in normal and charcoal-striped media by manipulating miR-423-3p expression level.

Whether miR-423-3p can be transferred via exosomes and be biologically active in the recipient cells will be investigated. The expression level of miR-423-3p in secreted exosomes of LNCaP, C4-2, and other PCa will be evaluated by RT-qPCR. Exosomes from LNCaP over-expressing miR-423-3p will be collected and the exosomal miR-423-3p expression level will be compared with wild type LNCaP exosomes. Different methods including using co-culture system, culturing in conditioned media and directly adding exosomes will be performed to evaluate if exosomes overexpressing miR-423-3p could increase PCa cell proliferation, migration and invasion under cell culture conditions with and without androgen.

7.2.3 Other plasma exosomal RNA in PCa

By aligning the RNA-sequencing data to mirBase mature miRNA, we have generated a plasma exosomal miRNA expression profile in treatment-naive PCa and CRPC by RNA-sequencing. Further analysis of RNA-sequencing data may be applied to identify other RNA species that could be related to CRPC. It has been demonstrated by RNA-sequencing that exosomes contain several RNA species such as tRNA, rRNA, small nuclear, small nucleolar and piwi-interacting RNA, lncRNA and mRNA [103, 175, 346, 350]. The value of these exosomal RNAs in PCa is largely unknown. Our RNA-sequencing data, without size selection, could be used to explore the expression profile of these RNAs and reveal potential biomarker value in future studies. The RNA-sequencing raw reads will be re-analysed mapping to Ensembl Release to identify other RNA species. The differentially expressed RNAs will be identified which may be associated to CRPC development.

7.2.4 CTC culture, molecular analysis and drug test

Although we were not able to establish CTC cell lines, the high success rate of short-term CTC culture may enable us to perform molecular analysis and potentially drug testing. The previous study was focused on the long-term expansion of CTCs. Future studies will be focused on the molecular characterisation of the cultured cells and investigation of the application of cultured CTCs. We will utilise cells frozen from previous cultured samples. The

cells will be recovered and further immunofluorescence staining will be performed to identify the cell type. Epithelial makers such as CK and EpCam, mescenchymal marker Vim, and macrophage markers such as CD68 and CD163 will be used. Patients with chemo-naive progressed disease may be recruited to test if cultured CTCs could be used to test therapy response. The CTCs will be cultured for short-term (approximately one month) and will be treated with drugs such as docetaxel, abiraterone and enzalutamide to test the cell sensitivity to these drugs, which may provide information guiding clinical decisions. Single cell RNA and exome sequencing of the CTCs may be performed to uncover markers that may help further validation of the cell origins in culture and uncover tumour-specific markers guiding treatment selection.

References

1. Timms, B.G., *Prostate development: a historical perspective.* Differentiation, 2008. **76**(6): p. 565-77.
2. Aaron, L., O.E. Franco, and S.W. Hayward, *Review of Prostate Anatomy and Embryology and the Etiology of Benign Prostatic Hyperplasia.* Urol Clin North Am, 2016. **43**(3): p. 279-88.
3. Verze, P., T. Cai, and S. Lorenzetti, *The role of the prostate in male fertility, health and disease.* Nat Rev Urol, 2016. **13**(7): p. 379-86.
4. Toivanen, R. and M.M. Shen, *Prostate organogenesis: tissue induction, hormonal regulation and cell type specification.* Development, 2017. **144**(8): p. 1382-1398.
5. Zhou, Y., E.C. Bolton, and J.O. Jones, *Androgens and androgen receptor signaling in prostate tumorigenesis.* J Mol Endocrinol, 2015. **54**(1): p. R15-29.
6. Marker, P.C., et al., *Hormonal, cellular, and molecular control of prostatic development.* Dev Biol, 2003. **253**(2): p. 165-74.
7. Bray, F., et al., *Global cancer statistics 2018: GLOBOCAN estimates of incidence and mortality worldwide for 36 cancers in 185 countries.* CA Cancer J Clin, 2018. **68**(6): p. 394-424.
8. *Cancer Research UK, https://www.cancerresearchuk.org/health-professional/cancer-statistics/statistics-by-cancer-type/prostate-cancer#heading-Zero, Accessed November 2018.*
9. *Cancer Research UK, https://www.cancerresearchuk.org/health-professional/cancer-statistics/statistics-by-cancer-type/prostate-cancer/mortality#heading-Two, Accessed November 2018.*
10. *Cancer Research UK, https://www.cancerresearchuk.org/health-professional/cancer-statistics/statistics-by-cancer-type/prostate-cancer/survival#heading-Zero, Accessed November 2018.*
11. Noone AM, H.N., Krapcho M, Miller D, Brest A, Yu M, Ruhl J, Tatalovich Z, Mariotto A, Lewis DR, Chen HS, Feuer EJ, Cronin KA (eds), *SEER Cancer Statistics Review, 1975-2015, National Cancer Institute. Bethesda, MD, https://seer.cancer.gov/csr/1975_2015/, based on November 2017 SEER data submission, posted to the SEER web site, April 2018.*
12. Johns, L.E. and R.S. Houlston, *A systematic review and meta-analysis of familial prostate cancer risk.* BJU Int, 2003. **91**(9): p. 789-94.
13. Bruner, D.W., et al., *Relative risk of prostate cancer for men with affected relatives: systematic review and meta-analysis.* Int J Cancer, 2003. **107**(5): p. 797-803.
14. Zeegers, M.P., A. Jellema, and H. Ostrer, *Empiric risk of prostate carcinoma for relatives of patients with prostate carcinoma: a meta-analysis.* Cancer, 2003. **97**(8): p. 1894-903.

15. Dai, F.Q., et al., *miR-150-5p Inhibits Non-Small-Cell Lung Cancer Metastasis and Recurrence by Targeting HMGA2 and beta-Catenin Signaling.* Mol Ther Nucleic Acids, 2019. **16**: p. 675-685.

16. Oderda, M., et al., *[Update on epidemiology and risk factors of prostate cancer].* Urologia, 2008. **75**(3): p. 143-8.

17. Lilja, H., D. Ulmert, and A.J. Vickers, *Prostate-specific antigen and prostate cancer: prediction, detection and monitoring.* Nat Rev Cancer, 2008. **8**(4): p. 268-78.

18. Mettlin, C., et al., *Defining and updating the American Cancer Society guidelines for the cancer-related checkup: prostate and endometrial cancers.* CA Cancer J Clin, 1993. **43**(1): p. 42-6.

19. Schroder, F.H., et al., *Screening and prostate-cancer mortality in a randomized European study.* N Engl J Med, 2009. **360**(13): p. 1320-8.

20. Andriole, G.L., et al., *Mortality results from a randomized prostate-cancer screening trial.* N Engl J Med, 2009. **360**(13): p. 1310-9.

21. Schroder, F.H., et al., *Screening and prostate cancer mortality: results of the European Randomised Study of Screening for Prostate Cancer (ERSPC) at 13 years of follow-up.* Lancet, 2014. **384**(9959): p. 2027-35.

22. Martin, R.M., et al., *Effect of a Low-Intensity PSA-Based Screening Intervention on Prostate Cancer Mortality: The CAP Randomized Clinical Trial.* JAMA, 2018. **319**(9): p. 883-895.

23. Mottet, N., et al., *EAU-ESTRO-SIOG Guidelines on Prostate Cancer. Part 1: Screening, Diagnosis, and Local Treatment with Curative Intent.* Eur Urol, 2017. **71**(4): p. 618-629.

24. Boorjian, S.A., et al., *Long-term risk of clinical progression after biochemical recurrence following radical prostatectomy: the impact of time from surgery to recurrence.* Eur Urol, 2011. **59**(6): p. 893-9.

25. Pezaro, C., et al., *Visceral disease in castration-resistant prostate cancer.* Eur Urol, 2014. **65**(2): p. 270-273.

26. Epstein, J.I., et al., *The 2005 International Society of Urological Pathology (ISUP) Consensus Conference on Gleason Grading of Prostatic Carcinoma.* Am J Surg Pathol, 2005. **29**(9): p. 1228-42.

27. Epstein, J.I., et al., *The 2014 International Society of Urological Pathology (ISUP) Consensus Conference on Gleason Grading of Prostatic Carcinoma: Definition of Grading Patterns and Proposal for a New Grading System.* Am J Surg Pathol, 2016. **40**(2): p. 244-52.

28. D'Amico, A.V., et al., *Biochemical outcome after radical prostatectomy, external beam radiation therapy, or interstitial radiation therapy for clinically localized prostate cancer.* JAMA, 1998. **280**(11): p. 969-74.

29. Stark, J.R., et al., *Gleason score and lethal prostate cancer: does 3 + 4 = 4 + 3?* J Clin Oncol, 2009. **27**(21): p. 3459-64.

30. Chan, T.Y., et al., *Prognostic significance of Gleason score 3+4 versus Gleason score 4+3 tumor at radical prostatectomy.* Urology, 2000. **56**(5): p. 823-7.

31. Tsao, C.K., et al., *Patients with Biopsy Gleason 9 and 10 Prostate Cancer Have Significantly Worse Outcomes Compared to Patients with Gleason 8 Disease.* J Urol, 2015. **194**(1): p. 91-7.

32. Epstein, J.I., et al., *A Contemporary Prostate Cancer Grading System: A Validated Alternative to the Gleason Score.* Eur Urol, 2016. **69**(3): p. 428-35.

33. Yeong, J., et al., *Gleason grade grouping of prostate cancer is of prognostic value in Asian men.* J Clin Pathol, 2017. **70**(9): p. 745-753.

34. Buyyounouski, M.K., et al., *Prostate cancer - major changes in the American Joint Committee on Cancer eighth edition cancer staging manual.* CA Cancer J Clin, 2017. **67**(3): p. 245-253.

35. Hamdy, F.C., et al., *10-Year Outcomes after Monitoring, Surgery, or Radiotherapy for Localized Prostate Cancer.* N Engl J Med, 2016. **375**(15): p. 1415-1424.

36. Bill-Axelson, A., et al., *Radical prostatectomy or watchful waiting in early prostate cancer.* N Engl J Med, 2014. **370**(10): p. 932-42.

37. Wilt, T.J., et al., *Radical prostatectomy versus observation for localized prostate cancer.* N Engl J Med, 2012. **367**(3): p. 203-13.

38. *American Cancer Society. Hormone therapy for prostate cancer. www.cancer.org/cancer/prostate-cancer/treating/hormone-therapy.html. Accessed October 30, 2019.*

39. Cornford, P., et al., *EAU-ESTRO-SIOG Guidelines on Prostate Cancer. Part II: Treatment of Relapsing, Metastatic, and Castration-Resistant Prostate Cancer.* Eur Urol, 2017. **71**(4): p. 630-642.

40. James, N.D., et al., *Addition of docetaxel, zoledronic acid, or both to first-line long-term hormone therapy in prostate cancer (STAMPEDE): survival results from an adaptive, multiarm, multistage, platform randomised controlled trial.* Lancet, 2016. **387**(10024): p. 1163-77.

41. Gravis, G., et al., *Androgen-deprivation therapy alone or with docetaxel in non-castrate metastatic prostate cancer (GETUG-AFU 15): a randomised, open-label, phase 3 trial.* Lancet Oncol, 2013. **14**(2): p. 149-58.

42. Sweeney, C.J., et al., *Chemohormonal Therapy in Metastatic Hormone-Sensitive Prostate Cancer.* N Engl J Med, 2015. **373**(8): p. 737-46.

43. Scher, H.I., et al., *Design and end points of clinical trials for patients with progressive prostate cancer and castrate levels of testosterone: recommendations of the Prostate Cancer Clinical Trials Working Group.* J Clin Oncol, 2008. **26**(7): p. 1148-59.

44. Chandrasekar, T., et al., *Mechanisms of resistance in castration-resistant prostate cancer (CRPC).* Transl Androl Urol, 2015. **4**(3): p. 365-80.

45. Kirby, M., C. Hirst, and E.D. Crawford, *Characterising the castration-resistant prostate cancer population: a systematic review.* Int J Clin Pract, 2011. **65**(11): p. 1180-92.

46. Petrylak, D.P., et al., *Docetaxel and estramustine compared with mitoxantrone and prednisone for advanced refractory prostate cancer.* N Engl J Med, 2004. **351**(15): p. 1513-20.

47. Tannock, I.F., et al., *Docetaxel plus prednisone or mitoxantrone plus prednisone for advanced prostate cancer.* N Engl J Med, 2004. **351**(15): p. 1502-12.

48. Ryan, C.J., et al., *Abiraterone acetate plus prednisone versus placebo plus prednisone in chemotherapy-naive men with metastatic castration-resistant prostate cancer (COU-AA-302): final overall survival analysis of a randomised, double-blind, placebo-controlled phase 3 study.* Lancet Oncol, 2015. **16**(2): p. 152-60.

49. Beer, T.M., et al., *Enzalutamide in metastatic prostate cancer before chemotherapy.* N Engl J Med, 2014. **371**(5): p. 424-33.

50. Kantoff, P.W., et al., *Overall survival analysis of a phase II randomized controlled trial of a Poxviral-based PSA-targeted immunotherapy in metastatic castration-resistant prostate cancer.* J Clin Oncol, 2010. **28**(7): p. 1099-105.

51. Parker, C., et al., *Alpha emitter radium-223 and survival in metastatic prostate cancer.* N Engl J Med, 2013. **369**(3): p. 213-23.

52. Mucci, L.A., et al., *Familial Risk and Heritability of Cancer Among Twins in Nordic Countries.* JAMA, 2016. **315**(1): p. 68-76.

53. Benafif, S., et al., *A Review of Prostate Cancer Genome-Wide Association Studies (GWAS).* Cancer Epidemiol Biomarkers Prev, 2018. **27**(8): p. 845-857.

54. Marzec, J., et al., *A genetic study and meta-analysis of the genetic predisposition of prostate cancer in a Chinese population.* Oncotarget, 2016. **7**(16): p. 21393-403.

55. Conti, D.V., et al., *Two Novel Susceptibility Loci for Prostate Cancer in Men of African Ancestry.* J Natl Cancer Inst, 2017. **109**(8).

56. Han, Y., et al., *Prostate Cancer Susceptibility in Men of African Ancestry at 8q24.* J Natl Cancer Inst, 2016. **108**(7).

57. Amundadottir, L.T., et al., *A common variant associated with prostate cancer in European and African populations.* Nat Genet, 2006. **38**(6): p. 652-8.

58. Matejcic, M., et al., *Germline variation at 8q24 and prostate cancer risk in men of European ancestry.* Nat Commun, 2018. **9**(1): p. 4616.

59. Ewing, C.M., et al., *Germline mutations in HOXB13 and prostate-cancer risk.* N Engl J Med, 2012. **366**(2): p. 141-9.

60. Breyer, J.P., et al., *Confirmation of the HOXB13 G84E germline mutation in familial prostate cancer.* Cancer Epidemiol Biomarkers Prev, 2012. **21**(8): p. 1348-53.

61. Shu, X., et al., *Genetic variants of the Wnt signaling pathway as predictors of aggressive disease and reclassification in men with early stage prostate cancer on active surveillance.* Carcinogenesis, 2016. **37**(10): p. 965-971.

62. Sanchez, A., et al., *Common variation in BRCA1 may have a role in progression to lethal prostate cancer after radiation treatment.* Prostate Cancer Prostatic Dis, 2016. **19**(2): p. 197-201.

63. Kim, Y.S., et al., *Genetic variants and risk of prostate cancer using pathway analysis of a genome-wide association study.* Neoplasma, 2016. **63**(4): p. 629-34.

64. Loo, L.W., et al., *In silico functional pathway annotation of 86 established prostate cancer risk variants.* PLoS One, 2015. **10**(2): p. e0117873.

65. Maurano, M.T., et al., *Systematic localization of common disease-associated variation in regulatory DNA.* Science, 2012. **337**(6099): p. 1190-5.

66. Farashi, S., et al., *Post-GWAS in prostate cancer: from genetic association to biological contribution.* Nat Rev Cancer, 2019. **19**(1): p. 46-59.

67. Weischenfeldt, J., et al., *Integrative genomic analyses reveal an androgen-driven somatic alteration landscape in early-onset prostate cancer.* Cancer Cell, 2013. **23**(2): p. 159-70.

68. Cancer Genome Atlas Research, N., *The Molecular Taxonomy of Primary Prostate Cancer.* Cell, 2015. **163**(4): p. 1011-25.

69. Beltran, H., et al., *Divergent clonal evolution of castration-resistant neuroendocrine prostate cancer.* Nat Med, 2016. **22**(3): p. 298-305.

70. Grasso, C.S., et al., *The mutational landscape of lethal castration-resistant prostate cancer.* Nature, 2012. **487**(7406): p. 239-43.

71. Wedge, D.C., et al., *Sequencing of prostate cancers identifies new cancer genes, routes of progression and drug targets.* Nat Genet, 2018. **50**(5): p. 682-692.

72. Tomlins, S.A., et al., *Recurrent fusion of TMPRSS2 and ETS transcription factor genes in prostate cancer.* Science, 2005. **310**(5748): p. 644-8.

73. Rubin, M.A., C.A. Maher, and A.M. Chinnaiyan, *Common gene rearrangements in prostate cancer.* J Clin Oncol, 2011. **29**(27): p. 3659-68.

74. Barbieri, C.E., et al., *Exome sequencing identifies recurrent SPOP, FOXA1 and MED12 mutations in prostate cancer.* Nat Genet, 2012. **44**(6): p. 685-9.

75. Beroukhim, R., et al., *The landscape of somatic copy-number alteration across human cancers.* Nature, 2010. **463**(7283): p. 899-905.

76. Phin, S., M.W. Moore, and P.D. Cotter, *Genomic Rearrangements of PTEN in Prostate Cancer.* Front Oncol, 2013. **3**: p. 240.

77. Robinson, D., et al., *Integrative clinical genomics of advanced prostate cancer.* Cell, 2015. **161**(5): p. 1215-1228.

78. Robbins, C.M., et al., *Copy number and targeted mutational analysis reveals novel somatic events in metastatic prostate tumors.* Genome Res, 2011. **21**(1): p. 47-55.

79. Smith, M.R., et al., *Natural history of rising serum prostate-specific antigen in men with castrate nonmetastatic prostate cancer.* J Clin Oncol, 2005. **23**(13): p. 2918-25.

80. Berthold, D.R., et al., *Docetaxel plus prednisone or mitoxantrone plus prednisone for advanced prostate cancer: updated survival in the TAX 327 study.* J Clin Oncol, 2008. **26**(2): p. 242-5.

81. de Bono, J.S., et al., *Abiraterone and increased survival in metastatic prostate cancer.* N Engl J Med, 2011. **364**(21): p. 1995-2005.

82. Scher, H.I., et al., *Increased survival with enzalutamide in prostate cancer after chemotherapy.* N Engl J Med, 2012. **367**(13): p. 1187-97.

83. Kawalec, P., et al., *Sipuleucel-T immunotherapy for castration-resistant prostate cancer. A systematic review and meta-analysis.* Arch Med Sci, 2012. **8**(5): p. 767-75.

84. de Bono, J.S., et al., *Prednisone plus cabazitaxel or mitoxantrone for metastatic castration-resistant prostate cancer progressing after docetaxel treatment: a randomised open-label trial.* Lancet, 2010. **376**(9747): p. 1147-54.

85. Huang, Y., et al., *Molecular and cellular mechanisms of castration resistant prostate cancer.* Oncol Lett, 2018. **15**(5): p. 6063-6076.

86. Waltering, K.K., et al., *Increased expression of androgen receptor sensitizes prostate cancer cells to low levels of androgens.* Cancer Res, 2009. **69**(20): p. 8141-9.

87. Gregory, C.W., et al., *Androgen receptor stabilization in recurrent prostate cancer is associated with hypersensitivity to low androgen.* Cancer Res, 2001. **61**(7): p. 2892-8.

88. Veldscholte, J., et al., *A mutation in the ligand binding domain of the androgen receptor of human LNCaP cells affects steroid binding characteristics and response to anti-androgens.* Biochem Biophys Res Commun, 1990. **173**(2): p. 534-40.

89. Hu, R., et al., *Ligand-independent androgen receptor variants derived from splicing of cryptic exons signify hormone-refractory prostate cancer.* Cancer Res, 2009. **69**(1): p. 16-22.

90. Qu, Y., et al., *Constitutively active AR-V7 plays an essential role in the development and progression of castration-resistant prostate cancer.* Sci Rep, 2015. **5**: p. 7654.

91. Sharp, A., et al., *Androgen receptor splice variant-7 expression emerges with castration resistance in prostate cancer.* J Clin Invest, 2019. **129**(1): p. 192-208.

92. Sung, Y.Y. and E. Cheung, *Androgen receptor co-regulatory networks in castration-resistant prostate cancer.* Endocr Relat Cancer, 2014. **21**(1): p. R1-R11.

93. Armandari, I., et al., *Intratumoral steroidogenesis in castration-resistant prostate cancer: a target for therapy.* Prostate Int, 2014. **2**(3): p. 105-13.

94. Halabi, S., et al., *Updated prognostic model for predicting overall survival in first-line chemotherapy for patients with metastatic castration-resistant prostate cancer.* J Clin Oncol, 2014. **32**(7): p. 671-7.

95. Armstrong, A.J., et al., *Biomarkers in the management and treatment of men with metastatic castration-resistant prostate cancer.* Eur Urol, 2012. **61**(3): p. 549-59.

96. de Bono, J.S., et al., *Circulating tumor cells predict survival benefit from treatment in metastatic castration-resistant prostate cancer.* Clin Cancer Res, 2008. **14**(19): p. 6302-9.

97. Goldkorn, A., et al., *Circulating tumor cell counts are prognostic of overall survival in SWOG S0421: a phase III trial of docetaxel with or without atrasentan for metastatic castration-resistant prostate cancer.* J Clin Oncol, 2014. **32**(11): p. 1136-42.

98. Shaffer, D.R., et al., *Circulating tumor cell analysis in patients with progressive castration-resistant prostate cancer.* Clin Cancer Res, 2007. **13**(7): p. 2023-9.

99. Antonarakis, E.S., et al., *Clinical Significance of Androgen Receptor Splice Variant-7 mRNA Detection in Circulating Tumor Cells of Men With Metastatic Castration-Resistant Prostate Cancer Treated With First- and Second-Line Abiraterone and Enzalutamide.* J Clin Oncol, 2017. **35**(19): p. 2149-2156.

100. Onstenk, W., et al., *Efficacy of Cabazitaxel in Castration-resistant Prostate Cancer Is Independent of the Presence of AR-V7 in Circulating Tumor Cells.* Eur Urol, 2015. **68**(6): p. 939-45.

101. Antonarakis, E.S., et al., *Androgen Receptor Splice Variant 7 and Efficacy of Taxane Chemotherapy in Patients With Metastatic Castration-Resistant Prostate Cancer.* JAMA Oncol, 2015. **1**(5): p. 582-91.

102. Li, H., et al., *Prognostic Value of Androgen Receptor Splice Variant 7 in the Treatment of Castration-resistant Prostate Cancer with Next generation Androgen Receptor Signal Inhibition: A Systematic Review and Meta-analysis.* Eur Urol Focus, 2018. **4**(4): p. 529-539.

103. Huang, X., et al., *Exosomal miR-1290 and miR-375 as prognostic markers in castration-resistant prostate cancer.* Eur Urol, 2015. **67**(1): p. 33-41.

104. Ross, R.W., et al., *A whole-blood RNA transcript-based prognostic model in men with castration-resistant prostate cancer: a prospective study.* Lancet Oncol, 2012. **13**(11): p. 1105-13.

105. Danila, D.C., et al., *Analytic and clinical validation of a prostate cancer-enhanced messenger RNA detection assay in whole blood as a prognostic biomarker for survival.* Eur Urol, 2014. **65**(6): p. 1191-7.

106. Gonzalez-Billalabeitia, E., et al., *Circulating tumor DNA in advanced prostate cancer: transitioning from discovery to a clinically implemented test.* Prostate Cancer Prostatic Dis, 2019. **22**(2): p. 195-205.

107. Mostaghel, E.A., et al., *Intraprostatic androgens and androgen-regulated gene expression persist after testosterone suppression: therapeutic*

implications for castration-resistant prostate cancer. Cancer Res, 2007. **67**(10): p. 5033-41.

108. Lee, Y., et al., *MicroRNA genes are transcribed by RNA polymerase II.* EMBO J, 2004. **23**(20): p. 4051-60.

109. Cai, X., C.H. Hagedorn, and B.R. Cullen, *Human microRNAs are processed from capped, polyadenylated transcripts that can also function as mRNAs.* RNA, 2004. **10**(12): p. 1957-66.

110. Han, J., et al., *The Drosha-DGCR8 complex in primary microRNA processing.* Genes Dev, 2004. **18**(24): p. 3016-27.

111. Han, J., et al., *Molecular basis for the recognition of primary microRNAs by the Drosha-DGCR8 complex.* Cell, 2006. **125**(5): p. 887-901.

112. Kim, V.N., *MicroRNA precursors in motion: exportin-5 mediates their nuclear export.* Trends Cell Biol, 2004. **14**(4): p. 156-9.

113. Lund, E., et al., *Nuclear export of microRNA precursors.* Science, 2004. **303**(5654): p. 95-8.

114. Hutvagner, G., et al., *A cellular function for the RNA-interference enzyme Dicer in the maturation of the let-7 small temporal RNA.* Science, 2001. **293**(5531): p. 834-8.

115. Romero-Cordoba, S.L., et al., *miRNA biogenesis: biological impact in the development of cancer.* Cancer Biol Ther, 2014. **15**(11): p. 1444-55.

116. Chendrimada, T.P., et al., *TRBP recruits the Dicer complex to Ago2 for microRNA processing and gene silencing.* Nature, 2005. **436**(7051): p. 740-4.

117. Kim, V.N., J. Han, and M.C. Siomi, *Biogenesis of small RNAs in animals.* Nat Rev Mol Cell Biol, 2009. **10**(2): p. 126-39.

118. Romero-Cordoba, S., et al., *Identification and pathway analysis of microRNAs with no previous involvement in breast cancer.* PLoS One, 2012. **7**(3): p. e31904.

119. Guo, H., et al., *Mammalian microRNAs predominantly act to decrease target mRNA levels.* Nature, 2010. **466**(7308): p. 835-40.

120. Eulalio, A., et al., *Deadenylation is a widespread effect of miRNA regulation.* RNA, 2009. **15**(1): p. 21-32.

121. Valinezhad Orang, A., R. Safaralizadeh, and M. Kazemzadeh-Bavili, *Mechanisms of miRNA-Mediated Gene Regulation from Common Downregulation to mRNA-Specific Upregulation.* Int J Genomics, 2014. **2014**: p. 970607.

122. Calin, G.A., et al., *Frequent deletions and down-regulation of micro- RNA genes miR15 and miR16 at 13q14 in chronic lymphocytic leukemia.* Proc Natl Acad Sci U S A, 2002. **99**(24): p. 15524-9.

123. Lu, J., et al., *MicroRNA expression profiles classify human cancers.* Nature, 2005. **435**(7043): p. 834-8.

124. Volinia, S., et al., *A microRNA expression signature of human solid tumors defines cancer gene targets.* Proc Natl Acad Sci U S A, 2006. **103**(7): p. 2257-61.

125. Rosenfeld, N., et al., *MicroRNAs accurately identify cancer tissue origin.* Nat Biotechnol, 2008. **26**(4): p. 462-9.

126. Varambally, S., et al., *Genomic loss of microRNA-101 leads to overexpression of histone methyltransferase EZH2 in cancer.* Science, 2008. **322**(5908): p. 1695-9.

127. Cao, P., et al., *MicroRNA-101 negatively regulates Ezh2 and its expression is modulated by androgen receptor and HIF-1alpha/HIF-1beta.* Mol Cancer, 2010. **9**: p. 108.

128. Hao, Y., et al., *Enforced expression of miR-101 inhibits prostate cancer cell growth by modulating the COX-2 pathway in vivo.* Cancer Prev Res (Phila), 2011. **4**(7): p. 1073-83.

129. Peng, Y. and C.M. Croce, *The role of MicroRNAs in human cancer.* Signal Transduct Target Ther, 2016. **1**: p. 15004.

130. Xi, Y., et al., *Systematic analysis of microRNA expression of RNA extracted from fresh frozen and formalin-fixed paraffin-embedded samples.* RNA, 2007. **13**(10): p. 1668-74.

131. Bucay, N., et al., *miRNA Expression Analyses in Prostate Cancer Clinical Tissues.* J Vis Exp, 2015(103).

132. Paziewska, A., et al., *Candidate diagnostic miRNAs that can detect cancer in prostate biopsy.* Prostate, 2018. **78**(3): p. 178-185.

133. Zedan, A.H., et al., *Heterogeneity of miRNA expression in localized prostate cancer with clinicopathological correlations.* PLoS One, 2017. **12**(6): p. e0179113.

134. Renwick, N., et al., *Multiplexed miRNA fluorescence in situ hybridization for formalin-fixed paraffin-embedded tissues.* Methods Mol Biol, 2014. **1211**: p. 171-87.

135. Pena, J.T., et al., *miRNA in situ hybridization in formaldehyde and EDC-fixed tissues.* Nat Methods, 2009. **6**(2): p. 139-41.

136. Filella, X. and L. Foj, *miRNAs as novel biomarkers in the management of prostate cancer.* Clin Chem Lab Med, 2017. **55**(5): p. 715-736.

137. Zhou, X., et al., *Prognostic value of miR-21 in various cancers: an updating meta-analysis.* PLoS One, 2014. **9**(7): p. e102413.

138. Zedan, A.H., et al., *microRNA expression in tumour tissue and plasma in patients with newly diagnosed metastatic prostate cancer.* Tumour Biol, 2018. **40**(5): p. 1010428318775864.

139. Hart, M., et al., *Comparative microRNA profiling of prostate carcinomas with increasing tumor stage by deep sequencing.* Mol Cancer Res, 2014. **12**(2): p. 250-63.

140. Endzelins, E., et al., *Detection of circulating miRNAs: comparative analysis of extracellular vesicle-incorporated miRNAs and cell-free*

miRNAs in whole plasma of prostate cancer patients. BMC Cancer, 2017. **17**(1): p. 730.

141. Stuopelyte, K., et al., *Detection of miRNAs in urine of prostate cancer patients.* Medicina (Kaunas), 2016. **52**(2): p. 116-24.

142. Ghorbanmehr, N., et al., *miR-21-5p, miR-141-3p, and miR-205-5p levels in urine-promising biomarkers for the identification of prostate and bladder cancer.* Prostate, 2019. **79**(1): p. 88-95.

143. Yaman Agaoglu, F., et al., *Investigation of miR-21, miR-141, and miR-221 in blood circulation of patients with prostate cancer.* Tumour Biol, 2011. **32**(3): p. 583-8.

144. Stuopelyte, K., et al., *The utility of urine-circulating miRNAs for detection of prostate cancer.* Br J Cancer, 2016. **115**(6): p. 707-15.

145. Brase, J.C., et al., *Circulating miRNAs are correlated with tumor progression in prostate cancer.* Int J Cancer, 2011. **128**(3): p. 608-16.

146. Bryant, R.J., et al., *Changes in circulating microRNA levels associated with prostate cancer.* Br J Cancer, 2012. **106**(4): p. 768-74.

147. Lekchnov, E.A., et al., *Searching for the Novel Specific Predictors of Prostate Cancer in Urine: The Analysis of 84 miRNA Expression.* Int J Mol Sci, 2018. **19**(12).

148. Mitchell, P.S., et al., *Circulating microRNAs as stable blood-based markers for cancer detection.* Proc Natl Acad Sci U S A, 2008. **105**(30): p. 10513-8.

149. Luu, H.N., et al., *miRNAs associated with prostate cancer risk and progression.* BMC Urol, 2017. **17**(1): p. 18.

150. Zhang, H.L., et al., *An elevated serum miR-141 level in patients with bone-metastatic prostate cancer is correlated with more bone lesions.* Asian J Androl, 2013. **15**(2): p. 231-5.

151. Song, C.J., et al., *The potential of microRNAs as human prostate cancer biomarkers: A meta-analysis of related studies.* J Cell Biochem, 2018. **119**(3): p. 2763-2786.

152. Harding, C., J. Heuser, and P. Stahl, *Receptor-mediated endocytosis of transferrin and recycling of the transferrin receptor in rat reticulocytes.* J Cell Biol, 1983. **97**(2): p. 329-39.

153. Pan, B.T., et al., *Electron microscopic evidence for externalization of the transferrin receptor in vesicular form in sheep reticulocytes.* J Cell Biol, 1985. **101**(3): p. 942-8.

154. Johnstone, R.M., et al., *Vesicle formation during reticulocyte maturation. Association of plasma membrane activities with released vesicles (exosomes).* J Biol Chem, 1987. **262**(19): p. 9412-20.

155. Hessvik, N.P. and A. Llorente, *Current knowledge on exosome biogenesis and release.* Cell Mol Life Sci, 2018. **75**(2): p. 193-208.

156. Huotari, J. and A. Helenius, *Endosome maturation.* EMBO J, 2011. **30**(17): p. 3481-500.

157. Borges, F.T., L.A. Reis, and N. Schor, *Extracellular vesicles: structure, function, and potential clinical uses in renal diseases.* Braz J Med Biol Res, 2013. **46**(10): p. 824-30.

158. Laulagnier, K., et al., *Characterization of exosome subpopulations from RBL-2H3 cells using fluorescent lipids.* Blood Cells Mol Dis, 2005. **35**(2): p. 116-21.

159. Willms, E., et al., *Cells release subpopulations of exosomes with distinct molecular and biological properties.* Sci Rep, 2016. **6**: p. 22519.

160. Andreu, Z. and M. Yanez-Mo, *Tetraspanins in extracellular vesicle formation and function.* Front Immunol, 2014. **5**: p. 442.

161. Schmidt, O. and D. Teis, *The ESCRT machinery.* Curr Biol, 2012. **22**(4): p. R116-20.

162. Colombo, M., et al., *Analysis of ESCRT functions in exosome biogenesis, composition and secretion highlights the heterogeneity of extracellular vesicles.* J Cell Sci, 2013. **126**(Pt 24): p. 5553-65.

163. Li, A., et al., *Exosomal proteins as potential markers of tumor diagnosis.* J Hematol Oncol, 2017. **10**(1): p. 175.

164. Yang, C., et al., *Comprehensive proteomics analysis of exosomes derived from human seminal plasma.* Andrology, 2017. **5**(5): p. 1007-1015.

165. Welton, J.L., et al., *Proteomics analysis of bladder cancer exosomes.* Mol Cell Proteomics, 2010. **9**(6): p. 1324-38.

166. Thery, C., et al., *Proteomic analysis of dendritic cell-derived exosomes: a secreted subcellular compartment distinct from apoptotic vesicles.* J Immunol, 2001. **166**(12): p. 7309-18.

167. Llorente, A., et al., *Molecular lipidomics of exosomes released by PC-3 prostate cancer cells.* Biochim Biophys Acta, 2013. **1831**(7): p. 1302-9.

168. Laulagnier, K., et al., *Mast cell- and dendritic cell-derived exosomes display a specific lipid composition and an unusual membrane organization.* Biochem J, 2004. **380**(Pt 1): p. 161-71.

169. Skotland, T., et al., *Exosomal lipid composition and the role of ether lipids and phosphoinositides in exosome biology.* J Lipid Res, 2019. **60**(1): p. 9-18.

170. Skotland, T., et al., *Molecular lipid species in urinary exosomes as potential prostate cancer biomarkers.* Eur J Cancer, 2017. **70**: p. 122-132.

171. Balaj, L., et al., *Tumour microvesicles contain retrotransposon elements and amplified oncogene sequences.* Nat Commun, 2011. **2**: p. 180.

172. Guescini, M., et al., *Astrocytes and Glioblastoma cells release exosomes carrying mtDNA.* J Neural Transm (Vienna), 2010. **117**(1): p. 1-4.

173. Thakur, B.K., et al., *Double-stranded DNA in exosomes: a novel biomarker in cancer detection.* Cell Res, 2014. **24**(6): p. 766-9.

174. Wang, L., et al., *Exosomal double-stranded DNA as a biomarker for the diagnosis and preoperative assessment of pheochromocytoma and paraganglioma.* Mol Cancer, 2018. **17**(1): p. 128.

175. Huang, X., et al., *Characterization of human plasma-derived exosomal RNAs by deep sequencing.* BMC Genomics, 2013. **14**: p. 319.

176. Batagov, A.O. and I.V. Kurochkin, *Exosomes secreted by human cells transport largely mRNA fragments that are enriched in the 3'-untranslated regions.* Biol Direct, 2013. **8**: p. 12.

177. Xu, J.F., et al., *Exosomes containing differential expression of microRNA and mRNA in osteosarcoma that can predict response to chemotherapy.* Oncotarget, 2017. **8**(44): p. 75968-75978.

178. Li, M., et al., *Analysis of the RNA content of the exosomes derived from blood serum and urine and its potential as biomarkers.* Philos Trans R Soc Lond B Biol Sci, 2014. **369**(1652).

179. Tsang, E.K., et al., *Small RNA Sequencing in Cells and Exosomes Identifies eQTLs and 14q32 as a Region of Active Export.* G3 (Bethesda), 2017. **7**(1): p. 31-39.

180. Li, P., et al., *Progress in Exosome Isolation Techniques.* Theranostics, 2017. **7**(3): p. 789-804.

181. Konoshenko, M.Y., et al., *Isolation of Extracellular Vesicles: General Methodologies and Latest Trends.* Biomed Res Int, 2018. **2018**: p. 8545347.

182. Melo, S.A., et al., *Glypican-1 identifies cancer exosomes and detects early pancreatic cancer.* Nature, 2015. **523**(7559): p. 177-82.

183. Mizutani, K., et al., *Isolation of prostate cancer-related exosomes.* Anticancer Res, 2014. **34**(7): p. 3419-23.

184. Park, Y.H., et al., *Prostate-specific extracellular vesicles as a novel biomarker in human prostate cancer.* Sci Rep, 2016. **6**: p. 30386.

185. Ding, M., et al., *Comparison of commercial exosome isolation kits for circulating exosomal microRNA profiling.* Anal Bioanal Chem, 2018. **410**(16): p. 3805-3814.

186. Helwa, I., et al., *A Comparative Study of Serum Exosome Isolation Using Differential Ultracentrifugation and Three Commercial Reagents.* PLoS One, 2017. **12**(1): p. e0170628.

187. Brownlee, Z., et al., *A novel "salting-out" procedure for the isolation of tumor-derived exosomes.* J Immunol Methods, 2014. **407**: p. 120-6.

188. Deregibus, M.C., et al., *Charge-based precipitation of extracellular vesicles.* Int J Mol Med, 2016. **38**(5): p. 1359-1366.

189. Yang, F., et al., *Exosome separation using microfluidic systems: size-based, immunoaffinity-based and dynamic methodologies.* Biotechnol J, 2017. **12**(4).

190. Contreras-Naranjo, J.C., H.J. Wu, and V.M. Ugaz, *Microfluidics for exosome isolation and analysis: enabling liquid biopsy for personalized medicine.* Lab Chip, 2017. **17**(21): p. 3558-3577.

191. Azmi, A.S., B. Bao, and F.H. Sarkar, *Exosomes in cancer development, metastasis, and drug resistance: a comprehensive review.* Cancer Metastasis Rev, 2013. **32**(3-4): p. 623-42.

192. Schorey, J.S. and C.V. Harding, *Extracellular vesicles and infectious diseases: new complexity to an old story.* J Clin Invest, 2016. **126**(4): p. 1181-9.

193. Martinez, M.C. and R. Andriantsitohaina, *Extracellular Vesicles in Metabolic Syndrome.* Circ Res, 2017. **120**(10): p. 1674-1686.

194. Mitchell, M.D., et al., *Placental exosomes in normal and complicated pregnancy.* Am J Obstet Gynecol, 2015. **213**(4 Suppl): p. S173-81.

195. Li, I. and B.Y. Nabet, *Exosomes in the tumor microenvironment as mediators of cancer therapy resistance.* Mol Cancer, 2019. **18**(1): p. 32.

196. Liao, J., et al., *Exosome-shuttling microRNA-21 promotes cell migration and invasion-targeting PDCD4 in esophageal cancer.* Int J Oncol, 2016. **48**(6): p. 2567-79.

197. Singh, R., et al., *Exosome-mediated transfer of miR-10b promotes cell invasion in breast cancer.* Mol Cancer, 2014. **13**: p. 256.

198. Singh, A., et al., *Exosome-mediated Transfer of alphavbeta3 Integrin from Tumorigenic to Nontumorigenic Cells Promotes a Migratory Phenotype.* Mol Cancer Res, 2016. **14**(11): p. 1136-1146.

199. Skog, J., et al., *Glioblastoma microvesicles transport RNA and proteins that promote tumour growth and provide diagnostic biomarkers.* Nat Cell Biol, 2008. **10**(12): p. 1470-6.

200. Hoshino, A., et al., *Tumour exosome integrins determine organotropic metastasis.* Nature, 2015. **527**(7578): p. 329-35.

201. Fong, M.Y., et al., *Breast-cancer-secreted miR-122 reprograms glucose metabolism in premetastatic niche to promote metastasis.* Nat Cell Biol, 2015. **17**(2): p. 183-94.

202. Zhang, H., et al., *Exosome-delivered EGFR regulates liver microenvironment to promote gastric cancer liver metastasis.* Nat Commun, 2017. **8**: p. 15016.

203. Costa-Silva, B., et al., *Pancreatic cancer exosomes initiate pre-metastatic niche formation in the liver.* Nat Cell Biol, 2015. **17**(6): p. 816-26.

204. Zhang, L., et al., *Microenvironment-induced PTEN loss by exosomal microRNA primes brain metastasis outgrowth.* Nature, 2015. **527**(7576): p. 100-104.

205. Wieckowski, E.U., et al., *Tumor-derived microvesicles promote regulatory T cell expansion and induce apoptosis in tumor-reactive activated CD8+ T lymphocytes.* J Immunol, 2009. **183**(6): p. 3720-30.

206. Klibi, J., et al., *Blood diffusion and Th1-suppressive effects of galectin-9-containing exosomes released by Epstein-Barr virus-infected nasopharyngeal carcinoma cells.* Blood, 2009. **113**(9): p. 1957-66.

207. Chen, G., et al., *Exosomal PD-L1 contributes to immunosuppression and is associated with anti-PD-1 response.* Nature, 2018. **560**(7718): p. 382-386.

208. Poggio, M., et al., *Suppression of Exosomal PD-L1 Induces Systemic Anti-tumor Immunity and Memory.* Cell, 2019. **177**(2): p. 414-427 e13.

209. Salimu, J., et al., *Dominant immunosuppression of dendritic cell function by prostate-cancer-derived exosomes.* J Extracell Vesicles, 2017. **6**(1): p. 1368823.

210. Plebanek, M.P., et al., *Pre-metastatic cancer exosomes induce immune surveillance by patrolling monocytes at the metastatic niche.* Nat Commun, 2017. **8**(1): p. 1319.

211. Hannafon, B.N., et al., *Plasma exosome microRNAs are indicative of breast cancer.* Breast Cancer Res, 2016. **18**(1): p. 90.

212. Wang, M., et al., *Effect of exosome biomarkers for diagnosis and prognosis of breast cancer patients.* Clin Transl Oncol, 2018. **20**(7): p. 906-911.

213. Domenyuk, V., et al., *Plasma Exosome Profiling of Cancer Patients by a Next Generation Systems Biology Approach.* Sci Rep, 2017. **7**: p. 42741.

214. McKiernan, J., et al., *A Novel Urine Exosome Gene Expression Assay to Predict High-grade Prostate Cancer at Initial Biopsy.* JAMA Oncol, 2016. **2**(7): p. 882-9.

215. Corcoran, C., S. Rani, and L. O'Driscoll, *miR-34a is an Intracellular and Exosomal Predictive Biomarker for Response to Docetaxel with Clinical Relevance to Prostate Cancer Progression.* Prostate, 2014. **74**(13): p. 1320-1334.

216. Rodriguez, M., et al., *Identification of non-invasive miRNAs biomarkers for prostate cancer by deep sequencing analysis of urinary exosomes.* Mol Cancer, 2017. **16**(1): p. 156.

217. Rabinowits, G., et al., *Exosomal microRNA: a diagnostic marker for lung cancer.* Clin Lung Cancer, 2009. **10**(1): p. 42-6.

218. Jakobsen, K.R., et al., *Exosomal proteins as potential diagnostic markers in advanced non-small cell lung carcinoma.* J Extracell Vesicles, 2015. **4**: p. 26659.

219. Liu, Q., et al., *Circulating exosomal microRNAs as prognostic biomarkers for non-small-cell lung cancer.* Oncotarget, 2017. **8**(8): p. 13048-13058.

220. Wang, J., et al., *Circulating exosomal miR-125a-3p as a novel biomarker for early-stage colon cancer.* Sci Rep, 2017. **7**(1): p. 4150.

221. Yan, S., et al., *Downregulation of circulating exosomal miR-638 predicts poor prognosis in colon cancer patients.* Oncotarget, 2017. **8**(42): p. 72220-72226.

222. Allenson, K., et al., *High prevalence of mutant KRAS in circulating exosome-derived DNA from early-stage pancreatic cancer patients.* Ann Oncol, 2017. **28**(4): p. 741-747.

223. Madhavan, B., et al., *Combined evaluation of a panel of protein and miRNA serum-exosome biomarkers for pancreatic cancer diagnosis increases sensitivity and specificity.* Int J Cancer, 2015. **136**(11): p. 2616-27.

224. McKiernan, J., et al., *A Prospective Adaptive Utility Trial to Validate Performance of a Novel Urine Exosome Gene Expression Assay to Predict*

High-grade Prostate Cancer in Patients with Prostate-specific Antigen 2-10ng/ml at Initial Biopsy. Eur Urol, 2018. **74**(6): p. 731-738.

225. Del Re, M., et al., *The Detection of Androgen Receptor Splice Variant 7 in Plasma-derived Exosomal RNA Strongly Predicts Resistance to Hormonal Therapy in Metastatic Prostate Cancer Patients.* Eur Urol, 2017. **71**(4): p. 680-687.
226. Turturici, G., et al., *Extracellular membrane vesicles as a mechanism of cell-to-cell communication: advantages and disadvantages.* Am J Physiol Cell Physiol, 2014. **306**(7): p. C621-33.
227. Kim, M.S., et al., *Engineering macrophage-derived exosomes for targeted paclitaxel delivery to pulmonary metastases: in vitro and in vivo evaluations.* Nanomedicine, 2018. **14**(1): p. 195-204.
228. Kalimuthu, S., et al., *A New Approach for Loading Anticancer Drugs Into Mesenchymal Stem Cell-Derived Exosome Mimetics for Cancer Therapy.* Front Pharmacol, 2018. **9**: p. 1116.
229. Ohno, S., et al., *Systemically injected exosomes targeted to EGFR deliver antitumor microRNA to breast cancer cells.* Mol Ther, 2013. **21**(1): p. 185-91.
230. Kamerkar, S., et al., *Exosomes facilitate therapeutic targeting of oncogenic KRAS in pancreatic cancer.* Nature, 2017. **546**(7659): p. 498-503.
231. Mendt, M., et al., *Generation and testing of clinical-grade exosomes for pancreatic cancer.* JCI Insight, 2018. **3**(8).
232. Zitvogel, L., et al., *Eradication of established murine tumors using a novel cell-free vaccine: dendritic cell-derived exosomes.* Nat Med, 1998. **4**(5): p. 594-600.
233. Escudier, B., et al., *Vaccination of metastatic melanoma patients with autologous dendritic cell (DC) derived-exosomes: results of thefirst phase I clinical trial.* J Transl Med, 2005. **3**(1): p. 10.
234. Morse, M.A., et al., *A phase I study of dexosome immunotherapy in patients with advanced non-small cell lung cancer.* J Transl Med, 2005. **3**(1): p. 9.
235. Hao, S., et al., *Mature dendritic cells pulsed with exosomes stimulate efficient cytotoxic T-lymphocyte responses and antitumour immunity.* Immunology, 2007. **120**(1): p. 90-102.
236. Segura, E., et al., *ICAM-1 on exosomes from mature dendritic cells is critical for efficient naive T-cell priming.* Blood, 2005. **106**(1): p. 216-23.
237. Utsugi-Kobukai, S., et al., *MHC class I-mediated exogenous antigen presentation by exosomes secreted from immature and mature bone marrow derived dendritic cells.* Immunol Lett, 2003. **89**(2-3): p. 125-31.
238. Besse, B., et al., *Dendritic cell-derived exosomes as maintenance immunotherapy after first line chemotherapy in NSCLC.* Oncoimmunology, 2016. **5**(4): p. e1071008.

239. Guo, T., et al., *Culture of Circulating Tumor Cells - Holy Grail and Big Challenge*. 2016: International Journal of Cancer and Clinical Research p. 065.

240. Pantel, K. and M.R. Speicher, *The biology of circulating tumor cells.* Oncogene, 2016. **35**(10): p. 1216-24.

241. Vanharanta, S. and J. Massague, *Origins of metastatic traits.* Cancer Cell, 2013. **24**(4): p. 410-21.

242. Alix-Panabieres, C. and K. Pantel, *Challenges in circulating tumour cell research.* Nat Rev Cancer, 2014. **14**(9): p. 623-31.

243. Shen, Z., A. Wu, and X. Chen, *Current detection technologies for circulating tumor cells.* Chem Soc Rev, 2017. **46**(8): p. 2038-2056.

244. Pantel, K. and C. Alix-Panabieres, *Functional Studies on Viable Circulating Tumor Cells.* Clin Chem, 2016. **62**(2): p. 328-34.

245. Yu, N., et al., *Circulating tumor cells in lung cancer: detection methods and clinical applications.* Lung, 2015. **193**(2): p. 157-71.

246. Gao, D., et al., *Organoid cultures derived from patients with advanced prostate cancer.* Cell, 2014. **159**(1): p. 176-87.

247. Hodgkinson, C.L., et al., *Tumorigenicity and genetic profiling of circulating tumor cells in small-cell lung cancer.* Nat Med, 2014. **20**(8): p. 897-903.

248. Lu, Y., et al., *Isolation and characterization of living circulating tumor cells in patients by immunomagnetic negative enrichment coupled with flow cytometry.* Cancer, 2015. **121**(17): p. 3036-45.

249. Cristofanilli, M., et al., *Circulating tumor cells, disease progression, and survival in metastatic breast cancer.* N Engl J Med, 2004. **351**(8): p. 781-91.

250. Cohen, S.J., et al., *Relationship of circulating tumor cells to tumor response, progression-free survival, and overall survival in patients with metastatic colorectal cancer.* J Clin Oncol, 2008. **26**(19): p. 3213-21.

251. Nagrath, S., et al., *Isolation of rare circulating tumour cells in cancer patients by microchip technology.* Nature, 2007. **450**(7173): p. 1235-9.

252. Murlidhar, V., et al., *A radial flow microfluidic device for ultra-high-throughput affinity-based isolation of circulating tumor cells.* Small, 2014. **10**(23): p. 4895-904.

253. Ozkumur, E., et al., *Inertial Focusing for Tumor Antigen-Dependent and -Independent Sorting of Rare Circulating Tumor Cells.* Science Translational Medicine, 2013. **5**(179).

254. Morrow, C.J., et al., *Tumourigenic non-small-cell lung cancer mesenchymal circulating tumour cells: a clinical case study.* Ann Oncol, 2016.

255. Sorg, N., et al., *Red blood cell depletion from bone marrow and peripheral blood buffy coat: a comparison of two new and three established technologies.* Transfusion, 2015. **55**(6): p. 1275-82.

256. Alix-Panabieres, C., et al., *Full-length cytokeratin-19 is released by human tumor cells: a potential role in metastatic progression of breast cancer.* Breast Cancer Research, 2009. **11**(3).

257. Kolostova, K., M. Cegan, and V. Bobek, *Circulating tumour cells in patients with urothelial tumours: Enrichment and in vitro culture.* Can Urol Assoc J, 2014. **8**(9-10): p. E715-20.

258. Kolostova, K., et al., *Isolation, primary culture, morphological and molecular characterization of circulating tumor cells in gynecological cancers.* Am J Transl Res, 2015. **7**(7): p. 1203-13.

259. Kolostova, K., et al., *The added value of circulating tumor cells examination in ovarian cancer staging.* Am J Cancer Res, 2015. **5**(11): p. 3363-75.

260. Bobek, V., et al., *Circulating tumor cells in pancreatic cancer patients: enrichment and cultivation.* World J Gastroenterol, 2014. **20**(45): p. 17163-70.

261. Xu, L., et al., *Optimization and Evaluation of a Novel Size Based Circulating Tumor Cell Isolation System.* PLoS One, 2015. **10**(9): p. e0138032.

262. Sarioglu, A.F., et al., *A microfluidic device for label-free, physical capture of circulating tumor cell clusters.* Nat Methods, 2015. **12**(7): p. 685-91.

263. Riahi, R., et al., *A novel microchannel-based device to capture and analyze circulating tumor cells (CTCs) of breast cancer.* Int J Oncol, 2014. **44**(6): p. 1870-8.

264. de Wit, S., G. van Dalum, and L.W. Terstappen, *Detection of circulating tumor cells.* Scientifica (Cairo), 2014. **2014**: p. 819362.

265. Ligthart, S.T., et al., *Circulating Tumor Cells Count and Morphological Features in Breast, Colorectal and Prostate Cancer.* PLoS One, 2013. **8**(6): p. e67148.

266. Vona, G., et al., *Isolation by size of epithelial tumor cells - A new method for the immunomorphological and molecular characterization of circulating tumor cells.* American Journal of Pathology, 2000. **156**(1): p. 57-63.

267. Huang, S.B., et al., *High-purity and label-free isolation of circulating tumor cells (CTCs) in a microfluidic platform by using optically-induced-dielectrophoretic (ODEP) force.* Lab on a Chip, 2013. **13**(7): p. 1371-1383.

268. Coumans, F.A., et al., *Filter characteristics influencing circulating tumor cell enrichment from whole blood.* PLoS One, 2013. **8**(4): p. e61770.

269. Chen, J.F., et al., *Subclassification of prostate cancer circulating tumor cells by nuclear size reveals very small nuclear circulating tumor cells in patients with visceral metastases.* Cancer, 2015. **121**(18): p. 3240-51.

270. Lu, J., et al., *Isolation of circulating epithelial and tumor progenitor cells with an invasive phenotype from breast cancer patients.* International Journal of Cancer, 2010. **126**(3): p. 669-683.

271. Paris, P.L., et al., *Functional phenotyping and genotyping of circulating tumor cells from patients with castration resistant prostate cancer.* Cancer Letters, 2009. **277**(2): p. 164-173.

272. Wang, H.Z., et al., *Detection and enumeration of circulating tumor cells based on their invasive property.* Oncotarget, 2015. **6**(29): p. 27304-27311.

273. Larson, C.J., et al., *Apoptosis of circulating tumor cells in prostate cancer patients.* Cytometry A, 2004. **62**(1): p. 46-53.

274. Sastre, J., et al., *Circulating tumor cells in colorectal cancer: correlation with clinical and pathological variables.* Annals of Oncology, 2008. **19**(5): p. 935-938.

275. Punnoose, E.A., et al., *Evaluation of Circulating Tumor Cells and Circulating Tumor DNA in Non-Small Cell Lung Cancer: Association with Clinical Endpoints in a Phase II Clinical Trial of Pertuzumab and Erlotinib.* Clinical Cancer Research, 2012. **18**(8): p. 2391-2401.

276. Tinhofer, I., et al., *Cancer stem cell characteristics of circulating tumor cells.* Int J Radiat Biol, 2014. **90**(8): p. 622-7.

277. Danila, D.C., et al., *Circulating tumor cell number and prognosis in progressive castration-resistant prostate cancer.* Clin Cancer Res, 2007. **13**(23): p. 7053-8.

278. Thalgott, M., et al., *Circulating tumor cells versus objective response assessment predicting survival in metastatic castration-resistant prostate cancer patients treated with docetaxel chemotherapy.* J Cancer Res Clin Oncol, 2015. **141**(8): p. 1457-64.

279. Scher, H.I., et al., *Circulating tumour cells as prognostic markers in progressive, castration-resistant prostate cancer: a reanalysis of IMMC38 trial data.* Lancet Oncology, 2009. **10**(3): p. 233-239.

280. Jiang, R.Z., et al., *A comparison of isolated circulating tumor cells and tissue biopsies using whole-genome sequencing in prostate cancer.* Oncotarget, 2015. **6**(42): p. 44781-44793.

281. Swennenhuis, J.F., et al., *Efficiency of whole genome amplification of single circulating tumor cells enriched by CellSearch and sorted by FACS.* Genome Medicine, 2013. **5**.

282. Mostert, B., et al., *Gene expression profiles in circulating tumor cells to predict prognosis in metastatic breast cancer patients.* Annals of Oncology, 2015. **26**(3): p. 510-516.

283. Blassl, C., et al., *Gene expression profiling of single circulating tumor cells in ovarian cancer - Establishment of a multi-marker gene panel.* Mol Oncol, 2016.

284. Cho, W.J., et al., *Gene expression analysis of bone metastasis and circulating tumor cells from metastatic castrate-resistant prostate cancer patients.* J Transl Med, 2016. **14**(1): p. 72.

285. Armstrong, C.M. and A.C. Gao, *Drug resistance in castration resistant prostate cancer: resistance mechanisms and emerging treatment strategies.* Am J Clin Exp Urol, 2015. **3**(2): p. 64-76.

286. Onstenk, W., et al., *The use of circulating tumor cells in guiding treatment decisions for patients with metastatic castration-resistant prostate cancer.* Cancer Treat Rev, 2016. **46**: p. 42-50.

287. Ting, D.T., et al., *Single-cell RNA sequencing identifies extracellular matrix gene expression by pancreatic circulating tumor cells.* Cell Rep, 2014. **8**(6): p. 1905-1918.

288. Cann, G.M., et al., *mRNA-Seq of single prostate cancer circulating tumor cells reveals recapitulation of gene expression and pathways found in prostate cancer.* PLoS One, 2012. **7**(11): p. e49144.

289. Lang, J.E., et al., *RNA-Seq of Circulating Tumor Cells in Stage II-III Breast Cancer.* Ann Surg Oncol, 2018. **25**(8): p. 2261-2270.

290. Zhu, Z., et al., *Progress and challenges of sequencing and analyzing circulating tumor cells.* Cell Biol Toxicol, 2018. **34**(5): p. 405-415.

291. Zhang, Z., et al., *Expansion of CTCs from early stage lung cancer patients using a microfluidic co-culture model.* Oncotarget, 2014. **5**(23): p. 12383-12397.

292. Kolostova, K., et al., *Circulating tumor cells in localized prostate cancer: isolation, cultivation in vitro and relationship to T-stage and Gleason score.* Anticancer Res, 2014. **34**(7): p. 3641-6.

293. Kolostova, K., et al., *Detection and cultivation of circulating tumor cells in gastric cancer.* Cytotechnology, 2015.

294. Khoo, B.L., et al., *Short-term expansion of breast circulating cancer cells predicts response to anti-cancer therapy.* Oncotarget, 2015. **6**(17): p. 15578-93.

295. Khoo, B.L., et al., *Expansion of patient-derived circulating tumor cells from liquid biopsies using a CTC microfluidic culture device.* Nat Protoc, 2018. **13**(1): p. 34-58.

296. Andree, K.C., et al., *Toward a real liquid biopsy in metastatic breast and prostate cancer: Diagnostic LeukApheresis increases CTC yields in a European prospective multicenter study (CTCTrap).* Int J Cancer, 2018. **143**(10): p. 2584-2591.

297. Lambros, M.B., et al., *Single-Cell Analyses of Prostate Cancer Liquid Biopsies Acquired by Apheresis.* Clin Cancer Res, 2018. **24**(22): p. 5635-5644.

298. Zhang, L., et al., *The identification and characterization of breast cancer CTCs competent for brain metastasis.* Sci Transl Med, 2013. **5**(180): p. 180ra48.

299. Yu, M., et al., *Cancer therapy. Ex vivo culture of circulating breast tumor cells for individualized testing of drug susceptibility.* Science, 2014. **345**(6193): p. 216-20.

300. Cayrefourcq, L., et al., *Establishment and characterization of a cell line from human circulating colon cancer cells.* Cancer Res, 2015. **75**(5): p. 892-901.

301. Lallo, A., et al., *Ex vivo culture of cells derived from circulating tumour cell xenograft to support small cell lung cancer research and experimental therapeutics.* Br J Pharmacol, 2018.

302. Rossi, E., et al., *Retaining the long-survive capacity of Circulating Tumor Cells (CTCs) followed by xeno-transplantation: not only from metastatic cancer of the breast but also of prostate cancer patients.* Oncoscience, 2014. **1**(1): p. 49-56.

303. Baccelli, I., et al., *Identification of a population of blood circulating tumor cells from breast cancer patients that initiates metastasis in a xenograft assay.* Nat Biotechnol, 2013. **31**(6): p. 539-44.

304. Fisher, R., L. Pusztai, and C. Swanton, *Cancer heterogeneity: implications for targeted therapeutics.* Br J Cancer, 2013. **108**(3): p. 479-85.

305. Di Meo, A., et al., *Liquid biopsy: a step forward towards precision medicine in urologic malignancies.* Mol Cancer, 2017. **16**(1): p. 80.

306. Siravegna, G., et al., *Integrating liquid biopsies into the management of cancer.* Nat Rev Clin Oncol, 2017. **14**(9): p. 531-548.

307. Tomlins, S.A., et al., *Urine TMPRSS2:ERG Plus PCA3 for Individualized Prostate Cancer Risk Assessment.* Eur Urol, 2016. **70**(1): p. 45-53.

308. Rigau, M., et al., *The present and future of prostate cancer urine biomarkers.* Int J Mol Sci, 2013. **14**(6): p. 12620-49.

309. Palmirotta, R., et al., *Liquid biopsy of cancer: a multimodal diagnostic tool in clinical oncology.* Ther Adv Med Oncol, 2018. **10**: p. 1758835918794630.

310. Elazezy, M. and S.A. Joosse, *Techniques of using circulating tumor DNA as a liquid biopsy component in cancer management.* Comput Struct Biotechnol J, 2018. **16**: p. 370-378.

311. Gormally, E., et al., *TP53 and KRAS2 mutations in plasma DNA of healthy subjects and subsequent cancer occurrence: a prospective study.* Cancer Res, 2006. **66**(13): p. 6871-6.

312. Zhou, B., et al., *[Exploratory study of circulating tumor DNA detection in early breast cancer: an analysis of 75 next-generation sequencing results].* Zhonghua Wai Ke Za Zhi, 2017. **55**(11): p. 847-852.

313. Aravanis, A.M., M. Lee, and R.D. Klausner, *Next-Generation Sequencing of Circulating Tumor DNA for Early Cancer Detection.* Cell, 2017. **168**(4): p. 571-574.

314. Lecomte, T., et al., *Detection of free-circulating tumor-associated DNA in plasma of colorectal cancer patients and its association with prognosis.* Int J Cancer, 2002. **100**(5): p. 542-8.

315. Dawson, S.J., et al., *Analysis of circulating tumor DNA to monitor metastatic breast cancer.* N Engl J Med, 2013. **368**(13): p. 1199-209.

316. Oshiro, C., et al., *PIK3CA mutations in serum DNA are predictive of recurrence in primary breast cancer patients.* Breast Cancer Res Treat, 2015. **150**(2): p. 299-307.

317. Tie, J., et al., *Circulating tumor DNA analysis detects minimal residual disease and predicts recurrence in patients with stage II colon cancer.* Sci Transl Med, 2016. **8**(346): p. 346ra92.

318. Garcia-Murillas, I., et al., *Mutation tracking in circulating tumor DNA predicts relapse in early breast cancer.* Sci Transl Med, 2015. **7**(302): p. 302ra133.

319. Frattini, M., et al., *Quantitative and qualitative characterization of plasma DNA identifies primary and recurrent colorectal cancer.* Cancer Lett, 2008. **263**(2): p. 170-81.

320. Wu, Y.L., et al., *First-line erlotinib versus gemcitabine/cisplatin in patients with advanced EGFR mutation-positive non-small-cell lung cancer: analyses from the phase III, randomized, open-label, ENSURE study.* Ann Oncol, 2015. **26**(9): p. 1883-9.

321. Schreuer, M., et al., *Quantitative assessment of BRAF V600 mutant circulating cell-free tumor DNA as a tool for therapeutic monitoring in metastatic melanoma patients treated with BRAF/MEK inhibitors.* J Transl Med, 2016. **14**: p. 95.

322. Administration., U.F.D., *Premarket approval P150044 — Cobas EGFR MUTATION TEST V2. FDA* http://www.accessdata.fda.gov/scripts/cdrh/cfdocs/cfpma/pma.cfm?id=P150044. 2016.

323. https://www.accessdata.fda.gov/scripts/cdrh/cfdocs/cfpma/pma_template.cfm?id=p130001. *Accessed in May, 2019.*

324. Fiala, C. and E.P. Diamandis, *Utility of circulating tumor DNA in cancer diagnostics with emphasis on early detection.* BMC Med, 2018. **16**(1): p. 166.

325. Cohen, J.D., et al., *Detection and localization of surgically resectable cancers with a multi-analyte blood test.* Science, 2018. **359**(6378): p. 926-930.

326. Fernando, M.R., et al., *New evidence that a large proportion of human blood plasma cell-free DNA is localized in exosomes.* PLoS One, 2017. **12**(8): p. e0183915.

327. Vagner, T., et al., *Large extracellular vesicles carry most of the tumour DNA circulating in prostate cancer patient plasma.* J Extracell Vesicles, 2018. **7**(1): p. 1505403.

328. Wu, Y., et al., *Circulating HER-2 mRNA in the peripheral blood as a potential diagnostic and prognostic biomarker in females with breast cancer.* Oncol Lett, 2018. **16**(3): p. 3726-3734.

329. Russo, F., et al., *miRandola 2017: a curated knowledge base of non-invasive biomarkers.* Nucleic Acids Res, 2018. **46**(D1): p. D354-D359.

330. Janowska-Wieczorek, A., et al., *Microvesicles derived from activated platelets induce metastasis and angiogenesis in lung cancer.* Int J Cancer, 2005. **113**(5): p. 752-60.

331. Jiang, X., et al., *Microfluidic isolation of platelet-covered circulating tumor cells.* Lab Chip, 2017. **17**(20): p. 3498-3503.

332. Schlesinger, M., *Role of platelets and platelet receptors in cancer metastasis.* J Hematol Oncol, 2018. **11**(1): p. 125.

333. Best, M.G., P. Wesseling, and T. Wurdinger, *Tumor-Educated Platelets as a Noninvasive Biomarker Source for Cancer Detection and Progression Monitoring.* Cancer Res, 2018. **78**(13): p. 3407-3412.

334. Best, M.G., et al., *RNA-Seq of Tumor-Educated Platelets Enables Blood-Based Pan-Cancer, Multiclass, and Molecular Pathway Cancer Diagnostics.* Cancer Cell, 2015. **28**(5): p. 666-676.

335. Best, M.G., et al., *Swarm Intelligence-Enhanced Detection of Non-Small-Cell Lung Cancer Using Tumor-Educated Platelets.* Cancer Cell, 2017. **32**(2): p. 238-252 e9.

336. Nilsson, R.J., et al., *Blood platelets contain tumor-derived RNA biomarkers.* Blood, 2011. **118**(13): p. 3680-3.

337. Calverley, D.C., et al., *Significant downregulation of platelet gene expression in metastatic lung cancer.* Clin Transl Sci, 2010. **3**(5): p. 227-32.

338. Tjon-Kon-Fat, L.A., et al., *Platelets harbor prostate cancer biomarkers and the ability to predict therapeutic response to abiraterone in castration resistant patients.* Prostate, 2018. **78**(1): p. 48-53.

339. Xu, L., et al., *The Novel Association of Circulating Tumor Cells and Circulating Megakaryocytes with Prostate Cancer Prognosis.* Clin Cancer Res, 2017. **23**(17): p. 5112-5122.

340. Ritchie, M.E., et al., *limma powers differential expression analyses for RNA-sequencing and microarray studies.* Nucleic Acids Res, 2015. **43**(7): p. e47.

341. Robinson, M.D. and A. Oshlack, *A scaling normalization method for differential expression analysis of RNA-seq data.* Genome Biol, 2010. **11**(3): p. R25.

342. Jiang, G., et al., *Effects of cadmium on proliferation and self-renewal activity of prostate stem/progenitor cells.* Environ Toxicol Pharmacol, 2011. **32**(2): p. 275-84.

343. Liu, X., et al., *ROCK inhibitor and feeder cells induce the conditional reprogramming of epithelial cells.* Am J Pathol, 2012. **180**(2): p. 599-607.

344. Bae, S., J. Brumbaugh, and B. Bonavida, *Exosomes derived from cancerous and non-cancerous cells regulate the anti-tumor response in the tumor microenvironment.* Genes Cancer, 2018. **9**(3-4): p. 87-100.

345. Maia, J., et al., *Exosome-Based Cell-Cell Communication in the Tumor Microenvironment.* Front Cell Dev Biol, 2018. **6**: p. 18.

346. Yuan, T., et al., *Plasma extracellular RNA profiles in healthy and cancer patients.* Sci Rep, 2016. **6**: p. 19413.

347. Ge, Q., et al., *miRNA in plasma exosome is stable under different storage conditions.* Molecules, 2014. **19**(2): p. 1568-75.

348. Liu, C.M., et al., *Exosomes from the tumor microenvironment as reciprocal regulators that enhance prostate cancer progression.* Int J Urol, 2016. **23**(9): p. 734-44.

349. Wahid, F., et al., *MicroRNAs: synthesis, mechanism, function, and recent clinical trials.* Biochim Biophys Acta, 2010. **1803**(11): p. 1231-43.

350. Cheng, L., et al., *Exosomes provide a protective and enriched source of miRNA for biomarker profiling compared to intracellular and cell-free blood.* J Extracell Vesicles, 2014. **3**.

351. Zhang, J., et al., *Exosome and exosomal microRNA: trafficking, sorting, and function.* Genomics Proteomics Bioinformatics, 2015. **13**(1): p. 17-24.

352. Keerthikumar, S., et al., *ExoCarta: A Web-Based Compendium of Exosomal Cargo.* J Mol Biol, 2016. **428**(4): p. 688-692.

353. Kim, D.K., et al., *EVpedia: a community web portal for extracellular vesicles research.* Bioinformatics, 2015. **31**(6): p. 933-9.

354. Li, S., et al., *exoRBase: a database of circRNA, lncRNA and mRNA in human blood exosomes.* Nucleic Acids Res, 2018. **46**(D1): p. D106-D112.

355. Liu, T., et al., *EVmiRNA: a database of miRNA profiling in extracellular vesicles.* Nucleic Acids Res, 2019. **47**(D1): p. D89-D93.

356. Khare, D., et al., *Plasma microRNA profiling: Exploring better biomarkers for lymphoma surveillance.* PLoS One, 2017. **12**(11): p. e0187722.

357. Ebrahimkhani, S., et al., *Deep sequencing of circulating exosomal microRNA allows non-invasive glioblastoma diagnosis.* NPJ Precis Oncol, 2018. **2**: p. 28.

358. Umu, S.U., et al., *A comprehensive profile of circulating RNAs in human serum.* RNA Biol, 2018. **15**(2): p. 242-250.

359. Freedman, J.E., et al., *Diverse human extracellular RNAs are widely detected in human plasma.* Nat Commun, 2016. **7**: p. 11106.

360. Tam, S., M.S. Tsao, and J.D. McPherson, *Optimization of miRNA-seq data preprocessing.* Brief Bioinform, 2015. **16**(6): p. 950-63.

361. Dillies, M.A., et al., *A comprehensive evaluation of normalization methods for Illumina high-throughput RNA sequencing data analysis.* Brief Bioinform, 2013. **14**(6): p. 671-83.

362. Mizokami, A., et al., *Understanding prostate-specific antigen dynamics in monitoring metastatic castration-resistant prostate cancer: implications for clinical practice.* Asian J Androl, 2017. **19**(2): p. 143-148.

363. Xu, G., et al., *Characterization of the small RNA transcriptomes of androgen dependent and independent prostate cancer cell line by deep sequencing.* PLoS One, 2010. **5**(11): p. e15519.

364. Zhu, J., et al., *Screening key microRNAs for castration-resistant prostate cancer based on miRNA/mRNA functional synergistic network.* Oncotarget, 2015. **6**(41): p. 43819-30.

365. Byron, S.A., et al., *Translating RNA sequencing into clinical diagnostics: opportunities and challenges.* Nat Rev Genet, 2016. **17**(5): p. 257-71.

366. Watahiki, A., et al., *Plasma miRNAs as biomarkers to identify patients with castration-resistant metastatic prostate cancer.* Int J Mol Sci, 2013. **14**(4): p. 7757-70.

367. Zhu, Y., et al., *Identification of a serum microRNA expression signature for detection of lung cancer, involving miR-23b, miR-221, miR-148b and miR-423-3p.* Lung Cancer, 2017. **114**: p. 6-11.

368. Watahiki, A., et al., *MicroRNAs associated with metastatic prostate cancer.* PLoS One, 2011. **6**(9): p. e24950.

369. Hsieh, I.S., et al., *MicroRNA-320 suppresses the stem cell-like characteristics of prostate cancer cells by downregulating the Wnt/beta-catenin signaling pathway.* Carcinogenesis, 2013. **34**(3): p. 530-8.

370. Sato, S., et al., *Histone Deacetylase Inhibition in Prostate Cancer Triggers miR-320-Mediated Suppression of the Androgen Receptor.* Cancer Res, 2016. **76**(14): p. 4192-204.

371. Okato, A., et al., *Direct regulation of LAMP1 by tumor-suppressive microRNA-320a in prostate cancer.* Int J Oncol, 2016. **49**(1): p. 111-22.

372. Luo, L., et al., *Decreased miR-320 expression is associated with breast cancer progression, cell migration, and invasiveness via targeting Aquaporin 1.* Acta Biochim Biophys Sin (Shanghai), 2018. **50**(5): p. 473-480.

373. Wang, H., et al., *miR-320b suppresses cell proliferation by targeting c-Myc in human colorectal cancer cells.* BMC Cancer, 2015. **15**: p. 748.

374. Tadano, T., et al., *MicroRNA-320 family is downregulated in colorectal adenoma and affects tumor proliferation by targeting CDK6.* World J Gastrointest Oncol, 2016. **8**(7): p. 532-42.

375. Pan, C., et al., *MiR-320 inhibits the growth of glioma cells through downregulating PBX3.* Biol Res, 2017. **50**(1): p. 31.

376. Lieb, V., et al., *Serum levels of miR-320 family members are associated with clinical parameters and diagnosis in prostate cancer patients.* Oncotarget, 2018. **9**(12): p. 10402-10416.

377. Yang, Z., et al., *Silencing of miR-193a-5p increases the chemosensitivity of prostate cancer cells to docetaxel.* J Exp Clin Cancer Res, 2017. **36**(1): p. 178.

378. Song, C., et al., *Expression profile analysis of microRNAs in prostate cancer by next-generation sequencing.* Prostate, 2015. **75**(5): p. 500-16.

379. He, H.C., et al., *Global analysis of the differentially expressed miRNAs of prostate cancer in Chinese patients.* BMC Genomics, 2013. **14**: p. 757.

380. Tsai, T.F., et al., *miR-99a-5p acts as tumor suppressor via targeting to mTOR and enhances RAD001-induced apoptosis in human urinary bladder urothelial carcinoma cells.* Onco Targets Ther, 2018. **11**: p. 239-252.

381. Lin, Y., et al., *Biomarker microRNAs for prostate cancer metastasis: screened with a network vulnerability analysis model.* J Transl Med, 2018. **16**(1): p. 134.

382. Wang, X., et al., *miR-148a-3p represses proliferation and EMT by establishing regulatory circuits between ERBB3/AKT2/c-myc and DNMT1 in bladder cancer.* Cell Death Dis, 2016. **7**(12): p. e2503.

383. Wang, W., et al., *miR-148a-3p suppresses epithelial ovarian cancer progression primarily by targeting c-Met.* Oncol Lett, 2018. **15**(5): p. 6131-6136.

384. Xie, Q., et al., *microRNA-148a-3p inhibited the proliferation and epithelial-mesenchymal transition progression of non-small-cell lung cancer via modulating Ras/MAPK/Erk signaling.* J Cell Physiol, 2018.

385. Murata, T., et al., *miR-148a is an androgen-responsive microRNA that promotes LNCaP prostate cell growth by repressing its target CAND1 expression.* Prostate Cancer Prostatic Dis, 2010. **13**(4): p. 356-61.

386. Yu, J., et al., *Aryl hydrocarbon receptor enhances the expression of miR-150-5p to suppress in prostate cancer progression by regulating MAP3K12.* Arch Biochem Biophys, 2018. **654**: p. 47-54.

387. Okato, A., et al., *Dual strands of pre-miR150 (miR1505p and miR1503p) act as antitumor miRNAs targeting SPOCK1 in naive and castration-resistant prostate cancer.* Int J Oncol, 2017. **51**(1): p. 245-256.

388. Lu, W., et al., *Long non-coding RNA linc00673 regulated non-small cell lung cancer proliferation, migration, invasion and epithelial mesenchymal transition by sponging miR-150-5p.* Mol Cancer, 2017. **16**(1): p. 118.

389. Dybos, S.A., et al., *Increased levels of serum miR-148a-3p are associated with prostate cancer.* APMIS, 2018. **126**(9): p. 722-731.

390. Jansson, M.D. and A.H. Lund, *MicroRNA and cancer.* Mol Oncol, 2012. **6**(6): p. 590-610.

391. Hessvik, N.P., K. Sandvig, and A. Llorente, *Exosomal miRNAs as Biomarkers for Prostate Cancer.* Front Genet, 2013. **4**: p. 36.

392. Zhu, J., et al., *Different miRNA expression profiles between human breast cancer tumors and serum.* Front Genet, 2014. **5**: p. 149.

393. Zhang, G., et al., *Decreased expression of microRNA-320a promotes proliferation and invasion of non-small cell lung cancer cells by increasing VDAC1 expression.* Oncotarget, 2016. **7**(31): p. 49470-49480.

394. Wang, J., et al., *MicroRNA-320a is downregulated in non-small cell lung cancer and suppresses tumor cell growth and invasion by directly targeting insulin-like growth factor 1 receptor.* Oncol Lett, 2017. **13**(5): p. 3247-3252.

395. Fortunato, O., et al., *Circulating mir-320a promotes immunosuppressive macrophages M2 phenotype associated with lung cancer risk.* Int J Cancer, 2019. **144**(11): p. 2746-2761.

396. Lee, I.H., et al., *A detailed analysis of next generation sequencing reads of microRNA expression in Barrett's esophagus: absolute versus relative quantification.* BMC Res Notes, 2014. **7**: p. 212.

397. Camarena, L., et al., *Molecular mechanisms of ethanol-induced pathogenesis revealed by RNA-sequencing.* PLoS Pathog, 2010. **6**(4): p. e1000834.

398. Git, A., et al., *Systematic comparison of microarray profiling, real-time PCR, and next-generation sequencing technologies for measuring differential microRNA expression.* RNA, 2010. **16**(5): p. 991-1006.

399. Takayama, K.I., A. Misawa, and S. Inoue, *Significance of microRNAs in Androgen Signaling and Prostate Cancer Progression.* Cancers (Basel), 2017. **9**(8).

400. Kristensen, H., et al., *Novel diagnostic and prognostic classifiers for prostate cancer identified by genome-wide microRNA profiling.* Oncotarget, 2016. **7**(21): p. 30760-71.

401. Kong, P., et al., *The microRNA-423-3p-Bim Axis Promotes Cancer Progression and Activates Oncogenic Autophagy in Gastric Cancer.* Mol Ther, 2017. **25**(4): p. 1027-1037.

402. Guan, G., et al., *microRNA-423-3p promotes tumor progression via modulation of AdipoR2 in laryngeal carcinoma.* Int J Clin Exp Pathol, 2014. **7**(9): p. 5683-91.

403. Xu, J., et al., *MicroRNA-423-3p promotes glioma growth by targeting PANX2.* Oncol Lett, 2018. **16**(1): p. 179-188.

404. Wu, T.T., et al., *Establishing human prostate cancer cell xenografts in bone: induction of osteoblastic reaction by prostate-specific antigen-producing tumors in athymic and SCID/bg mice using LNCaP and lineage-derived metastatic sublines.* Int J Cancer, 1998. **77**(6): p. 887-94.

405. Li, H.T., et al., *MiR-423-3p enhances cell growth through inhibition of p21Cip1/Waf1 in colorectal cancer.* Cell Physiol Biochem, 2015. **37**(3): p. 1044-54.

406. Sun, G., et al., *Molecular predictors of brain metastasis-related microRNAs in lung adenocarcinoma.* PLoS Genet, 2019. **15**(2): p. e1007888.

407. Chen, X., et al., *TDP-43 regulates cancer-associated microRNAs.* Protein Cell, 2018. **9**(10): p. 848-866.

408. Hussain, M., et al., *Enzalutamide in Men with Nonmetastatic, Castration-Resistant Prostate Cancer.* N Engl J Med, 2018. **378**(26): p. 2465-2474.

409. Bhanvadia, R.R., et al., *MEIS1 and MEIS2 Expression and Prostate Cancer Progression: A Role For HOXB13 Binding Partners in Metastatic Disease.* Clin Cancer Res, 2018. **24**(15): p. 3668-3680.

410. Chen, J.L., et al., *Deregulation of a Hox protein regulatory network spanning prostate cancer initiation and progression.* Clin Cancer Res, 2012. **18**(16): p. 4291-302.

411. Cui, L., et al., *MEIS1 functions as a potential AR negative regulator.* Exp Cell Res, 2014. **328**(1): p. 58-68.

412. Lin, J., et al., *MicroRNA-423 promotes cell growth and regulates G(1)/S transition by targeting p21Cip1/Waf1 in hepatocellular carcinoma.* Carcinogenesis, 2011. **32**(11): p. 1641-7.

413. Fizazi, K., et al., *The association of p21((WAF-1/CIP1)) with progression to androgen-independent prostate cancer.* Clin Cancer Res, 2002. **8**(3): p. 775-81.

414. Aaltomaa, S., et al., *Prognostic value and expression of p21(waf1/cip1) protein in prostate cancer.* Prostate, 1999. **39**(1): p. 8-15.

415. Sugibayashi, R., et al., *Up-regulation of p21(WAF1/CIP1) levels leads to growth suppression of prostate cancer cell lines.* Anticancer Res, 2002. **22**(2A): p. 713-9.

416. Roy, S., et al., *Downregulation of both p21/Cip1 and p27/Kip1 produces a more aggressive prostate cancer phenotype.* Cell Cycle, 2008. **7**(12): p. 1828-35.

417. Kawakubo-Yasukochi, T., et al., *miR-200c-3p spreads invasive capacity in human oral squamous cell carcinoma microenvironment.* Mol Carcinog, 2018. **57**(2): p. 295-302.

418. Hsu, Y.L., et al., *Hypoxic Lung-Cancer-Derived Extracellular Vesicle MicroRNA-103a Increases the Oncogenic Effects of Macrophages by Targeting PTEN.* Mol Ther, 2018. **26**(2): p. 568-581.

419. Zhou, C.F., et al., *Cervical squamous cell carcinoma-secreted exosomal miR-221-3p promotes lymphangiogenesis and lymphatic metastasis by targeting VASH1.* Oncogene, 2019. **38**(8): p. 1256-1268.

420. Niranjan, B., et al., *Primary culture and propagation of human prostate epithelial cells.* Methods Mol Biol, 2013. **945**: p. 365-82.

421. Leibiger, C., et al., *First molecular cytogenetic high resolution characterization of the NIH 3T3 cell line by murine multicolor banding.* J Histochem Cytochem, 2013. **61**(4): p. 306-12.

422. Shamir, E.R. and A.J. Ewald, *Three-dimensional organotypic culture: experimental models of mammalian biology and disease.* Nat Rev Mol Cell Biol, 2014. **15**(10): p. 647-64.

423. Edmondson, R., et al., *Three-dimensional cell culture systems and their applications in drug discovery and cell-based biosensors.* Assay Drug Dev Technol, 2014. **12**(4): p. 207-18.

424. Hockel, M. and P. Vaupel, *Tumor hypoxia: definitions and current clinical, biologic, and molecular aspects.* J Natl Cancer Inst, 2001. **93**(4): p. 266-76.

425. Heldin, C.H., et al., *High interstitial fluid pressure - an obstacle in cancer therapy.* Nat Rev Cancer, 2004. **4**(10): p. 806-13.

426. Nathan, S.S., et al., *Elevated physiologic tumor pressure promotes proliferation and chemosensitivity in human osteosarcoma.* Clin Cancer Res, 2005. **11**(6): p. 2389-97.

427. Walsh, M.F., et al., *Extracellular pressure stimulates colon cancer cell proliferation via a mechanism requiring PKC and tyrosine kinase signals.* Cell Prolif, 2004. **37**(6): p. 427-41.

428. Muller, V., et al., *Circulating tumor cells in breast cancer: correlation to bone marrow micrometastases, heterogeneous response to systemic*

therapy and low proliferative activity. Clin Cancer Res, 2005. **11**(10): p. 3678-85.

429. Hwang, E., et al., *Cancer gene panel analysis of cultured circulating tumor cells and primary tumor tissue from patients with breast cancer.* Oncol Lett, 2017. **13**(6): p. 4627-4632.

430. Most, J., et al., *Formation of multinucleated giant cells in vitro is dependent on the stage of monocyte to macrophage maturation.* Blood, 1997. **89**(2): p. 662-71.

431. Powell, A.E., et al., *Fusion between Intestinal epithelial cells and macrophages in a cancer context results in nuclear reprogramming.* Cancer Res, 2011. **71**(4): p. 1497-505.

432. Clawson, G.A., et al., *Macrophage-tumor cell fusions from peripheral blood of melanoma patients.* PLoS One, 2015. **10**(8): p. e0134320.

433. Gast, C.E., et al., *Cell fusion potentiates tumor heterogeneity and reveals circulating hybrid cells that correlate with stage and survival.* Sci Adv, 2018. **4**(9): p. eaat7828.

434. Llames, S., et al., *Feeder Layer Cell Actions and Applications.* Tissue Eng Part B Rev, 2015. **21**(4): p. 345-53.

435. Searles, S.C., E.K. Santosa, and J.D. Bui, *Cell-cell fusion as a mechanism of DNA exchange in cancer.* Oncotarget, 2018. **9**(5): p. 6156-6173.

436. Wang, R., et al., *Spontaneous cancer-stromal cell fusion as a mechanism of prostate cancer androgen-independent progression.* PLoS One, 2012. **7**(8): p. e42653.

437. Siegel, R.L., K.D. Miller, and A. Jemal, *Cancer statistics, 2019.* CA Cancer J Clin, 2019. **69**(1): p. 7-34.

438. Hussain, M., et al., *Absolute prostate-specific antigen value after androgen deprivation is a strong independent predictor of survival in new metastatic prostate cancer: data from Southwest Oncology Group Trial 9346 (INT-0162).* J Clin Oncol, 2006. **24**(24): p. 3984-90.

439. Choueiri, T.K., et al., *Time to prostate-specific antigen nadir independently predicts overall survival in patients who have metastatic hormone-sensitive prostate cancer treated with androgen-deprivation therapy.* Cancer, 2009. **115**(5): p. 981-7.

440. Caram, M.E., T.A. Skolarus, and K.A. Cooney, *Limitations of Prostate-specific Antigen Testing After a Prostate Cancer Diagnosis.* Eur Urol, 2016. **70**(2): p. 209-10.

441. Yamamoto, S., et al., *M1 prostate cancer with a serum level of prostate-specific antigen less than 10 ng/mL.* Int J Urol, 2001. **8**(7): p. 374-9.

442. Sella, A., et al., *Low PSA metastatic androgen- independent prostate cancer.* Eur Urol, 2000. **38**(3): p. 250-4.

443. Lee, D.K., et al., *Progression of prostate cancer despite an extremely low serum level of prostate-specific antigen.* Korean J Urol, 2010. **51**(5): p. 358-61.

444. Leibovici, D., et al., *Prostate cancer progression in the presence of undetectable or low serum prostate-specific antigen level.* Cancer, 2007. **109**(2): p. 198-204.

445. Rahman, M.A., et al., *Lung cancer exosomes as drivers of epithelial mesenchymal transition.* Oncotarget, 2016. **7**(34): p. 54852-54866.

446. Franzen, C.A., et al., *Urothelial cells undergo epithelial-to-mesenchymal transition after exposure to muscle invasive bladder cancer exosomes.* Oncogenesis, 2015. **4**: p. e163.

447. Tang, W., et al., *MicroRNA-150 suppresses triple-negative breast cancer metastasis through targeting HMGA2.* Onco Targets Ther, 2018. **11**: p. 2319-2332.

448. Antonarakis, E.S., et al., *AR-V7 and resistance to enzalutamide and abiraterone in prostate cancer.* N Engl J Med, 2014. **371**(11): p. 1028-38.

449. Scher, H.I., et al., *Association of AR-V7 on Circulating Tumor Cells as a Treatment-Specific Biomarker With Outcomes and Survival in Castration-Resistant Prostate Cancer.* JAMA Oncol, 2016. **2**(11): p. 1441-1449.

450. Park, S., et al., *Morphological differences between circulating tumor cells from prostate cancer patients and cultured prostate cancer cells.* PLoS One, 2014. **9**(1): p. e85264.

451. Kallergi, G., et al., *Apoptotic circulating tumor cells in early and metastatic breast cancer patients.* Mol Cancer Ther, 2013. **12**(9): p. 1886-95.

452. Hiltermann, T.J., et al., *Circulating tumor cells in small-cell lung cancer: a predictive and prognostic factor.* Ann Oncol, 2012. **23**(11): p. 2937-42.

453. Seashols-Williams, S.J., et al., *miR-9 Acts as an OncomiR in Prostate Cancer through Multiple Pathways That Drive Tumour Progression and Metastasis.* PLoS One, 2016. **11**(7): p. e0159601.

Appendix 1. Clinical characteristics of patients for exosome study.

ID	Grouping	RNA-seq	RT-qPCR	Fluidigm	Age(year)	Gleason Score	PSA at collection(ng/ml)	Metastasis
BCI001	treatment-naive		√		74.8	3+3, 1/12	10	None
BCI002	treatment-naive		√		57.8	4+4, 13/13	22	None
BCI003	treatment-naive		√		56.0	4+3, 12/13	15	None
BCI004	treatment-naive		√		58.1	3+3, 3/13	5	None
BCI005	treatment-naive		√		57.7	3+3, 2/14	5	None
BCI006	treatment-naive		√		58.1	3+3, 1/27	1	None
BCI007	treatment-naive		√		67.2	3+4, 5/15	12	None
BCI008	treatment-naive		√		63.0	3+3, 4/13	5	None
BCI009	treatment-naive		√		62.3	4+5, 12/12	26	None
BCI010	treatment-naive	√	√		65.8	3+3, 1/12	6	None
BCI011	treatment-naive		√		56.0	3+3, 1/59	45	None
BCI012	treatment-naive	√	√		69.3	3+3, 1/45	7.5	None
BCI013	treatment-naive	√	√		34.1	3+3, 4/14	4	None
BCI014	treatment-naive	√	√		74.8	4+3, 5/17	8	None
BCI015	treatment-naive		√		77.2	4+3, 6/12	9.12	None

BCI016	treatment-naive		√		76.3	4+3, 11/12	10	None
BCI017	treatment-naive		√		69.5	3+4, 7/12	3.2	None
BCI018	treatment-naive	√	√		71.2	3+4, 5/12	9.49	None
BCI019	treatment-naive	√	√		50.0	3+3, 3/12	5.42	None
BCI020	treatment-naive	√	√		72.8	4+3, 7/13	6.8	None
BCI021	treatment-naive	√	√		72.2	3+4, 3/16	13	None
BCI022	treatment-naive	√	√		54.6	4+3, 2/14	5.32	None
BCI023	treatment-naive	√	√		66.9	4+3, 3/13	20	None
BCI024	treatment-naive		√		69.1	3+4, 8/12	7.8	None
BCI025	treatment-naive	√	√		56.2	3+4, 6/12	9.8	None
BCI026	treatment-naive	√	√		59.8	4+3, 7/13	11	None
BCI027	treatment-naive	√	√		73.5	3+4, 8/20	7.9	None
BCI028	treatment-naive		√		65.3	3+4, 3/50	7.81	None
BCI029	treatment-naive	√	√		66.5	3+3, 1/19	12	None
BCI030	treatment-naive	√	√		51.7	3+4, 7/12	16	None
BCI031	treatment-naive	√	√		64.5	4+3, 6/12	18	None
BCI032	treatment-naive	√	√		55.7	3+4, 9/12	7.2	None
BCI033	treatment-naive	√	√		60.5	3+3,1/15	10	None

BCI034	treatment-naive	√	√		56.9	4+3, 7/12	19	None
BCI035	treatment-naive		√		68.6	4+3,10/16	23	None
BCI036	treatment-naive	√	√		58.6	3+4, 7/16	12	None
BCI037	treatment-naive	√	√		66.3	3+3, 4/17	12	None
BCI038	treatment-naive		√		51.3	3+4, 2/14	9.66	None
BCI039	treatment-naive		√		67.8	3+3, 3/15	11	None
BCI040	treatment-naive		√		64.5	3+4, 4/12	7.19	None
BCI041	treatment-naive		√		55.4	3+3, 5/14	5.5	None
BCI042	treatment-naive		√		79.8	3+4, 2/13	13	None
BCI043	treatment-naive		√		57.7	3+4, 4/12	5.13	None
BCI044	treatment-naive		√		71.2	4+3, 8/19	6.4	None
BCI045	treatment-naive		√		68.2	4+4, 7/14	9	None
BCI046	treatment-naive		√		66.3	3+3, 1/33	6.46	None
BCI047	treatment-naive		√		54.3	3+3, 2/12	6.9	None
BCI048	treatment-naive		√		76.5	3+4, 4/14	12	None
BCI049	treatment-naive		√		73.2	3+3, 4/11	9.92	None
BCI050	treatment-naive		√		64.8	4+5, 6/6	310	T3bN1M0
BCI051	treatment-naive		√		83.5	4+4, 5/14	21	None

BCI052	treatment-naive		√		81.1	4+5, 12/14	23	None
BCI053	treatment-naive		√		78.6	3+3, 1/22	18	None
BCI054	treatment-naive	√	√		56.1	3+3, 3/12	6.27	None
BCI055	treatment-naive	√	√		72.5	3+4,13/15	83	None
BCI056	treatment-naive		√		68.2	3+4, 1/36	5.9	None
BCI057	treatment-naive	√	√		68.2	3+4, 3/16	12	None
BCI058	treatment-naive		√		63.0	3+4, 8/12	9.28	None
BCI059	treatment-naive		√		67.3	5+5, all cores	26	regional LYM
BCI060	treatment-naive		√		69.4	3+4, 11/13	17	None
BCI061	treatment-naive		√		66.2	3+4, 15/23	18	None
BCI062	treatment-naive		√		62.8	3+3, 3/14	12	None
BCI063	treatment-naive		√		78.8	4+5, 3/45	17.6	None
BCI064	treatment-naive		√		78.1	3+4, 4/12	9.69	None
BCI065	treatment-naive		√		66.9	4+4, 2/12	7.5	None
BCI066	treatment-naive		√		55.8	3+4, 8/52	13	None
BCI067	treatment-naive		√		71.8	3+3, 13/29	17	None
BCI068	treatment-naive		√		65.6	3+4, 6/12	5.6	None
BCI069	treatment-naive		√		58.3	3+4, 3/11	4.57	None

BCI070	treatment-naive		√		72.3	3+4, 5/18	5.54	None
BCI071	treatment-naive		√		53.8	3+4, 8/12	8.29	None
BCI072	treatment-naive		√		53.3	4+3	7.7	None
BCI073	treatment-naive		√		76.0	4+4, 8/17	7.21	None
BCI074	treatment-naive		√		58.6	3+4, 1/12	4.3	None
BCI075	treatment-naive		√		74.6	3+4, 2/16	10	None
BCI076	treatment-naive		√		61.8	3+3, 9/74	5	None
BCI077	treatment-naive		√		70.0	3+4, 3/24	8.33	None
BCI078	treatment-naive		√		62.8	4+3, 1/17	11	None
BCI079	treatment-naive		√		50.9	3+3, 8/12	6.5	None
BCI080	treatment-naive		√		48.8	3+3, 2/12	4.2	None
BCI081	treatment-naive		√		43.0	3+3, 3/15	2.4	None
BCI082	treatment-naive		√		58.6	3+4, 4/13	5.7	None
BCI083	treatment-naive		√		72.9	4+4, 6/11	13	T2N0M1, bone
BCI084	treatment-naive		√		59.2	3+3, 1/53	4.34	None
BCI085	treatment-naive		√		66.0	3+4, 1/13	5.27	None
BCI086	treatment-naive		√		58.5	3+4, 8/14	4.8	None
BCI087	treatment-naive		√		76.0	4+3, 7/14	19.71	None

BCI088	treatment-naive		√		64.5	4+3,18/26	6	None
BCI089	treatment-naive		√		69.3	3+4, 4/43	6.56	None
BCI090	treatment-naive		√		76.2	3+4, 8/12	5.41	None
BCI091	treatment-naive		√		65.3	3+3, 5/12	5.09	None
BCI092	treatment-naive		√		60.3	3+3, 7/12	7.96	None
BCI093	treatment-naive		√		79.9	4+3, 14/14	13	None
BCI094	treatment-naive		√		68.2	3+4, 7/15	15.9	None
BCI095	treatment-naive		√		63.8	4+3, 11/15	26.8	None
BCI096	CRPC			√	60.1	4+5	399	LYM
BCI097	treatment-naive		√		71.0	3+3, 2/12	8.73	None
BCI098	treatment-naive		√		58.8	3+3, 4/18	4.3	None
BCI099	treatment-naive		√		43.6	3+3, 1/13	3.3	None
BCI100	treatment-naive		√		69.4	4+5	21.1	None
BCI101	treatment-naive		√		51.3	3+3, 7/17	7.87	None
BCI102	treatment-naive		√		74.4	3+4, 8/14	11	None
BCI103	treatment-naive		√		48.8	4+3, 2/13	8.8	None
BCI104	treatment-naive		√		55.4	3+3, 7/11	20	None
BCI105	treatment-naive		√		57.3	3+3, 2/12	4.81	None

BCI106	treatment-naive		√		66.1	3+4, 5/13	6.5	None
BCI107	treatment-naive		√		76.8	right 5+4, 6/6; left 4+5, 3/3	131	bone
BCI108	treatment-naive		√		73.0	4+5,7/7	4.52	T4N1M1
BCI109	CRPC	√	√		72.8	5+4	255	LYM, multiple bone
BCI110	CRPC			√	65.8	3+4	204	multiple bone
BCI111	CRPC			√	79.5	3+5	250	LYM, multiple bone
BCI112	CRPC	√	√		68.7	4+4	66	bone
BCI113	CRPC		√		70.2	4+5	1574	LYM, multiple bone
BCI114	CRPC			√	81.2	3+3	2781	multiple bone
BCI115	CRPC	√	√	√	81.6		525	LYM, multiple bone
BCI116	CRPC		√	√	70.9	3+4	609	from lymphadenopathy
BCI117	CRPC	√	√		80.7	4+4	52	None
BCI118	CRPC	√	√	√	81.8		2	multiple bone
BCI119	CRPC	√	√	√	60.2	5+5	39	LYM, multiple bone
BCI120	CRPC			√	74.0	NEC	53	bladder, LYM
BCI121	CRPC	√	√	√	68.9	5+4	900	multiple bone

BCI122	CRPC			√	79.9	4+5	260	Liver, LYM, multiple bone
BCI123	CRPC			√	80.4	3+4	12	single bone
BCI124	CRPC	√	√	√	83.9		119	LYM
BCI125	CRPC	√	√	√	63.5	4+3	16	LYM
BCI126	CRPC	√	√	√	83.9	3+3	1	LYM, multiple bone
BCI127	CRPC	√	√	√	76.2	4+4	2	multiple bone
BCI128	CRPC	√	√	√	87.8	4+3	1027	multiple bone
BCI129	CRPC		√		66.7	5+5	4	LYM
BCI130	CRPC	√	√	√	67.4		43	multiple bone
BCI131	CRPC	√	√	√	81.4		77	multiple bone
BCI132	CRPC	√	√	√	86.5	5+3	29	LYM, multiple bone
BCI133	CRPC	√	√	√	62.5	5+5	9	multiple bone
BCI134	CRPC	√	√	√	60.1	4+4	202	multiple bone
BCI135	CRPC		√		54.3	4+5	176	bone and lymph nodes
BCI136	CRPC		√		61.4	9	168.2	T2bN1M1
BCI137	CRPC			√	69.4	4+4	60	multiple bone
BCI138	CRPC		√		70.2	4+4	123	M1b

BCI139	CRPC			√	77.0	4+4	11	multiple bone
BCI140	CRPC	√	√	√	74.4		550	multiple bone, LYM
BCI141	CRPC		√		76.4	4+3	56	M1b
BCI142	CRPC		√		54.8	4+5	52	M1b
BCI143	CRPC		√		71.2	3+4	58	N1
BCI144	CRPC	√	√	√	74.2	4+5	23	multiple bone, lung, regional LYM
BCI145	CRPC		√		84.0	3+5	18	M1b
BCI146	CRPC		√		71.3	4+5	58	T3bN1M1
BCI147	CRPC		√		71.9		22	M1b
BCI148	CRPC		√		73.8		514	N/A
BCI149	CRPC		√		59.8	4+4	24	N/A
BCI150	CRPC	√	√	√	72.5	5+5	50	multiple bone, LYM
BCI151	treated non-CRPC		√		72.4	4+5	9	multiple bone, LYM
BCI152	treated non-CRPC		√		69.0	3+4	16	None

BCI153	treated non-CRPC		√		79.3	4+5	11	single bone
BCI154	treated non-CRPC		√		59.9		5	multiple bone
BCI155	treated non-CRPC		√		60.9	4+4	153	multiple bone, lung
BCI156	treated non-CRPC		√		62.2	4+5	60	multiple bone, LYM
BCI157	treated non-CRPC		√		60.0	Adenocarcinoma from LYM	204	multiple bone, LYM
BCI158	treated non-CRPC		√		80.0	4+3, 12/12	5.34	T2N0M1, isolated pelvic bone (questioned)
BCI159	treated non-CRPC		√		80.6		152	multiple bone, LYM
BCI160	treated non-CRPC		√		63.7	4+3	9.4	multiple bone
BCI161	treated non-CRPC		√		57.4	5+4, 5/15	55	None

BCI162	treated non-CRPC		√		63.9	5+5	15	multiple bone
BCI163	treated non-CRPC		√		65.9	3+4	367	None
BCI164	treated non-CRPC		√		78.9	5+5	6.09	N1
BCI165	treated non-CRPC		√		66.1	4+3,4/11	13.4	None
BCI166	treated non-CRPC		√		70.1	5+4,3/4	343	multiple bone
BCI167	treated non-CRPC		√		74.0	5+4, 12/12	22	None
BCI168	treated non-CRPC		√		53.8	4+5	138	N/A
BCI169	treated non-CRPC		√		77.0	4+4, 6/8	51	T3bN1M1
BCI170	treated non-CRPC		√		74.5	3+3	7.8	None

BCI171	treated non-CRPC		√		68.3	4+3, 6/6	126.6	None
BCI172	treated non-CRPC		√		65.6	4+3, 13/15	2.69	T3a/T3bN1M1a
BCI173	treated non-CRPC		√		76.6		1913	T3bN1M1c, lung
BCI174	treated non-CRPC		√		63.0	4+5	9	T4N2M1
BCI175	treated non-CRPC		√		61.3	4+5,14/14	57.39	bone
BCI176	treated non-CRPC		√		57.0	4+5	90.61	T3bN1M1
BCI177	treated non-CRPC		√		65.9	4+4	31.4	T3aN1M1, bone
BCI178	treated non-CRPC		√		64.7	4+5	0.74	M1b
BCI179	treated non-CRPC		√		69.3	3+4	10.46	LYM, bone

BCI180	treated non-CRPC		√		53.1	4+3	6.75	T3N1M1b
BCI181	treated non-CRPC		√		63.3	4+4	5.7	M1b
BCI182	treated non-CRPC		√		71.4		3.4	M1b
BCI183	treated non-CRPC		√		67.0	4+4,19/19	2.79	N1M1b
BCI184	treated non-CRPC		√		73.1	4+3,7/10	3.46 (10/01/18)	M1b
BCI185	treated non-CRPC		√		83.8	4+3	30	None
BCI186	treated non-CRPC		√		57.7	4+5	120	T3bM1b
BCI187	CRPC	√	√	√	81.9	4+5	4	N/A
BCI188	CRPC			√	70.9	4+5	49	multiple bone, T4N2M1
BCI189	CRPC	√	√	√	84.2	4+5	189	lung, liver
BCI190	CRPC	√	√	√	77.2		346	N/A
BCI191	treatment-naive			√	61.8	4+5, 9/22	11	None

BCI192	treatment-naive			√	75.8	3+4, 4/35	12	None
BCI193	treatment-naive			√	68.9	3+3, 1/13	15	None
BCI194	treatment-naive			√	71.7	3+4, 6/14	7.05	None
BCI195	treatment-naive			√	53.5	3+3, 5/12	4.86	None
BCI196	treatment-naive			√	80.8	3+3, 1/13	8.4	None
BCI197	treatment-naive			√	63.9	4+5, 12/12	23	N1
BCI198	treatment-naive			√	68.7	4+5, 12/12	40	N1
BCI199	treatment-naive			√	66.9	3+3,1/15	6.7	None
BCI200	treatment-naive		√	√	73.8	3+4, 5/15	19.1	None
BCI201	treatment-naive			√	57.1	3+3, 1/16	8.03	None
BCI202	treatment-naive			√	57.8	4+3,12/12	12	N1
BCI203	treatment-naive			√	60.1	4+3, 8/12	5.93	None
BCI204	treatment-naive			√	58.3	4+3	29	None
BCI205	treatment-naive			√	69.6	3+4, 8/15	6.15	None
BCI206	treatment-naive			√	61.2	3+4, 8/15	18	None
BCI207	treatment-naive			√	66.5	3+4, 10/13	7.34	None
BCI208	treatment-naive			√	71.2	4+3	2	None
BCI209	treatment-naive			√	57.0	3+3	4.84	None

BCI210	treatment-naive			√	83.3		52.4	None
BCI211	treatment-naive			√	68.8	3+3, 7/30	NA	None
BCI212	treatment-naive			√	65.2	3+4, 7/20	7.5	None
BCI213	treatment-naive			√	66.5	3+4, 5/14	7.33	None
BCI214	treatment-naive			√	49.2	3+3, 6/13	3.15	None
BCI215	treatment-naive			√	61.1	5+4, all cores	127	N1
BCI216	treatment-naive			√	69.1	3+4, 2/13	11	None
BCI217	treatment-naive			√	82.3	3+3, 2/14	1.37	None
BCI218	treatment-naive			√	56.5	3+3	7.64	None
BCI219	treatment-naive			√	52.1	3+3, 3/14		None
BCI220	treatment-naive			√	59.6	3+3, 1/16	6.73	None
BCI221	treatment-naive			√	68.4	4+4, 11/22	8.2	None
BCI222	treatment-naive			√	61.2	3+3, 3/28	5.38	None
BCI223	treatment-naive			√	75.8	3+3, 3/17	9.2	None
BCI224	treatment-naive			√	67.0	3+4, 5/12	6.4	None
BCI225	treatment-naive			√	58.2	3+3, 3/41	11.9	None
BCI226	treatment-naive			√	70.0	4+4, 1/12	8.7	None
BCI227	treatment-naive			√	55.7	3+4, 5/37	5.09	None

BCI228	treatment-naive			√	55.3	3+3	9.77	None
BCI229	treatment-naive			√	65.7	3+3, 6/28	6	None
BCI230	treatment-naive			√	54.3	3+3, 1/12	6.5	None
BCI231	treatment-naive			√	74.1	3+4, 3/17	17	None
BCI232	treatment-naive			√	73.7	3+3, 2/14	9.06	None
BCI233	treatment-naive			√	51.9	3+3, 1/14	6.6	None
BCI234	treatment-naive			√	77.2	3+3, 6/14	7.5	None
BCI235	treatment-naive			√	60.9	3+3	0.45	None
BCI236	treatment-naive			√	61.2	3+3, 1/13	5.14	None
BCI237	treatment-naive			√	61.0	3+3, 2/13	5.1	None
BCI238	treatment-naive			√	68.7	3+3, 2/15	11	None
BCI239	treatment-naive			√	69.8	3+4, 2/13	24.4	None
BCI240	treatment-naive			√	60.8	3+3, 2/14	3.68	None
BCI241	treatment-naive			√	66.8	3+3, 8/13	5.14	None
BCI242	treatment-naive			√	61.3	4+5	4.99	None
BCI243	CRPC			√	78.5	4+4	387	bone
BCI244	CRPC			√	78.8	4+5	17	bone
BCI245	CRPC			√	49.5	4+4, 7/14	307	bone

BCI246	CRPC			√	60.8	5+4	392.8	bone
BCI247	CRPC		√	√	74.6	4+5	65	N/A
BCI248	CRPC		√	√	69.5		20	M1b
BCI249	CRPC		√	√	73.9	3+4	134	N1M1b
BCI250	CRPC	√	√	√	74.9	4+5	29	None
BCI251	CRPC		√	√	69.1	4+3	14	N/A
BCI252	CRPC			√	72.0	4+3	21	None
BCI253	CRPC			√	83.0		324	bone

CRPC: castration-resistant prostate cancer; NEC: neuroendocrine carcinoma; LYM: lymph nodes metastasis.

Appendix 2. Read counts of plasma exosomal miRNAs in all samples.

	CRPC																							
ID	BCI 109	BCI 115	BCI 112	BCI 118	BCI 121	BCI 117	BCI 124	BCI 125	BCI 126	BCI 128	BCI 130	BCI 131	BCI 132	BCI 133	BCI 134	BCI 140	BCI 144	BCI 190	BCI 119	BCI 127	BCI 250	BCI 150	BCI 187	BCI 189
let-7a-3p	0	0	1	0	0	5	0	0	0	1	6	0	0	2	0	1	0	4	2	1	0	0	0	0
let-7a-5p	201	134	253	266	1283	658	144	164	170	879	1746	586	171	764	205	1545	418	684	49	289	517	490	124	783
let-7b-3p	2	0	0	2	8	3	2	0	5	8	11	1	1	4	0	21	0	2	2	3	0	0	0	3
let-7b-5p	240	149	802	369	813	846	256	372	359	465	12318	511	255	387	343	927	363	1419	271	479	870	451	245	618
let-7c-3p	0	0	0	0	0	0	0	0	0	0	0	0	0	0	0	1	0	0	0	0	0	0	0	0
let-7c-5p	23	18	27	23	77	47	24	16	16	57	161	55	19	53	7	86	37	58	8	28	59	44	15	65
let-7d-3p	14	12	20	13	57	85	4	13	15	42	284	14	13	26	29	191	17	136	17	28	28	22	10	47

let-7d-5p	20	4	13	7	66	53	7	4	10	29	186	18	7	75	14	107	16	33	0	14	13	35	10	61
let-7e-3p	0	0	0	0	0	0	0	0	0	0	0	0	0	0	0	0	0	0	0	0	0	0	0	0
let-7e-5p	14	8	9	13	64	39	3	5	20	19	15	9	5	24	7	43	7	15	1	10	24	40	5	31
let-7f-1-3p	0	0	0	0	0	2	0	0	0	0	2	1	0	0	0	0	0	0	0	0	0	0	0	0
let-7f-5p	77	52	128	73	407	372	65	59	65	323	858	199	78	377	87	745	160	261	26	119	189	186	37	355
let-7g-5p	36	12	69	38	130	158	23	32	30	75	842	72	30	127	47	267	82	180	5	28	69	54	19	114
let-7i-3p	0	0	0	0	0	0	0	0	0	0	0	0	0	0	0	0	1	0	0	1	0	0	0	0
let-7i-5p	134	97	289	140	409	1148	128	108	140	281	6298	273	198	395	172	1188	221	694	81	323	407	396	108	492
miR-1	0	1	0	1	2	0	1	0	0	6	8	3	3	11	1	6	2	0	0	1	0	7	0	2
miR-100-5p	1	5	0	1	4	4	25	2	1	89	22	7	3	25	0	27	1	6	0	35	24	6	2	4

miR-101-3p	6	8	18	7	12	19	6	5	10	13	171	5	16	10	17	16	4	68	0	4	22	2	3	15
miR-103a-3p	4	2	5	1	15	11	3	2	0	10	64	5	0	18	4	30	7	16	2	4	1	6	3	14
miR-105-5p	0	0	0	0	0	0	0	0	0	0	0	0	0	0	0	1	0	0	0	0	0	0	0	0
miR-106a-5p	0	0	0	0	0	0	0	0	0	0	0	2	0	0	0	2	0	0	0	0	0	0	0	1
miR-106b-3p	2	3	4	3	13	19	0	3	1	9	79	9	6	6	6	31	3	22	2	8	6	5	3	6
miR-106b-5p	1	0	3	0	0	0	0	0	0	0	18	1	0	3	0	1	0	4	0	1	0	0	0	1
miR-107	1	0	1	2	6	2	0	0	1	0	18	0	0	1	1	4	3	6	0	3	1	0	0	1
miR-10a-3p	0	0	0	0	1	0	0	0	0	0	2	0	0	0	0	0	0	1	0	0	0	0	0	1
miR-10a-5p	12	19	24	20	81	40	14	13	30	36	87	38	24	26	9	82	23	77	7	18	51	16	9	70

miR-10b-3p	0	0	0	0	2	0	0	0	1	1	1	0	0	0	0	1	0	0	0	0	0	0	0	0
miR-10b-5p	30	24	20	38	134	52	14	25	52	61	157	72	34	59	20	127	36	155	24	62	17	24	16	75
miR-1180-3p	1	3	6	0	12	5	0	1	4	4	42	9	0	7	1	5	2	11	1	1	1	2	1	3
miR-1183	0	0	0	0	1	1	0	0	0	0	0	0	0	0	1	0	1	0	0	0	0	1	0	1
miR-1185-1-3p	0	0	0	0	0	0	0	0	0	0	0	0	0	0	0	2	0	0	0	0	0	0	0	0
miR-1193	0	0	0	0	0	1	0	0	0	0	0	0	0	0	0	0	0	0	0	0	0	0	0	0
miR-1224-5p	0	0	1	0	0	0	0	0	0	0	0	0	0	0	0	0	0	1	0	0	0	0	0	0
miR-1225-5p	0	0	0	0	0	0	0	0	0	0	0	0	0	0	0	0	0	0	0	0	0	0	0	0
miR-122-5p	145	34	163	911	385	145	125	39	284	152	3139	6283	119	112	34	18730	101	782	141	396	128	77	10	96

miR-1226-3p	0	0	0	0	0	1	0	0	0	0	0	0	0	0	0	3	0	0	0	0	0	0	0	0
miR-1228-5p	1	0	0	1	0	0	2	0	0	0	3	1	0	1	1	0	0	0	0	0	0	1	0	1
miR-1229-3p	0	0	0	0	0	0	0	0	0	0	1	0	0	0	0	1	0	0	0	0	0	0	0	1
miR-124-3p	0	0	0	0	0	0	0	0	0	0	0	0	0	0	0	0	0	0	0	0	0	0	0	0
miR-1246	2	2	0	0	11	1	1	0	1	6	0	0	0	5	0	4	0	0	0	0	0	2	0	3
miR-1248	0	4	1	0	0	0	0	0	0	0	0	0	0	0	0	0	1	1	0	0	0	0	0	0
miR-1249	0	0	0	0	0	0	0	0	0	0	0	0	0	1	0	0	0	0	0	0	0	0	0	0
miR-1254	0	0	0	0	0	0	0	0	0	0	0	0	0	0	0	0	0	0	0	0	0	0	0	0
miR-1255a	0	0	0	0	0	0	0	0	0	0	0	0	0	0	0	0	0	0	0	1	0	0	0	0

miR-1255b-5p	0	0	0	0	0	0	0	0	0	0	1	0	0	0	0	0	0	0	0	0	0	0	0	0
miR-125a-3p	1	0	0	0	1	1	0	1	0	3	2	0	0	0	0	2	1	2	0	1	1	3	1	0
miR-125a-5p	10	8	2	13	79	15	6	10	9	22	41	21	3	28	2	59	14	40	2	6	9	26	1	28
miR-125b-1-3p	0	0	0	0	0	0	0	0	0	0	0	0	0	0	0	1	0	0	0	0	0	0	0	0
miR-125b-2-3p	0	0	0	0	1	0	0	0	0	0	0	0	0	0	0	0	0	1	0	0	0	0	0	0
miR-125b-5p	2	1	1	1	21	2	0	1	0	7	14	10	0	2	0	29	0	11	2	0	1	3	2	1
miR-1261	0	0	0	0	0	0	0	0	0	0	0	0	0	0	0	0	0	0	0	0	0	0	0	0
miR-126-3p	377	203	379	519	2570	1532	345	228	602	502	2265	911	412	891	253	1861	720	1657	255	1074	280	840	212	1556

miR-126-5p	3	2	3	1	15	9	1	1	1	2	12	3	2	11	1	2	2	11	0	3	0	6	0	3
miR-1270	0	0	0	0	0	0	0	0	0	0	0	0	0	0	0	0	0	0	0	0	0	0	0	0
miR-1271-5p	0	0	0	0	1	0	0	0	1	0	1	0	0	0	0	2	0	0	0	0	0	0	0	0
miR-1273h-3p	0	0	0	0	0	1	0	0	0	0	0	0	0	0	0	0	0	0	0	0	0	0	0	0
miR-127-3p	0	0	0	0	0	0	0	1	0	0	1	0	0	0	0	0	0	0	1	0	0	0	1	0
miR-1277-5p	0	0	0	0	0	0	0	0	0	0	0	0	0	0	0	0	0	0	0	0	0	0	0	0
miR-1278	0	0	0	0	0	0	0	0	0	0	0	0	0	0	0	0	0	0	0	0	0	0	0	0
miR-128-3p	9	6	15	14	41	96	7	12	7	15	189	19	10	40	15	137	12	127	9	21	16	20	2	54
miR-1284	0	0	0	0	2	0	0	0	0	0	1	0	0	0	0	1	0	0	0	1	0	0	0	0

miR-1287-5p	0	0	0	0	0	1	0	0	0	0	0	0	0	0	0	0	0	0	0	0	0	0	0	0
miR-1288-3p	0	0	0	0	0	1	0	0	0	1	0	0	0	0	0	0	0	0	0	0	0	0	0	0
miR-1292-5p	0	0	0	0	0	2	0	0	0	0	1	1	0	0	0	1	1	2	0	0	0	0	0	0
miR-1293	0	0	0	0	0	0	0	0	0	0	0	0	0	0	0	0	0	0	0	0	0	0	0	0
miR-1294	0	0	0	0	1	0	0	0	0	0	0	0	0	0	1	1	0	0	0	0	1	0	0	0
miR-1295a	0	0	0	0	0	0	0	0	0	0	0	0	0	0	0	0	0	0	0	0	0	0	0	0
miR-129-5p	0	0	0	0	0	0	0	0	2	2	3	0	0	0	0	1	0	7	0	1	0	0	0	0
miR-1299	0	0	0	0	0	0	0	0	0	0	0	0	0	0	0	0	0	0	0	0	0	0	0	0
miR-1301-3p	0	0	0	0	1	9	0	0	1	2	0	1	0	2	0	11	0	1	0	0	0	4	0	2

miR-1304-3p	0	0	0	0	0	0	0	0	0	0	0	0	0	0	0	0	0	0	0	0	0	0	0	0
miR-1306-3p	0	0	0	0	0	0	0	0	0	0	0	0	0	0	0	0	0	0	0	0	0	0	0	0
miR-1306-5p	0	0	0	0	0	0	0	0	0	0	1	0	0	0	0	1	0	1	0	1	0	2	0	0
miR-1307-3p	0	2	2	1	9	8	1	1	1	4	28	4	1	12	1	24	3	20	0	4	2	4	0	11
miR-1307-5p	0	0	0	0	2	1	0	1	1	0	2	0	0	0	0	3	0	1	0	0	0	0	0	1
miR-130a-3p	0	0	2	0	1	1	2	0	0	0	2	0	0	0	0	1	0	0	0	0	0	1	0	0
miR-130b-3p	1	0	0	1	0	0	0	0	0	2	0	0	0	0	0	5	0	0	0	0	0	0	0	0
miR-130b-5p	0	0	1	0	0	3	0	0	0	1	4	0	0	1	1	4	0	4	0	0	1	0	0	0
miR-1323	0	0	0	0	0	2	0	0	0	0	0	1	0	0	0	0	0	0	0	0	0	0	0	0

miR-132-3p	0	0	0	0	0	0	0	0	0	0	0	0	0	0	0	0	0	0	0	0	0	0	0	0
miR-132-5p	0	0	0	0	0	1	0	0	1	0	2	0	0	0	0	0	0	2	0	0	0	0	0	0
miR-1343-3p	0	0	0	0	0	0	0	0	0	0	0	0	0	0	0	0	0	0	0	0	0	0	0	0
miR-134-5p	0	1	2	0	0	11	0	0	0	0	3	0	0	2	0	4	1	0	0	1	0	1	0	2
miR-135a-5p	0	0	0	0	0	0	0	0	0	0	0	0	0	0	0	0	0	0	0	0	0	0	0	0
miR-136-3p	0	0	0	0	0	0	0	0	0	0	1	0	0	1	0	0	0	0	0	0	0	0	0	0
miR-136-5p	0	0	0	0	0	0	0	0	0	0	1	0	0	0	0	0	0	1	0	0	0	0	0	0
miR-138-5p	0	0	0	0	0	0	0	0	0	0	0	0	0	0	0	0	0	0	0	0	0	0	0	1
miR-139-3p	1	2	4	3	8	11	1	3	1	6	16	2	3	4	1	9	5	8	0	5	3	6	1	6

miR-139-5p	5	3	3	13	36	19	2	9	14	18	52	20	6	18	15	31	12	34	9	34	3	14	0	32
miR-140-3p	2	0	5	0	6	5	0	2	2	4	22	2	1	0	5	1	2	9	0	2	2	0	0	4
miR-140-5p	1	0	1	0	2	3	0	0	0	2	10	1	3	2	0	5	1	6	0	0	1	1	0	5
miR-141-3p	0	1	0	0	0	0	0	0	0	0	1	0	0	1	0	0	0	3	0	0	0	0	0	0
miR-142-3p	2	0	4	1	10	10	4	2	2	1	16	3	1	6	2	9	9	10	0	6	3	6	3	16
miR-142-5p	1	0	2	3	7	5	0	3	2	1	24	5	0	1	2	1	5	6	0	4	0	3	1	1
miR-143-3p	4	14	5	4	20	32	4	4	10	22	112	2	6	12	3	29	10	94	4	7	12	5	5	31
miR-144-3p	1	0	3	1	4	2	0	1	3	0	52	0	0	5	0	1	1	4	1	1	2	1	0	6
miR-144-5p	2	1	2	2	9	4	2	0	1	0	16	0	0	1	1	3	2	9	1	1	1	2	0	9

miR-145-3p	0	0	0	1	0	0	0	2	3	0	3	3	0	1	0	4	0	0	0	0	0	0	0	0
miR-145-5p	0	0	0	0	0	0	0	0	0	0	0	0	0	0	0	0	0	0	0	0	0	0	0	0
miR-1468-5p	0	0	0	0	0	0	0	0	0	0	0	0	0	0	0	0	0	0	0	0	0	0	0	0
miR-146a-5p	4	1	7	2	17	56	5	4	12	7	88	5	4	22	5	104	5	27	5	17	3	10	3	17
miR-146b-3p	0	0	0	0	0	0	0	0	0	0	0	0	0	0	0	1	0	0	0	0	0	0	0	1
miR-146b-5p	0	3	4	1	2	11	5	0	2	2	43	5	2	16	0	10	4	8	1	10	2	1	1	18
miR-147b	0	0	0	0	0	0	0	0	0	0	0	0	0	0	0	0	0	0	0	0	0	0	0	0
miR-148a-3p	90	675	129	151	737	1023	73	36	131	1442	3106	619	136	327	152	2644	110	1090	67	254	363	373	117	322
miR-148a-5p	0	0	0	0	0	0	0	0	0	2	0	0	0	1	0	3	1	0	0	0	0	1	0	1

miR-148b-3p	2	6	9	5	18	44	2	2	6	6	76	11	4	15	7	33	4	33	0	5	9	5	0	8
miR-149-5p	0	0	0	0	0	0	0	0	0	0	0	0	0	0	0	0	0	0	0	0	2	0	0	1
miR-150-3p	0	0	0	1	11	4	0	1	0	1	11	3	3	1	1	2	0	6	0	0	0	1	0	3
miR-150-5p	2	1	9	7	34	11	5	7	5	10	47	6	5	17	2	23	6	24	1	11	7	3	2	29
miR-151a-3p	11	16	25	13	55	141	8	8	23	37	146	31	24	28	16	236	13	91	14	36	55	45	15	34
miR-151a-5p	0	0	0	0	0	0	0	0	0	0	0	0	0	0	1	0	0	0	0	0	0	0	0	0
miR-152-3p	0	0	0	0	0	0	0	0	0	1	1	0	1	0	0	3	0	2	0	0	2	0	0	0
miR-152-5p	0	0	0	0	0	0	0	0	0	0	0	0	0	0	0	0	0	0	0	1	0	0	0	0
miR-153-3p	0	0	0	0	0	0	0	0	0	0	0	0	0	0	0	0	0	0	0	0	0	0	0	0

miR-155-5p	8	4	6	8	36	9	6	3	13	10	18	17	2	12	7	27	12	12	7	20	2	7	2	3
miR-15a-5p	0	0	0	0	0	0	0	0	0	0	4	0	0	0	0	0	0	0	0	0	0	0	0	0
miR-15b-3p	1	0	0	0	1	0	0	0	0	0	7	0	0	0	1	0	0	5	0	0	1	0	0	2
miR-15b-5p	0	0	4	2	3	0	1	2	1	2	19	0	0	4	3	1	1	8	1	0	0	0	2	1
miR-16-2-3p	4	0	9	4	8	2	2	8	4	1	71	5	0	7	11	5	3	27	0	3	3	1	2	8
miR-16-5p	7	0	30	5	27	17	3	4	9	7	345	22	5	35	14	21	9	88	1	5	5	7	1	27
miR-17-3p	0	0	0	0	0	0	0	0	0	0	0	0	0	0	0	2	0	0	0	0	0	0	0	0
miR-17-5p	0	0	0	0	3	2	0	0	0	0	20	3	0	2	1	6	1	4	0	1	2	2	0	6
miR-181a-2-3p	0	0	0	0	5	0	0	0	0	0	1	0	0	1	0	2	0	0	0	1	1	1	1	2

miR-181a-3p	0	0	0	0	0	0	0	0	0	0	1	0	0	1	0	0	0	0	0	0	0	0	0	0
miR-181a-5p	11	8	6	9	44	31	10	3	17	17	146	9	8	32	8	42	12	58	8	28	5	14	2	25
miR-181b-5p	1	1	0	2	9	5	1	0	1	2	11	2	0	3	1	7	1	6	2	1	2	0	2	6
miR-181c-3p	0	0	0	0	0	0	0	0	0	0	0	0	0	0	0	0	0	0	0	0	0	0	0	0
miR-181c-5p	0	0	0	0	0	0	0	0	0	0	0	0	0	0	0	0	0	0	0	0	0	0	0	0
miR-181d-5p	0	0	0	0	0	0	0	0	0	0	0	0	0	3	0	0	0	1	0	0	0	0	0	0
miR-182-5p	8	8	14	6	24	8	6	7	1	12	119	9	5	11	7	18	9	28	0	12	23	5	0	16
miR-183-5p	4	6	18	1	31	9	7	11	10	10	145	20	6	13	12	17	8	16	2	7	24	8	1	20
miR-184	0	0	0	3	4	7	0	0	0	0	1	5	2	1	2	18	3	1	0	2	0	3	2	0

miR-185-3p	0	0	0	0	0	2	0	0	0	0	4	0	0	2	0	0	0	0	0	0	0	0	0	0
miR-185-5p	9	8	19	9	125	56	9	14	7	53	175	21	3	98	39	194	22	150	0	3	9	20	2	42
miR-186-5p	5	2	15	2	34	11	2	4	4	9	138	13	2	15	5	11	3	38	1	5	5	2	0	8
miR-188-3p	0	0	0	0	0	0	0	0	0	0	0	0	0	0	0	0	0	0	0	0	0	0	0	0
miR-188-5p	0	0	0	0	1	0	0	0	0	0	0	0	0	1	0	0	0	0	0	0	0	0	0	0
miR-18a-3p	0	0	0	0	0	0	0	0	0	1	1	0	0	0	0	1	0	0	0	0	0	0	0	0
miR-18a-5p	1	0	0	0	1	1	0	0	0	1	1	2	0	0	0	0	0	1	0	0	1	1	0	1
miR-18b-5p	0	0	0	0	0	2	0	0	0	0	0	0	0	2	0	0	0	0	0	0	0	0	0	0
miR-1908-5p	1	1	1	0	2	10	0	0	0	3	7	0	1	3	0	14	1	0	0	0	0	3	0	5

miR-190a-5p	0	0	0	0	0	0	0	0	0	0	0	0	0	0	0	0	0	0	0	0	0	0	0	0
miR-191-3p	0	0	0	0	0	0	0	0	0	0	0	0	0	1	0	1	0	0	0	0	0	0	0	0
miR-1914-5p	0	0	0	0	0	0	0	0	0	0	0	0	0	0	0	1	0	0	0	0	0	0	0	0
miR-191-5p	15	5	18	8	66	139	6	4	6	32	114	20	18	80	10	162	24	62	2	28	9	43	2	71
miR-192-5p	1	2	11	6	18	7	2	1	3	7	110	46	2	5	7	134	5	68	1	4	7	2	1	11
miR-193a-5p	1	4	2	9	15	1	0	1	0	9	6	11	2	15	1	140	2	9	1	2	0	7	2	2
miR-193b-5p	0	2	0	2	0	0	0	0	1	4	3	4	0	0	0	15	0	1	0	1	0	2	0	0
miR-194-3p	0	0	0	0	0	0	0	0	0	0	0	4	0	0	0	0	0	0	0	0	0	0	0	0
miR-194-5p	4	1	7	3	6	2	2	1	6	1	74	26	0	5	3	33	4	68	0	7	1	1	2	4

miR-195-3p	0	0	0	0	5	0	0	0	0	0	0	0	0	0	0	1	0	3	0	0	0	0	0	0
miR-195-5p	0	0	0	0	0	1	1	0	0	0	1	0	0	0	0	1	0	1	0	0	0	0	0	0
miR-196a-5p	0	0	0	0	0	0	0	0	0	0	1	0	0	0	0	0	0	0	0	0	0	0	0	0
miR-196b-5p	0	0	0	0	0	0	0	0	0	0	2	0	0	0	0	1	0	2	0	0	0	0	0	0
miR-197-3p	0	0	0	1	5	5	0	0	1	0	2	0	1	2	0	9	0	1	0	0	0	2	0	5
miR-197-5p	0	0	0	0	0	0	0	0	0	0	1	0	0	0	0	0	0	0	0	0	0	0	0	0
miR-1976	0	0	0	0	0	0	0	0	0	0	0	0	0	0	0	0	0	1	0	0	0	0	0	0
miR-199a-3p	2	0	1	1	12	13	3	0	1	2	12	6	1	4	0	14	1	8	0	2	0	5	0	4
miR-199a-5p	0	0	0	0	0	16	0	0	1	1	5	1	2	4	1	4	3	2	2	2	3	0	0	2

miR-199b-3p	0	0	2	0	4	3	0	0	1	2	8	1	0	0	0	4	1	4	0	2	0	2	0	1
miR-199b-5p	0	0	0	1	0	0	0	0	0	0	2	0	1	0	0	0	0	1	0	0	0	0	0	1
miR-19a-3p	1	0	0	0	0	1	1	2	0	1	4	0	0	0	0	1	0	8	0	0	0	0	0	1
miR-19b-1-5p	0	0	0	0	0	0	0	0	0	0	0	0	0	0	0	0	0	1	0	0	0	0	0	0
miR-19b-3p	0	0	4	0	2	2	0	0	0	0	20	0	0	2	0	1	0	8	0	0	1	0	0	1
miR-200a-3p	1	0	0	1	5	1	2	1	0	10	4	3	0	0	1	1	1	29	0	0	8	1	0	4
miR-200a-5p	0	0	0	0	0	0	0	0	0	1	0	0	0	2	0	0	0	0	0	0	5	0	0	0
miR-200b-3p	0	0	0	0	2	0	0	0	0	7	0	0	0	3	0	0	0	4	0	0	3	0	0	0
miR-200b-5p	0	0	0	0	0	0	0	0	0	7	0	0	0	0	0	0	0	0	0	0	0	0	1	1

miR-200c-3p	0	0	0	0	3	0	1	0	1	6	1	0	0	3	0	0	2	4	0	0	3	1	0	1
miR-202-3p	0	0	0	0	0	0	0	0	0	0	0	0	0	0	0	0	0	0	0	0	0	0	0	0
miR-203a	1	0	1	0	4	1	0	0	1	0	1	0	2	0	0	3	0	0	3	1	0	3	0	3
miR-204-3p	0	5	0	0	1	1	0	0	0	0	0	0	0	0	0	0	1	0	0	0	0	0	0	2
miR-204-5p	0	0	0	0	0	0	0	0	0	0	0	0	0	0	0	0	0	0	0	0	0	0	0	0
miR-206	0	0	0	1	1	0	4	0	3	0	1	0	0	0	0	0	0	7	0	0	0	0	0	1
miR-20a-5p	1	0	1	0	11	3	0	3	0	1	42	4	0	9	0	5	1	6	0	0	2	3	1	4
miR-20b-3p	0	0	0	0	0	0	0	0	0	0	0	0	0	0	0	0	0	0	0	0	0	0	0	0
miR-20b-5p	0	0	1	0	8	0	0	0	1	0	6	2	0	2	0	1	0	1	0	2	0	0	0	1

miR-210-3p	0	0	0	0	0	0	0	0	0	0	1	0	0	0	0	0	0	0	0	0	0	0	0	0
miR-2110	2	3	3	4	1	1	0	2	0	4	39	3	0	2	1	16	3	13	0	1	4	1	2	4
miR-2115-5p	0	1	0	0	0	0	0	0	0	0	0	0	0	0	1	0	0	0	0	0	0	0	0	0
miR-21-3p	0	0	0	0	0	0	0	0	0	0	1	0	0	1	0	0	0	0	0	0	0	0	0	0
miR-214-3p	2	0	0	0	0	0	0	0	0	0	0	0	0	0	0	0	0	0	0	0	0	0	0	0
miR-214-5p	0	1	0	0	0	0	0	0	0	0	0	0	0	0	0	0	0	0	0	0	0	0	0	0
miR-215-3p	0	0	0	0	0	0	0	0	0	0	0	0	0	0	0	0	0	0	0	0	0	0	0	0
miR-215-5p	0	0	0	0	0	0	0	0	1	1	12	0	0	1	0	4	0	43	0	0	0	0	0	0
miR-21-5p	41	17	58	26	224	156	26	13	45	74	901	60	16	103	38	409	30	331	23	73	41	69	13	103

miR-216a-5p	0	0	0	0	0	0	0	0	0	0	1	0	0	0	0	0	0	0	0	0	0	0	0	0
miR-216b-5p	0	0	0	0	0	0	0	0	0	0	0	0	0	0	0	0	0	1	0	0	0	0	0	0
miR-218-5p	0	4	0	0	0	2	0	0	0	0	0	0	0	0	0	0	0	0	0	0	0	0	0	0
miR-219a-1-3p	0	0	0	2	0	0	0	0	0	0	2	0	0	0	0	0	0	0	0	0	0	0	0	0
miR-219a-2-3p	0	0	0	0	0	0	0	0	0	0	0	0	0	0	0	0	0	0	0	0	0	0	0	0
miR-221-3p	1	0	2	1	11	10	0	2	0	5	19	1	2	4	1	16	1	5	0	1	2	1	0	8
miR-221-5p	0	0	0	0	0	0	0	0	0	0	2	0	0	1	0	0	0	1	0	0	0	1	0	0
miR-222-3p	0	0	2	4	11	7	0	2	2	4	36	5	2	2	2	10	0	10	1	0	4	0	0	9

miR-222-5p	0	0	0	0	0	0	0	0	0	0	0	0	0	0	0	0	0	1	0	0	0	0	0	0
miR-223-3p	0	0	0	0	1	3	0	0	2	1	2	0	0	4	1	0	0	0	0	0	0	0	0	2
miR-223-5p	2	0	0	4	0	2	1	0	1	3	9	2	1	1	1	6	1	8	1	1	1	2	0	3
miR-22-3p	34	14	76	31	159	131	24	26	35	73	769	64	11	90	48	384	29	386	27	76	29	52	5	70
miR-224-5p	0	0	0	2	2	1	0	0	0	0	1	3	0	0	0	13	0	1	0	0	0	0	0	0
miR-22-5p	0	0	3	0	9	4	0	0	0	6	12	3	0	5	0	12	0	6	1	1	1	2	0	3
miR-2278	0	0	0	0	0	0	0	0	0	0	0	0	0	0	0	0	0	0	0	0	0	0	0	0
miR-2355-3p	0	0	0	0	0	1	0	0	0	0	0	0	0	0	0	0	0	0	0	0	0	0	0	0
miR-23a-3p	0	1	1	0	2	3	0	0	0	0	0	0	2	3	0	5	0	2	0	1	0	0	0	1

miR-23a-5p	0	0	0	0	1	0	0	0	0	0	0	1	0	0	0	0	0	0	0	0	0	0	0	0
miR-23b-3p	0	0	0	0	0	0	0	0	0	0	0	0	0	1	0	0	1	0	0	0	0	0	0	0
miR-23b-5p	0	0	0	0	0	0	0	0	0	1	0	0	0	0	0	0	1	0	0	0	0	0	0	1
miR-24-3p	21	24	30	22	110	162	14	12	24	51	312	49	26	77	11	361	32	128	11	42	14	36	7	106
miR-25-3p	50	29	175	26	253	183	36	54	48	55	1860	139	20	184	142	200	47	676	17	62	113	37	18	116
miR-25-5p	0	0	0	0	0	1	0	0	0	0	5	0	0	1	0	1	0	2	0	0	0	0	0	0
miR-26a-2-3p	0	0	0	0	0	0	0	0	0	0	0	0	0	0	0	0	0	0	0	2	0	0	0	0
miR-26a-5p	51	28	54	44	263	411	23	37	58	62	287	84	38	211	47	341	83	146	35	198	19	229	17	265
miR-26b-3p	0	0	0	0	0	0	0	0	0	0	0	0	0	0	0	0	0	0	0	0	0	0	0	0

miR-26b-5p	1	0	3	1	12	6	2	2	8	3	75	7	0	14	3	11	5	8	1	2	0	3	1	8
miR-27a-3p	18	4	11	10	76	29	4	4	12	20	178	22	5	15	11	70	25	92	6	33	6	32	5	47
miR-27a-5p	0	2	1	2	3	4	0	1	0	3	3	2	1	4	0	7	3	2	3	1	2	0	1	0
miR-27b-3p	9	8	6	6	25	21	2	5	10	10	76	26	6	11	0	95	11	48	6	12	5	6	1	29
miR-27b-5p	0	0	0	0	0	0	0	0	0	0	0	0	0	0	0	1	0	0	0	1	0	0	0	0
miR-28-3p	0	0	0	1	7	19	0	0	1	7	13	0	2	6	0	21	1	3	0	2	0	1	0	1
miR-28-5p	0	0	0	0	2	0	0	0	0	0	4	1	2	2	0	5	0	1	0	2	0	1	0	0
miR-296-3p	0	0	0	0	1	0	0	0	0	0	0	0	0	0	0	0	0	0	0	0	0	0	0	0
miR-296-5p	0	0	0	0	0	0	0	0	0	0	0	0	0	1	0	0	0	0	0	0	0	0	0	0

miR-29a-3p	2	0	1	4	9	5	0	0	3	9	21	3	1	2	1	20	3	6	0	2	3	2	1	1
miR-29b-1-5p	0	0	0	0	0	0	0	0	0	0	0	1	0	0	0	0	0	0	0	0	0	0	0	0
miR-29b-3p	0	0	0	0	0	0	0	0	0	0	2	0	0	0	0	1	0	1	0	0	0	0	0	0
miR-29c-3p	2	0	0	0	1	0	0	0	0	0	2	0	0	0	0	0	0	1	0	0	0	0	0	0
miR-29c-5p	0	0	0	0	0	0	1	0	0	0	0	0	0	0	0	0	0	0	0	0	0	0	0	0
miR-301a-3p	0	0	0	0	0	0	0	0	0	0	0	0	0	0	0	0	0	0	0	1	0	0	0	0
miR-301b	0	0	0	0	0	0	0	0	0	0	0	0	0	0	0	0	0	0	0	0	0	0	0	0
miR-30a-3p	5	7	1	2	20	10	3	1	4	12	17	14	5	8	3	20	9	15	4	8	7	5	2	10
miR-30a-5p	4	2	1	3	51	17	3	1	14	14	36	12	5	7	3	29	6	37	1	4	5	7	3	15

miR-30b-3p	0	0	0	0	0	0	0	0	0	0	0	1	0	0	0	0	0	0	0	0	0	0	0	0
miR-30b-5p	0	0	1	0	2	0	0	0	0	0	1	0	0	0	1	0	1	1	0	0	0	0	0	0
miR-30c-1-3p	0	0	0	0	1	1	0	0	0	0	0	0	0	0	0	0	0	0	0	0	0	0	0	0
miR-30c-2-3p	1	0	0	0	0	0	0	0	0	0	0	0	0	0	0	0	1	0	0	0	0	0	1	0
miR-30c-5p	3	1	3	6	21	15	2	4	1	6	16	6	2	13	3	10	3	9	0	9	4	6	4	17
miR-30d-3p	0	0	0	0	0	1	0	0	0	0	0	0	0	0	1	0	1	0	0	0	0	0	0	0
miR-30d-5p	38	50	49	41	286	106	21	33	38	120	601	58	14	114	35	223	22	257	7	33	53	37	3	87
miR-30e-3p	2	6	6	3	18	39	3	3	9	9	34	6	3	12	8	57	11	17	1	10	17	11	9	18

miR-30e-5p	1	1	2	3	4	1	0	0	1	2	30	4	0	1	1	11	1	16	0	0	1	0	2	3
miR-3122	0	0	0	0	0	0	0	0	0	0	1	0	0	0	0	0	0	0	0	0	0	0	0	0
miR-3127-3p	0	0	0	0	0	0	0	0	0	0	0	0	0	0	0	0	1	0	0	0	0	0	0	0
miR-3127-5p	0	0	0	0	0	0	0	0	0	0	0	0	0	0	0	1	0	0	0	0	0	0	0	0
miR-3128	0	0	0	0	0	0	0	0	0	0	0	0	0	0	0	0	0	0	0	0	0	0	0	0
miR-3136-5p	0	0	0	0	0	0	0	0	0	0	0	0	0	0	0	0	0	0	0	0	0	0	0	0
miR-3138	0	0	0	0	0	0	0	0	0	0	0	0	0	0	0	0	0	0	0	1	0	0	0	0
miR-3143	0	0	0	0	0	0	0	0	0	0	0	0	0	0	0	0	0	0	0	0	0	0	0	0
miR-3150a-5p	0	0	0	0	0	0	0	0	0	0	0	0	0	0	0	2	0	0	0	0	0	0	0	0

miR-3150b-3p	0	0	0	0	1	0	0	0	0	0	0	2	0	0	0	1	1	0	0	0	0	0	0	0
miR-3157-3p	0	0	0	0	0	0	0	0	0	0	1	0	0	0	0	0	0	0	0	0	0	0	0	0
miR-3158-3p	3	0	6	1	0	4	2	2	1	1	27	6	1	2	4	6	2	3	0	0	0	0	0	2
miR-3168	13	4	4	2	6	8	6	4	9	4	23	11	5	6	3	13	2	9	5	3	4	0	1	6
miR-3173-5p	0	0	0	0	0	0	0	0	0	0	0	0	0	0	0	0	0	0	0	0	0	0	0	0
miR-3174	0	0	0	0	0	0	0	0	0	0	0	0	0	0	0	1	0	0	0	0	0	0	0	0
miR-3179	0	0	0	0	0	0	0	0	0	0	0	0	0	1	0	0	0	1	0	0	0	0	0	0
miR-3180-3p	0	0	0	0	0	0	0	0	0	0	2	0	0	0	0	2	0	0	0	0	0	0	0	0
miR-3187-3p	0	0	0	0	0	0	0	0	0	0	0	0	0	0	0	1	0	0	0	0	0	0	0	0

miR-3191-3p	0	0	0	0	0	0	0	0	0	0	0	1	0	0	0	0	0	0	0	0	0	0	0	0
miR-3197	0	0	0	0	0	0	0	0	0	1	0	0	0	0	0	0	0	0	0	0	0	0	0	0
miR-3200-3p	0	0	0	0	0	0	0	0	0	0	0	0	0	0	0	0	0	0	0	0	0	0	0	0
miR-320a	68	117	67	85	384	201	42	39	50	268	763	134	46	320	72	1071	93	601	16	55	88	161	33	192
miR-320b	6	48	13	15	80	19	11	7	18	74	93	14	7	67	11	257	6	80	5	8	19	36	3	29
miR-320c	0	22	0	3	39	1	1	2	1	26	20	5	3	16	1	90	2	19	2	1	5	11	3	13
miR-320d	0	5	3	1	11	1	1	0	0	5	3	2	1	5	0	30	1	7	1	0	1	2	3	7
miR-320e	0	0	0	0	0	0	0	0	0	0	0	0	0	0	0	1	0	0	0	0	0	0	0	0
miR-323a-3p	0	0	0	0	0	2	0	0	0	0	0	0	0	0	0	0	0	0	0	0	0	0	0	0

miR-323a-5p	0	0	0	0	0	1	0	0	0	0	0	0	0	0	0	0	0	0	0	0	0	0	0	0
miR-323b-3p	0	0	0	0	0	4	0	0	0	0	0	0	1	0	0	0	0	0	0	0	0	0	0	0
miR-324-5p	0	0	0	0	0	0	0	0	0	0	1	0	0	1	0	0	0	0	0	0	0	0	0	1
miR-32-5p	0	0	2	2	1	5	0	1	1	1	16	0	0	1	0	5	0	6	0	2	0	1	1	0
miR-326	0	0	0	0	0	2	0	0	0	0	4	0	1	0	0	3	0	1	0	0	0	0	0	0
miR-328-3p	2	1	3	1	6	40	2	0	1	3	17	4	5	12	1	55	2	5	0	10	1	13	0	11
miR-330-3p	0	0	0	0	0	1	0	0	0	2	0	0	0	0	0	0	0	0	0	1	0	1	0	0
miR-330-5p	0	0	0	0	0	3	0	0	0	0	2	0	1	0	0	0	0	0	0	0	0	0	0	0
miR-331-5p	0	0	0	0	0	0	0	0	0	1	1	0	0	0	0	1	0	0	0	0	0	1	0	0

miR-335-3p	0	0	0	0	0	3	0	0	0	0	2	0	1	1	0	6	0	3	0	1	0	0	0	4
miR-335-5p	0	0	0	0	2	2	0	0	0	0	2	0	0	0	0	4	0	2	0	1	1	0	0	0
miR-337-3p	0	0	0	0	0	0	0	0	0	0	0	0	0	0	0	0	0	0	0	0	0	0	0	0
miR-337-5p	0	0	0	0	0	0	0	0	0	0	0	0	0	0	0	0	0	0	0	0	0	0	0	0
miR-338-5p	0	0	0	0	0	1	0	0	0	1	3	0	0	0	0	1	0	2	0	0	1	0	0	1
miR-339-3p	0	0	0	0	0	1	0	0	1	0	11	0	0	0	1	8	0	5	0	0	0	1	0	0
miR-339-5p	0	0	0	0	0	0	0	0	0	0	0	0	0	1	0	0	0	0	0	0	0	0	0	0
miR-340-3p	0	0	0	0	1	1	0	0	0	0	0	0	0	1	0	1	2	0	0	0	0	0	0	0
miR-340-5p	2	0	1	0	7	10	1	0	3	1	14	1	1	3	0	16	0	0	2	4	0	2	1	3

miR-342-3p	0	0	0	1	2	4	0	0	0	0	2	2	1	0	0	0	0	2	0	2	0	2	0	2
miR-342-5p	1	1	1	3	5	8	2	0	1	0	49	0	0	0	2	8	2	13	2	3	6	1	0	2
miR-345-5p	0	0	0	1	1	1	2	0	0	0	1	2	0	1	0	2	0	0	0	0	0	0	0	0
miR-34a-5p	0	0	0	0	0	0	0	0	0	0	1	0	0	0	0	0	0	0	0	0	0	0	0	0
miR-3591-5p	0	0	0	0	0	0	0	0	0	0	0	2	0	0	0	0	0	0	0	0	0	0	0	0
miR-3605-3p	2	0	1	0	8	1	1	0	0	0	6	0	0	1	0	3	0	0	0	0	0	1	1	0
miR-3605-5p	0	0	1	0	0	0	0	0	0	0	0	0	0	0	0	0	0	2	0	0	0	0	1	1
miR-3613-3p	0	0	0	0	1	0	0	0	0	0	0	0	0	0	0	0	0	0	0	0	0	0	0	0
miR-3613-5p	0	0	0	2	1	2	0	0	0	1	3	0	0	0	0	2	0	0	0	1	0	1	0	1

miR-361-3p	0	0	0	0	1	0	0	0	0	0	3	0	1	1	1	0	0	1	0	3	0	0	0	0
miR-3614-5p	0	0	0	0	0	0	0	0	0	0	0	0	0	0	0	0	0	0	0	0	0	1	0	0
miR-3615	5	4	1	0	6	0	0	3	0	2	19	0	1	7	1	21	1	7	0	0	2	1	0	3
miR-361-5p	0	0	0	0	4	1	0	0	0	0	2	1	0	3	0	7	1	1	0	2	0	4	0	0
miR-3621	0	0	0	0	0	0	0	0	0	0	1	0	0	0	1	0	0	0	0	0	0	0	0	0
miR-362-5p	0	0	0	0	0	0	0	0	0	0	0	0	0	0	0	0	0	0	0	0	0	1	0	0
miR-363-3p	16	4	25	4	48	25	2	4	9	9	371	22	6	30	14	20	7	78	4	14	36	13	0	23
miR-363-5p	0	0	0	0	1	0	0	0	1	0	7	0	0	0	0	0	0	2	0	0	0	0	0	1
miR-3656	0	0	0	0	0	1	0	0	0	0	0	0	0	0	0	0	0	0	0	0	0	1	0	0

miR-365a-3p	0	0	0	0	0	0	0	0	0	0	0	0	0	0	0	0	0	0	0	0	0	0	0	0
miR-365a-5p	0	0	0	0	0	0	0	0	0	0	0	0	0	0	0	0	0	0	0	0	0	0	0	0
miR-365b-3p	0	0	0	0	0	0	0	0	0	0	0	1	0	0	0	0	0	0	0	0	0	0	0	0
miR-3663-5p	0	0	0	0	0	0	0	0	0	0	0	0	0	0	0	0	0	0	0	0	0	0	0	0
miR-3675-5p	0	0	0	0	0	0	0	0	0	0	0	1	0	0	0	0	0	0	0	0	0	0	0	0
miR-3682-3p	0	0	0	0	1	0	0	0	0	0	0	0	0	0	0	0	0	0	0	0	0	0	0	0
miR-3688-3p	0	0	0	0	0	0	0	0	0	0	1	0	0	0	0	0	0	0	0	0	0	0	0	0
miR-3690	0	0	0	0	0	0	0	0	0	0	0	0	0	0	0	0	0	0	0	0	0	0	0	0
miR-3691-5p	0	0	0	0	0	0	0	0	0	0	0	0	0	0	0	0	0	1	0	0	0	0	0	0

miR-369-5p	0	0	0	0	0	0	0	0	0	0	0	0	0	0	0	0	0	0	0	0	0	0	0	0
miR-370-3p	0	0	0	1	0	12	0	0	0	2	9	1	4	6	0	9	1	0	5	0	0	1	3	6
miR-370-5p	0	0	0	0	0	2	0	0	0	0	0	0	0	0	0	0	0	0	0	0	0	0	0	0
miR-372-3p	0	0	0	0	0	0	0	0	0	0	1	0	0	0	0	0	0	0	0	0	0	0	0	0
miR-374a-3p	0	0	0	0	1	1	0	0	1	0	8	0	0	0	0	2	0	1	0	0	0	0	1	1
miR-374a-5p	1	1	1	0	1	4	0	0	1	1	12	2	0	4	0	3	0	4	0	2	1	1	0	2
miR-374b-5p	0	0	0	0	0	1	0	0	0	0	4	0	0	0	0	0	0	1	0	0	0	0	0	0
miR-375	7	219	6	2	25	3	3	0	3	578	58	11	5	67	8	124	7	861	1	0	29	4	0	0
miR-378a-3p	1	1	5	2	11	5	1	0	1	8	28	6	0	4	3	21	3	31	0	6	3	4	0	6

miR-378a-5p	0	0	0	0	0	0	0	0	0	0	0	0	0	0	0	0	0	0	0	0	0	0	0	0
miR-378c	0	0	1	0	1	1	0	0	0	0	0	0	0	0	0	0	0	1	0	1	0	0	0	0
miR-378d	0	0	0	0	0	0	0	0	0	0	2	0	0	0	0	0	0	0	0	0	0	0	0	1
miR-379-3p	0	0	0	0	0	0	0	0	0	0	0	0	0	0	0	0	0	0	0	0	0	0	0	0
miR-379-5p	0	0	1	0	0	11	0	0	0	0	2	1	2	2	0	1	2	0	0	1	0	0	1	1
miR-381-3p	0	0	0	0	0	19	0	0	0	0	8	0	1	4	0	3	0	4	0	0	1	1	2	1
miR-381-5p	0	2	0	0	0	0	0	0	0	0	0	0	0	0	0	0	0	0	0	0	0	0	0	0
miR-382-5p	0	0	0	0	0	10	0	0	0	1	3	2	0	1	0	4	0	1	1	0	0	0	0	1
miR-3909	0	1	0	0	0	0	0	0	0	0	1	0	0	0	0	1	0	0	0	0	0	0	0	0

miR-3911	0	0	0	0	0	0	0	0	0	0	0	0	0	0	0	0	0	0	0	0	0	0	0	0
miR-3912-3p	0	0	0	0	0	1	0	0	0	0	0	0	0	0	0	2	0	0	0	0	0	0	0	0
miR-3913-5p	0	0	0	0	0	0	0	1	0	0	1	0	0	0	2	0	0	1	0	0	1	0	0	0
miR-3928-3p	0	0	0	0	0	0	0	0	0	0	0	0	0	0	0	1	0	0	0	0	0	0	0	0
miR-3934-5p	0	0	0	0	0	0	0	0	0	0	1	0	0	0	0	0	0	0	0	0	0	0	0	0
miR-3936	0	0	0	0	0	0	0	0	0	0	0	0	0	0	0	0	0	0	0	0	0	0	0	0
miR-3940-3p	0	0	0	0	0	0	0	0	0	0	0	0	0	0	0	0	0	0	0	0	0	0	0	0
miR-409-3p	0	0	2	0	0	20	0	0	0	0	25	0	7	5	2	9	2	3	1	0	4	0	1	5
miR-409-5p	0	0	0	0	0	0	0	0	0	0	0	0	0	0	0	0	0	0	0	0	0	0	0	0

miR-410-3p	0	0	0	0	0	0	0	0	0	0	0	0	0	1	0	0	0	0	0	0	0	0	0	0
miR-411-3p	0	0	0	0	0	2	0	0	0	0	1	0	1	2	0	0	0	0	0	0	0	0	0	2
miR-411-5p	0	0	0	0	0	1	0	0	0	0	1	0	0	1	0	0	0	0	0	0	0	0	0	1
miR-421	0	0	0	0	1	0	0	0	0	0	1	0	0	1	0	0	0	1	0	0	0	0	0	0
miR-423-3p	14	16	22	30	91	122	6	11	18	52	194	35	20	69	14	297	18	92	5	28	31	48	12	55
miR-423-5p	272	193	765	259	834	1137	232	296	306	316	5072	481	256	426	550	907	105	3239	272	481	1077	451	137	651
miR-424-3p	0	1	2	1	3	3	0	0	1	5	30	2	0	1	1	5	1	11	1	1	7	2	0	3
miR-424-5p	0	0	0	0	1	0	0	0	0	0	1	0	0	0	0	1	0	0	0	1	0	0	0	0
miR-425-5p	1	1	12	0	15	8	0	4	2	6	88	6	0	11	7	5	2	20	0	2	3	3	0	8

miR-4259	0	0	0	0	0	0	0	0	0	0	0	0	0	0	0	0	0	0	0	0	0	0	0	0
miR-429	0	0	0	0	0	0	0	0	0	1	0	0	0	0	0	0	0	3	0	0	1	0	0	0
miR-431-5p	0	0	0	0	0	1	0	0	0	0	0	0	1	0	0	0	0	1	0	0	0	0	0	1
miR-4322	0	0	0	0	0	0	0	0	0	0	0	0	0	0	0	0	0	0	0	1	0	0	0	0
miR-432-5p	1	0	0	0	0	17	0	0	0	0	22	0	2	6	0	9	0	3	0	0	0	0	0	4
miR-4326	0	0	0	0	0	0	0	0	0	0	0	0	0	0	0	0	0	0	0	0	0	0	0	0
miR-433-3p	0	0	0	0	0	1	0	0	0	0	2	0	0	1	0	1	0	0	0	0	0	0	0	0
miR-4433-3p	0	0	0	0	0	0	0	0	0	0	0	0	0	0	0	0	0	0	0	0	0	0	0	0
miR-4433-5p	0	0	0	0	0	0	0	0	0	0	0	0	0	0	0	0	0	1	0	0	0	0	0	0

miR-4433b-3p	0	0	1	0	0	8	0	0	0	1	1	2	1	2	0	1	0	1	0	1	0	0	0	0
miR-4433b-5p	0	0	0	0	0	4	0	0	0	0	0	0	0	0	0	3	1	0	0	0	0	0	0	1
miR-4443	1	0	0	0	1	1	1	0	1	0	2	0	0	0	0	1	0	2	0	0	1	0	0	4
miR-4446-3p	0	0	0	0	0	10	0	0	0	0	2	0	1	0	0	5	0	0	0	2	0	1	0	0
miR-4467	0	0	0	0	1	0	0	0	0	0	0	0	0	0	0	0	0	0	0	0	0	0	0	0
miR-4473	0	0	0	0	0	0	0	0	0	0	0	0	0	0	0	0	0	0	0	0	0	0	0	0
miR-4474-3p	0	0	0	0	0	0	0	0	1	0	0	0	0	0	0	0	0	0	0	0	0	0	0	0
miR-4477b	0	0	0	0	0	0	0	0	0	0	0	0	0	0	0	0	0	0	0	0	0	1	0	0

miR-4482-3p	0	0	1	0	0	0	0	0	0	0	0	0	0	0	0	1	0	0	0	0	0	0	0	0
miR-4488	0	0	0	0	0	0	0	0	0	0	0	0	0	0	1	0	0	0	0	0	0	0	0	0
miR-4489	0	0	0	0	0	0	0	0	0	0	0	0	0	0	0	0	0	0	0	0	0	0	0	0
miR-4497	0	0	0	0	0	1	0	0	1	0	0	3	0	1	0	3	0	0	0	0	1	0	0	2
miR-4500	0	0	0	0	0	0	0	0	0	0	0	0	0	0	0	0	0	0	0	0	0	0	0	0
miR-4504	0	0	0	0	0	0	0	0	0	1	1	0	0	0	0	0	0	0	0	0	0	0	0	0
miR-4508	0	0	0	0	1	0	0	0	0	0	0	2	0	0	0	0	0	0	0	0	0	0	0	1
miR-450a-5p	1	0	0	0	1	1	1	0	0	0	0	0	0	0	0	1	0	1	0	0	0	0	0	1
miR-450b-5p	0	0	0	0	0	1	0	0	0	0	3	0	0	0	0	1	0	0	0	0	1	0	0	0

miR-4510	0	0	0	0	0	1	0	0	0	0	0	0	0	0	0	0	0	0	0	0	0	0	0	0
miR-4511	0	0	0	0	0	0	0	0	0	0	0	0	0	0	0	0	0	0	0	0	0	0	0	0
miR-4513	0	0	0	0	0	0	0	0	0	0	0	0	0	0	0	0	0	0	0	0	0	0	0	0
miR-4516	0	0	0	0	0	0	0	0	0	1	0	0	0	0	0	0	0	0	2	0	0	0	0	0
miR-451a	601	72	3482	463	2480	2128	461	779	687	692	29702	1492	404	2318	1855	1124	1069	6826	314	613	1525	275	325	1820
miR-452-5p	0	0	0	0	0	0	0	0	0	0	0	0	0	0	0	1	0	0	0	0	0	0	0	0
miR-454-3p	0	0	0	0	0	0	0	0	0	0	0	0	0	0	0	0	0	1	0	0	0	0	0	0
miR-454-5p	0	0	0	0	0	0	0	0	0	0	0	0	0	0	0	0	0	0	0	0	0	0	0	0
miR-455-5p	0	0	0	0	0	0	0	0	0	0	0	0	0	0	0	0	0	0	0	0	0	0	0	1

miR-4635	0	0	0	0	0	0	0	0	0	0	0	0	0	0	0	0	0	0	0	0	0	0	0	0
miR-4647	0	0	1	0	0	0	0	0	0	0	0	0	0	0	0	0	0	0	0	0	0	0	0	0
miR-4658	0	0	0	0	0	0	0	0	0	0	0	0	0	0	0	1	0	0	0	0	0	0	0	0
miR-4661-5p	0	0	0	0	0	1	0	0	0	0	0	0	0	0	0	0	0	0	0	0	0	0	0	0
miR-4662a-5p	0	0	0	0	0	1	0	0	0	0	0	0	0	0	0	0	0	0	0	0	0	0	0	0
miR-4663	0	0	0	0	0	0	0	0	0	0	0	0	0	0	0	0	0	0	0	0	0	0	0	0
miR-4664-3p	0	0	0	0	0	0	0	0	0	0	0	0	0	0	0	0	0	0	0	0	0	0	0	0
miR-4665-5p	0	1	1	0	1	3	1	0	0	0	0	0	0	0	0	2	0	1	0	1	0	0	0	0
miR-4667-5p	0	0	0	0	0	0	0	0	0	0	0	0	0	0	0	0	0	0	0	0	0	0	0	0

miR-4669	0	0	0	0	0	1	0	0	0	1	0	0	0	0	0	0	0	0	0	1	0	0	0	0
miR-4670-5p	0	0	0	0	0	0	0	0	0	0	0	0	0	0	0	0	0	1	0	0	0	0	0	0
miR-4671-5p	0	0	0	0	0	0	0	0	1	0	0	0	1	1	0	0	0	0	1	0	0	0	2	1
miR-4672	0	0	0	0	0	0	0	0	0	0	0	0	0	0	0	0	0	0	0	0	0	0	0	0
miR-4676-5p	0	0	0	0	0	0	0	0	2	0	0	0	0	0	0	0	0	0	0	0	0	0	0	0
miR-4677-5p	0	0	0	0	0	0	0	0	0	0	0	0	0	0	0	0	0	0	0	0	0	0	0	0
miR-4683	0	0	0	0	0	0	0	0	0	0	0	0	0	0	0	0	0	0	0	0	0	0	0	0
miR-4685-3p	0	0	0	0	0	0	0	0	0	0	2	0	0	0	0	2	0	0	0	0	0	0	0	0
miR-4688	0	0	0	0	0	1	0	0	0	0	0	0	0	0	0	0	0	0	0	0	0	0	0	0

miR-4697-3p	0	0	0	0	0	0	0	0	0	0	0	0	0	0	0	0	0	0	0	0	0	0	0	0
miR-4709-5p	0	0	0	0	0	0	0	0	0	0	0	0	0	0	0	0	0	1	0	0	0	0	0	0
miR-4714-5p	0	0	0	0	0	0	0	0	0	0	0	0	0	1	0	0	0	0	0	0	0	0	0	0
miR-4723-3p	0	0	1	0	0	0	0	0	0	0	0	0	0	0	0	0	0	1	0	0	0	0	0	0
miR-4727-5p	0	0	0	0	0	0	0	0	0	0	0	0	0	0	0	0	0	0	0	0	0	0	0	0
miR-4731-5p	0	0	0	0	0	0	0	0	0	0	0	0	0	0	0	0	0	0	0	0	0	0	0	0
miR-4732-3p	0	0	1	0	1	0	0	0	0	3	13	1	0	1	2	0	0	4	0	1	3	0	0	2
miR-4732-5p	0	1	5	0	3	2	0	1	2	3	19	6	0	5	3	2	0	10	0	1	6	0	2	4
miR-4741	0	0	0	0	0	0	0	0	0	0	0	0	0	0	0	0	0	0	0	0	0	0	0	1

miR-4742-3p	0	0	0	0	1	0	0	0	0	0	3	0	0	0	0	0	0	0	0	2	0	0	0	0
miR-4742-5p	0	0	0	0	0	0	0	0	0	0	0	0	0	0	0	0	0	0	0	0	0	1	0	0
miR-4743-5p	0	0	0	0	0	0	0	0	0	0	0	0	0	0	0	1	0	0	0	0	0	0	0	0
miR-4745-5p	0	0	0	0	1	0	0	0	0	0	0	0	0	0	0	0	0	0	0	0	0	0	0	0
miR-4746-5p	0	0	1	1	0	0	0	0	0	1	4	0	0	0	0	4	0	0	0	0	0	0	0	1
miR-4750-5p	0	0	0	0	0	0	0	0	0	0	0	0	0	0	0	0	0	0	0	0	0	0	0	0
miR-4763-3p	0	0	0	0	0	0	0	0	0	0	0	0	0	0	0	0	0	0	0	0	0	0	0	0
miR-4773	0	0	0	0	0	0	0	0	0	0	0	0	0	0	1	0	0	0	0	0	0	0	0	0
miR-4779	0	0	0	0	0	0	0	0	0	0	0	0	0	0	0	0	0	0	0	0	0	0	0	0

miR-4781-3p	0	0	0	0	0	0	0	0	0	0	0	0	0	0	0	2	0	0	0	0	0	0	0	2
miR-4800-5p	0	0	0	0	0	0	0	0	0	0	0	0	0	0	0	0	0	0	0	0	0	0	0	0
miR-4804-5p	0	0	0	0	0	0	0	0	2	0	0	0	0	0	0	0	0	0	0	0	0	0	0	0
miR-483-3p	0	0	0	0	0	0	0	0	0	0	0	2	0	0	0	0	0	0	0	0	0	0	0	0
miR-483-5p	0	0	1	0	5	3	0	1	3	0	0	1	0	0	0	8	0	3	5	5	0	1	0	2
miR-484	2	1	4	0	10	5	2	0	0	7	42	3	0	14	1	19	2	12	0	0	3	1	0	5
miR-485-3p	0	0	1	0	0	5	0	0	0	0	2	0	0	1	0	3	0	0	1	0	0	1	0	0
miR-485-5p	0	0	0	0	0	0	0	0	0	1	3	0	0	0	0	2	0	1	0	0	0	0	0	1
miR-486-3p	1	3	16	6	32	7	5	4	4	21	102	19	3	29	19	58	12	64	2	2	14	3	4	25

miR-486-5p	346	170	1355	524	1443	1271	319	585	354	874	11196	1055	224	1201	971	2158	407	3807	187	237	998	225	231	926
miR-490-3p	0	0	0	0	0	1	0	0	0	0	0	0	0	0	0	0	0	0	0	0	0	0	0	0
miR-493-3p	0	0	0	0	0	3	0	0	0	0	1	0	0	2	0	1	2	2	0	0	0	0	0	0
miR-493-5p	0	0	0	0	0	3	0	0	0	0	0	0	1	0	1	4	0	0	0	0	0	0	0	0
miR-495-3p	0	0	0	0	0	3	0	0	1	0	2	0	0	0	0	1	0	1	0	0	0	0	0	0
miR-499a-5p	0	0	0	0	3	0	0	0	0	0	0	0	0	0	0	0	0	0	0	0	0	0	0	1
miR-5009-5p	0	0	0	0	0	0	0	0	0	0	0	1	0	0	0	0	0	0	0	0	0	0	0	0
miR-500a-3p	0	0	0	0	4	0	0	0	0	0	0	1	0	2	0	0	0	1	0	0	0	0	0	1
miR-5010-3p	0	0	0	0	0	0	0	0	0	0	2	0	0	0	0	0	0	1	0	0	0	0	0	0

miR-5010-5p	0	0	0	0	0	0	0	0	0	0	1	0	0	0	0	0	1	4	0	0	0	0	0	1
miR-501-3p	0	0	0	2	7	6	0	0	3	3	21	2	0	7	2	9	0	8	0	2	1	0	0	2
miR-502-3p	0	0	0	1	0	2	0	0	0	0	1	0	0	0	0	1	0	0	0	0	0	0	0	0
miR-503-5p	0	0	2	0	3	3	0	0	0	1	3	2	0	3	0	0	0	1	0	0	2	1	0	1
miR-504-5p	0	0	0	0	0	0	0	0	0	0	0	1	1	0	0	1	0	1	0	0	0	0	1	0
miR-505-3p	0	0	0	0	0	0	0	0	0	0	0	0	0	0	0	1	0	0	0	0	0	0	0	0
miR-505-5p	0	0	0	0	1	4	1	0	1	1	11	3	1	1	0	1	0	4	0	0	0	0	0	1
miR-5090	0	0	0	0	0	0	1	1	1	0	0	0	0	0	0	0	0	0	0	0	0	0	0	0
miR-5091	0	0	0	0	0	0	0	0	0	0	0	0	0	0	0	0	0	0	0	0	0	0	0	0

miR-509-3-5p	0	0	0	0	0	0	0	0	0	0	0	0	0	0	0	0	0	0	0	0	0	0	0	0
miR-509-3p	0	0	0	0	0	0	0	0	0	0	0	1	0	0	0	0	0	0	0	0	0	0	0	0
miR-5100	0	0	0	0	1	0	0	0	0	0	0	0	0	0	0	0	0	0	0	0	0	0	0	0
miR-511-5p	0	1	0	0	1	0	0	0	7	0	8	0	0	0	0	2	0	2	0	0	0	0	0	0
miR-514a-3p	0	0	0	0	0	1	0	0	0	0	0	0	0	0	0	0	0	0	0	0	0	0	0	0
miR-516a-5p	0	0	0	0	0	0	0	0	0	0	0	1	0	0	0	0	0	0	0	0	0	0	0	0
miR-516b-5p	0	0	0	0	0	0	0	0	0	0	0	0	0	0	0	0	0	0	0	0	0	0	0	0
miR-5187-5p	0	0	0	0	0	0	0	0	0	0	0	0	0	0	0	0	0	0	0	1	0	0	0	0
miR-5189-5p	0	0	0	1	0	1	0	1	0	0	0	0	0	0	0	0	0	1	0	0	0	0	0	0

miR-520a-3p	0	0	0	0	0	0	0	0	0	0	0	0	0	0	0	0	0	0	0	0	0	0	0	0
miR-532-3p	0	0	0	0	0	0	0	0	0	0	0	0	0	0	0	0	0	1	0	0	0	0	0	1
miR-532-5p	6	4	15	5	19	20	4	4	9	14	126	14	5	10	11	36	9	59	2	6	12	7	3	16
miR-541-5p	0	0	0	0	1	0	0	0	0	0	0	0	0	0	0	0	0	0	0	0	1	0	0	0
miR-542-3p	0	0	1	0	0	0	0	0	0	0	0	0	0	0	0	0	0	0	0	0	0	0	0	0
miR-543	0	0	1	2	1	28	0	0	0	0	10	1	1	2	0	7	1	0	0	0	0	0	2	7
miR-548ac	0	0	0	0	0	0	0	0	0	0	0	0	0	0	0	0	0	0	0	0	0	0	0	0
miR-548e-3p	0	0	0	0	0	0	0	0	0	0	0	0	0	0	0	1	0	0	0	0	0	0	0	0
miR-548j-5p	0	0	0	0	0	1	0	0	0	0	1	0	0	0	0	0	0	0	0	0	0	0	0	1

miR-548o-3p	0	0	0	1	0	1	0	0	0	0	0	0	0	0	0	0	1	1	0	0	0	0	0	0
miR-550a-3-5p	0	0	0	0	0	0	0	0	0	0	0	0	0	3	0	1	0	0	0	0	0	0	0	0
miR-550a-5p	0	0	0	0	0	1	0	0	1	3	12	3	0	2	0	0	0	3	0	1	1	1	0	4
miR-551a	0	0	0	0	0	0	0	0	0	0	1	0	0	0	0	0	0	0	0	0	0	0	0	0
miR-556-5p	0	0	0	0	0	0	0	0	0	0	0	0	0	0	0	0	0	0	0	0	0	0	0	1
miR-570-3p	0	0	0	0	0	0	0	0	0	0	0	0	0	0	0	0	0	0	0	0	0	0	0	0
miR-574-3p	0	0	0	0	0	3	1	0	0	0	0	0	0	0	0	5	1	0	0	0	0	0	0	1
miR-574-5p	0	0	0	0	1	1	0	0	0	0	0	0	0	0	0	1	0	0	0	0	0	0	0	0
miR-576-3p	0	0	0	0	0	0	0	0	0	1	1	0	0	0	0	0	0	0	0	0	0	0	0	0

miR-576-5p	0	1	0	0	0	0	0	0	0	1	1	0	0	1	0	0	0	0	0	0	0	0	0	0
miR-579-5p	0	1	0	0	0	0	0	0	0	0	0	1	0	0	0	0	0	0	0	0	0	0	0	0
miR-580-3p	0	0	0	0	0	0	0	0	0	0	1	0	0	0	0	0	0	0	0	0	0	0	0	0
miR-581	0	0	0	0	0	0	0	0	0	0	0	0	0	0	0	0	0	0	0	0	0	0	0	0
miR-582-3p	0	1	0	1	1	0	0	0	1	1	2	0	0	0	0	2	0	0	1	0	0	1	0	0
miR-582-5p	0	0	0	0	0	0	0	0	0	0	0	0	0	0	0	0	0	0	1	0	0	0	0	0
miR-584-5p	0	3	5	1	12	16	0	2	2	5	45	12	5	5	4	54	1	27	1	1	7	4	2	6
miR-589-5p	0	0	0	0	0	1	0	0	0	0	2	1	0	0	0	0	0	1	0	0	0	0	0	0
miR-598-3p	0	0	0	0	0	0	0	0	0	0	0	0	0	0	0	0	0	0	0	0	0	0	0	0

miR-6068	0	0	0	0	0	0	0	0	0	0	0	0	0	0	0	0	0	0	0	0	0	0	0	0
miR-6087	0	0	0	0	0	0	0	0	0	0	0	0	0	0	0	0	0	0	0	0	0	0	0	0
miR-615-3p	0	0	0	0	0	0	0	0	0	3	2	0	0	0	0	11	0	3	0	0	0	0	0	1
miR-618	0	0	0	0	0	1	0	0	0	1	0	0	0	0	0	2	1	0	0	0	0	0	0	0
miR-624-5p	0	0	0	0	0	0	0	0	0	0	1	0	0	0	0	0	0	0	0	0	0	0	0	0
miR-625-3p	0	0	0	0	0	2	0	1	0	0	2	0	0	0	0	17	0	1	0	1	0	0	0	0
miR-625-5p	0	0	0	0	0	0	0	0	0	0	0	0	0	1	0	0	0	0	0	0	0	0	0	0
miR-627-5p	0	0	0	0	0	0	0	0	0	0	0	0	0	0	0	0	0	1	0	0	0	0	0	0
miR-628-3p	0	0	0	0	0	0	0	0	0	0	1	0	0	0	0	1	0	0	0	0	0	0	0	0

miR-628-5p	0	0	0	0	0	0	0	0	0	0	0	0	0	0	0	0	0	0	0	0	0	0	0	0
miR-629-3p	0	0	0	0	0	0	0	0	0	0	0	1	0	0	0	0	0	0	0	0	0	0	0	0
miR-629-5p	10	7	15	7	10	14	2	3	4	10	97	10	2	12	9	27	3	67	0	7	23	9	2	11
miR-636	0	0	0	0	0	0	0	0	0	0	0	0	0	0	0	0	0	0	0	0	0	0	0	0
miR-642a-3p	0	0	0	0	0	0	0	0	1	0	0	0	0	0	0	0	0	0	0	0	0	0	0	0
miR-6503-3p	0	1	0	0	0	0	0	0	0	0	0	0	0	0	0	0	0	0	0	0	0	0	0	0
miR-6509-5p	0	0	0	0	0	0	0	0	0	0	0	0	0	0	0	1	0	0	0	0	0	0	0	0
miR-6510-3p	0	0	0	0	1	0	0	0	0	0	0	0	0	0	0	0	0	0	0	0	1	0	0	0
miR-6511a-3p	0	0	0	0	0	0	0	0	0	0	0	0	0	0	0	0	0	1	0	0	0	0	0	0

miR-6511b-3p	0	0	0	0	0	0	0	0	0	0	1	0	0	0	0	0	0	0	0	0	0	0	0	0
miR-6511b-5p	0	0	0	0	0	0	0	0	0	0	0	0	0	0	0	0	0	0	0	0	0	0	0	0
miR-6515-5p	0	0	0	0	0	0	0	0	0	0	1	0	0	0	0	0	0	0	0	0	0	0	0	0
miR-651-5p	0	0	1	0	0	0	0	0	0	0	0	0	0	0	0	0	0	2	0	0	0	0	0	0
miR-6516-5p	0	0	0	0	0	0	0	0	0	0	0	0	0	0	0	0	0	0	0	0	0	0	0	0
miR-652-3p	0	0	0	0	1	2	0	0	0	0	19	1	0	1	0	2	0	1	0	0	0	0	0	0
miR-654-3p	0	0	0	0	0	2	0	0	0	0	2	1	0	1	0	1	0	0	1	0	0	0	0	0
miR-654-5p	0	0	0	0	0	3	0	0	0	0	1	0	1	0	0	1	0	1	0	0	0	0	0	0

miR-655-3p	0	0	0	0	0	0	0	0	0	0	0	0	0	0	0	0	0	0	0	0	0	0	0	0
miR-658	0	0	0	0	0	0	0	0	0	0	0	0	0	0	0	0	0	0	0	0	0	0	0	0
miR-659-5p	0	0	0	0	0	0	0	0	0	0	0	0	0	0	0	0	1	0	0	0	0	0	0	0
miR-660-5p	0	0	0	0	0	0	0	0	0	0	0	0	0	0	0	0	0	1	0	0	0	0	0	0
miR-661	0	0	0	0	0	0	0	0	0	0	0	1	0	0	0	0	0	0	0	0	0	0	0	0
miR-664a-3p	0	0	0	0	0	1	0	0	0	0	0	0	0	0	0	0	0	0	0	0	0	0	0	0
miR-664a-5p	1	2	0	2	2	2	0	0	1	1	6	0	0	4	0	17	0	4	0	0	1	1	0	0
miR-664b-5p	0	0	0	0	0	0	0	0	0	0	0	0	0	0	0	0	0	0	0	0	0	0	0	0
miR-671-3p	0	0	0	0	1	0	0	0	0	0	0	1	0	0	0	1	0	0	0	0	0	0	0	0

miR-6715a-3p	0	0	0	0	0	0	0	0	0	0	0	0	0	0	0	0	0	0	0	0	0	0	0	0
miR-6716-3p	0	0	0	0	0	0	0	0	0	0	1	0	0	0	0	0	0	0	0	0	0	0	0	0
miR-6717-5p	0	0	1	0	0	0	0	0	0	0	0	0	0	0	0	0	0	0	0	1	0	0	0	0
miR-6721-5p	0	0	0	0	0	1	0	0	0	0	0	0	0	0	0	0	0	0	0	0	0	0	0	0
miR-6723-5p	0	0	0	0	0	0	0	0	0	0	0	0	0	0	0	0	0	0	0	0	0	0	0	0
miR-6727-5p	0	0	0	2	0	0	0	0	0	0	0	0	0	0	0	0	0	0	0	0	0	0	0	0
miR-6730-5p	0	0	0	0	0	0	0	0	0	0	0	0	0	0	0	1	0	0	0	0	0	0	0	0
miR-6734-3p	0	0	0	0	0	0	0	0	0	0	0	0	0	0	0	0	0	0	0	0	0	0	0	0
miR-6734-5p	0	0	0	0	0	0	0	0	0	0	2	0	0	0	0	0	0	0	0	0	0	0	0	0

miR-6735-3p	0	0	0	0	0	0	0	0	0	0	0	0	0	0	0	0	0	0	0	0	0	0	0	0
miR-6735-5p	0	0	0	0	0	0	0	0	0	0	0	0	0	1	0	0	0	2	0	0	0	0	0	0
miR-6736-5p	0	0	0	0	0	0	0	0	0	0	0	0	0	0	0	0	0	1	0	0	0	0	0	0
miR-6738-3p	0	0	0	0	0	0	0	0	0	0	0	0	0	0	0	0	0	0	1	0	0	0	0	0
miR-6741-3p	0	0	0	0	0	2	0	2	0	1	0	0	0	0	0	0	0	0	0	0	0	0	0	0
miR-6741-5p	0	0	0	0	0	0	0	0	0	0	0	0	0	0	0	0	0	2	0	0	0	0	0	0
miR-6747-3p	0	0	0	0	1	0	0	0	0	0	0	0	0	0	0	0	0	0	0	0	0	0	0	1
miR-6750-3p	0	0	0	0	0	0	0	0	0	0	0	0	0	0	0	0	0	1	0	0	0	0	0	0
miR-6750-5p	0	0	0	1	0	0	0	0	0	0	0	0	0	0	0	0	0	0	0	0	0	0	0	0

miR-6767-5p	0	0	0	0	0	0	0	0	0	0	0	1	0	0	0	0	0	1	0	0	0	0	0	0
miR-6770-3p	0	0	0	0	0	0	0	0	0	0	0	0	0	0	0	0	0	2	0	0	0	0	0	0
miR-6772-3p	0	0	0	0	0	1	0	0	0	0	0	0	0	0	0	0	0	0	0	0	0	0	0	0
miR-6777-5p	0	0	1	0	0	0	0	0	0	0	0	0	0	0	0	0	0	1	0	0	0	0	0	0
miR-6780a-5p	0	0	0	0	0	0	1	0	0	0	0	0	0	0	0	0	0	1	0	0	0	0	0	0
miR-6781-5p	0	0	0	0	0	0	0	0	0	0	0	0	0	0	0	0	0	0	0	0	0	0	0	0
miR-6785-5p	0	0	0	0	0	0	0	0	0	0	0	0	0	0	1	0	0	0	0	0	0	0	0	0
miR-6786-3p	0	0	0	0	0	0	0	0	0	0	2	0	0	0	0	0	0	0	0	0	0	0	0	0
miR-6787-3p	0	0	0	0	0	0	0	0	0	0	0	0	0	0	0	0	0	0	0	0	0	0	0	0

miR-6788-3p	0	0	0	0	0	0	0	0	0	0	0	0	0	0	0	0	0	0	1	0	0	0	0	0
miR-6790-3p	0	0	0	0	0	0	0	0	0	0	0	0	0	0	0	0	0	0	0	0	0	0	0	0
miR-6793-5p	0	0	0	0	0	0	0	0	0	0	0	0	0	0	0	0	0	0	0	0	0	0	0	0
miR-6802-5p	0	0	0	0	0	0	0	0	0	0	0	0	0	0	0	1	0	0	0	0	0	0	0	0
miR-6803-3p	0	0	0	0	0	0	0	0	0	0	0	0	0	0	0	0	0	0	0	0	0	0	0	0
miR-6805-5p	0	0	0	0	0	0	0	0	0	0	1	0	0	0	0	0	0	0	0	0	1	0	0	0
miR-6806-3p	0	0	0	0	0	0	0	0	0	0	0	0	0	0	0	0	0	1	0	0	0	0	0	0
miR-6808-3p	0	0	0	0	0	0	0	0	0	0	0	0	0	0	0	1	0	0	0	0	0	0	0	1
miR-6812-3p	0	0	0	0	0	0	0	0	0	0	0	0	0	0	0	0	0	0	0	0	0	0	0	0

miR-6813-5p	0	0	0	0	0	0	0	0	0	0	0	0	0	0	0	2	0	0	0	0	0	0	0	0
miR-6815-5p	0	0	1	0	0	0	0	0	0	0	3	1	0	0	0	1	0	0	0	0	0	0	0	0
miR-6821-5p	0	0	0	0	0	0	0	0	0	0	0	0	0	0	0	0	0	0	0	0	0	0	0	0
miR-6826-5p	1	0	0	0	0	0	0	0	0	0	0	0	0	0	0	0	0	0	0	0	0	0	0	0
miR-6837-3p	0	0	0	0	0	1	0	0	0	0	0	0	1	0	0	0	0	0	0	0	0	0	0	0
miR-6839-5p	0	0	0	0	0	0	0	0	0	1	0	0	0	0	0	0	0	0	0	0	0	0	0	0
miR-6842-3p	0	0	0	0	0	0	0	0	0	1	0	2	0	0	0	0	0	2	0	0	1	0	0	0
miR-6842-5p	0	0	0	0	0	1	0	0	0	0	0	0	0	0	0	4	0	0	0	1	0	0	0	0
miR-6847-5p	0	0	0	0	0	0	0	0	0	0	0	0	0	0	0	0	0	0	0	0	0	0	0	0

miR-6849-5p	0	0	0	0	0	0	0	0	0	0	0	0	0	0	0	0	0	0	0	0	0	0	0	0
miR-6850-5p	0	0	1	0	0	0	0	0	0	0	0	0	0	0	0	0	0	0	0	0	0	1	0	0
miR-6852-5p	0	0	0	0	0	0	0	0	0	0	0	0	0	0	0	1	0	0	0	0	0	0	1	1
miR-6859-5p	0	0	0	0	0	0	0	0	0	0	0	0	0	0	0	0	0	0	0	0	1	0	0	0
miR-6862-5p	0	0	1	0	0	0	0	0	0	0	0	0	0	0	0	0	0	0	0	0	0	0	0	0
miR-6865-5p	0	0	0	0	0	0	0	0	0	0	0	0	0	0	0	0	0	0	0	0	0	0	0	0
miR-6866-5p	0	0	0	0	0	0	0	0	0	0	0	0	0	0	0	0	0	1	0	0	1	0	0	0
miR-6868-3p	0	0	0	0	0	0	0	0	0	0	0	0	0	0	0	0	0	0	0	0	1	0	0	0
miR-6869-5p	0	0	0	0	1	1	1	0	0	0	1	0	0	0	0	0	0	0	1	0	1	1	0	0

miR-6873-3p	0	0	0	0	0	0	0	0	1	0	0	0	0	0	0	0	0	0	0	0	0	0	0	0
miR-6877-5p	0	0	0	0	0	0	0	0	0	0	0	0	0	0	0	0	0	1	0	0	0	0	0	0
miR-6881-3p	0	0	0	0	0	0	0	0	0	0	1	0	0	0	0	0	0	0	0	0	0	0	0	0
miR-6884-5p	0	0	0	0	0	0	0	0	0	0	0	0	0	0	0	0	0	0	0	0	0	0	0	0
miR-7107-3p	0	1	3	0	0	0	0	0	1	0	0	0	0	0	0	0	0	0	0	0	0	2	0	1
miR-7110-3p	0	0	0	0	0	0	0	0	0	0	0	0	0	1	0	0	0	0	0	0	0	0	0	0
miR-744-5p	1	2	2	0	7	46	1	1	2	7	22	4	4	15	1	59	1	6	3	7	3	12	1	4
miR-758-3p	0	0	0	0	0	1	0	0	0	0	0	0	1	0	0	0	0	0	0	0	0	0	0	2
miR-7-5p	3	0	6	1	19	2	0	3	0	10	77	8	0	12	7	10	2	23	4	3	7	3	0	11

miR-760	0	1	0	0	0	0	0	0	0	0	0	1	0	0	0	1	0	0	0	0	0	1	0	0
miR-766-5p	0	0	0	0	0	0	0	0	0	0	0	0	0	1	0	0	0	0	0	0	0	0	0	1
miR-769-5p	0	0	0	0	2	0	0	0	0	1	5	0	0	0	0	2	0	1	0	0	1	0	0	1
miR-7704	0	0	0	0	3	0	0	0	1	0	0	1	0	1	0	3	0	0	0	0	0	0	0	2
miR-7706	0	1	1	0	2	1	0	0	1	1	13	0	0	0	0	3	0	2	0	0	2	0	0	0
miR-7848-3p	0	0	0	0	0	0	0	0	0	1	0	0	0	0	0	0	1	0	0	0	0	0	0	0
miR-7854-3p	0	0	0	0	0	0	0	0	0	0	0	0	0	0	0	1	0	0	0	0	0	0	0	0
miR-7976	0	0	0	0	0	0	0	0	0	0	2	0	0	0	0	1	0	0	0	0	0	0	0	0
miR-873-5p	0	1	0	0	0	0	0	0	1	0	0	0	0	0	0	0	0	0	0	0	0	0	0	0

miR-874-3p	0	0	0	0	0	0	0	0	0	0	0	0	0	0	0	0	0	0	0	0	0	0	0	0
miR-877-5p	0	0	0	0	0	0	0	0	0	0	1	0	0	0	0	0	0	0	0	0	0	0	0	0
miR-885-3p	0	0	0	0	0	0	0	0	0	0	0	0	0	0	0	7	0	0	0	0	0	0	0	0
miR-885-5p	0	0	0	0	0	0	0	0	0	0	0	0	0	0	0	4	0	0	0	0	0	0	0	0
miR-889-3p	0	0	0	0	0	0	0	0	0	0	0	0	0	1	0	0	0	0	0	0	0	0	1	0
miR-92a-1-5p	0	0	0	0	0	0	0	0	0	0	1	0	0	0	0	1	1	0	0	0	0	0	0	0
miR-92a-2-5p	0	0	0	0	1	0	0	0	0	0	0	0	0	0	0	0	0	0	0	0	0	0	0	0
miR-92a-3p	142	106	545	199	1038	620	114	180	162	374	4255	527	145	644	424	985	178	2320	65	216	489	251	75	464

miR-92b-3p	1	2	6	5	18	7	0	3	5	24	35	4	2	23	3	28	3	20	1	2	2	2	3	4
miR-92b-5p	1	0	0	1	1	0	0	0	0	2	11	0	0	4	0	1	0	2	0	1	5	0	0	0
miR-93-5p	0	0	3	3	11	3	0	3	0	0	34	3	0	3	2	3	3	10	0	1	4	1	1	2
miR-937-3p	0	0	0	0	0	0	0	0	0	0	0	0	0	0	0	0	0	0	0	0	0	0	0	0
miR-939-5p	0	0	0	0	0	0	0	0	0	0	1	0	0	0	0	0	0	0	0	0	0	0	0	0
miR-9-3p	0	0	0	0	0	0	0	0	0	0	0	0	0	0	0	0	0	0	0	0	0	0	0	0
miR-941	1	1	1	0	1	5	3	0	1	5	23	1	0	4	2	10	2	4	0	2	1	0	1	2
miR-942-3p	0	0	0	0	0	0	0	0	0	0	0	0	0	0	0	0	0	0	0	0	0	0	0	0
miR-942-5p	0	0	0	0	0	0	0	0	0	0	5	0	0	1	0	1	0	0	0	0	0	0	0	0

miR-95-3p	0	0	0	0	0	0	0	0	0	0	2	0	1	1	0	3	0	1	0	0	0	0	0	0
miR-9-5p	0	0	0	0	1	0	0	0	0	0	8	0	0	1	1	0	0	1	0	0	3	3	0	2
miR-96-5p	1	2	1	0	0	0	1	0	0	1	6	0	0	0	0	0	0	1	0	0	0	0	0	1
miR-98-5p	3	2	2	1	14	35	0	1	2	2	31	4	3	12	2	19	5	9	0	4	0	10	1	10
miR-99a-5p	37	21	38	54	353	68	25	8	41	155	416	115	21	35	23	550	34	549	21	56	59	157	7	87
miR-99b-3p	0	0	0	0	4	2	0	0	0	1	2	0	0	0	0	2	0	0	0	5	1	0	0	0
miR-99b-5p	19	17	6	23	96	71	5	11	24	34	50	18	13	31	7	107	17	62	4	23	43	31	9	26
	treatment-naive Pca																							
ID	BCI 010	BCI 012	BCI 013	BCI 014	BCI 018	BCI 019	BCI 020	BCI 021	BCI 022	BCI 023	BCI 025	BCI 026	BCI 027	BCI 029	BCI 030	BCI 031	BCI 032	BCI 033	BCI 034	BCI 036	BCI 037	BCI 054	BCI 055	BCI 057
let-7a-3p	2	0	0	0	1	0	0	2	0	2	1	2	0	0	0	0	0	1	0	1	1	0	2	4

let-7a-5p	192	84	77	371	348	307	155	2550	477	152	209	175	170	56	105	425	128	763	193	293	992	73	808	899
let-7b-3p	0	1	0	1	1	1	1	15	3	0	2	1	0	0	0	3	0	2	1	0	3	1	4	2
let-7b-5p	338	427	400	564	466	343	283	7160	936	218	964	259	635	176	207	973	229	832	678	467	1604	251	918	1499
let-7c-3p	0	0	0	0	0	0	0	0	0	0	0	0	0	0	0	0	0	0	0	0	0	0	0	0
let-7c-5p	11	13	9	25	31	30	17	156	53	11	26	23	15	1	9	57	7	68	27	32	103	12	74	79
let-7d-3p	7	12	13	27	14	22	10	169	44	9	28	12	15	0	2	35	15	23	25	17	70	14	46	56
let-7d-5p	5	3	4	12	14	20	10	194	20	16	5	14	4	2	2	19	2	42	8	14	62	2	47	51
let-7e-3p	0	0	0	0	0	0	0	0	0	0	0	0	0	0	0	0	0	0	0	0	1	0	0	0
let-7e-5p	7	8	3	8	24	8	0	74	15	3	8	2	8	2	4	10	5	20	14	6	59	5	20	38

let-7f-1-3p	0	0	0	0	0	0	0	0	0	0	0	0	0	0	0	0	0	0	0	0	0	0	0	0
let-7f-5p	90	38	40	156	157	103	72	936	187	57	95	61	80	16	37	167	34	259	77	101	425	42	351	365
let-7g-5p	32	15	46	72	70	65	40	659	108	26	47	40	25	8	27	103	28	147	28	47	233	23	151	199
let-7i-3p	0	0	0	0	0	0	0	0	0	0	0	0	0	0	0	0	0	0	0	0	0	0	0	0
let-7i-5p	175	143	115	466	252	129	193	2538	414	125	294	134	176	54	143	369	107	412	213	283	705	123	541	832
miR-1	1	0	3	0	2	2	0	1	0	0	1	1	7	0	8	0	5	1	0	0	0	0	2	2
miR-100-5p	6	0	9	0	2	6	1	36	5	26	1	1	46	1	127	2	90	5	0	11	26	1	10	16
miR-101-3p	6	3	10	20	21	14	13	277	27	5	33	13	13	5	4	29	12	17	6	20	38	3	18	41
miR-103a-3p	1	1	1	5	4	4	4	49	3	1	2	5	0	0	1	6	3	12	5	2	15	2	12	16
miR-105-5p	0	0	0	0	0	0	0	0	0	0	0	0	0	0	0	0	0	0	0	0	0	0	0	0

miR-106a-5p	0	0	0	0	0	0	0	1	1	0	0	0	0	0	0	0	0	0	0	0	0	0	0	3
miR-106b-3p	0	1	7	16	5	0	3	84	8	1	9	2	3	2	4	8	4	6	3	10	9	2	8	7
miR-106b-5p	0	0	0	0	2	3	0	5	1	1	0	1	0	0	0	0	0	0	0	0	1	0	2	0
miR-107	1	1	2	0	1	1	1	17	2	0	1	1	0	0	0	0	0	1	0	0	0	0	3	2
miR-10a-3p	0	0	0	0	0	0	0	1	0	0	0	0	0	0	0	0	0	0	0	0	0	0	1	0
miR-10a-5p	16	16	11	33	30	20	10	164	30	14	19	12	35	2	13	48	8	52	43	24	114	13	52	62
miR-10b-3p	0	0	0	0	0	0	0	0	0	0	0	0	0	0	0	0	0	0	0	0	0	0	0	1
miR-10b-5p	28	30	18	60	71	57	20	268	59	22	21	25	59	5	19	85	16	89	61	38	213	8	110	132
miR-1180-3p	1	1	2	3	2	1	0	36	2	4	0	3	0	0	0	2	2	6	0	2	5	0	6	15

miR-1183	0	1	0	0	0	0	0	1	0	0	0	0	0	0	1	0	0	0	0	0	0	0	0	0
miR-1185-1-3p	0	0	0	0	0	0	0	0	0	0	1	0	0	0	0	0	0	0	0	0	0	0	0	0
miR-1193	0	0	0	0	0	0	0	0	0	0	0	0	0	0	0	0	0	0	0	0	0	0	0	0
miR-1224-5p	0	0	0	0	0	0	0	0	2	0	0	0	0	0	0	0	0	0	0	1	0	0	0	0
miR-1225-5p	0	0	0	0	0	0	0	0	0	0	0	0	0	0	0	1	0	0	0	0	0	0	0	0
miR-122-5p	63	55	104	126	237	53	212	536	1595	63	239	125	110	75	55	115	161	176	337	111	1244	200	178	574
miR-1226-3p	0	0	0	0	0	0	0	0	0	0	0	0	0	0	0	0	0	0	0	0	0	0	0	0
miR-1228-5p	0	0	0	0	0	0	0	3	0	0	0	0	1	0	0	0	0	1	0	0	0	0	0	0
miR-1229-3p	0	0	0	0	0	0	0	0	0	0	0	0	0	0	0	0	0	0	0	0	0	0	0	0

miR-124-3p	0	0	0	0	0	0	0	0	0	0	0	0	0	0	0	0	0	0	0	0	3	0	0	0
miR-1246	0	0	1	0	1	0	0	2	1	0	0	0	0	0	0	0	2	0	0	0	2	0	0	0
miR-1248	0	0	0	0	0	0	1	2	0	0	2	0	0	0	0	0	0	0	0	0	0	0	0	1
miR-1249	0	0	0	0	0	0	0	0	1	0	0	0	0	0	0	0	0	0	0	0	1	0	0	0
miR-1254	0	0	0	0	0	0	0	0	0	0	0	1	0	0	0	0	0	0	0	0	0	0	0	0
miR-1255a	0	0	0	0	0	0	0	0	0	0	0	0	0	0	0	0	0	0	0	1	0	0	0	1
miR-1255b-5p	0	0	0	0	0	0	0	0	0	0	0	0	0	0	0	0	0	0	0	0	0	0	0	0
miR-125a-3p	0	0	0	0	0	0	0	2	0	1	1	0	0	0	0	0	0	0	0	1	0	0	1	0
miR-125a-5p	8	4	8	12	8	11	7	80	8	4	5	8	10	0	3	14	2	27	21	6	74	4	18	38

miR-125b-1-3p	0	0	0	0	0	0	0	0	0	0	0	0	0	0	0	0	0	0	0	0	0	0	0	0
miR-125b-2-3p	0	0	0	0	0	0	0	0	1	0	0	0	0	0	0	0	0	0	0	0	0	0	0	0
miR-125b-5p	0	1	0	1	2	0	1	5	5	2	0	2	1	0	0	1	2	1	1	1	11	0	1	5
miR-1261	0	0	0	0	0	0	0	1	0	0	0	0	0	0	0	0	0	0	0	0	0	0	0	0
miR-126-3p	415	548	238	933	1006	733	274	5767	1051	465	229	380	379	101	225	1213	160	1437	934	573	3183	145	1791	2174
miR-126-5p	1	2	0	5	0	3	1	18	1	4	0	2	0	0	0	1	0	6	1	3	8	0	6	12
miR-1270	0	0	0	0	0	0	0	0	0	0	1	0	0	0	0	0	0	0	0	0	0	0	0	0
miR-1271-5p	0	0	0	0	0	0	0	0	0	0	0	0	0	0	0	0	0	0	0	0	0	0	0	0

miR-1273h-3p	0	0	0	0	0	0	0	0	0	0	0	0	0	0	0	0	0	0	0	0	0	0	0	0
miR-127-3p	0	0	0	0	0	0	0	0	0	0	2	0	0	0	0	0	0	1	1	0	0	1	0	0
miR-1277-5p	0	0	0	0	1	0	0	0	0	0	0	0	0	0	0	0	0	0	0	0	0	0	0	0
miR-1278	0	0	0	0	0	0	0	3	0	0	0	0	0	0	0	0	1	0	0	0	0	0	0	0
miR-128-3p	6	9	18	26	24	26	7	143	30	4	11	10	10	4	6	45	9	17	12	17	106	9	42	73
miR-1284	0	0	0	0	0	0	0	1	0	0	0	0	0	0	0	0	0	0	0	0	0	0	0	0
miR-1287-5p	0	0	0	0	0	0	0	0	0	0	0	0	0	0	0	1	0	0	0	0	0	0	0	0
miR-1288-3p	0	0	0	0	0	0	0	0	0	0	0	0	0	0	0	0	0	0	0	0	0	0	0	0
miR-1292-5p	0	0	0	0	0	0	0	0	1	0	0	1	0	0	0	0	0	0	0	1	0	0	0	0

miR-1293	0	0	0	0	0	0	0	1	0	0	0	0	0	0	0	0	0	0	0	0	0	0	0	0
miR-1294	0	0	0	0	0	1	0	3	0	0	0	0	0	0	0	0	0	1	0	0	0	0	1	1
miR-1295a	0	0	0	0	0	0	0	0	0	0	0	0	1	0	0	0	0	0	0	0	0	0	0	0
miR-129-5p	0	0	0	0	1	0	0	1	0	0	0	0	0	0	1	0	0	0	3	0	8	0	0	0
miR-1299	0	0	0	1	0	0	0	2	0	0	0	0	0	0	0	0	0	0	0	0	0	0	0	2
miR-1301-3p	0	0	0	1	4	1	0	0	1	0	2	0	0	0	0	1	0	1	5	1	2	0	0	0
miR-1304-3p	0	0	0	0	0	0	0	0	2	0	0	0	0	0	0	0	0	0	0	0	0	0	0	0
miR-1306-3p	0	0	0	0	0	0	0	1	0	0	0	0	0	0	0	0	0	0	0	0	0	0	0	0
miR-1306-5p	0	0	0	0	0	0	0	0	0	1	0	0	0	0	0	1	0	0	0	0	2	0	0	0

miR-1307-3p	1	1	2	8	3	7	1	38	5	0	4	4	1	0	0	3	2	4	0	1	7	2	12	6
miR-1307-5p	0	1	0	0	1	0	0	8	0	0	2	0	1	0	0	0	0	1	0	0	2	1	1	0
miR-130a-3p	0	0	1	0	0	0	0	1	0	0	0	0	0	0	0	0	0	1	0	2	0	0	2	2
miR-130b-3p	1	0	1	0	0	0	0	0	0	0	0	1	0	1	0	0	0	0	0	0	0	0	0	1
miR-130b-5p	0	0	0	0	0	1	0	0	0	0	0	0	0	0	0	2	0	0	0	1	0	0	0	1
miR-1323	0	0	0	0	0	0	0	0	0	0	0	0	0	0	0	0	0	0	0	0	0	0	0	0
miR-132-3p	0	0	0	0	0	0	0	0	0	0	0	0	0	0	0	0	0	1	0	0	0	0	0	0
miR-132-5p	0	0	0	0	0	0	0	2	0	1	0	0	0	0	0	0	0	0	0	0	0	0	1	0
miR-1343-3p	0	0	0	0	0	0	0	0	0	0	0	0	0	0	0	0	0	0	0	1	0	0	0	0

miR-134-5p	0	0	2	0	1	0	0	0	1	0	0	0	0	0	0	0	0	0	0	1	1	0	0	1
miR-135a-5p	0	0	0	0	0	0	0	0	0	0	0	0	2	0	0	0	0	0	0	0	0	0	0	0
miR-136-3p	0	0	0	0	0	0	0	0	0	0	0	0	0	0	0	0	0	0	0	0	0	0	0	0
miR-136-5p	0	0	0	0	0	0	0	0	0	0	0	0	0	0	0	0	0	0	0	0	0	0	0	0
miR-138-5p	0	0	0	0	0	0	0	1	0	0	0	0	0	0	0	0	0	0	0	0	0	0	0	0
miR-139-3p	1	1	0	9	4	0	0	11	2	1	2	0	7	1	1	4	1	4	3	1	21	2	5	5
miR-139-5p	16	6	4	24	13	17	3	69	14	12	2	3	9	0	4	22	3	27	15	12	65	3	17	34
miR-140-3p	0	1	3	2	2	2	2	21	3	0	2	4	2	1	2	2	0	1	2	2	12	0	2	4
miR-140-5p	0	0	0	1	0	0	0	2	1	0	0	1	0	0	0	1	0	1	1	3	3	0	1	7

miR-141-3p	0	0	0	0	0	0	0	0	0	0	0	0	0	0	0	0	0	0	0	0	0	0	0	0
miR-142-3p	2	0	1	6	5	7	4	27	1	1	1	5	0	0	0	5	0	5	7	5	11	2	11	12
miR-142-5p	0	1	3	1	5	4	1	22	3	1	1	1	0	0	2	3	3	1	1	5	9	1	11	3
miR-143-3p	5	3	0	19	8	5	2	20	10	3	5	6	16	1	5	11	0	8	7	13	35	1	22	22
miR-144-3p	0	1	1	1	2	2	1	21	3	0	0	0	1	0	0	3	1	6	3	3	10	0	2	2
miR-144-5p	0	0	3	2	2	1	1	15	2	1	0	4	0	0	0	3	0	5	1	3	12	2	12	6
miR-145-3p	0	0	0	1	0	0	0	0	0	0	0	0	0	0	0	0	0	0	0	0	1	0	1	1
miR-145-5p	0	0	0	0	0	0	0	0	0	0	0	0	0	0	0	0	0	0	0	0	1	0	0	0
miR-1468-5p	0	0	0	0	0	0	0	0	0	0	0	0	0	1	0	0	0	1	0	0	0	0	0	0

miR-146a-5p	1	1	1	9	6	8	7	45	8	0	7	4	1	1	5	10	1	17	9	5	24	2	14	20
miR-146b-3p	0	0	0	0	0	0	0	0	0	0	0	0	0	0	0	0	0	0	0	0	0	0	0	0
miR-146b-5p	0	1	2	1	4	4	1	45	8	1	0	4	0	1	2	8	0	18	8	3	23	1	6	15
miR-147b	0	0	0	1	0	0	0	0	0	0	0	0	0	0	0	0	0	0	0	0	0	0	0	0
miR-148a-3p	80	75	103	317	160	111	146	1234	321	57	315	111	228	42	105	227	109	137	175	151	325	110	260	475
miR-148a-5p	0	0	0	0	0	0	0	0	0	0	0	0	0	0	0	0	0	0	0	0	0	0	2	1
miR-148b-3p	1	6	8	19	6	11	7	77	12	4	10	2	4	0	6	13	7	7	4	8	17	4	6	26
miR-149-5p	0	0	0	0	0	0	0	0	0	0	0	0	0	0	0	0	0	0	0	0	2	0	0	0
miR-150-3p	0	0	0	3	1	4	0	4	6	0	4	3	2	0	0	5	0	6	0	2	1	0	2	4

miR-150-5p	4	1	12	15	6	17	6	93	8	3	4	11	1	1	4	18	2	45	14	10	66	6	40	42
miR-151a-3p	16	10	10	67	18	14	12	168	34	6	53	11	32	2	17	27	15	20	14	23	55	8	26	70
miR-151a-5p	0	0	0	0	0	0	0	1	0	0	0	0	0	0	0	0	0	0	0	0	0	0	0	0
miR-152-3p	0	3	0	1	0	0	0	3	0	1	0	0	0	0	0	0	0	0	3	0	2	0	0	4
miR-152-5p	0	0	0	0	0	0	0	0	0	0	0	0	0	0	0	0	0	0	0	0	0	0	0	0
miR-153-3p	0	0	1	0	0	0	0	0	0	0	0	0	0	0	0	0	0	0	0	0	0	0	0	0
miR-155-5p	2	11	5	4	4	6	5	32	6	2	0	2	1	3	3	12	1	10	13	6	39	0	20	15
miR-15a-5p	0	0	0	0	1	0	0	1	0	0	0	0	0	0	0	1	0	0	0	0	0	0	1	1
miR-15b-3p	0	0	0	0	0	0	0	3	0	0	0	0	0	0	0	1	0	0	0	1	1	0	0	1

miR-15b-5p	1	1	0	7	3	1	1	37	2	1	1	1	0	0	4	3	2	2	2	1	5	0	2	3
miR-16-2-3p	0	3	1	4	11	7	3	64	11	0	5	4	0	1	0	8	3	9	2	5	7	1	10	13
miR-16-5p	7	3	11	16	24	23	6	204	28	7	9	19	5	4	3	23	6	30	4	20	37	5	34	29
miR-17-3p	0	0	0	0	0	0	0	0	0	0	0	0	0	1	0	1	0	0	0	0	0	0	0	0
miR-17-5p	0	0	0	2	0	0	1	6	0	1	0	1	0	0	0	1	1	4	0	1	8	0	2	3
miR-181a-2-3p	0	0	0	1	1	0	0	4	0	0	0	0	1	0	0	2	0	0	0	0	2	0	0	2
miR-181a-3p	0	0	0	0	0	1	0	0	0	0	1	0	0	0	0	0	0	0	0	0	0	0	0	0
miR-181a-5p	4	10	4	16	25	11	3	124	12	13	6	6	10	1	5	25	8	21	15	8	50	2	29	47
miR-181b-5p	1	0	0	2	1	1	1	15	3	0	1	0	1	0	0	2	0	3	1	1	13	0	5	3

miR-181c-3p	0	0	0	0	0	0	0	0	0	0	0	0	0	0	0	0	0	0	0	1	0	0	0	0
miR-181c-5p	0	0	0	0	0	0	0	0	0	0	0	0	0	0	0	0	0	0	0	0	1	0	0	0
miR-181d-5p	0	0	0	0	0	0	0	0	0	0	0	1	0	0	0	0	0	1	0	1	1	0	0	0
miR-182-5p	10	3	2	12	2	4	4	112	12	4	5	2	1	0	2	6	6	17	3	3	27	1	20	26
miR-183-5p	3	4	5	14	7	8	1	86	9	6	5	3	2	2	2	8	11	24	1	17	24	6	21	35
miR-184	3	1	0	1	2	3	2	26	2	0	2	2	0	1	118	0	1	3	0	1	0	0	1	8
miR-185-3p	0	0	0	0	0	0	1	1	1	0	0	0	0	0	0	1	0	0	2	0	0	0	0	0
miR-185-5p	6	3	14	17	10	44	4	228	36	9	11	27	9	2	5	19	7	35	7	10	50	2	37	46
miR-186-5p	5	3	6	7	11	6	3	86	17	0	8	9	3	1	1	6	6	15	1	8	25	2	5	14

miR-188-3p	0	0	0	0	0	0	0	0	0	0	0	0	0	0	0	0	0	0	0	1	0	0	0	0
miR-188-5p	0	0	0	0	0	1	0	0	0	0	0	0	0	0	0	0	0	0	0	0	0	0	0	0
miR-18a-3p	0	0	0	0	0	0	0	0	0	0	0	1	0	0	0	1	0	0	0	0	1	0	0	4
miR-18a-5p	0	0	0	0	0	2	0	0	0	0	0	0	0	0	0	0	0	1	0	0	2	0	0	0
miR-18b-5p	0	0	0	0	0	0	0	0	0	0	0	0	0	0	0	0	0	0	0	0	0	0	2	0
miR-1908-5p	0	1	1	2	0	0	1	17	1	0	0	3	0	0	1	1	1	3	0	0	4	0	4	7
miR-190a-5p	0	0	0	0	0	0	0	0	0	0	0	0	0	0	0	0	0	1	0	0	0	0	0	0
miR-191-3p	0	0	0	0	0	0	0	0	0	0	0	0	0	0	0	0	0	0	0	0	0	0	0	0
miR-1914-5p	0	0	0	0	0	0	0	0	0	0	0	0	0	0	0	0	0	0	0	0	0	0	0	0

miR-191-5p	9	6	12	28	28	23	5	139	27	10	11	17	3	1	5	42	32	34	22	9	73	2	54	86
miR-192-5p	2	1	9	9	9	7	9	137	12	4	6	16	6	2	3	9	2	24	5	5	21	3	7	19
miR-193a-5p	0	0	0	1	1	2	1	3	8	0	0	0	0	0	0	4	0	2	0	1	7	0	3	3
miR-193b-5p	0	0	0	0	0	0	0	1	4	0	0	0	0	0	0	0	0	0	3	0	1	0	2	0
miR-194-3p	0	0	0	0	0	0	0	1	0	0	0	0	0	0	0	0	0	0	0	0	0	0	0	0
miR-194-5p	2	0	4	2	6	9	2	52	13	1	0	3	1	1	3	9	1	5	0	1	13	0	10	15
miR-195-3p	1	0	0	1	0	0	0	4	1	1	0	0	0	0	0	0	0	0	0	2	1	0	1	0
miR-195-5p	0	0	0	0	1	0	0	0	0	0	0	0	0	0	0	0	0	0	0	0	2	0	0	0
miR-196a-5p	0	0	0	0	0	0	0	0	0	0	0	0	0	0	0	0	0	0	0	0	0	0	0	0

miR-196b-5p	0	0	1	3	0	0	0	0	0	0	0	0	0	0	0	0	0	0	0	0	0	0	0	1
miR-197-3p	0	0	0	2	1	1	0	4	0	0	0	1	0	0	0	0	0	1	1	1	0	0	0	0
miR-197-5p	0	0	0	0	0	0	0	0	0	0	0	0	0	0	0	0	0	0	0	0	0	0	0	1
miR-1976	0	0	0	0	0	0	0	4	0	1	0	0	0	0	0	0	0	0	0	0	0	0	0	0
miR-199a-3p	0	0	0	4	4	1	0	5	1	0	0	0	0	0	0	4	0	4	5	0	1	0	3	4
miR-199a-5p	0	0	0	1	0	0	0	2	2	0	2	1	0	1	1	0	0	1	0	0	3	0	4	6
miR-199b-3p	0	0	0	3	1	0	0	1	0	0	0	1	0	0	0	1	0	0	0	0	3	0	1	2
miR-199b-5p	0	0	0	0	0	1	0	0	0	0	0	0	0	0	0	1	0	0	0	0	0	0	0	4
miR-19a-3p	0	0	0	1	2	4	2	10	1	0	0	1	0	0	0	0	0	2	0	2	0	2	0	6

miR-19b-1-5p	0	0	0	0	0	0	0	0	0	0	0	0	0	0	0	0	0	0	0	0	0	0	0	0
miR-19b-3p	0	0	0	1	0	2	0	7	0	0	0	1	0	0	0	1	1	0	0	1	2	0	3	1
miR-200a-3p	1	1	0	0	0	0	0	0	0	0	1	0	0	0	0	0	0	1	1	0	0	0	1	0
miR-200a-5p	0	0	0	0	0	0	0	0	0	0	0	0	0	0	0	0	0	0	0	0	0	1	0	0
miR-200b-3p	0	0	0	0	0	0	0	0	0	0	0	0	0	0	0	0	0	0	0	0	1	0	0	0
miR-200b-5p	0	0	0	0	0	0	0	0	0	0	0	0	0	0	0	1	0	0	0	0	0	0	0	0
miR-200c-3p	0	0	2	0	1	0	0	2	0	0	0	0	1	0	0	0	0	0	1	0	1	0	2	0
miR-202-3p	0	0	0	0	0	0	0	3	0	0	0	0	0	0	0	0	0	0	0	0	0	0	0	0
miR-203a	0	8	0	0	1	1	1	0	0	1	0	0	1	0	0	6	0	1	1	0	1	0	1	6

miR-204-3p	0	0	0	0	0	0	0	2	0	0	0	0	0	0	0	0	0	0	0	0	0	0	0	0
miR-204-5p	0	0	0	1	0	0	0	1	0	0	0	0	0	0	0	0	0	2	0	0	1	0	0	0
miR-206	0	0	0	1	0	0	0	3	6	0	0	0	1	0	1	1	0	0	3	1	1	0	2	1
miR-20a-5p	1	1	1	1	2	5	5	19	3	0	0	2	0	0	0	4	0	2	2	4	12	0	4	3
miR-20b-3p	0	0	0	0	0	0	0	0	0	0	0	0	0	0	0	0	0	0	0	0	0	0	0	1
miR-20b-5p	0	0	0	0	0	0	0	2	0	0	0	1	0	0	0	1	0	0	0	0	1	0	0	1
miR-210-3p	0	0	0	0	0	0	0	0	0	0	0	0	0	0	0	0	0	0	0	0	0	0	0	0
miR-2110	1	0	2	3	2	1	0	28	8	0	1	4	1	0	2	6	0	5	1	1	4	0	1	9
miR-2115-5p	0	0	0	0	0	0	0	0	0	0	0	0	0	0	0	0	0	0	0	0	0	0	0	0

miR-21-3p	0	0	0	0	0	0	0	0	0	0	0	0	0	0	0	0	0	0	0	0	0	0	0	0
miR-214-3p	0	0	0	0	0	0	0	0	0	0	0	0	0	0	0	0	0	0	0	0	0	0	0	0
miR-214-5p	0	0	0	0	0	0	0	0	0	0	0	0	0	0	0	0	0	0	0	0	0	0	0	1
miR-215-3p	0	0	0	0	0	0	0	0	0	0	0	0	0	0	0	0	0	0	0	0	0	0	0	1
miR-215-5p	1	0	0	0	0	1	0	6	3	0	0	0	0	0	0	2	0	1	0	2	1	0	1	0
miR-21-5p	16	14	38	50	53	40	18	582	85	24	24	40	18	8	9	65	34	72	44	30	134	5	81	156
miR-216a-5p	0	0	0	0	0	0	0	0	0	0	0	0	0	0	0	0	0	0	0	0	0	0	0	0
miR-216b-5p	0	0	0	0	0	0	0	0	0	0	0	0	0	0	0	0	0	0	0	0	0	0	0	0
miR-218-5p	0	0	0	0	0	0	0	0	0	0	0	0	0	0	0	0	0	0	0	0	2	0	2	4

miR-219a-1-3p	0	0	0	0	0	0	0	0	0	0	0	0	0	0	0	0	0	0	0	0	0	0	0	0
miR-219a-2-3p	0	0	0	0	0	0	0	0	0	0	0	0	0	0	0	0	0	0	0	0	10	0	0	0
miR-221-3p	0	0	0	3	1	1	0	6	1	0	0	2	0	1	0	3	3	1	1	2	7	0	3	9
miR-221-5p	0	0	0	0	0	0	0	0	0	0	0	0	0	0	0	0	0	0	0	0	2	0	0	0
miR-222-3p	2	1	3	3	4	1	1	11	5	1	0	1	1	1	1	6	0	9	0	1	12	1	4	12
miR-222-5p	0	0	0	0	0	0	0	0	0	0	0	0	0	0	0	0	0	0	0	0	0	0	0	0
miR-223-3p	0	0	0	0	2	0	0	2	0	0	0	1	0	0	0	0	0	1	0	0	5	0	1	1
miR-223-5p	0	0	0	2	0	0	0	2	1	1	1	1	2	0	1	1	0	3	3	0	2	0	1	6

miR-22-3p	18	32	32	50	46	51	28	740	86	11	42	34	15	12	15	83	37	54	29	40	107	14	126	140
miR-224-5p	0	0	0	0	0	0	0	0	0	0	0	0	0	0	0	0	0	0	0	0	0	0	0	0
miR-22-5p	0	0	1	0	0	0	0	18	1	0	1	0	1	0	0	1	0	0	1	0	1	0	3	2
miR-2278	0	0	0	0	0	0	0	0	0	0	0	0	0	0	0	0	0	0	0	0	0	0	1	0
miR-2355-3p	0	0	0	0	0	0	0	0	0	0	0	0	0	0	0	0	0	0	0	0	0	0	0	0
miR-23a-3p	0	0	0	2	0	0	0	1	1	0	0	0	0	0	0	1	3	2	0	0	0	0	2	1
miR-23a-5p	0	0	0	0	0	0	0	0	0	0	0	0	0	0	0	0	0	0	0	0	0	0	0	2
miR-23b-3p	0	1	0	0	0	0	0	0	0	0	0	0	0	0	0	0	0	1	0	0	1	0	3	0
miR-23b-5p	0	0	0	0	0	0	0	0	0	0	0	0	0	0	0	0	0	0	0	0	0	0	0	0

miR-24-3p	11	13	18	51	31	22	8	164	47	15	8	12	11	4	12	59	8	68	18	28	140	2	83	98
miR-25-3p	30	18	94	123	86	124	64	1415	154	42	114	108	57	32	56	201	69	135	46	120	268	36	152	279
miR-25-5p	0	0	0	0	0	0	1	5	0	1	2	1	0	0	0	3	0	0	0	0	2	0	2	0
miR-26a-2-3p	0	0	0	0	0	0	0	0	0	0	0	0	0	0	0	0	0	0	0	0	1	0	0	0
miR-26a-5p	36	53	47	81	159	95	24	522	101	45	19	62	17	7	19	112	14	179	182	58	416	14	230	295
miR-26b-3p	0	0	0	0	0	0	0	0	0	0	0	0	0	0	0	0	0	0	0	0	1	0	0	0
miR-26b-5p	4	1	6	2	7	4	3	36	8	3	1	4	2	0	0	7	0	9	3	6	14	0	7	11
miR-27a-3p	4	16	9	15	30	13	10	116	31	10	3	16	6	4	6	36	6	35	19	10	76	5	42	51
miR-27a-5p	1	1	0	1	2	1	0	6	0	0	0	1	0	0	0	0	1	1	1	2	1	4	1	5

miR-27b-3p	5	8	6	10	12	8	3	50	29	6	4	8	4	0	3	23	4	16	4	6	49	2	19	23
miR-27b-5p	0	0	0	0	0	0	0	0	0	0	0	0	0	0	0	0	0	0	0	0	0	0	0	0
miR-28-3p	0	0	1	0	0	1	0	10	1	0	1	1	3	0	0	4	0	4	1	5	9	0	2	7
miR-28-5p	0	0	0	2	1	0	0	1	0	0	0	0	0	0	0	0	0	2	0	0	0	0	1	1
miR-296-3p	0	0	0	0	0	0	0	0	0	0	0	0	0	0	0	0	0	0	0	0	0	0	0	0
miR-296-5p	0	0	0	1	0	0	0	0	0	0	0	0	0	0	0	0	0	0	0	0	0	0	0	0
miR-29a-3p	0	1	1	2	3	2	1	19	7	3	0	1	2	0	1	2	0	6	1	3	9	0	3	9
miR-29b-1-5p	0	0	0	0	0	0	0	0	0	0	0	0	0	0	0	0	0	0	0	0	0	0	0	0
miR-29b-3p	0	0	0	0	0	0	0	0	0	0	0	0	0	0	0	0	0	0	2	1	1	0	0	1

miR-29c-3p	0	0	0	0	0	1	0	1	0	0	0	1	0	0	0	0	0	0	0	0	0	0	0	0
miR-29c-5p	0	0	0	0	0	1	0	1	0	0	0	0	0	0	0	0	0	0	0	0	0	0	0	0
miR-301a-3p	0	0	0	0	0	0	0	0	0	0	0	0	0	0	0	0	0	0	0	0	0	0	0	0
miR-301b	0	0	0	0	0	0	0	0	0	0	0	0	0	0	0	0	0	0	1	0	0	0	0	0
miR-30a-3p	7	4	1	12	4	9	4	49	7	5	9	5	5	1	4	10	2	9	9	4	26	3	22	23
miR-30a-5p	4	3	0	6	10	5	7	64	14	5	3	6	4	3	1	10	0	11	10	5	25	0	19	15
miR-30b-3p	0	0	0	0	0	0	0	0	0	0	0	0	0	0	0	0	0	0	0	0	0	0	0	0
miR-30b-5p	0	0	0	0	0	0	0	1	0	0	0	1	1	0	0	0	0	0	0	0	0	0	0	3
miR-30c-1-3p	0	0	0	0	0	1	1	0	0	0	0	0	0	0	0	0	0	0	0	0	1	0	0	2

miR-30c-2-3p	0	0	0	0	0	0	0	0	1	0	0	0	0	0	0	0	0	0	0	0	1	0	1	1
miR-30c-5p	6	4	1	4	16	7	1	48	9	2	4	5	4	1	3	9	3	13	5	6	22	2	19	22
miR-30d-3p	0	0	0	0	0	0	0	0	0	0	1	0	0	0	0	0	0	1	0	0	0	0	0	1
miR-30d-5p	13	13	29	40	33	33	29	487	79	14	19	49	16	9	23	100	17	86	26	42	150	9	104	147
miR-30e-3p	3	4	2	9	13	8	4	40	6	3	11	5	6	2	5	12	5	21	7	12	24	5	23	20
miR-30e-5p	0	0	1	4	1	3	1	38	4	2	0	0	0	1	0	1	5	4	4	2	3	0	2	6
miR-3122	0	0	0	0	0	0	0	0	0	0	0	0	0	0	0	0	0	0	0	0	0	0	0	0
miR-3127-3p	0	0	0	0	0	0	0	0	0	0	0	0	0	0	0	0	0	0	0	0	0	0	0	0
miR-3127-5p	0	0	0	0	0	0	0	0	0	0	0	0	0	0	0	0	0	0	0	0	1	0	0	0

miR-3128	0	0	0	0	0	0	0	0	0	0	1	0	0	0	0	0	0	0	0	0	0	0	0	0
miR-3136-5p	0	0	0	0	0	0	0	0	0	0	0	0	0	1	0	0	0	0	0	0	0	0	0	0
miR-3138	0	0	0	0	0	0	0	1	0	0	0	0	0	0	0	0	0	0	0	0	0	0	0	0
miR-3143	0	0	0	2	0	0	0	1	1	0	0	0	0	0	0	0	0	0	0	0	0	0	0	0
miR-3150a-5p	0	0	0	0	0	0	0	0	0	0	0	0	0	0	0	0	0	0	0	0	0	0	0	0
miR-3150b-3p	0	0	0	0	0	0	0	0	0	0	0	0	0	0	1	0	0	0	0	0	0	0	0	0
miR-3157-3p	0	0	0	0	0	0	0	0	0	0	0	0	0	0	0	0	0	0	0	0	0	0	0	0
miR-3158-3p	0	0	0	1	3	8	0	40	3	1	5	2	3	0	3	3	0	1	0	3	2	0	0	4

miR-3168	9	4	11	5	4	12	5	52	7	1	3	3	1	1	4	5	2	6	5	3	21	5	9	16
miR-3173-5p	0	0	0	0	0	0	0	0	0	0	0	0	1	0	0	1	0	1	0	0	0	0	0	0
miR-3174	0	0	0	0	0	0	0	0	0	0	0	0	0	0	0	0	0	0	0	0	0	0	0	0
miR-3179	0	0	0	0	0	0	0	0	0	0	0	0	0	0	0	0	0	0	0	0	0	0	0	0
miR-3180-3p	0	0	0	0	0	0	0	0	0	0	0	0	0	0	0	0	0	0	0	0	0	0	0	0
miR-3187-3p	0	0	0	0	0	0	0	0	0	0	0	0	0	0	0	0	0	0	0	0	0	0	0	0
miR-3191-3p	0	0	0	0	0	0	0	0	0	0	0	0	0	0	0	0	0	0	0	0	0	0	0	0
miR-3197	0	0	0	0	0	0	0	0	0	0	0	0	0	0	0	0	0	1	0	0	0	0	0	0
miR-3200-3p	0	0	0	0	0	0	0	0	0	0	0	0	0	0	1	0	0	0	0	0	0	0	0	0

miR-320a	25	33	31	60	58	136	35	894	134	33	54	63	24	14	17	111	32	179	86	62	233	20	276	229
miR-320b	4	16	3	6	7	14	10	132	36	3	10	5	6	1	2	13	4	31	9	5	25	4	31	31
miR-320c	3	11	2	1	0	4	1	29	6	3	4	3	1	1	1	1	0	4	2	2	7	1	7	8
miR-320d	1	0	0	1	0	0	1	11	0	1	0	0	0	0	0	2	0	4	3	0	4	0	2	1
miR-320e	0	0	0	0	0	0	0	0	0	0	0	0	0	0	0	0	0	0	0	0	0	0	0	0
miR-323a-3p	0	0	0	0	0	0	0	0	0	0	0	0	0	0	0	0	0	0	0	0	1	0	0	0
miR-323a-5p	0	0	0	0	0	0	0	0	0	0	0	0	0	0	0	0	0	0	0	0	0	0	0	0
miR-323b-3p	0	0	0	0	0	0	0	1	0	0	0	0	0	0	0	0	0	0	0	0	0	0	0	0
miR-324-5p	0	0	0	0	0	0	0	0	1	0	0	0	0	0	0	0	0	0	0	0	0	0	0	0

miR-32-5p	1	1	1	2	2	2	0	5	3	0	0	0	0	0	0	1	0	2	0	0	4	0	5	7
miR-326	0	0	0	0	0	0	0	0	1	0	0	1	0	0	0	0	0	0	0	0	1	0	0	0
miR-328-3p	0	0	2	7	5	5	0	12	5	1	1	2	1	1	1	9	0	6	2	4	19	1	4	8
miR-330-3p	0	0	0	0	0	0	0	0	0	0	0	1	0	0	0	1	0	0	0	1	2	0	0	1
miR-330-5p	0	0	0	0	0	0	0	0	0	0	0	1	0	0	0	0	0	1	0	0	0	0	1	0
miR-331-5p	0	0	0	0	0	0	0	0	0	0	0	0	0	0	0	0	0	0	0	0	0	0	0	0
miR-335-3p	0	0	1	0	0	0	0	2	1	0	0	0	0	0	0	0	0	1	0	0	0	0	1	0
miR-335-5p	2	0	1	0	1	0	0	3	0	0	0	0	0	0	1	1	0	1	0	0	0	0	0	0
miR-337-3p	0	0	0	0	0	0	0	0	0	0	0	0	0	0	0	0	0	0	1	0	0	0	0	0

miR-337-5p	0	0	0	0	0	0	0	0	0	0	0	0	0	0	0	0	0	0	0	0	0	0	0	2
miR-338-5p	0	0	0	1	0	0	0	0	0	0	0	0	0	0	0	1	0	3	0	0	4	0	0	3
miR-339-3p	0	0	0	1	1	0	1	1	2	0	0	0	0	0	0	1	2	0	0	0	1	0	1	3
miR-339-5p	0	0	0	0	1	0	0	0	0	0	0	0	0	0	0	0	0	0	0	0	0	0	0	0
miR-340-3p	0	0	0	0	0	0	0	0	0	0	1	0	1	0	0	1	0	0	0	0	1	0	0	3
miR-340-5p	1	0	0	4	4	1	0	5	0	1	1	3	2	0	1	0	1	2	1	0	2	0	2	7
miR-342-3p	2	0	1	0	1	1	0	1	0	0	0	0	0	0	0	0	1	5	1	2	1	0	1	1
miR-342-5p	2	2	1	7	2	3	0	33	4	1	4	1	2	1	1	2	3	4	6	3	14	1	6	16
miR-345-5p	0	0	0	1	0	1	0	2	1	0	0	1	0	0	0	1	0	1	0	0	1	0	2	0

miR-34a-5p	0	0	0	0	0	0	0	0	0	0	0	0	0	0	0	0	0	0	0	0	0	0	0	0
miR-3591-5p	0	0	0	0	0	0	0	0	0	0	0	0	0	0	0	0	0	0	0	0	0	0	0	0
miR-3605-3p	0	0	0	1	1	0	0	5	1	0	0	0	1	0	0	0	0	1	0	0	1	0	1	3
miR-3605-5p	0	0	0	0	0	0	0	1	1	0	0	0	0	0	1	0	0	0	0	0	0	0	0	0
miR-3613-3p	0	0	0	0	0	0	0	2	0	0	0	0	0	0	0	0	0	0	0	0	0	0	0	0
miR-3613-5p	0	0	0	0	0	0	0	0	0	0	0	0	0	0	0	0	0	0	0	0	0	0	1	0
miR-361-3p	0	0	0	0	0	0	1	1	0	0	0	0	0	0	0	0	0	0	0	1	0	0	0	0
miR-3614-5p	0	0	0	0	0	1	0	0	0	0	0	0	0	1	0	0	0	0	0	0	0	0	0	0
miR-3615	0	1	1	2	1	1	1	15	4	0	3	0	1	0	2	2	0	4	2	2	2	0	2	7

miR-361-5p	0	1	0	0	1	1	0	2	4	0	0	1	0	0	0	0	1	0	0	0	1	0	0	2
miR-3621	0	0	0	0	0	0	0	0	0	0	0	0	0	0	0	0	0	0	0	0	0	0	0	0
miR-362-5p	0	0	0	0	0	0	0	0	0	0	0	0	0	0	0	0	0	1	0	0	0	0	0	0
miR-363-3p	7	5	3	23	19	16	3	171	24	9	16	17	8	6	1	39	5	30	7	12	34	8	57	77
miR-363-5p	0	0	0	0	1	0	0	0	0	0	0	0	0	0	0	0	0	1	0	0	0	0	1	2
miR-3656	0	0	0	0	0	0	0	0	1	0	1	0	0	0	0	0	0	0	0	0	0	0	0	0
miR-365a-3p	0	0	0	0	0	0	0	0	0	0	0	0	0	0	0	0	1	0	0	0	0	0	0	0
miR-365a-5p	0	0	0	0	0	0	0	0	1	0	0	0	0	0	0	1	0	0	0	0	0	0	0	0
miR-365b-3p	0	0	0	0	0	0	0	0	0	0	0	0	0	0	0	0	0	0	0	0	0	0	0	0

miR-3663-5p	0	0	0	0	0	0	0	0	0	0	0	0	0	0	0	0	0	0	0	0	0	1	0	0
miR-3675-5p	0	0	0	0	0	0	0	0	0	0	0	0	0	0	0	0	0	0	0	0	0	0	0	0
miR-3682-3p	0	0	0	0	0	0	0	1	0	0	0	0	0	0	0	0	0	0	0	0	0	0	0	0
miR-3688-3p	0	0	0	0	0	0	0	0	0	0	0	0	0	0	0	0	0	0	0	0	1	0	0	0
miR-3690	0	0	0	0	0	0	0	0	0	0	0	0	0	0	0	0	0	0	0	0	0	2	0	0
miR-3691-5p	0	0	0	0	0	0	0	0	0	0	0	0	0	0	0	0	0	0	0	0	0	0	0	0
miR-369-5p	0	0	0	0	0	0	0	0	0	0	0	0	0	0	0	0	0	1	0	0	0	0	0	0
miR-370-3p	0	0	1	3	2	0	1	15	1	0	0	0	0	0	1	0	0	2	0	0	3	1	0	8
miR-370-5p	0	0	0	0	0	0	0	0	0	0	0	0	0	0	0	0	0	0	0	0	0	0	0	0

miR-372-3p	0	0	0	0	0	0	0	0	0	0	0	0	0	0	0	0	0	1	0	0	0	0	0	0
miR-374a-3p	0	0	0	0	0	0	0	4	0	0	0	0	0	0	0	0	0	1	0	0	1	0	2	0
miR-374a-5p	0	0	1	0	0	3	0	4	3	1	0	3	0	0	0	1	0	2	0	0	3	1	1	5
miR-374b-5p	0	0	0	1	0	4	1	0	0	1	0	0	0	0	0	0	0	1	0	1	0	0	1	1
miR-375	1	0	2	0	5	1	3	6	9	1	0	2	1	1	2	1	0	0	1	4	7	1	7	7
miR-378a-3p	1	1	1	1	7	2	2	21	5	1	2	2	0	0	0	1	4	1	4	0	8	2	4	7
miR-378a-5p	0	0	0	0	0	0	0	0	0	0	0	0	0	0	0	1	0	0	0	0	0	0	0	0
miR-378c	0	0	1	0	0	1	0	2	1	0	0	0	0	0	0	1	0	0	0	0	0	0	0	0
miR-378d	0	0	0	0	1	0	0	0	0	0	0	0	0	0	0	0	0	0	0	0	0	0	0	0

miR-379-3p	0	0	0	0	0	0	0	1	0	0	0	0	0	0	0	0	0	0	0	0	0	0	0	0
miR-379-5p	0	0	2	0	0	0	1	1	0	0	0	0	0	1	0	0	0	2	0	0	2	0	3	1
miR-381-3p	1	0	0	1	0	3	0	7	0	0	3	0	1	0	2	2	0	0	6	0	5	0	1	3
miR-381-5p	0	0	0	0	0	0	0	0	0	0	0	0	0	0	0	0	0	0	0	0	0	0	0	0
miR-382-5p	0	1	0	0	1	0	0	3	1	0	0	1	0	0	0	3	0	2	1	0	4	0	1	2
miR-3909	0	0	0	0	0	1	0	0	0	0	0	0	0	0	0	0	0	0	0	0	1	0	0	0
miR-3911	0	0	0	0	0	0	0	0	0	0	0	0	0	0	0	0	0	0	0	0	0	0	0	1
miR-3912-3p	0	0	0	0	0	0	0	0	0	0	0	0	0	0	0	0	0	0	0	0	0	0	0	0
miR-3913-5p	1	0	0	0	0	0	0	5	1	0	1	0	0	0	0	0	1	0	0	0	0	0	0	0

miR-3928-3p	0	0	0	0	0	0	0	0	0	0	0	0	0	0	0	0	0	0	0	0	0	0	0	0
miR-3934-5p	0	0	0	0	0	0	0	0	0	0	0	0	0	0	1	0	0	0	0	0	0	0	0	0
miR-3936	0	0	0	0	0	0	0	0	0	0	0	0	0	0	0	0	0	0	0	0	0	0	0	3
miR-3940-3p	0	0	0	0	0	0	0	0	0	0	0	0	0	0	0	0	0	1	0	0	0	0	0	1
miR-409-3p	0	1	3	4	0	0	0	4	1	0	4	0	0	2	1	1	1	2	0	2	9	1	0	15
miR-409-5p	0	0	0	0	0	0	0	0	0	0	0	0	0	0	0	0	0	0	0	0	1	0	0	0
miR-410-3p	0	0	0	0	0	0	0	0	0	0	0	0	0	0	0	0	0	0	0	0	0	0	0	0
miR-411-3p	0	0	0	0	1	0	0	0	0	0	0	0	0	0	0	0	0	0	0	0	0	0	0	0
miR-411-5p	0	0	0	1	0	0	0	4	1	0	0	0	0	0	0	0	0	0	0	0	0	0	0	1

miR-421	0	0	1	0	0	0	0	2	1	0	0	0	0	0	0	1	2	0	0	0	0	0	0	0
miR-423-3p	7	8	6	40	16	22	11	168	32	6	27	19	12	1	4	34	11	27	17	18	97	14	41	65
miR-423-5p	247	265	293	682	316	196	386	5449	558	130	906	256	475	141	238	880	373	556	408	387	1026	272	626	1995
miR-424-3p	0	0	0	0	1	1	0	11	1	2	0	1	1	0	0	5	0	5	0	1	2	0	7	1
miR-424-5p	0	0	0	0	0	0	0	0	0	0	0	0	0	0	0	0	0	0	0	0	0	0	0	0
miR-425-5p	3	1	5	1	5	7	2	68	9	0	6	2	2	2	4	8	3	9	0	4	13	2	9	20
miR-4259	0	0	0	0	0	0	0	0	0	0	0	0	0	0	0	0	0	0	0	0	0	0	0	1
miR-429	1	0	0	0	0	0	0	0	0	0	0	0	0	0	0	0	0	0	0	0	0	0	0	0
miR-431-5p	0	0	0	0	0	0	0	0	0	0	0	0	0	0	0	0	0	0	0	0	0	0	0	0

miR-4322	0	0	0	0	0	0	0	0	0	0	0	0	0	0	0	0	0	0	0	0	0	0	0	0
miR-432-5p	0	0	1	1	0	0	0	4	1	0	2	0	0	0	1	3	0	5	1	0	3	1	0	3
miR-4326	0	0	0	0	0	0	0	0	0	0	0	0	0	0	0	1	0	0	0	0	0	0	0	0
miR-433-3p	0	0	0	0	1	0	0	0	0	0	0	0	0	0	0	0	0	0	0	0	1	0	0	0
miR-4433-3p	0	0	0	0	0	0	0	0	0	0	0	0	0	0	0	0	0	0	2	0	0	0	0	0
miR-4433-5p	0	0	0	0	0	0	0	0	0	0	0	0	0	0	0	0	0	0	0	0	0	0	0	0
miR-4433b-3p	0	0	0	1	0	0	0	1	0	0	0	0	0	0	0	0	0	0	0	0	0	0	0	1
miR-4433b-5p	0	0	0	0	0	0	0	1	0	0	0	0	0	0	0	0	0	0	0	0	0	0	0	4

miR-4443	2	0	0	2	0	0	0	4	0	0	1	0	0	0	0	4	0	1	2	0	0	0	2	3
miR-4446-3p	0	0	1	0	0	0	0	3	3	0	0	1	0	0	0	0	0	1	0	0	2	0	0	0
miR-4467	0	0	0	0	0	0	0	0	0	0	0	0	0	0	1	0	0	0	0	1	0	0	1	1
miR-4473	0	0	1	0	0	0	0	0	0	0	0	0	0	0	0	0	0	0	0	0	0	0	0	0
miR-4474-3p	0	0	0	0	0	0	0	0	0	0	0	0	0	0	0	0	0	0	0	0	0	0	0	0
miR-4477b	0	0	0	0	0	0	0	0	0	0	0	0	0	0	0	0	0	0	0	0	0	0	0	0
miR-4482-3p	0	0	0	0	0	0	0	4	0	0	0	0	0	0	0	0	0	0	0	0	0	0	0	0
miR-4488	0	0	0	0	0	0	0	0	0	0	0	0	0	0	0	0	0	0	0	0	0	0	0	0
miR-4489	0	0	0	0	1	0	0	0	0	0	0	0	0	0	0	0	0	0	0	0	0	0	0	0

miR-4497	0	0	0	0	1	0	0	3	0	0	0	0	0	0	0	0	0	0	0	0	1	0	0	2
miR-4500	0	0	0	1	0	0	0	1	0	0	0	0	0	0	0	0	0	0	0	0	0	0	0	0
miR-4504	0	0	0	0	0	0	0	1	0	0	0	0	0	0	0	0	0	0	0	0	0	0	0	0
miR-4508	0	0	0	0	0	0	0	1	0	0	0	0	0	0	0	0	0	0	0	0	0	0	1	0
miR-450a-5p	0	0	0	0	0	0	0	1	0	0	0	0	0	0	0	1	0	0	0	0	0	0	0	1
miR-450b-5p	0	0	0	0	0	0	0	0	1	0	0	0	0	0	0	0	0	0	0	0	1	0	2	0
miR-4510	0	0	0	0	1	0	0	0	0	0	0	0	0	0	0	0	0	0	0	0	0	1	0	0
miR-4511	0	0	0	0	0	0	0	1	0	0	0	0	0	0	0	0	0	0	0	0	0	0	0	0
miR-4513	0	0	0	0	0	0	0	0	0	0	0	0	0	0	17	0	0	0	0	0	0	0	0	0

miR-4516	0	0	0	0	0	0	1	1	0	0	0	0	0	0	0	0	0	0	0	0	0	0	0	0
miR-451a	572	312	1976	1148	1772	2115	1055	25325	2234	482	1881	1710	763	668	832	3360	1268	3436	524	1302	2498	715	3577	4504
miR-452-5p	0	0	0	0	0	0	0	0	0	0	0	0	0	0	0	0	0	0	0	0	0	0	0	0
miR-454-3p	0	0	0	0	0	0	0	0	0	0	0	0	0	0	0	0	0	0	0	0	0	0	0	0
miR-454-5p	0	0	0	0	0	0	0	0	0	0	0	0	0	0	0	0	0	0	0	0	0	0	1	0
miR-455-5p	0	0	0	0	0	0	0	0	0	0	0	0	0	0	0	0	0	0	0	0	0	0	0	0
miR-4635	0	0	0	0	0	1	0	0	0	0	0	0	0	0	0	0	1	1	0	0	0	0	0	1
miR-4647	0	0	0	0	0	0	0	0	0	0	0	0	0	0	0	0	0	0	0	0	0	0	0	0
miR-4658	0	0	0	0	0	0	0	0	0	0	0	0	0	0	0	0	0	0	0	0	0	0	0	0

miR-4661-5p	0	0	0	0	0	0	0	0	1	0	0	0	0	0	0	0	0	0	0	0	0	0	0	0
miR-4662a-5p	0	0	0	0	0	0	0	0	0	0	0	0	0	0	0	0	0	0	1	0	0	0	0	0
miR-4663	0	0	0	0	0	0	0	0	0	0	0	0	0	0	0	0	0	0	0	1	0	0	0	0
miR-4664-3p	0	0	0	0	0	0	0	0	1	0	0	0	0	0	0	0	0	0	0	0	0	0	0	0
miR-4665-5p	0	0	0	0	1	0	0	0	0	0	0	0	0	0	0	0	0	0	2	0	0	0	0	1
miR-4667-5p	0	0	0	0	0	0	0	1	0	0	0	0	0	0	0	0	0	0	0	0	0	0	0	0
miR-4669	0	0	0	0	0	0	0	0	0	0	2	0	0	0	0	0	0	0	1	0	0	0	0	0
miR-4670-5p	0	0	0	0	0	0	0	0	0	0	0	0	0	0	0	0	0	0	0	0	0	0	0	0
miR-4671-5p	0	0	0	0	0	0	1	0	0	0	0	1	0	0	0	0	0	0	0	1	0	0	0	0

miR-4672	0	0	0	0	0	0	0	1	0	0	0	0	0	0	0	0	0	0	0	0	0	0	0	0
miR-4676-5p	0	0	0	0	0	0	0	0	0	0	0	0	0	0	0	0	0	0	0	0	0	0	0	0
miR-4677-5p	0	0	0	0	0	0	0	0	0	1	0	0	0	0	0	0	0	0	0	0	0	0	0	0
miR-4683	0	0	0	0	0	0	0	0	0	0	0	0	1	0	0	0	0	0	1	0	0	0	0	0
miR-4685-3p	0	0	0	0	0	0	0	1	0	0	0	0	0	0	0	0	0	0	0	0	0	0	0	0
miR-4688	0	0	0	0	0	0	0	0	0	0	0	0	0	0	0	0	0	0	0	0	0	0	0	0
miR-4697-3p	0	0	0	0	0	0	0	0	1	0	0	0	0	0	0	0	0	0	0	0	0	0	0	0
miR-4709-5p	0	0	0	0	0	0	0	0	0	0	0	0	0	0	0	0	0	0	0	0	0	0	0	0
miR-4714-5p	0	0	0	0	0	0	0	0	0	0	0	0	0	0	0	0	0	0	0	0	0	0	0	0

miR-4723-3p	0	0	0	0	0	0	0	0	0	0	0	0	0	0	0	0	0	0	0	0	0	0	0	0
miR-4727-5p	0	0	0	0	0	0	0	0	0	0	0	0	0	0	0	0	0	0	0	0	0	0	1	0
miR-4731-5p	0	0	0	0	0	0	0	0	0	0	0	0	0	0	0	0	0	0	0	0	0	0	1	0
miR-4732-3p	1	1	0	1	0	1	0	6	2	0	2	0	0	0	1	1	0	0	0	0	1	2	3	3
miR-4732-5p	0	0	0	2	3	3	1	29	7	1	2	2	0	0	1	5	0	3	1	0	5	1	9	12
miR-4741	0	0	0	0	0	0	0	0	0	0	0	0	0	0	0	0	0	0	0	0	0	0	0	0
miR-4742-3p	0	0	0	0	0	0	0	0	0	0	0	0	0	0	0	0	0	0	0	0	1	0	0	0
miR-4742-5p	0	0	0	0	0	0	0	0	0	0	0	0	0	0	0	0	0	0	0	0	0	0	0	0
miR-4743-5p	0	0	0	0	0	0	0	0	0	0	0	0	0	0	0	0	0	0	0	0	0	0	0	0

miR-4745-5p	0	0	0	0	0	0	0	0	0	0	0	0	0	0	0	0	0	0	0	0	0	0	0	0
miR-4746-5p	0	0	3	2	0	0	0	3	0	0	1	0	0	0	0	0	0	0	0	0	0	0	0	0
miR-4750-5p	0	0	0	0	0	0	0	3	0	0	0	0	0	0	0	0	0	0	0	0	0	0	0	0
miR-4763-3p	0	0	0	0	0	0	0	0	1	0	0	0	0	0	0	0	0	0	0	0	0	0	0	0
miR-4773	0	0	0	0	0	0	0	0	0	0	0	0	0	0	0	0	0	0	0	0	0	0	0	0
miR-4779	0	0	0	0	0	0	0	0	0	0	0	0	0	0	0	0	0	0	0	0	0	0	0	1
miR-4781-3p	0	0	0	0	0	0	0	0	0	0	0	0	0	0	0	0	0	0	0	0	0	0	0	0
miR-4800-5p	0	0	0	0	0	0	0	0	0	0	0	0	0	0	1	0	0	0	0	0	0	1	0	0
miR-4804-5p	0	0	0	0	0	0	0	1	0	0	1	0	0	0	0	1	0	0	0	0	0	0	0	0

miR-483-3p	0	0	0	0	0	0	0	0	0	0	0	0	0	0	0	0	0	0	0	0	0	0	0	0
miR-483-5p	1	3	1	1	2	0	0	23	3	2	2	0	1	0	0	1	0	1	2	2	8	0	2	4
miR-484	2	1	0	0	1	7	2	33	6	0	1	3	0	0	1	1	1	5	0	4	7	0	6	3
miR-485-3p	0	0	0	0	1	0	0	0	0	0	0	0	0	0	0	0	0	0	3	0	1	0	2	0
miR-485-5p	0	0	0	0	1	0	0	2	0	0	0	0	0	0	0	0	0	0	1	0	0	1	1	0
miR-486-3p	3	0	5	4	2	11	6	146	25	2	22	7	9	6	1	12	2	18	4	2	39	1	10	16
miR-486-5p	306	170	770	909	479	859	535	12415	1164	241	1240	633	717	243	366	1556	398	1021	244	631	2398	541	1644	2533
miR-490-3p	0	0	0	0	0	0	0	0	0	0	0	0	0	0	0	0	0	0	0	0	0	0	0	0
miR-493-3p	0	0	0	0	0	0	0	0	0	0	0	0	0	0	0	0	0	0	1	0	0	0	0	1

miR-493-5p	0	0	0	0	0	0	0	0	0	0	0	0	0	0	0	0	0	0	0	0	0	0	0	1
miR-495-3p	0	0	0	0	0	0	0	0	0	0	0	0	0	0	0	0	0	0	0	1	0	0	0	0
miR-499a-5p	0	0	0	0	1	0	0	0	0	0	0	0	0	0	0	0	0	0	2	0	0	0	0	0
miR-5009-5p	0	0	0	0	0	0	0	0	0	0	0	0	0	0	0	0	0	0	0	0	0	0	0	0
miR-500a-3p	0	0	0	0	0	0	0	0	1	0	0	0	1	0	0	0	0	0	0	0	0	0	0	0
miR-5010-3p	0	0	0	0	1	0	0	0	0	0	0	0	0	0	0	0	0	0	0	0	0	0	0	0
miR-5010-5p	0	0	0	0	0	0	0	1	0	0	0	0	0	0	0	0	0	1	0	1	0	0	0	0
miR-501-3p	0	0	0	0	1	1	0	31	2	1	0	0	0	0	1	2	1	6	0	1	4	0	6	6
miR-502-3p	0	0	0	0	1	0	0	2	0	0	0	1	0	0	0	0	0	0	0	0	1	0	1	0

miR-503-5p	0	1	0	1	0	0	0	5	1	0	0	2	0	0	0	2	1	2	1	0	0	0	3	1
miR-504-5p	0	0	0	0	0	0	0	0	0	0	0	0	0	0	0	0	0	2	1	0	1	0	0	0
miR-505-3p	0	0	0	0	0	0	0	0	0	0	0	0	0	0	0	0	0	0	0	0	0	0	0	0
miR-505-5p	0	0	0	0	0	1	1	11	1	1	0	1	1	0	0	1	0	2	0	1	1	0	2	0
miR-5090	0	0	0	0	0	0	0	0	0	0	0	0	0	0	0	0	0	0	0	0	0	0	0	0
miR-5091	0	0	0	0	0	0	0	0	0	0	0	0	1	0	0	0	0	0	0	0	0	0	0	0
miR-509-3-5p	0	0	0	0	0	0	0	0	0	0	0	0	0	0	0	0	0	0	0	0	0	0	0	1
miR-509-3p	0	0	0	0	0	0	0	0	0	0	0	0	0	0	0	0	0	0	0	0	0	0	0	0
miR-5100	0	0	0	0	0	0	0	0	0	0	0	0	0	0	0	0	0	0	0	0	0	0	0	0

miR-511-5p	0	0	0	0	0	1	0	0	3	0	1	0	0	0	0	0	0	0	1	1	0	0	2	0
miR-514a-3p	0	0	0	0	0	0	0	0	0	0	0	0	0	0	0	0	0	0	0	0	1	0	0	0
miR-516a-5p	0	0	0	0	0	0	0	0	0	0	0	0	0	0	0	0	0	0	0	0	0	0	0	0
miR-516b-5p	0	0	0	0	0	0	0	1	0	0	0	0	0	0	0	0	0	0	0	0	0	0	0	0
miR-5187-5p	0	0	0	0	0	0	0	0	0	0	0	0	0	0	0	0	0	0	0	0	0	0	0	0
miR-5189-5p	0	0	0	0	0	0	0	0	1	0	0	1	0	0	0	0	0	0	0	0	1	0	0	0
miR-520a-3p	0	0	0	0	1	0	0	0	0	0	0	0	0	0	0	0	0	0	0	0	0	0	0	0
miR-532-3p	0	0	0	0	0	0	0	4	0	0	0	0	0	0	0	0	0	0	0	0	0	0	0	0
miR-532-5p	5	1	9	11	9	11	6	128	12	3	13	3	6	5	6	20	8	14	4	6	31	5	14	26

miR-541-5p	0	0	0	0	0	0	0	1	0	0	0	0	0	0	0	0	0	0	0	0	0	0	0	0
miR-542-3p	0	0	0	0	0	0	0	1	0	0	0	0	0	0	0	0	0	0	0	0	0	0	0	0
miR-543	1	0	3	3	1	1	1	11	2	1	0	0	0	0	1	6	1	2	4	1	8	1	2	7
miR-548ac	0	0	0	0	0	0	0	1	0	0	0	0	0	0	0	0	0	0	0	0	0	1	0	0
miR-548e-3p	0	0	0	0	0	0	0	0	0	0	0	0	0	0	0	0	0	1	0	0	0	0	0	1
miR-548j-5p	0	0	0	1	0	0	0	1	1	0	0	0	0	0	0	0	0	0	1	1	0	0	0	0
miR-548o-3p	0	0	0	0	0	0	0	2	0	0	0	0	0	0	1	0	0	0	0	3	0	0	0	1
miR-550a-3-5p	0	0	0	0	0	0	0	2	0	0	0	0	0	0	0	1	0	0	0	0	0	0	0	0
miR-550a-5p	1	0	1	0	0	0	0	7	1	0	1	0	0	0	0	2	0	0	0	0	1	0	0	2

miR-551a	0	0	0	0	0	0	0	0	0	0	0	0	0	0	0	0	0	0	0	0	0	0	0	0
miR-556-5p	0	0	0	0	0	0	0	0	0	0	0	0	0	0	0	0	0	0	0	0	0	0	0	0
miR-570-3p	0	0	0	1	0	0	0	0	0	0	0	0	0	0	0	0	0	0	0	0	0	0	0	0
miR-574-3p	0	0	0	0	1	0	0	0	0	0	0	1	0	0	0	0	1	0	3	0	1	0	0	0
miR-574-5p	0	0	0	0	0	0	0	0	0	0	0	0	0	0	0	0	0	1	0	1	0	0	0	0
miR-576-3p	0	0	0	0	0	0	0	1	0	0	0	0	0	1	0	0	0	0	0	0	0	0	0	0
miR-576-5p	0	0	0	0	1	0	1	0	0	0	0	0	0	0	0	3	0	1	0	0	0	0	0	0
miR-579-5p	0	0	0	0	0	0	0	0	0	0	0	0	0	0	0	0	0	0	0	0	0	0	0	0
miR-580-3p	0	0	0	0	0	0	0	0	0	0	0	0	0	0	0	0	0	0	0	0	0	0	0	0

miR-581	0	0	0	0	0	0	0	0	0	0	0	0	0	0	0	0	0	0	0	1	0	0	0	0
miR-582-3p	0	1	0	0	2	0	0	0	0	0	0	0	1	0	0	0	0	1	3	0	1	0	1	0
miR-582-5p	0	0	0	0	0	0	0	0	0	0	0	0	0	0	0	0	0	0	0	0	0	0	0	0
miR-584-5p	1	0	1	10	2	3	5	25	2	0	4	2	4	0	0	6	0	2	5	9	7	2	3	22
miR-589-5p	0	0	0	0	0	0	0	0	1	0	0	0	0	0	0	0	0	0	0	0	0	1	0	0
miR-598-3p	0	0	0	0	0	0	0	0	0	0	0	0	0	0	0	0	0	0	1	0	0	0	0	0
miR-6068	0	0	0	0	0	0	0	0	0	0	0	0	0	0	0	0	0	0	0	0	0	0	1	0
miR-6087	0	0	0	0	0	0	0	0	0	0	0	0	0	0	0	0	0	0	0	0	0	0	0	1
miR-615-3p	0	0	0	0	0	0	0	0	0	0	0	0	0	0	0	0	0	0	0	0	0	0	0	0

miR-618	0	0	0	0	0	0	0	0	0	0	0	0	0	0	0	0	0	1	1	0	0	0	0	0
miR-624-5p	0	0	0	0	0	0	0	0	0	0	0	0	0	0	0	0	0	0	0	0	0	0	0	0
miR-625-3p	1	0	0	0	1	0	0	1	0	0	0	0	0	0	0	1	0	0	0	0	0	0	0	2
miR-625-5p	0	0	0	0	0	0	0	0	0	0	0	0	0	0	0	0	0	0	0	0	1	0	0	0
miR-627-5p	0	0	0	0	0	0	0	0	0	0	0	0	0	0	0	0	0	0	0	0	0	0	0	0
miR-628-3p	0	0	0	0	0	0	0	1	1	0	0	0	0	0	0	0	0	0	0	0	0	0	0	0
miR-628-5p	0	0	0	0	0	0	0	1	0	0	0	0	0	0	0	0	0	0	0	0	0	0	0	0
miR-629-3p	0	0	0	0	0	0	0	0	0	0	0	0	0	0	0	0	0	0	0	0	0	0	0	0
miR-629-5p	1	10	4	6	4	5	7	127	4	5	11	13	7	2	4	18	8	14	8	10	11	6	19	35

miR-636	0	0	0	0	0	0	0	1	0	0	0	0	0	0	0	0	0	0	0	0	0	0	0	1
miR-642a-3p	0	0	0	0	0	0	0	0	0	0	0	0	0	0	0	0	0	0	0	0	0	0	0	0
miR-6503-3p	0	0	0	0	0	0	0	1	0	0	0	0	0	0	0	0	0	0	0	0	0	0	0	0
miR-6509-5p	0	0	0	0	0	0	0	0	0	0	0	0	0	0	0	0	0	0	0	0	0	0	0	0
miR-6510-3p	0	0	0	0	0	0	0	0	0	0	0	0	0	0	0	0	0	0	0	0	0	0	0	0
miR-6511a-3p	0	0	0	0	0	0	0	0	0	0	0	0	0	0	0	0	0	0	0	0	0	0	0	0
miR-6511b-3p	0	0	0	0	0	0	0	0	0	0	0	0	0	0	0	0	0	0	0	0	0	0	0	0
miR-6511b-5p	0	0	0	0	0	0	0	0	0	0	0	0	0	0	0	0	1	0	0	0	0	0	0	0

miR-6515-5p	0	0	0	0	0	0	0	0	0	0	0	0	0	0	0	0	0	0	0	0	0	0	0	0
miR-651-5p	0	0	0	0	0	1	0	0	0	0	1	0	0	0	1	0	1	0	0	0	0	0	0	0
miR-6516-5p	0	0	0	0	0	0	0	0	0	0	0	0	0	0	0	0	0	0	1	0	1	0	0	0
miR-652-3p	0	0	0	0	0	2	0	4	1	0	0	0	0	0	0	1	0	0	0	2	1	0	0	1
miR-654-3p	0	0	2	0	0	0	0	1	0	0	0	0	0	0	0	1	0	0	0	0	1	0	0	1
miR-654-5p	0	1	0	0	0	0	0	0	0	0	1	1	0	0	0	0	0	1	1	0	0	0	0	0
miR-655-3p	0	0	0	0	0	0	0	0	0	0	0	0	0	0	0	0	0	0	0	0	1	0	0	0
miR-658	0	0	0	0	0	0	0	0	0	0	0	0	0	0	0	0	0	0	0	0	0	0	1	0
miR-659-5p	0	0	0	0	0	0	2	0	0	0	0	0	0	0	0	0	0	0	0	0	0	0	0	0

miR-660-5p	0	0	0	0	0	0	0	0	0	0	0	0	0	0	0	0	0	0	0	0	0	0	0	0
miR-661	0	0	0	0	0	0	0	0	0	0	0	0	0	0	0	0	0	0	0	0	0	0	0	0
miR-664a-3p	0	0	0	0	0	0	0	0	0	0	0	0	0	0	0	0	0	0	0	0	0	0	0	0
miR-664a-5p	0	2	1	0	1	0	0	4	1	0	0	0	0	0	0	1	0	1	0	0	0	0	1	0
miR-664b-5p	0	0	0	0	0	0	0	0	0	0	0	0	0	0	0	0	0	0	0	0	1	0	0	0
miR-671-3p	0	0	0	0	0	0	0	1	0	0	0	0	0	0	0	0	0	0	0	0	1	0	2	1
miR-6715a-3p	0	0	0	0	0	0	0	1	0	0	0	0	0	0	0	0	0	0	0	0	0	0	0	0
miR-6716-3p	0	0	0	0	0	0	0	1	0	0	0	0	0	0	0	0	0	0	0	0	0	0	0	1
miR-6717-5p	0	0	0	0	0	0	4	0	0	0	0	0	0	0	0	0	2	1	0	0	0	0	0	1

miR-6721-5p	0	0	0	0	0	0	0	0	0	0	0	0	0	0	0	0	0	0	0	0	0	0	0	0
miR-6723-5p	0	0	0	1	0	0	0	0	0	0	0	0	0	0	0	0	0	0	0	0	0	0	0	0
miR-6727-5p	0	0	0	0	0	0	0	0	0	0	0	0	0	0	0	0	0	0	0	0	0	0	0	0
miR-6730-5p	0	0	0	0	0	0	0	0	0	0	0	0	0	0	0	0	0	0	0	0	0	0	0	0
miR-6734-3p	0	0	0	1	0	0	0	0	0	0	0	0	0	0	0	0	0	0	0	0	0	0	0	0
miR-6734-5p	0	0	0	0	0	0	0	0	1	0	0	0	0	0	0	0	0	0	0	0	1	0	0	0
miR-6735-3p	0	0	0	0	0	0	0	0	0	0	0	0	0	0	0	0	0	0	0	1	0	0	0	0
miR-6735-5p	0	0	0	0	0	0	0	0	0	0	0	0	0	0	0	0	0	0	0	0	1	0	0	0
miR-6736-5p	0	0	0	0	0	0	0	0	0	0	0	0	0	0	0	0	0	0	0	0	0	0	0	0

miR-6738-3p	0	0	0	0	0	0	0	0	0	0	0	0	0	0	0	0	0	0	0	0	0	0	0	0
miR-6741-3p	0	0	0	0	0	1	0	0	0	0	0	0	0	0	0	0	0	0	0	0	0	0	0	2
miR-6741-5p	0	0	0	0	1	0	0	1	0	0	0	0	0	0	0	0	0	0	0	0	0	0	0	0
miR-6747-3p	0	0	0	0	0	0	0	0	0	0	0	0	0	0	0	0	0	0	0	0	0	0	0	0
miR-6750-3p	0	0	0	0	0	0	0	0	0	0	0	0	0	0	0	0	0	0	0	0	0	0	0	0
miR-6750-5p	0	0	0	0	0	0	0	4	0	0	0	0	0	0	0	0	0	0	0	0	0	0	0	0
miR-6767-5p	0	0	0	0	0	0	0	1	0	0	0	0	0	0	0	0	0	0	0	0	0	0	0	0
miR-6770-3p	0	0	0	0	0	0	0	0	0	0	0	0	0	0	0	0	0	0	0	0	0	0	0	0
miR-6772-3p	0	0	0	0	0	0	0	0	0	0	0	0	0	0	0	0	0	0	0	0	0	0	0	0

miR-6777-5p	0	0	0	0	0	0	0	3	0	0	0	0	0	0	0	0	0	0	0	0	0	0	0	1
miR-6780a-5p	0	0	0	0	0	0	1	2	0	0	0	0	0	0	0	0	0	0	0	0	0	0	0	0
miR-6781-5p	0	0	0	0	0	1	0	0	0	0	0	0	0	0	0	0	0	0	0	3	0	0	1	0
miR-6785-5p	0	0	0	0	0	0	0	1	0	0	0	0	0	0	0	0	0	0	0	0	0	0	0	0
miR-6786-3p	0	0	0	0	0	0	0	0	0	0	0	0	0	0	0	0	0	0	0	0	0	0	0	0
miR-6787-3p	0	0	0	0	0	0	0	0	0	0	0	0	0	0	0	0	0	1	0	0	0	0	0	0
miR-6788-3p	0	0	0	0	0	0	0	0	0	0	0	0	0	0	0	0	0	0	0	0	0	0	0	0
miR-6790-3p	1	0	0	0	0	0	0	0	0	0	0	0	0	0	0	0	0	0	0	0	0	0	0	0
miR-6793-5p	0	0	0	0	0	0	0	0	0	0	0	0	0	0	0	0	0	0	0	0	1	0	0	0

miR-6802-5p	0	0	0	0	0	0	0	0	0	0	0	0	0	0	0	0	0	0	0	0	0	0	0	0
miR-6803-3p	0	0	0	0	0	0	0	1	0	0	0	0	0	0	0	0	0	0	0	0	1	0	0	0
miR-6805-5p	0	0	0	1	0	0	0	0	0	0	0	0	0	0	0	0	0	0	0	0	0	0	0	0
miR-6806-3p	0	0	0	0	0	0	0	0	0	0	0	0	0	0	0	0	0	0	0	0	0	0	0	0
miR-6808-3p	0	0	0	0	0	0	0	0	0	0	0	0	0	0	0	0	0	0	0	0	0	0	0	0
miR-6812-3p	0	0	0	0	0	0	0	0	0	0	1	0	0	0	0	0	0	0	0	0	0	0	1	0
miR-6813-5p	0	0	0	0	0	0	0	0	0	0	0	0	0	0	0	0	0	0	0	0	0	0	0	0
miR-6815-5p	0	0	1	0	0	0	0	4	1	0	0	0	0	0	0	0	0	0	0	0	0	0	1	3
miR-6821-5p	0	0	0	0	0	0	0	0	0	0	0	0	0	0	0	0	0	0	0	0	1	0	0	0

miR-6826-5p	0	0	0	0	0	0	0	0	0	0	0	0	0	0	0	0	0	0	0	0	0	0	0	0
miR-6837-3p	0	0	0	0	0	0	0	0	0	0	0	0	0	0	0	0	0	0	0	1	0	0	0	0
miR-6839-5p	0	0	0	0	0	0	0	0	0	0	0	0	0	0	0	0	0	0	0	0	0	0	0	0
miR-6842-3p	1	0	0	0	0	0	0	0	0	0	0	0	0	0	0	0	0	1	0	0	1	0	0	0
miR-6842-5p	0	0	0	0	0	0	0	0	0	0	0	0	0	0	0	0	0	0	0	0	0	0	0	0
miR-6847-5p	0	0	0	0	0	0	0	0	0	0	0	0	0	0	0	1	0	0	0	0	0	0	0	0
miR-6849-5p	0	0	0	0	0	0	0	0	0	0	0	0	0	0	0	0	0	0	0	1	0	0	0	0
miR-6850-5p	0	0	0	0	0	0	0	2	0	0	0	0	0	0	0	0	0	0	0	0	1	0	0	1
miR-6852-5p	0	0	0	0	0	0	0	0	0	0	0	0	0	0	0	0	0	0	0	0	0	0	0	0

miR-6859-5p	0	0	0	0	0	0	0	0	0	0	0	1	0	0	0	0	0	0	0	0	0	0	0	0
miR-6862-5p	0	0	0	0	0	0	0	0	0	0	0	0	0	0	0	0	0	0	0	0	0	0	0	0
miR-6865-5p	0	0	0	0	0	0	0	0	0	0	0	0	0	0	0	0	1	0	0	0	0	0	0	0
miR-6866-5p	0	0	0	0	0	0	0	0	0	0	0	0	0	0	1	0	0	0	0	0	0	0	0	0
miR-6868-3p	0	0	0	0	0	0	0	0	0	0	0	0	0	0	0	0	0	0	0	0	0	0	0	0
miR-6869-5p	1	0	0	1	1	0	0	1	0	2	0	0	0	0	0	1	0	0	0	1	1	0	1	0
miR-6873-3p	1	0	0	0	0	0	0	0	0	0	0	0	0	0	0	0	0	0	0	0	0	0	0	0
miR-6877-5p	0	0	0	0	0	0	0	0	0	0	0	0	0	0	0	0	0	0	0	0	0	0	0	0
miR-6881-3p	0	0	0	0	0	0	0	0	0	0	0	0	0	0	0	0	0	0	0	0	0	0	0	0

miR-6884-5p	0	0	0	0	0	0	0	3	0	0	0	0	0	0	0	0	0	0	0	0	0	0	0	0
miR-7107-3p	0	0	0	0	0	0	0	1	0	0	0	0	1	0	0	0	0	0	0	0	0	0	0	1
miR-7110-3p	0	0	0	0	0	0	0	0	0	0	0	0	0	0	0	0	0	0	0	0	0	0	0	0
miR-744-5p	1	1	1	9	6	0	0	12	5	0	4	3	1	0	3	5	0	3	5	4	5	0	4	10
miR-758-3p	0	0	0	0	0	0	0	0	0	0	0	0	0	0	0	0	0	0	0	0	0	0	0	1
miR-7-5p	6	0	2	3	6	9	0	39	1	1	1	1	0	1	8	6	5	9	0	2	8	0	4	9
miR-760	0	0	0	0	0	0	0	0	0	0	0	0	0	0	0	0	0	0	0	0	0	0	0	0
miR-766-5p	0	0	0	0	0	0	0	0	0	0	0	0	0	0	0	0	0	0	0	0	2	0	0	1
miR-769-5p	0	0	0	0	1	0	1	3	2	0	0	1	0	0	0	0	0	0	0	0	0	0	1	1

miR-7704	0	1	0	0	1	0	0	0	1	0	0	0	0	0	0	0	0	0	0	1	0	0	0	0
miR-7706	0	0	0	1	0	0	0	18	6	0	2	0	3	2	1	2	1	3	0	0	3	0	1	3
miR-7848-3p	0	0	0	0	0	0	0	2	0	0	0	0	0	0	0	0	0	0	0	0	0	0	0	1
miR-7854-3p	0	0	0	0	0	0	0	0	0	0	0	0	0	0	0	0	0	0	0	0	1	0	0	0
miR-7976	0	0	0	0	0	0	0	0	0	0	0	0	0	0	0	0	0	0	0	0	0	0	0	0
miR-873-5p	0	0	0	0	0	0	0	0	0	0	0	0	0	0	0	0	0	0	0	0	1	0	0	0
miR-874-3p	0	0	0	0	0	0	0	0	0	0	0	1	0	0	0	0	0	0	0	0	1	0	0	0
miR-877-5p	0	0	0	0	0	0	0	0	0	0	0	0	0	0	0	0	0	0	0	0	0	0	0	0
miR-885-3p	0	0	0	0	0	0	0	0	1	0	0	0	0	0	0	0	0	0	0	0	0	0	0	0

miR-885-5p	0	0	0	0	0	0	0	0	0	0	0	0	0	0	0	0	0	0	0	0	0	0	0	0
miR-889-3p	0	0	0	0	0	0	0	2	0	0	0	0	0	0	0	0	0	0	0	0	0	0	0	1
miR-92a-1-5p	0	0	0	0	0	0	0	0	0	0	0	0	0	0	0	0	0	0	1	0	1	0	0	0
miR-92a-2-5p	0	0	0	0	0	0	0	0	0	0	0	0	0	0	0	0	0	0	0	0	0	0	0	0
miR-92a-3p	176	60	183	474	265	356	253	3917	456	118	470	290	258	91	176	671	258	578	184	333	864	166	724	1349
miR-92b-3p	5	2	7	1	1	8	1	20	1	0	1	7	6	0	1	6	2	4	7	3	5	2	7	7
miR-92b-5p	0	1	0	0	1	0	0	4	1	0	1	0	1	0	0	1	0	0	0	0	1	1	0	0
miR-93-5p	1	0	4	3	3	1	0	27	4	0	1	3	0	2	1	4	1	1	1	4	8	1	6	7

miR-937-3p	0	0	0	0	0	0	0	0	0	0	0	0	0	0	0	0	0	0	0	0	0	0	0	1
miR-939-5p	0	0	0	0	0	0	0	2	1	0	0	0	0	0	0	0	0	0	0	0	1	0	0	0
miR-9-3p	0	0	0	0	0	0	0	0	0	0	0	0	0	0	0	0	0	0	0	0	1	0	0	0
miR-941	1	0	1	1	0	1	0	5	2	0	2	1	4	0	0	4	0	5	2	1	3	1	1	4
miR-942-3p	0	0	0	0	0	0	0	0	0	0	0	0	0	0	0	0	0	0	0	0	0	0	1	0
miR-942-5p	0	0	0	0	0	0	0	2	0	0	0	0	0	0	0	0	0	0	0	0	0	0	1	0
miR-95-3p	0	0	0	1	0	0	0	1	0	0	0	0	0	0	0	0	0	0	0	1	1	0	0	0
miR-9-5p	0	0	6	0	1	0	1	0	0	0	1	0	18	0	3	0	40	0	1	0	91	0	0	1
miR-96-5p	1	0	0	1	0	0	0	1	0	0	0	0	0	0	0	0	0	0	0	0	1	0	0	0

miR-98-5p	2	0	2	6	6	0	2	27	6	2	1	3	4	0	0	7	0	6	1	9	20	3	4	13
miR-99a-5p	30	19	14	39	41	35	15	129	93	12	14	23	24	5	11	42	8	82	46	29	197	21	114	130
miR-99b-3p	0	0	0	0	0	0	0	3	3	0	1	0	0	0	0	0	0	0	0	1	1	0	0	2
miR-99b-5p	23	6	8	24	21	14	15	168	20	18	10	13	24	3	8	33	14	42	31	19	110	5	53	71